Alanyl-phosphatidylglycerol-dependent lipid homeostasis in *Pseudomonas aeruginosa*

Von der Fakultät für Lebenswissenschaften

der Technischen Universität Carolo-Wilhelmina

zu Braunschweig

zur Erlangung des Grades einer

Doktorin der Naturwissenschaften

(Dr. rer. nat.)

genehmigte

D i s s e r t a t i o n

von Wiebke Arendt
aus Northeim

1. Referent:	Professor Dr. Dieter Jahn
2. Referentin:	Privatdozentin Dr. Gunhild Layer
3. Referent:	Professor Dr. Ralf-Rainer Mendel
eingereicht am:	26.06.2013
mündliche Prüfung (Disputation) am:	26.08.2013

Druckjahr 2013

Vorveröffentlichungen der Dissertation

Teilergebnisse aus dieser Arbeit wurden mit Genehmigung der Fakultät für Lebenswissenschaften, vertreten durch den Mentor der Arbeit, in folgenden Beiträgen vorab veröffentlicht:

Publikationen

Arendt, W., Hebecker, S., Jäger, S., Nimtz, M. & Moser, J. Resistance phenotypes mediated by aminoacyl-phosphatidylglycerol synthases. Journal of Bacteriology 194(6):1401-1416 (2012).

Arendt, W., Groenewold, M., Hebecker, S., Dickschat, J. S. & Moser, J. Identification of a periplasmic Aminoacyl-Phosphatidylglycerol Hydrolase responsible for *Pseudomonas aeruginosa* lipid homeostasis. *In revision*.

Tagungsbeiträge

Arendt, W. & Moser, J.: Phänotypische Effekte verschiedener Aminoacyl-Phosphatidyl-glycerol Synthasen. (Vortrag) Retreat mit der AG Frankenberg aus Bochum, Bochum (2011)

Arendt, W., Hebecker, S., Jäger, S., Nimtz, M. & Moser, J.: Resistance phenotypes mediated by aminoacyl-phosphatidylglycerol synthases. (Poster) VAAM Jahrestagung, Tübingen (2012)

Arendt, W. & Moser, J.: Phenotypical impact and homeostasis of Alanyl-phosphatidylglycerol in *Pseudomonas aeruginosa*. (Vortrag) Karlsruher Institut für Technologie, Karlsruhe (2012)

Arendt, W., Groenewold, M., Hebecker, S., Dickschat, J. S. & Moser, J.: Identification and characterization of a periplasmic Aminoacyl-Phosphatidylglycerol Hydrolase responsible for *Pseudomonas aeruginosa* lipid homeostasis. (Poster) VAAM Jahrestagung, Bremen (2013)

Table of contents

Abbreviations

aaPG	aminoacyl-phosphatidylglycerol
aaPGS	aminoacyl-phosphatidylglycerol synthase
ALA	5-aminolevulinic acid
Ap	ampicillin
A-PG	alanyl-phosphatidylglycerol
A-PGS	alanyl-phosphatidylglycerol synthase
ATP	adenosine triphosphate
AtvA	acid tolerance and virulence
BCIP	5-bromo-4-chloro-3-indolyl phosphate
BLAST	basic local alignment search tool
Boc	*tert*-butyloxycarbonyl
Boc_2O	di-*tert*-butyl dicarbonate
CAMP	cationic antimicrobial peptide
Cb	carbenicillin
CDP-DAG	cytidine diphosphate-diacylglycerol
CFTR	cystic fibrosis transmembrane conductance regulator
Cm	chloramphenicol
CMP	cytidine monophosphate
CTP	cytidine triphosphate
CV	column volume(s)
DCC	dicyclohexylcarbodiimide
DMSO	dimethyl sulfoxide
DPG	diphosphatidylglycerol
DSMZ	German Collection of Microorganisms and Cell Cultures
dNTP	deoxynucleotide triphosphate
GTP	guanosine triphosphate
EDTA	ethylenediaminetetraacetic acid
EMBL	European Molecular Biotechnology Laboratory
$FADH_2$	flavine adenine dinucleotide
FRT	FLP recombinase target
Gm	gentamicin
GTP	guanosine triphosphate
HABA	2-(4'-hydroxyl-benzeneazo)benzoic acid
HEPES	4-(2-hydoxyethyl)-1-piperazineethanesulfonic acid
ICP-MS	inductively coupled plasma – mass spectrometry
IPTG	isopropyl-β-D-thiogalactopyranoside
iTOL	interactive tree of life
Kan	kanamycin
LB	Luria-Bertani

L-PG	lysyl-phosphatidylglycerol
L-PGS	lysyl-phosphatidylglycerol synthase
MIC	minimal inhibitory concentration
MprF	multiple peptide resistance factor
MU	Miller Unit(s)
NADH	nicotinamide adenine dinucleotide
NADPH	nicotinamide adenine dinucleotide phosphate
NBT	nitrotetrazolium blue
NTA	nitrilotriacetic acid
OD_{λ}	optical density at λ nm
ONPG	2-nitrophenyl-β-D-galactopyranoside
PA	phosphatidic acid
PAGE	polyacrylamide gel electrophoresis
PC	phosphatidylcholine
PCR	polymerase chain reaction
PE	phosphatidylethanolamine
PG	phosphatidylglycerol
PI	phosphatidylinositol
PIPES	piperazine-N,N'-bis(2-ethanesulfonic acid)
PMSF	phenylmethylsulfonyl fluorid
PP_i	pyrophosphate
PS	phosphatidylserine
PVDF	polyvinylchloride
RBS	ribosome binding site
R-PG	arginyl-phosphatidylglycerol
RT	room temperature
R2A	Reasoner's 2A medium
SAH	*S*-adenosyl homocysteine
SAM	*S*-adenosyl methionine
SDS	sodium dodecyl sulfate
SMM	Spizizen's minimal medium
SRP	signal recognition particle
Tet	tetracycline
THF	tetrahydrofuran
TLC	thin-layer chromatography
TLCK	N_{α}-tosyl-L-lysine chloromethyl ketone
Tris	tris(hydrolxymethyl)aminomethane
TSB	trypticase soy broth

Glossary

et al.	*et alteri* (and others)
M_r	relative molecular weight
R_f	retardation factor, ratio of migration distance of the sample substance to migration distance of the solvent front
p.a.	*pro analysi* (quality grade)
v/v	volume per volume
w/v	weight per volume

1 Introduction

1.1 The era of bacterial infectious diseases has just begun

Bacterial infections often resulted in death before World War II. In 1848, 60 % of death were caused by infectious diseases in England (Cutler *et al.*, 2006) and 80 % of patients infected with *Staphylococcus aureus* died in the early 1940s (Deurenberg and Stobberingh, 2008). After Koch and Pasteur gained first insights into the principles of bacterial infections proposed as the germ theory in the second half of the 19th century (Lederberg, 2000), first substances with antimicrobial activity were detected in the begin of the 20th century: Salvarsan was used for syphilis treatment since 1910 and prontosil was employed for general purposes since 1935 (Kingston, 2000). The first antibiotics according to today's definition were applied during World War II. In 1937, sulfonamides were employed to treat streptococcal infections and in 1942, penicillin was applied against e.g. tetanus, gas gangrene and wound infections (Manring *et al.*, 2009; Davies and Davies, 2010). Streptomycin was introduced in 1944 to treat patients suffering from tuberculosis (Davies and Davies, 2010). With the development of the first semi-synthetic β-lactam antibiotic methicillin in 1959 and the isolation or development of several other antibiotics like cephalosporins, macrolides or fluorochinolones, the age of infectious diseases caused by bacteria seemed to be successfully overcome (Davies and Davies, 2010).

This was unfortunately not the case: First pathogens being resistant against the applied antibiotics were observed only a few years after the respective antibiotic was employed for clinical treatments (Davies and Davies, 2010; Deurenberg and Stobberingh, 2008). Subsequently, resistant strains were found in hospitals and were also established in the community (Goossens and Sprenger, 1998; Deurenberg and Stobberingh, 2008). The accumulation of resistances against several classes of antibiotics in one organism lead to the development of nosocomial superbugs like multidrug-resistant strains of *S. aureus*, *Mycobacterium tuberculosis* or *Pseudomonas aeruginosa* (Davies and Davies, 2010). Infections with these bacteria resulted in increased mortality and morbidity, in elongated hospitalization and also in increased health care costs (Cosgrove, 2006). Since the beginning of the 21st century, the bacterial membrane targeting lipopeptide daptomycin was employed to treat infections caused by multi-resistant gram positive bacteria (Enoch *et al.*, 2007).

Unfortunately, daptomycin resistant *S. aureus* strains were observed recently (Baltz, 2009; Friedman *et al.*, 2006).

Infections caused by highly-resistant bacteria represent only one aspect of the problem today: In developing countries and in crisis regions, many people die due to infectious diseases promoted by malnutrition, poor sanitation, climate changes or insufficient medical supply often additionally complicated by emerging antimicrobial resistances (Wilson, 1995; Byarugaba, 2004). For example, 2.7 million people died due to tuberculosis and 8.1 million were worldwide infected in 1993 (Dobson and Carper, 1996). Therefore, the era of bacterial infections has only just begun.

1.2 The opportunistic pathogen *Pseudomonas aeruginosa*

P. aeruginosa is a ubiquitous gram negative bacterium found in coastal marine habitats, soil and swamp. It was also isolated from animals and plants. Due to its ability to form biofilms on wet surfaces, it can grow on rocks and is found in almost every environment (Stover *et al.*, 2000; van Delden and Iglewski, 1998; Hancock, 1998). This is facilitated by its versatile and flexible metabolism concerning e.g. carbon source utilization, growth in the presence or absence of oxygen and denitrification (Oberhardt *et al.*, 2008).

P. aeruginosa is able to infect humans as opportunistic pathogen by colonializing burn wounds or catheters inserted into urinary tracts or respiration systems (Stover *et al.*, 2000). It is the most common gram negative nosocomial pathogen with 10 – 15 % nosocomial infections worldwide and provides a wide variety of virulence factors (van Delden and Iglewski, 1998; Strateva and Yordanov, 2009). It is related to hospital-acquired acute infections of surgical wounds (8 %), bloodstreams (10 %), urinary tracts (12 %) and pneumonia (16 %) of immunocompetent patients. Nosocomial *P. aeruginosa* infections of intubated, immunocompetent patients exhibit a death rate of 38 %. Instead, community-acquired infections of immunocompetent humans are rare. For immunocomprimized patients, *P. aeruginosa* infections are fatal: Pneumonia and septicemia resulted in 30 % deaths and AIDS patients died due to *P. aeruginosa* infections with a rate of 50 % (van Delden and Iglewski, 1998).

The treatment of *P. aeruginosa* infections is challenging due to its high intrinsic resistance and its ability to acquire resistance mechanisms (Breidenstein *et al.*, 2011; Hancock, 1998; Strateva and Yordanov, 2009). Especially in patients suffering from cystic fibrosis producing high viscous mucus, *P. aeruginosa* infections are often chronically established (Gaspar *et al.*, 2013; Callaghan and McClean, 2012).

1.2.1 Antibiotic resistance of *P. aeruginosa*

In general, bacteria become resistant mainly by two conventional mechanisms called acquired and adaptive resistance. Acquired (also called genetic) resistance results from the uptake of specific resistance genes by horizontal gene transfer and from mutations leading to increased expression or de-repression of efflux pump components and other resistance related systems or due to target site modifications. This kind of resistance mechanism is genetically encoded and is therefore inherited to daughter cells. Instead, adaptive resistance is induced by the presence of an antibiotic or by environmental stresses. Resistance related genes become upregulated and the bacterium is less susceptible to specific compounds. When the stimulus is removed, the adaptive resistance is lost and is therefore uninheritable (Breidenstein *et al.*, 2011; Hancock, 1998).

Beside these conventional types of resistance, *P. aeruginosa* exhibits a special, high intrinsic resistance against antibiotics like aminoglycosides, fluorochinolones or β-lactams mainly provided by three different systems. First, *P. aeruginosa* possesses an outer membrane with very low permeability (12 – 100x less compared to *E. coli*; Hancock, 1998). Outer membranes are regarded as selective, molecular sieves. Hydrophilic compounds pass this barrier by diffusing through water filled channels of porins. The size of the hydrophilic compounds is limited by porin channel sizes and their uptake is restricted by the low quantity of porins in the outer membrane of *P. aeruginosa*. Furthermore, antibiotics are taken up by specific porins or self-promoted ways. Alternatively, hydrophobic compounds can pass the outer membrane bilayer (Breidenstein *et al.*, 2011; Hancock, 1998). The second aspect of *P. aeruginosa* intrinsic resistance is the rapid efflux of accumulated antibiotics. Efflux pumps with wide substrate specificity, especially the resistance-nodulation-division efflux systems MexAB-OprM and MexXY-OprM, are constitutively expressed and export harmful antibiotics. Additionally, representing the third part of intrinsic resistance, *P. aeruginosa* exhibits a

chromosomally encoded β-lactamase which is constitutively expressed and confers resistance against a wide variety of β-lactam-type antibiotics (Breidenstein *et al.*, 2011; Strateva and Yordanov, 2009; Hancock, 1998).

1.2.2 Cystic fibrosis and *P. aeruginosa* infection

Cystic fibrosis is an inheritable disease and is caused by mutations affecting the cystic fibrosis transmembrane conductance regulator (CFTR) localized in epithelial cells. The defective CFTR influences the function of several organs like the gastrointestinal tract, the pancreas, the liver and particularly the respiratory system (Gaspar *et al.*, 2013). In lung epithelial cells, the CFTR mediated chloride secretion into the airways is decreased. Consequently, the sodium absorption from the airway liquid is increased resulting in depletion of airway surface liquid, mucus dehydration and volume reduction. The increased mucus viscosity impairs the mucociliary clearance normally exporting contaminated mucus. Purulent sputum is accumulated resulting in chronic infections of cystic fibrosis patients (Gaspar *et al.*, 2013; Callaghan and McClean, 2012). The surface liquid pH of cystic fibrosis lung epithelial cells was found acidified due to the impaired bicarbonate ion secretion by CFTR (Coakley *et al.*, 2003). Additionally, acidification of infection sites was proposed as a general aspect of inflammation (Simmen *et al.*, 1994).

When the cystic fibrosis lung becomes infected by a non-mucoid *P. aeruginosa*, the bacterium penetrates the nutrient rich mucus due to its flagellar activity and secrets high amounts of virulence factors. By the time, virulence factor secretion is reduced and *P. aeruginosa* forms biofilms protective against antimicrobial compounds and phagocytosis. Mutations are accumulated often resulting in the increased production of the exopolysaccharide alginate representing a physical barrier against host defense components (Gaspar *et al.*, 2013; Callaghan and McClean, 2012; Schobert and Jahn, 2010; van Delden and Iglewski, 1998; Breidenstein *et al.*, 2011). In viscous mucus, oxygen becomes limited and *P. aeruginosa* adapts to microaerophilic or anaerobic conditions by changing its physiology. It uses denitrification or special types of fermentation being accompanied by a diminished antibiotic sensitivity to antimicrobial compounds (Schobert and Jahn, 2010; Callaghan and McClean, 2012).

Chronic *P. aeruginosa* infections are associated with a decline in lung function. 54 % of cystic fibrosis patients are infected with *P. aeruginosa* being most prominent in adults (80 %), whereas *S. aureus* is the main pathogen in children (approximately 80 %) (Gaspar *et al.*, 2013). Microbial communities within the lung mucus include also anaerobic bacteria and evolve with the patient's age. Mostly, chronic *P. aeruginosa* infections cannot be eradicated by any therapy (Gaspar *et al.*, 2013; Schobert and Jahn, 2010). Therefore, the understanding of *P. aeruginosa* processes resulting in increased antibiotic tolerance and the subsequent development of new antimicrobials are highly important.

1.3 Prokaryotic cell envelopes and compounds

Prokaryotes can be divided in different classes according to their cell envelope architecture and components. These are summarized in the following sections focusing on bacterial membranes.

1.3.1 Different prokaryotic cell envelopes

The prokaryotic cytoplasm is surrounded by the cytoplasmic membrane separating the cell from its environment consisting of a phospholipid bilayer with inserted membrane proteins. Transport across the membrane is highly selective and energy generating processes depending on the proton motive force are located there. Membranes are highly variable structures described initially by the fluid mosaic model (Madigan and Martinko, 2009).

Cytoplasmic membranes are surrounded by stabilizing structures: Gram positive bacteria exhibit a massive peptidoglycan layer containing teichonic and teichuronic acids. In contrast, gram negative bacteria provide a thin peptidoglycan layer but also an additional outer membrane separating the peptidoglycan harboring periplasmic space from the environment. The outer membrane consists of an inner phospholipid leaflet and an outer lipopolysaccharide leaflet. Archaea do not possess peptidoglycan but their membranes are also surrounded by stabilizing structures consisting of pseudopeptidoglycan, other poly-saccharides or proteinogenic structures forming the S-layer (Madigan and Martinko, 2009).

1.3.2 Phospholipids

Prokaryotic phospholipids share a common basic amphiphilic structure. They consist of a glycerol backbone coupled to two hydrophobic side chains and a phosphate group and differ in their hydrophilic head groups (Koga, 2011).

Bacterial phospholipids are synthesized based on the precursor phosphatidic acid (PA) which is synthesized as follows: A fatty acid is transferred to the 1-position of glycerol-3-phosphate by the glycerol-3-phosphate acyltransferase PlsB or alternatively in a two-step process by PlsX and PlsY yielding lysophosphatidic acid (1-acyl-glycerol-3-phosphate). Subsequently, a second fatty acid is coupled to the remaining hydroxyl group of lysophosphatidic acid by the 1-acyl-glycerol-3-phosphate acyltransferase PlsC yielding the phospholipid precursor PA (Zhang and Rock, 2008; Geiger *et al.*, 2010b; Geiger *et al.*, 2010a). Saturated fatty acids are predominantly found in the 1-position, whereas unsaturated fatty acids are often located in the 2-position (Dowhan, 1997). The hydrophilic phosphate group of PA is coupled to several other hydrophilic molecules resulting in diversified phospholipids as summarized in Figure 1 based on selected reviews (Zhang and Rock, 2008; Geiger *et al.*, 2010a; Geiger *et al.*, 2010b).

The phospholipid synthesis was proposed to be located at the inner leaflet of the cytoplasmic membrane (Cronan, 2003). Initially, PA is activated using cytidine triphosphate (CTP) resulting in cytidine diphosphate-diacylglycerol (CDP-DAG) representing the central intermediate of phospholipid synthesis. The zwitterionic phosphatidylserine (PS) is synthesized by replacing cytidine monophosphate (CMP) with L-serine by the phosphatidyl-serine synthase. PS is further converted to the zwitterionic phosphatidylethanolamine (PE) by the phosphatidylserine decarboxylase by releasing CO_2. CDP-DAG is also the basis for the anionic phosphatidylglycerol (PG) synthesis using glycerol-3-phosphate *via* the intermediate phosphatidylglycerol phosphate by phosphatidylglycerol phosphate synthase and phosphatidylglycerol phosphate phosphatase. Two PG molecules are condensed by the cardiolipin synthase yielding the anionic diphosphatidylglycerol (DPG, also named cardiolipin). PE, PG and DPG are the major phospholipids of many bacteria. E.g. *Escherichia coli* contains 70 – 80 % PE, 15 – 20 % PG and up to 5 % DPG (Huijbregts *et al.*, 2000).

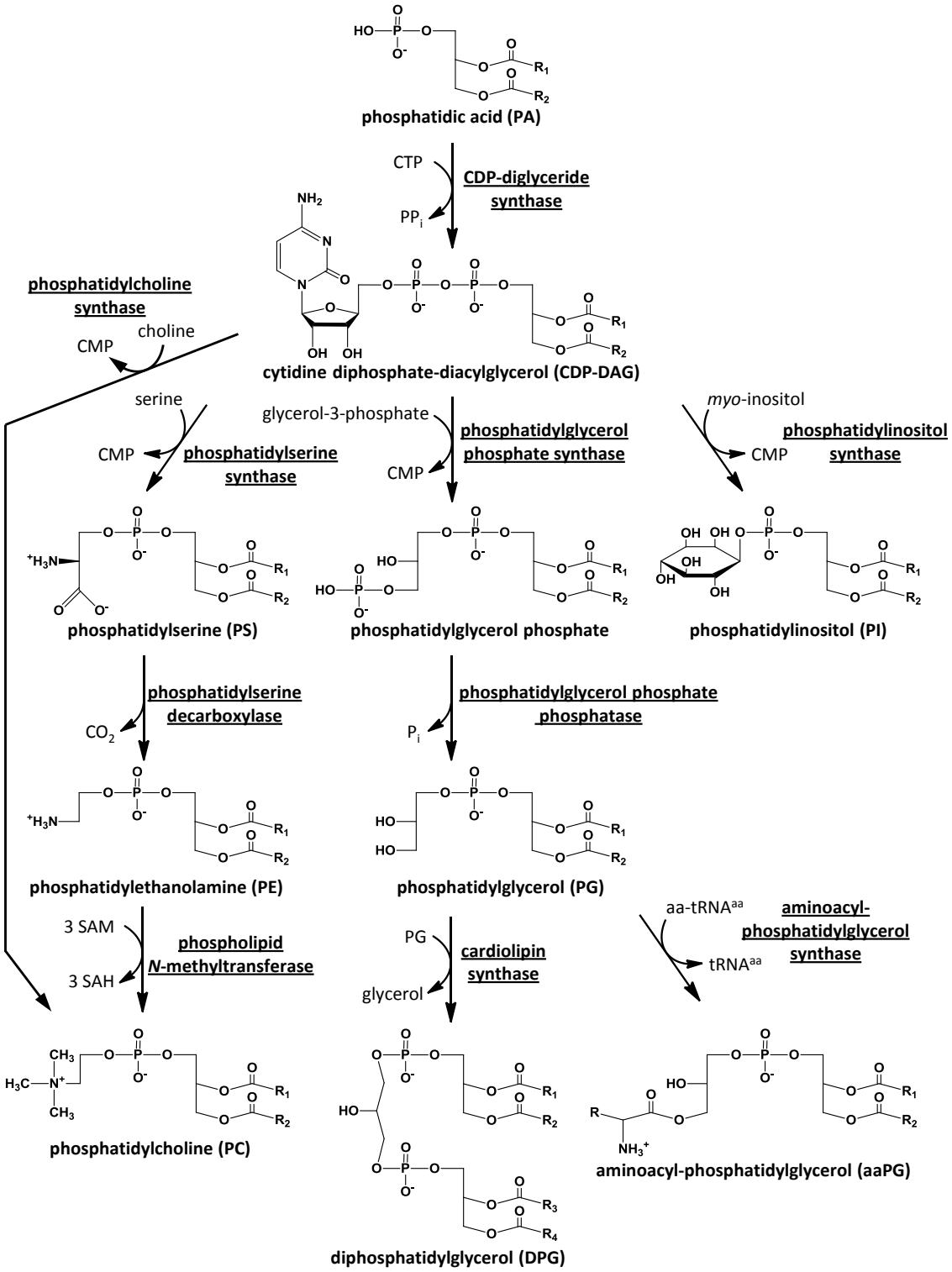

Figure 1: Diversification of phospholipid head groups (according to Geiger *et al.*, 2010a)
Bacterial phospholipids possessing different polar head groups are synthesized based on a common ancestor. One reaction pathway results in the formation of phosphatidylserine, phosphatidylethanolamine and phosphatidylcholine, whereas phosphatidylglycerol, diphosphatidylglycerol and aminoacyl-phosphatidylglycerols are synthesized in a second pathway. A third branch leads to the formation of phosphatidylinositol.
Phospholipid synthesizing enzymes are underlined. aa: amino acid, CMP: cytidine monophosphate, CTP: cytidine triphosphate, PP_i: pyrophosphate, R: amino acid side chain, $R_{1\text{-}4}$: fatty acid residues, SAH: *S*-adenosyl homocysteine, SAM: *S*-adenosyl methionine. See scheme for further abbreviations.

Additionally, several bacteria provide phospholipids with other modified head groups: The zwitterionic phosphatidylcholine (PC) present in only 10 % of the bacteria (Geiger *et al.*, 2010b) is synthesized by two different pathways: First, PE is methylated threefold by phospholipid *N*-methyltransferase using *S*-adenosyl methionine (SAM). Alternatively, PC is directly obtained by the condensation of CDP-DAG with choline catalyzed by the phosphatidylcholine synthase. The anionic phosphatidylinositol (PI) rarely found in bacteria is synthesized by CDP-DAG condensation with *myo*-inositol promoted by the phosphatidylinositol synthase e.g. in *M. tuberculosis* (Geiger *et al.*, 2010b). The formation of aminoacyl-phosphatidylglycerol (aaPG) by the transfer of an amino acid to PG by an aminoacyl-phosphatidylglycerol synthase (aaPGS) is also a process restricted to certain bacterial species. The charge characteristic of this molecule depends on the employed amino acid (Zhang and Rock, 2008; Geiger *et al.*, 2010b; Geiger *et al.*, 2010a; Roy, 2009). Several bacteria like *Bacillus subtilis* synthesize glucosylated diacylglycerols by transferring up to four uridine diphosphate-activated glucose molecules to diacylglycerol (Geiger *et al.*, 2010b). Other lipids like sphingolipids and steroids or hopanoids are rarely found in bacteria (Geiger *et al.*, 2010b) and not further discussed here.

Different bacterial phospholipids have distinct functions in cellular processes. E.g. anionic phospholipids are involved in DNA replication initiation, the control of cell division and protein translocation. PE is necessary for the accurate topology of certain membrane proteins (Geiger *et al.*, 2010b; Dowhan, 1997). Phospholipids have been found to aggregate to lipid microdomains and rafts localizing and compartmentalizing distinct membrane proteins and processes. E.g. DPG and PE enriched domains were located together with several phospholipid synthases in bacterial septal membranes (Dowhan and Bogdanov, 2002; Matsumoto *et al.*, 2006; Barák and Muchová, 2013). The aaPGs confer resistance against several antimicrobial compounds (Geiger *et al.*, 2010b) as further described in detail in following chapters.

Phospholipids are degraded by phospholipases cleaving specifically the ester bonds of the fatty acyl side chains or the phosphodiesterbond of the hydrophilic part with varying specificities (Schmiel and Miller, 1999; Ramrakhiani and Chand, 2011). Most bacterial phospholipases are secreted for phosphate and carbon source acquisition. Additionally, they act as virulence factors by degrading host phospholipids and destabilizing host membranes

resulting in tissue destruction during infection (Schmiel and Miller, 1999). Instead, eukaryotic phospholipases are mainly employed in lipid metabolism and signal transduction processes but are also components of e.g. snake venoms (Schmiel and Miller, 1999; Ramrakhiani and Chand, 2011).

Archaeal phospholipids provide a glycerol-1-phosphate backbone which is sequentially linked to geranylgeranyl side chains yielding archaetidic acid (in analogy to PA). CTP activation results in CDP-archaeol (in analogy to CDP-DAG) and archaetidylserine, archaetidylglycerol and archaetidylinositol are proposed to be synthesized analogously to bacterial pathways because homologous enzymes were identified in archaea by sequence analysis. The unsaturated geranylgeranyl side chains are hydrogenated during phospholipid synthesis using nicotinamide adenine dinucleotide (NADH) resulting in saturated isoprenoid residues predominant in archaeal lipids (Koga, 2010; Koga, 2011).

1.3.3 Membrane proteins and protein secretion

Proteins are integrated into membranes or are associated with membranes. Extracyto-plasmatic proteins are transported across the membrane employing the same machineries (Dalbey *et al.*, 2011). They are necessary for solute transport, signal transduction, energy production, cell-to-cell signaling, membrane biogenesis and several other processes (Dowhan and Bogdanov, 2009). Basic principles of membrane protein insertion and protein transfer across cytoplasmic membranes in bacteria are summarized.

Proteins represent the second major class of membrane components comprising 20 – 30 % of total cellular proteins (Dalbey *et al.*, 2011). Integral cytoplasmic membrane proteins consist of several α-helices inserted into the membrane by a highly conserved process present in bacteria, archaea and eukaryotes (Natale *et al.*, 2008). After translation of the first amino acids, the nascent peptide chain emerges from the ribosome. The N-terminal located signal sequence with an average length of 20 amino acids (Natale *et al.*, 2008) provides a hydrophobic core region which is bound by the signal recognition particle (SRP) consisting of a 4.5 S RNA molecule and the Ffh protein binding guanosine triphosphate (GTP). The SRP directs the ribosome to the membrane and binds to the membrane associated FtsY receptor also providing GTP. After SRP-FtsY complex formation, the nascent protein chain is

transferred to the SecYEG translocon, GTP is hydrolyzed and subsequently, SRP and FtsY dissociate (Dalbey *et al.*, 2011). Transmembrane helices of the nascent peptide chain are inserted co-translationally into the membrane by leaving the translocon laterally and cytoplasmic and extracytoplasmic domains are released into the respective compartment. Membrane insertion processes might be assisted by the YidC insertase (Dalbey *et al.*, 2011). The transport of the nascent peptide chain into and through the translocon is promoted by the cytoplasmic adenosine triphosphate (ATP) hydrolyzing motor protein SecA and also by the proton motive force (Dalbey *et al.*, 2011; Natale *et al.*, 2008).

Several factors influencing the topology of membrane proteins are encoded within the proteinogenic amino acid sequence. The signal sequence, the position of charged amino acids and the hydrophobicity of transmembrane domains determine the topology together with factors directly associated with the translocation process (YidC) (Dalbey *et al.*, 2011; Bogdanov *et al.*, 2009; Dowhan and Bogdanov, 2009). The most prominent initial membrane protein topology determinant is the localization of positively and negatively charged residues within the cytoplasmic and periplasmic loops of the integral membrane protein according to the 'positive-inside' rule. It describes the preferred localization of positively charged amino acid residues in cytoplasmic loops but the molecular basics are not solved in detail (Dalbey *et al.*, 2011; Bogdanov *et al.*, 2009; Dowhan and Bogdanov, 2009). This type of orientation determination is also observed for proteins with a single membrane-spanning helix (Dalbey *et al.*, 2011). The final membrane topology is additionally influenced by the interaction of membrane helices and extramembrane domains and especially by the biophysical properties of phospholipids surrounding the membrane protein. This was demonstrated by analyzing the PE-dependent topology of the *E. coli* lactose permease LacY (Dalbey *et al.*, 2011; von Heijne, 2006; Bogdanov *et al.*, 2009; Dowhan and Bogdanov, 2009).

Proteins are transported across the membrane and secreted into the periplasm (gram negatives) or to the extracellular space (gram positives) employing the same SecYEG translocon. During translation, the nascent peptide chain is bound by several copies of the cytoplasmic chaperone SecB maintaining the protein in an unfolded state. After translation, SecB interacts with SecA transferring the substrate protein to the SecYEG translocon and the protein is transported across the membrane mediated by the ATP-dependent SecA. SecB is not present in all bacteria but its function might be replaced by general chaperones (Natale

et al., 2008). In gram negative bacteria, periplasmic proteins are folded by periplasmic chaperones and disulfide-bonds are introduced by the redox-active Dsb-system well-elucidated in *E. coli*. Related compounds were also detected in gram positives (Kadokura and Beckwith, 2010).

Alternatively, proteins are transported across the membrane after translation and protein folding using the TatABC machinery. For this, the protein provides an N-terminal secretion signal sequence exhibiting two arginine residues. Most Tat-secreted proteins contain redox-active co-factors available only in the cytoplasm e.g. respiratory chain proteins. In contrast to the Sec-pathway, the Tat-machinery is driven solely by proton motive force (Dalbey *et al.*, 2011; Holland, 2004; Natale *et al.*, 2008).

Proteins designated for environmental release like nutrient degrading enzymes and virulence factors are secreted by gram positive bacteria employing the systems presented above. In gram negatives, proteins are secreted either in a two-step process combining the Sec- and Tat-machineries with outer membrane channels, e.g. by secretion systems type II and V, or in one-step processes spanning the whole bacterial envelope, e.g. by secretion systems type I and III (Holland, 2004; Bleves *et al.*, 2010; Filloux, 2011).

1.3.4 Bacterial membrane homeostasis

The barrier function of bacterial membranes depends on the characteristics of their phospholipids which are altered to adapt the cell in response to changing environmental conditions like temperature, osmolarity, salinity, pH or to defend antimicrobial compounds (Zhang and Rock, 2008). Phospholipid adaptation is obtained by linking more/minor unsaturated *cis*-fatty acids or *iso*/*anteiso*-branched fatty acids determining the membrane viscosity to the glycerol backbone. Additionally, the fatty acid side chains of existing phospholipids are modified by introducing *cis*-double bonds by desaturases (Martinez *et al.*, 2010; Zhang and Rock, 2008). These side chains can be further converted into cyclopropane structures employing SAM. Alternatively, some bacteria can transform *cis*-fatty acids irreversible into their *trans*-isomers exhibiting nearly saturated fatty acid characteristics (Zhang and Rock, 2008). By elevating the ratio of unsaturated to saturated fatty acids, membrane fluidity and permeability are increased e.g. in response to decreasing

temperatures. In contrast, high amounts of saturated fatty acids result in a closely packed, highly ordered phospholipid architecture associated with low fluidity and low permeability. In addition to the fatty acid alteration, the phospholipid head group composition is altered to balance the ratio of neutral or zwitterionic phospholipids to anionic ones regulating membrane associated processes (Zhang and Rock, 2008). For several bacteria, the formation of aaPG from PG in response to acidic pH conditions resulting in altered membrane surface charges was described and associated with antibiotic resistance (Roy, 2009).

1.4 Aminoacyl esters of PG: synthesis and impact

PG modification by aminoacylation was first described about 50 years ago (MacFarlane, 1962; Lennarz *et al.*, 1966). Up to now, several organisms containing aaPG molecules were identified (Dare and Ibba, 2012; Roy, 2009) and many of them are associated with eukaryotes as pathogens, symbionts or commensals (Geiger *et al.*, 2010a).

1.4.1 Aminoacylated PG variants

Aminoacylated PG is present in membranes of different bacteria. Most prominent is the utilization of L-lysine for PG modification, followed by L-alanine, but the use of several other amino acids was also observed (Dare and Ibba, 2012; Roy, 2009). The structures of the resulting lysyl-phosphatidylglycerol (L-PG) and alanyl-phosphatidylglycerol (A-PG) are presented in Figure 2.

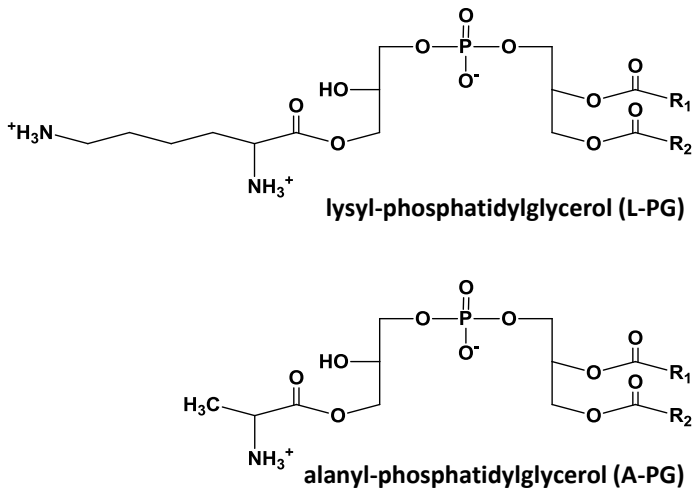

Figure 2: Structures of aminoacylated PG variants
L-PG and A-PG are synthesized by transferring the respective amino acid from its corresponding tRNA to the 3' hydroxyl group of PG (Roy, 2009). Alternatively, the respective amino acid might be coupled to the 2' hydroxyl group (not shown).
R_1 and R_2: fatty acid side chains.

A specific amino acid is transferred by the respective aaPGS from its corresponding tRNA to the 2' or the 3' hydroxyl group of PG (Dare and Ibba, 2012; Klein *et al.*, 2009). The migration of the amino acid moiety between the 2' and the 3' position was observed *in vitro* (Tocanne *et al.*, 1974a). Due to the addition of L-lysine to the anionic PG, the resulting L-PG is carrying a positive net charge resulting in altered membrane surface charge characteristics. In contrast, the utilization of L-alanine yields to the zwitterionic A-PG (Roy, 2009; Klein *et al.*, 2009). Based on *in vitro* experiments it was proposed that the hydrophilic head groups of both L-PG and A-PG do not prefer an elongated conformation. Instead, loop structures resulting from intramolecular salt bridge formation were postulated (Tocanne *et al.*, 1974b; Tocanne *et al.*, 1974c; Sacre *et al.*, 1977). It was assumed that the formation of aaPG molecules (e.g. 6 % A-PG in *P. aeruginosa* and 45 % L-PG in *S. aureus*; Klein *et al.*, 2009; Slavetinsky *et al.*, 2012) allows for the optimal fine-tuning of membrane properties like fluidity and phospholipid head group interaction (Tocanne *et al.*, 1974b; Tocanne *et al.*, 1974c; Sacre *et al.*, 1977; Dare and Ibba, 2012; Roy, 2009).

1.4.2 AaPG synthesizing enzymes

For almost 50 years, not only the existence of aaPG molecules but also the involvement of aminoacylated tRNAs in PG modification had been identified (MacFarlane, 1962; Lennarz *et al.*, 1966). The preparation of the *S. aureus* aaPGS enzyme by solvent extraction had been described (Nesbitt and Lennarz, 1968). In 2001, the *S. aureus* aaPGS (also termed MprF; multiple peptide resistance factor) was reinvestigated due to the observed association to the resistance of *S. aureus* to components of the host innate immune system (Peschel *et al.*, 2001). This was the starting point for the investigation of several other aaPGS enzymes (for review, see Roy, 2009). These investigations resulted in the following model of the domain architecture of aaPGS enzymes and their enzymatic mechanism (Figure 3).

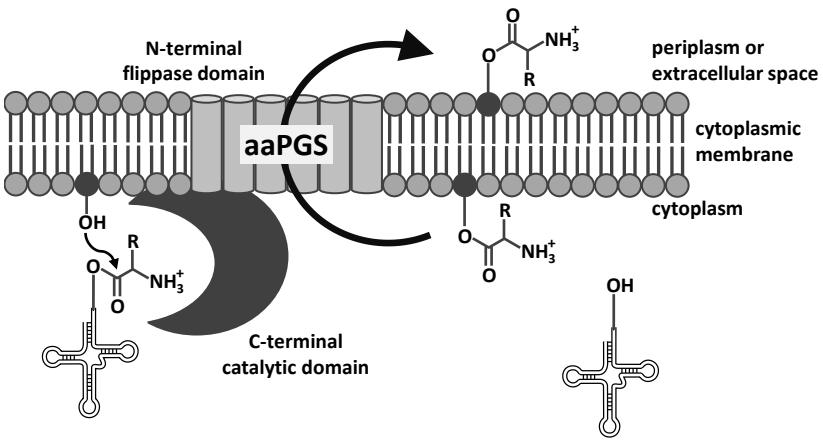

Figure 3: AaPG synthesis mediated by aaPGS enzymes
AaPGS enzymes consist of a highly conserved, cytoplasmic C-terminal domain (dark gray enzyme domain) catalyzing the synthesis of aaPG by transferring an amino acid from its tRNA to a hydroxyl group of the phospholipid PG (dark gray lipid). The hydrophobic N-terminal flippase domain (light gray) consists of a varying number of transmembrane helices and translocates the aaPG across the cytoplasmic membrane (see text for references).
AaPG: aminoacyl-phosphatidylglycerol, aaPGS: aaPG synthase, PG: phosphatidylglycerol, R: amino acid side chain.

AaPGS enzymes provide two domains with different functions and are localized in the cytoplasmic membrane of bacteria (Roy, 2009; Klein *et al.*, 2009; Ernst *et al.*, 2009; Slavetinsky *et al.*, 2012). The highly conserved, cytoplasmic C-terminal domain (Figure 3, dark gray) transfers an amino acid from its tRNA to a hydroxyl group of the phospholipid PG yielding aaPG and the respective tRNA. The key amino acid residues for catalysis were identified within this domain in an extended mutagenesis study of all highly conserved

amino acid residues of the *P. aeruginosa* enzyme (Hebecker *et al.*, 2011). The synthesis of aaPG was observed to be catalyzed by the C-terminal domains of the *P. aeruginosa* A-PGS and the *Clostridium perfringens* lysyl-phosphatidylglycerol synthase (L-PGS) devoid of any N-terminal helices (Hebecker *et al.*, 2011; Roy and Ibba, 2009; Ernst *et al.*, 2009). However, the *S. aureus* C-terminal enzyme domain catalyzes the aminoacylation of PG only in the presence of specific transmembrane helices (Ernst *et al.*, 2009; Slavetinsky *et al.*, 2012).

In an extended study, Hebecker and coworkers elucidated the substrate recognition of the water soluble, C-terminal alanyl-phosphatidylglycerol synthase (A-PGS) domain of *P. aeruginosa* (Hebecker *et al.*, 2011): The PG substrate is recognized by the A-PGS mainly due to its polar head group. In contrast, the architecture of the fatty acid side chains is of minor importance as observed by maintained catalysis even in the absence of one fatty acid. The substrate recognition of the aminoacyl-tRNA substrate was investigated using several aminoacylated tRNA derivatives including alanylated ribonucleic microhelices. The study revealed that only five terminal base pairings of the amino acid acceptor stem are necessary for effective substrate recognition. Instead, the architecture of the tRNA bound amino acid is the determinant for the substrate recognition (Roy and Ibba, 2008b; Hebecker *et al.*, 2011). On the basis of site-directed mutagenesis experiments, an enzymatic mechanism was proposed for the *P. aeruginosa* A-PGS: The nucleophilic hydroxyl group of PG attacks the enzymatically activated ester bond linking the amino acid to the tRNA without the involvement of a covalent enzyme-substrate intermediate (Hebecker *et al.*, 2011).

The second domain of aaPGS enzymes, the hydrophobic N-terminal domain (Figure 3, light gray), consists of 4 to 14 transmembrane helices showing a low level of sequence conservation (Roy, 2009). It was shown that this part of the protein is responsible for the translocation of synthesized aaPG from the inner to the outer leaflet of the cytoplasmic membrane. The *S. aureus* and *C. perfringens* flippase domains exhibit relaxed substrate specificity as indicated by the observed flipping of A-PG and L-PG in the presence of a chimeric aaPGS enzyme (Ernst *et al.*, 2009; Slavetinsky *et al.*, 2012). AaPG translocation is essential for the observed resistance of *S. aureus* to antimicrobial substances (Slavetinsky *et al.*, 2012; Ernst *et al.*, 2009). However, some aaPGS enzymes are devoid of this flippase domain (Roy and Ibba, 2009) and aaPG translocation might be processed by phospholipid flippases with broad substrate spectra (Ernst and Peschel, 2011). Since A-PG was also

detected in the outer membrane of *P. aeruginosa*, an aaPGS independent transfer of A-PG from the outer leaflet of the inner membrane to the inner leaflet of the outer membrane was proposed (Klein *et al.*, 2009).

In most organisms, a single aaPGS homologous gene was identified. However, the gram positive *C. perfringens* provides two homologs identified as an A-PGS and an L-PGS, respectively (Roy and Ibba, 2008b). In contrast, aaPGS enzymes from *B. subtilis*, *Enterococcus faecium* and *Enterococcus faecalis* were identified to accept at least two aminoacyl-tRNA substrates (Roy and Ibba, 2009; Bao *et al.*, 2012). Interestingly, for the *Listeria monocytogenes* L-PGS enzyme, the modification of PG with lysine and in parallel the presence of lysyl-DPG was observed (Thedieck *et al.*, 2006).

1.4.3 AaPG related physiology and antibiotic resistance

AaPG deficient strains of several bacteria did not show a growth phenotype (Peschel *et al.*, 2001; Klein *et al.*, 2009; Thedieck *et al.*, 2006) and the membrane proteome of the *S. aureus* deletion mutant strain was not dramatically altered (Sievers *et al.*, 2010). However, for aaPGS defective strains of *S. aureus*, *M. tuberculosis* and *L. monocytogenes*, a reduced virulence was observed *in vivo* (Peschel *et al.*, 2001; Maloney *et al.*, 2009; Thedieck *et al.*, 2006) and an L-PGS deficient *Rhizobium tropici* strain showed a reduced nodulation efficiency (Vinuesa *et al.*, 2003).

The *S. aureus* L-PGS (also termed MprF) was identified by a screening approach searching for factors mediating the bacterial resistance against antimicrobial peptides of the host innate immune system. L-PGS deficient strains devoid of any L-PG were found significantly more susceptible to cationic defensins, protegrins and other antimicrobial peptides of different origin when compared to the respective control strains (Peschel *et al.*, 2001). Cationic antimicrobial peptides (CAMPs) provide an amphipathic architecture containing positively charged amino acid residues and providing hydrophobic surfaces and they are part of the innate defense mechanisms of various organisms (Zasloff, 2002). They have been proposed to interact with anionic phospholipid head groups, thereby disrupting the membrane integrity and in some cases pore formation followed by membrane depolarization was assumed (Zasloff, 2002; Peschel and Sahl, 2006). During evolution, bacteria established

several mechanisms to cope with CAMPs. One of these mechanisms is the specific aminoacylation of PG (Peschel and Sahl, 2006; Koprivnjak and Peschel, 2011). Based on the results obtained for the L-PGS deficient *S. aureus* strain, the 'charge repulsion' model schematically presented in Figure 4 was proposed by A. Peschel and coworkers as a potential mechanism of L-PG mediated resistance against CAMPs (Peschel *et al.*, 2001).

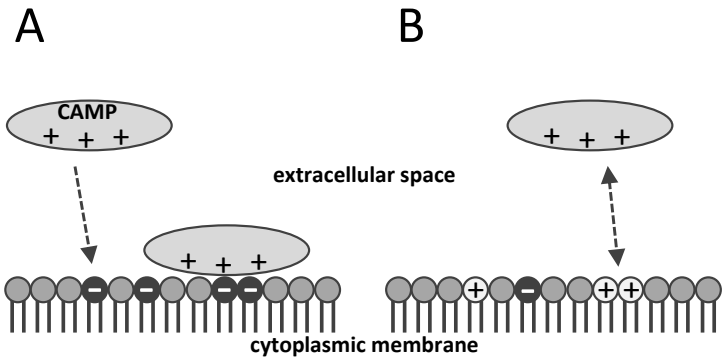

Figure 4: Scheme of the 'charge repulsion' mechanism (according to Peschel *et al.*, 2001)
The proposed 'charge repulsion' model describes the interaction of CAMPs with *S. aureus* membranes in the presence and in the absence of L-PG (Peschel *et al.*, 2001).

A. Positively charged CAMPs interact with negatively charged phospholipid head groups, attach to the membrane surface and disrupt the membrane order.

B. The presence of the cationic phospholipid L-PG prevents the CAMP interaction which results in the CAMP resistance of *S. aureus*.

Dark gray: anionic phospholipids, middle gray: zwitterionic and uncharged phospholipids, light gray: cationic L-PG. CAMP: cationic antimicrobial peptide, L-PG: lysyl-phosphatidylglycerol.

In bacterial strains which provide a negatively charged membrane surface due to anionic phospholipids like PG, positively charged CAMPs interact with the anionic head groups which result in a disordered membrane structure. In contrast, L-PG containing membranes provide a more positively charged surface resulting in the repulsion of CAMPs and leading to the observed CAMP resistance (Peschel *et al.*, 2001). However, recent results indicate a more complex L-PG mediated CAMP or daptomycin resistance mechanism. The anionic lipopeptide antibiotic daptomycin represents a CAMP when it is complexed with calcium ions (Bayer *et al.*, 2013). *In vitro* studies with artificial membranes revealed that CAMP repulsion cannot be correlated directly to the L-PG content of the membrane (Bayer *et al.*, 2013). Other reports emphasize rather a reduced anionic phospholipid content than an increased aaPG level for the observed CAMP resistance in *S. aureus*, *B. subtilis* and *P. aeruginosa* (Mishra *et al.*, 2012a; Hachmann *et al.*, 2011; Conrad and Gilleland, 1981). Furthermore, the substitution of

the cationic L-PG by the zwitterionic A-PG in *S. aureus* membranes resulted in a comparable resistance phenotype. This indicates that a simple repulsion is not sufficient to explain the observed effects further supporting the 'PG reduction' hypothesis (Bayer *et al.*, 2013; Slavetinsky *et al.*, 2012). AaPG formation was also associated with the resistance of different pathogens against daptomycin, oxacillin, methicillin, polymyxins and nisin (Hachmann *et al.*, 2009; Komatsuzawa *et al.*, 2001; Nishi *et al.*, 2004; Bao *et al.*, 2012; Jones *et al.*, 2008). Moreover, A-PG production was related to the increased resistance of *P. aeruginosa* against the CAMP protamine, the β-lactam cefsulodin, the heavy metal ion chromium(III) and osmotic stress conditions induced by lactate (Klein *et al.*, 2009). Especially in the context of *P. aeruginosa* containing up to 6 % A-PG, both postulated CAMP resistance mechanisms ('charge repulsion' and 'PG reduction') do not explain the observed resistance phenotypes. Membrane permeability and fluidity alterations or an influence of A-PG on membrane protein function and activity are also discussed in the literature (Klein *et al.*, 2009; Roy *et al.*, 2009). Furthermore, the consequences of parallel synthesis of different aaPGs described for several bacteria have not been elucidated in detail. Although the synthesis of A-PG in an L-PG deficient *S. aureus* strain resulted in comparable daptomycin resistance phenotypes (Slavetinsky *et al.*, 2012), it is not clear if this is also the case for bacteria synthesizing low amounts of aaPG or for gram negative bacteria showing a completely different cell envelope architecture.

1.4.4 Regulation of aaPG synthesis

For several aaPGS synthesizing bacteria like *S. aureus* and *P. aeruginosa*, increased aaPG amounts were detected under acidic conditions while the growth of the respective aaPGS defective strains was not affected (Houtsmuller and van Deenen, 1965; Klein *et al.*, 2009; Sohlenkamp *et al.*, 2007; Vinuesa *et al.*, 2003; op den Kamp *et al.*, 1969; Minnikin and Abdolrahimzadeh, 1974). In contrast, a transposon mutagenesis study identified an aaPGS homolog essential for the growth of *R. tropici* in acidic environments (Vinuesa *et al.*, 2003). Promoter sequences located upstream of the aaPGS encoding genes of *P. aeruginosa* and *R. tropici* were identified and the upregulation of the aaPG synthesis under acidic growth conditions was demonstrated (Klein *et al.*, 2009; Vinuesa *et al.*, 2003). To date, the underlying regulatory system has not been characterized.

In *S. aureus*, the GraRS two component system sensing specific antimicrobial peptides was identified to increase the expression of the L-PGS. However, this system only responds to very specific compounds and has not the ability to sense antimicrobial peptides in general (Yang *et al.*, 2012). In *L. monocytogenes*, the expression of the L-PGS is regulated by the VirSR two component system for which the induction of cell envelope stress response genes was demonstrated. However, the signal that activates the VirSR system has not been identified (Roy, 2009).

The extracytoplasmic functioning sigma factor σ^{22} of *P. aeruginosa* regulates the expression of various genes in response to cell wall stresses and controls the synthesis of alginate in mucoid strains associated with lung infections. The A-PGS was identified as a component of the σ^{22} regulon and it was further demonstrated that the stress response system was also affected in A-PGS defective strains. In this context, an essential role of A-PG was concluded. However, the molecular details are not resolved yet (Wood and Ohman, 2012).

1.4.5 AaPGS enzymes are encoded in a potential operon in gram negative bacteria

In many aaPG synthesizing gram negatives, the aaPGS encoding gene is located upstream of a second gene. In *P. aeruginosa*, the respective orf PA0919 is separated from the A-PGS encoding orf PA0920 by one single base pair. PA0919 homologous genes like *acvB* of *Agrobacterium tumefaciens* and *atvA* (acid tolerance and virulence) of *R. tropici* were previously detected (Vinuesa *et al.*, 2003). First, *acvB* was identified by a transposon mutagenesis study screening for virulence defective *A. tumefaciens* strains (Wirawan *et al.*, 1993). Further investigation also revealed the VirJ protein in *A. tumefaciens* which is highly homologous to the AcvB protein (Pan *et al.*, 1995). Cellular fractionation analysis identified AcvB and VirJ in the periplasm of *A. tumefaciens* (Kang *et al.*, 1994; Pan *et al.*, 1995). Due to the affected virulence it was proposed that AcvB/VirJ is a periplasmic component of the *A. tumefaciens* type IV secretion system (Pantoja *et al.*, 2002).

Vinuesa and coworkers identified that AcvB of *A. tumefaciens* and AtvA of *R. tropici* are relevant for bacterial growth under acidic conditions (Vinuesa *et al.*, 2003). Bioinformatic analyses revealed a serine containing lipase active site sequence motif (LIPASE_SER motif) within the sequence of the *R. tropici* AtvA. The substitution of the specific active site serine

to alanine resulted in an acid sensitive phenotype indicating the relevance of this specific serine for the function of AtvA. Due to the obtained results it was proposed that AtvA might be a member of an as yet unidentified class of lipolytic enzymes (Vinuesa *et al.*, 2003). It was speculated that high L-PG amounts might not be detectable in *R. tropici* due to the proposed lipolytic function of AtvA (Sohlenkamp *et al.*, 2007). However, up to now the characterization of an AcvB/AtvA homolog has not been reported.

1.5 Aim of this study

Under various stress conditions several pathogenic bacteria have the ability to modify the phospholipid PG mainly with lysine or alanine yielding the cationic L-PG or the zwitterionic A-PG. This reaction is mediated by aaPGS enzymes showing different aminoacyl-tRNA specificities (Ernst and Peschel, 2011). AaPGS deficient strains exhibited an increased susceptibility to host innate immune system components and to several antibiotics. Therefore, the inhibition of aaPGS enzymes was proposed as a promising strategy to treat bacterial infections (Ernst and Peschel, 2011). The first part of this study is dealing with the identification of the aminoacyl-tRNA substrate specificity of several as yet uncharacterized aaPGS enzymes. These results will then allow for the characterization of potential determinants of the aminoacyl-tRNA substrate specificity and also for the analysis of the evolutionary origin of A-PG and L-PG synthesis.

To date, it is not clear if L-PG and A-PG synthesis results in comparable resistance phenotypes as indicated by results obtained for the gram positive model organism *S. aureus* (Slavetinsky *et al.*, 2012) or if these molecules result in different physiological consequences possibly depending on the respective host. To address this question, an A-PGS deficient mutant strain of the gram negative model organism *P. aeruginosa* had to be complemented with various aaPGS enzymes to generate strains with artificially altered membrane composition. The obtained strains had to be characterized phenotypically to figure out the specific impact of the respective aaPG in the *P. aeruginosa* model system. Furthermore, the response of the A-PGS promoter to several antimicrobial compounds had to be investigated to analyze the A-PG homeostasis under antimicrobial stress conditions.

AaPGS enzymes are encoded in combination with a second protein with a proposed lipolytic function in gram negative bacteria (Vinuesa *et al.*, 2003). In *P. aeruginosa*, this protein is encoded by orf PA0919 whose function had to be elucidated in the present study. For this, a PA0919 deficient mutant had to be constructed and to be characterized with respect to growth phenotype, lipid composition and susceptibility to antimicrobials. Furthermore, the protein had to be analyzed biochemically after recombinant production and purification concerning its substrate specificity. Therefore, an appropriate *in vitro* activity assay had to be developed. Besides this, the cellular localization of the PA0919 protein in *P. aeruginosa* had to be elucidated.

2 Materials and methods

2.1 Materials

Instruments, chemicals, bacterial strains, plasmids and oligodeoxynucleotides employed in this study are summarized in the following sections.

2.1.1 Instruments

Instruments used in this study are summarized in Table 1.

Table 1: Instruments

Instrument	Model	Manufacturer
agarose gel electrophoresis chamber	Agagel	Biometra
agarose gel documentation	DeVision G system	Decon Science Tec
autoclave	LVSA 50/70	Zirbus
blotting apparatus	Trans-Blot® SD system	Bio-Rad
	Trans-Blot® Turbo™ system	Bio-Rad
centrifuge	Avanti® J-E	Beckman Coulter
	Megafuge	Heraeus®
	Minispin®	Eppendorf
	Optima™ L-90K ultracentrifuge with rotors SW 40 Ti or 70.1 Ti	Beckman Coulter
cell disruptor	FastPrep®	MP Biomedicals
fluorescence spectrometer	LS50B	PerkinElmer
FPLC	ÄKTApurifier™	GE Healthcare
French® Press	French® Pressure Cell Press	Polytec
French® Press cell	French® Pressure Cell	SLM Aminco
lyophilization	Lyovac GT2	Finn-Aqua
magnetic stirrer	KM02 basic	IKA Werke
microplate incubator	OmniLog®	Biology
	PHMP-4	Grant bio
microplate reader	Model 680	Bio-Rad
photometer	NanoDrop	PEQLAB Biotechnologie
	Ultrospec 2000	Amersham Pharmacia
	Ultrospec 2100pro	Amersham Pharmacia
pH determination	CG 842	Schott
pipettes	0.5 – 10 µL Reference	Eppendorf
	2 – 20 µL Reference	Eppendorf
	10 – 100 µL Reference	Eppendorf
	50 – 200 µL Reference	Eppendorf
	100 – 1000 µL Reference	Eppendorf
	LAB-Mate 10 mL	ABI Med
	20 – 200 µL Transferpette®-8	Brand

Instrument	Model	Manufacturer
power supply	PowerPac300	Bio-Rad
SDS-PAGE	Mini-Protean III™	Bio-Rad
shaker	3020	GFL
	TR-150	Infors
scintillation counter	Tri-Carb® 2900TR	PerkinElmer
thermocycler	Tpersonal	Biometra
	C1000™ Thermal Cycler	Bio-Rad
thermomixer	Thermomixer compact	Eppendorf
UV-Vis spectrometer	V-650	Jasco
vortex	REAX2000	Heidolph
water purification	Milli-Q system	Millipore
X-ray film processor	Optimax®	Protec®

2.1.2 Chemicals, enzymes and appliance

Chemicals and enzymes used in this study are summarized in Table 2. Unspecified chemicals were obtained from Fluka, Roth, Riedel-de Haen, Roche and Sigma-Aldrich (quality grade p.a.). Kits and appliances are indicated in Table 3.

Table 2: Chemicals and enzymes

Application	Product	Manufacturer
antibodies and accessory	5-bromo-4-chloro-3-indolyl phosphate (BCIP)	Sigma-Aldrich
	nitrotetrazolium blue (NBT)	Sigma-Aldrich
	Strep-Tactin® AP conjugate	IBA
antimicrobial compounds employed for susceptibility tests	ampicillin	Roth
	benzethonium chloride	Sigma-Aldrich
	cefsulodin	Sigma-Aldrich
	daptomycin	Novartis
	domiphen bromide	Sigma-Aldrich
	methicillin	Sigma-Aldrich
	nisin	Sigma-Aldrich
	oxacillin	Sigma-Aldrich
	poly-L-lysine	Sigma-Aldrich
	polymyxin B	Sigma-Aldrich
	polymyxin E	Sigma-Aldrich
	protamine sulfate	Sigma-Aldrich
	vancomycin	Roth
^{14}C-labeled compounds	[1-^{14}C]-L-alanine	Moravec Biochemicals
	[U-^{14}C]-L-lysine	Moravec Biochemicals
chemicals	adenosine triphosphate (ATP)	Sigma-Aldrich
	L-alanine	Sigma-Aldrich
	avidin	Calbiochem®
	bovine serume albumin	Roth
	Bradford reagent	Sigma-Aldrich

Application	Product	Manufacturer
chemicals (continued)	cOmplete protease inhibitor cocktail	Roche
	creatine phosphate	Sigma-Aldrich
	desthiobiotin	IBA
	deoxynucleotide triphosphate (dNTP) mix	New England Biolabs
	GelStar™ Nucleic Acid Gel Stain	Lonza
	isopropyl-β-D-thiogalactopyranoside (IPTG)	GERBU
	molybdatophosphoric acid	Roth
	ninhydrin spray solution	Merck
	OptiPhase HighSafe 2	PerkinElmer
	PBS-Tween® tablets	Medicago
	phenylmethylsulfonyl fluoride (PMSF)	Sigma-Aldrich
	Redox Dye Mix A	Biolog
	Strep-tag® regeneration buffer	IBA
	N_{α}-tosyl-L-lysine chloromethyl ketone (TLCK)	Sigma-Aldrich
chromogenic compounds	Ala-ONp	Bachem
	Gly-ONp	Bachem
	Ac-Gly-ONp	Bachem
	Boc-Ala-ONp	Bachem
	Ala-pNA	Bachem
	4-nitrophenol butyrate	Sigma-Aldrich
	4-nitrophenol acetate	Sigma-Aldrich
	4-nitrophenol phosphate	Sigma-Aldrich
	2-nitrophenyl-β-D-galactopyranoside (ONPG)	Roth
enzymes	creatine phosphate kinase	Sigma-Aldrich
	DNase I, RNase free	ambion®
	lysozyme (from chicken egg white)	Fluka
	Phusion® High-Fidelity DNA-Polymerase	Thermo Fisher Scientific
	restriction endonucleases	New England Biolabs
	RNase A	Invitrogen
	Taq DNA Polymerase	New England Biolabs
	T4 DNA Ligase	New England Biolabs
media components	Bacto™ Proteose Peptone no. 3	BD
	Bacto™ Tryptone	BD
	Bacto™ Soytone	BD
	Casamino acids	Roth
	IF-0 medium	Biolog
	IF-10a medium	Biolog
markers	GeneRuler™ DNA Ladder Mix	Thermo Fisher Scientific
	RNA Molecular Weight Marker I, DIG-labeled, 0.3 – 6.9 kb	Roche
	PageRuler™ Prestained Protein Ladder	Thermo Fisher Scientific
	Unstained Protein Molecular Weight Marker	Thermo Fisher Scientific

Table 3: Kits and appliances

Application	Product	Manufacturer
kits	QIAquick PCR Purification Kit	Qiagen
	QIAquick Gel Extraction Kit	Qiagen
	QuikChange® II Site-Directed Mutagenesis Kit	Stratagene
microplate appliance	gas permeable membrane (Breath-Easy™ sealing membrane)	Diversified Biotech
	microplates, 96-well flat bottom (No. 82.1581.001)	Sarstedt
	Phenotype MicroArray™ plates PM9 – PM20	Biolog
protein purification	Amicon® Ultra-0.5 device	Merck
	dialysis tubing membrane visking (molecular weight cutoff: 14 kDa)	Roth
	Poly-Prep chromatography columns (0.8 x 4 cm)	BioRad
	Protino® Ni-NTA agarose	Macherey-Nagel
	Strep-Tactin® Superflow® high capacity resin	IBA
	Superdex 200 5/150 GL column	GE Healthcare
radioactivity analysis	exposure cassette K 20 – 25 cm	Bio-Rad
	scintillation vials (PE-LD), 20 mL	A. Hartenstein
	X-ray film Fuji Super RX	BEMA
others	pH indicator test stripes (pH Fix 2.0 – 9.0 and 4.5 – 10.0)	Macherey-Nagel
	PVDF membrane, pore size 0.45 µm	Millipore, Merck
	sterile filters (Ø 0.2 µm)	Sarstedt
	thin-layer chromatography plates (Alugram®SIL G/UV254)	Macherey-Nagel

2.1.3 Strains and plasmids

Table 4 lists the bacterial strains used in this study and Table 5 summarizes the employed plasmids.

Table 4: Bacterial strains

Strain	Genotype	Reference
Escherichia coli		
BL21 (λDE3)	B F$^-$ *dcm ompT hsdS*(r_B^- m_B^-) *gal* λ(DE3)	Stratagene Studier *et al.*, 1990
DH10B	F$^-$ *mcrA* Δ(*mrr-hsdRMS-mcrBC*) Δ*lacX74* Φ80*lacZ*ΔM15 *recA1 endA1 ara*Δ139 Δ(*ara-leu*)7697 *galU galK* λ$^-$ *rpsL nupG* (Str^r)	Invitrogen Grant *et al.*, 1990
Rosetta^{TM}(λDE3)pLys	F$^-$ *ompT hsdS*$_B$(r_B^- m_B^-) *gal dcm* (DE3) pLysSRARE (Cm^r)	Novagen®
TOP10	F$^-$ *mcrA* Δ(*mrr-hsdRMS-mcrBC*) Δ*lacX74* Φ80*lacZ*ΔM15 *recA1 ara*Δ139 Δ(*ara-leu*)7697 *galU galK rpsL endA1 nupG* (Str^r)	Invitrogen
ST18	S17 λ-pir Δ*hemA*	Thoma and Schobert, 2009
***Pseudomonas aeruginosa* PAO1 and MPAO1 derivatives**		
PAO1	wild-type	Stover *et al.*, 2000
PAO1 ΔPA0920	markerless deletion mutant of orf PA0920 from *P. aeruginosa* PAO1	Lorenzo, 2006 Klein *et al.*, 2009
PAO1 ΔSa_{comp}	PAO1 ΔPA0920 *attB*::(P_{PA0920}-SamprF-t_{rrnB}); complementation of PAO1 ΔPA0920 by the integration of the *mprF* gene (Sa113) from *S. aureus* NCTC 8352, controlled by the P_{PA0920} promoter, into the *attB* site	this work
PAO1 ΔBs_{comp}	PAO1 ΔPA0920 *attB*::(P_{PA0920}-BsmprF-t_{rrnB}); complementation of PAO1 ΔPA0920 by the integration of the *mprF* gene (BSU08425) from *B. subtilis* subsp. *subtilis* str. 168, controlled by the P_{PA0920} promoter, into the *attB* site	this work
PAO1 ΔEf_{comp}	PAO1 ΔPA0920 *attB*::(P_{PA0920}-EfmprF-t_{rrnB}); complementation of PAO1 ΔPA0920 by the integration of the *aaPGS2* gene (gi:69249189) from *E. faecium* DO, controlled by the P_{PA0920} promoter, into the *attB* site	this work

Strain	Genotype	Reference
PAO1 ΔPa_{comp}	PAO1 ΔPA0920 *attB*::(P_{PA0920}-PA0920-t_{rrnB}); complementation of PAO1 ΔPA0920 by the integration of orf PA0920 from *P. aeruginosa* PAO1, controlled by the P_{PA0920} promoter, into the *attB* site	this work
PAO1 ΔPa-aa543-881_{comp}	PAO1 ΔPA0920 *attB*::(P_{PA0920}-PA0920-aa543-881-t_{rrnB}); complementation of PAO1 ΔPA0920 by the integration of the coding sequence for amino acids 543 – 881 of orf PA0920 from *P. aeruginosa* PAO1, controlled by the P_{PA0920} promoter, into the *attB* site	this work
PAO1 ΔPA0919	markerless deletion mutant of orf PA0919 from *P. aeruginosa* PAO1	Groenewold, 2011
PAO1 ΔPA0919/P_{PA0919}-PA0919-T (Δ19 P_{19}-19)	PAO1 ΔPA0919 *attB*::(P_{PA0919}-PA0919-t_{rrnB}); complementation of PAO1 ΔPA0919 by the integration of orf PA0919 from *P. aeruginosa* PAO1, controlled by the P_{PA0919} promoter, into the *attB* site	this work
PAO1 ΔPA0919/P_{PA0920}-PA0919-T (Δ19 P_{20}-19)	PAO1 ΔPA0919 *attB*::(P_{PA0920}-PA0919-t_{rrnB}); complementation of PAO1 ΔPA0919 by the integration of orf PA0919 from *P. aeruginosa* PAO1, controlled by the P_{PA0920} promoter, into the *attB* site	this work
PAO1 ΔPA0919/P_{PA0919}-T (Δ19 P_{19})	PAO1 ΔPA0919 *attB*::(P_{PA0919}-t_{rrnB}); derivative of PAO1 ΔPA0919 containing the P_{PA0919} promoter within the *attB* site	this work
PAO1 ΔPA0919/P_{PA0920}-T (Δ19 P_{20})	PAO1 ΔPA0919 *attB*::(P_{PA0920}-t_{rrnB}); derivative of PAO1 ΔPA0919 containing the P_{PA0920} promoter within the *attB* site	this work
PAO1 ΔPA0919/P_{PA0919}-PA0919-Strep-T (Δ19 19)	PAO1 ΔPA0919 *attB*::(P_{PA0919}-PA0919-Strep-t_{rrnB}); complementation of PAO1 ΔPA0919 by the integration of orf PA0919 from *P. aeruginosa* PAO1, C-terminally fused to a *Strep*-tag II coding sequence, controlled by the P_{PA0919} promoter, into the *attB* site	this work
PAO1 ΔPA0919/P_{PA0919}-PA0919-Δaa1-34-Strep-T (Δ19 $19_{35\text{-}427}$)	PAO1 ΔPA0919 *attB*::(P_{PA0919}-PA0919-Δaa1-34-Strep-t_{rrnB}); complementation of PAO1 ΔPA0919 by the integration of the coding sequence for amino acids 35 – 427 of orf PA0919 from *P. aeruginosa* PAO1, C-terminally fused to a *Strep*-tag II coding sequence, controlled by the P_{PA0919} promoter, into the *attB* site	this work
PAO1 ΔPA0919 pUCP20T (Δ19 pUC)	PAO1 ΔPA0919 containing the empty pUCP20T vector, Cb^r	this work

Strain	Genotype	Reference
PAO1 ΔPA0919 pUCP20T/P_{PA0919}-PA0919-Strep (Δ19 pUC/19)	PAO1 ΔPA0919 containing vector pUCP20T/P_{PA0919}-PA0919-Strep, Cb^r; complementation of PAO1 ΔPA0919 by the pUCP20T-encoded orf PA0919 from *P. aeruginosa* PAO1, C-terminally fused to a *Strep*-tag II coding sequence, controlled by the P_{PA0919} promoter	this work
PAO1 ΔPA0919 pUCP20T/P_{PA0919}-PA0919-Δaa1-34-Strep (Δ19 pUC/19_{35-427})	PAO1 ΔPA0919 containing vector pUCP20T/P_{PA0919}-PA0919-Δaa1-34-Strep, Cb^r; complementation of PAO1 ΔPA0919 by the pUCP20T-encoded coding sequence for amino acids 35 – 427 of orf PA0919 from *P. aeruginosa* PAO1, C-terminally fused to a *Strep*-tag II coding sequence, controlled by the P_{PA0919} promoter	this work
PAO1 KS11	PAO1 *attB*::(mini-CTX2-*lacZ*); PAO1 containing the *lacZ* reporter gene without any promoter in the *attB* site	Schreiber *et al.*, 2006
PAO1-P_{PA0920}-*lacZ*	PAO1 *attB*::(P_{PA0920}-*lacZ*); PAO1 containing the P_{PA0920} promoter fragment fused to the *lacZ* reporter gene in the *attB* site	Klein *et al.*, 2009 Spier, 2007
PAO1 P_{PA0919}-*430-lacZ*	PAO1 *attB*::(P_{PA0919}-*430-lacZ*); PAO1 containing a 430 bp P_{PA0919} promoter fragment fused to the *lacZ* reporter gene in the *attB* site	this work
PAO1 P_{PA0919}-*206-lacZ*	PAO1 *attB*::(P_{PA0919}-*206-lacZ*); PAO1 containing a 206 bp P_{PA0919} promoter fragment fused to the *lacZ* reporter gene in the *attB* site	this work
PAO1 P_{PA0919}-*140-lacZ*	PAO1 *attB*::(P_{PA0919}-*140-lacZ*); PAO1 containing a 140 bp P_{PA0919} promoter fragment fused to the *lacZ* reporter gene in the *attB* site	this work
MPAO1	wild-type	Jacobs *et al.*, 2003
MPAO1 17368	mutant of MPAO1 with transposon IS*lacZ*/hah inserted at base position 711 of orf PA0919	Jacobs *et al.*, 2003
MPAO1 53595	mutant of MPAO1 with transposon IS*phoA*/hah inserted at base position 532 of orf PA0919	Jacobs *et al.*, 2003
Others		
Bacillus licheniformis ATCC 14580	wild-type (DSM 13)	Veith *et al.*, 2004
Bacillus thuringiensis serovar Berliner ATCC 10792	wild-type (DSM 2046)	German Collection of Microorganisms and Cell Cultures (DSMZ)
Bacillus subtilis subsp. *subtilis* str. 168	wild-type	Kunst *et al.*, 1997

Strain	Genotype	Reference
Burkholderia phymatum STM 815	wild-type (DSM 17167)	DSMZ
Kineococcus radiotolerans SRS 30216	wild-type (DSM 14245)	Bagwell *et al.*, 2008 Phillips *et al.*, 2002
Methanosarcina barkeri str. Fusaro ATCC 29787	wild-type	Maeder *et al.*, 2006
Paenibacillus polymyxa ATCC 842	wild-type (DSM 36)	Jeong *et al.*, 2011
Pseudomonas aeruginosa UCBPP-PA14	wild-type	Lee *et al.*, 2006
Pseudomonas putida KT2440	wild-type	Nelson *et al.*, 2002
Streptococcus salivarius subsp. *thermophilus* ATCC 19258	wild-type (DSM 20617)	DSMZ

Table 5: Plasmids

Insert sequences introduced into the respective vector were verified by sequencing.

Plasmid	Description	Reference
pBAD-His-A	*E. coli* recombinant protein production vector, L(+)-arabinose-inducible expression system, N-terminal His_6-tag, Ap^r	Invitrogen
pBAD-His-A/A2435	pBAD-His-A containing orf Mbar_A2435 from *M. barkeri* ATCC 29787 cloned into *XhoI* site, Ap^r	S. Hebecker, unpublished
pBAD-His-A/Bp4019	pBAD-His-A containing orf Bphy_4019 from *B. phymatum* STM 815 cloned into *XhoI*/*HindIII* site, Ap^r	this work
pBAD-His-A/Bthur0008_13400	pBAD-His-A containing orf Bthur0008_13400 from *B. thuringiensis* ATCC 10792 cloned into *XhoI*/*KpnI* site, Ap^r	this work
pBAD-His-A/Krad4555	pBAD-His-A containing orf Krad_4555 from *K. radiotolerans* SRS 30216 cloned into *SacI*/*HindIII* site, Ap^r	S. Hebecker, unpublished
pBAD-His-A/Ppoly_aaPGS	pBAD-His-A containing aaPGS coding sequence from *P. polymyxa* ATCC 842 cloned into *SacI*/*KpnI* site, Ap^r	this work
pGEX-6P-1	*E. coli* recombinant protein production vector, P_{tac} promoter, N-terminal GST-tag, PreScission protease specific cleavage site, Ap^r	GE Healthcare
pGEX-6P-1/StMprFΔaa1-503	pGEX-6P-1 containing coding sequence of amino acids 504 – 851 of *S. thermophilus* ATCC 19258 aaPGS, cloned into *BamHI*/*XhoI* site, Ap^r	Jäger, 2011
pGEX-6P-1/YfiXΔaa1-518	pGEX-6P-1 containing coding sequence of amino acids 519 – 850 of *B. licheniformis* ATCC 14580 YfiX, cloned into *BamHI*/*XhoI* site, Ap^r	Jäger, 2011
mini-CTX2	chromosomal integration vector for *P. aeruginosa*, Tet^r	Hoang *et al.*, 2000

Plasmid	Description	Reference
mini-CTX2-PTC	mini-CTX2 containing the promoter-terminator-construct (PTC) fragment: native P_{PA0920} promoter (187 bp) followed by a linker (containing *SphI* and *BamHI* sites) and the *rrnB* terminator sequence (158 bp; Invitrogen) cloned into *SacI*/*HindIII* site, Tet^r	this work
mini-CTX2-P-SamprF-T	mini-CTX2-PTC vector containing *mprF* (Sa113) from *S. aureus* NCTC 8325 cloned into *SphI*/*BamHI* site, Tet^r	this work
mini-CTX2-P-BsmprF-T	mini-CTX2-PTC vector containing *mprF* (BSU08425) from *B. subtilis* subsp. *subtilis* str. 168 cloned into *SphI*/*BamHI* site, Tet^r	this work
mini-CTX2-P-EfmprF-T	mini-CTX2-PTC vector containing aaPGS2 coding sequence (gi:69249189) from *E. faecium* DO cloned into *SphI*/*BamHI* site, Tet^r	this work
mini-CTX2-P-PA0920-T	mini-CTX2-PTC vector containing orf PA0920 (A-PGS) from *P. aeruginosa* PAO1 cloned into *SphI*/*BamHI* site, Tet^r	this work
mini-CTX2-P-PA0920-aa543-881-T	mini-CTX2-PTC vector containing sequence encoding A-PGS amino acids 543 – 881 (PA0920 C-terminal domain) from *P. aeruginosa* PAO1 cloned into *SphI*/*BamHI* site, Tet^r	this work
mini-CTX2-P_{PA0920}-PA0919-T	mini-CTX2-PTC derivative containing the native P_{PA0920} promoter (187 bp upstream of orf PA0920) followed by orf PA0919, inserted into *SacI*/*BamHI* site, Tet^r	this work
mini-CTX2-P_{PA0919}-PA0919-T	mini-CTX2-PTC derivative containing the native P_{PA0919} promoter (430 bp upstream of orf PA0919) followed by orf PA0919, inserted into *SacI*/*BamHI* site, Tet^r	this work
mini-CTX2-P_{PA0919}-T	mini-CTX2-PTC derivative containing the native P_{PA0919} promoter (430 bp upstream of orf PA0919) inserted into *SacI*/*BamHI* site, Tet^r	this work
mini-CTX2-P_{PA0919}-PA0919-Strep-T	mini-CTX2-PTC derivative containing the native P_{PA0919} promoter (430 bp upstream of orf PA0919) followed by orf PA0919, fused to a *Strep*-tag II coding sequence, inserted into *SacI*/*BamHI* site, Tet^r	this work
mini-CTX2-P_{PA0919}-PA0919-Δaa1-34-Strep-T	mini-CTX2-P_{PA0919}-PA0919-Strep-T derivative, PA0919 secretion signal sequence (amino acids 1 – 34) removed, inserted into *SacI*/*BamHI* site, Tet^r	this work
pUCP20T	*E. coli – P. aeruginosa* shuttle vector, Cb^r	Schweizer *et al.*, 1996
pUCP20T/P_{PA0919}-PA0919-Strep	pUCP20T derivative containing the native P_{PA0919} promoter (430 bp upstream of orf PA0919) followed by orf PA0919, fused to a *Strep*-tag II coding sequence, inserted into *KpnI*/*BamHI* site, Cb^r	this work

Plasmid	Description	Reference
pUCP20T/P_{PA0919}-PA0919-Δaa1-34-Strep	pUCP20T/P_{PA0919}-PA0919-Strep derivative, PA0919 secretion signal sequence (amino acids 1 – 34) removed, inserted into *KpnI*/*BamHI* site, Cb^r	this work
mini-CTX-*lacZ*	chromosomal integration vector for *P. aeruginosa* carrying a promoter-less *lacZ,* Tet^r	Becher and Schweizer, 2000
mini-CTX-P_{PA0919}-*430-lacZ*	mini-CTX-*lacZ* derivative containing the 430 bp P_{PA0919} promoter fragment upstream of orf PA0919 inserted into *KpnI*/*BamHI* site, Tet^r	this work
mini-CTX-P_{PA0919}-*206-lacZ*	mini-CTX-*lacZ* derivative containing the 206 bp P_{PA0919} promoter fragment upstream of orf PA0919 inserted into *KpnI*/*BamHI* site, Tet^r	this work
mini-CTX-P_{PA0919}-*140-lacZ*	mini-CTX-*lacZ* derivative containing the 140 bp P_{PA0919} promoter fragment upstream of orf PA0919 inserted into *KpnI*/*BamHI* site, Tet^r	this work
pPS858	source of gentamicin resistance cassette, Ap^r, Gm^r	Hoang *et al.*, 1998
pEX18Ap	gene replacement vector with multiple cloning site from pUC18, $oriT^+$, $sacB^+$, Ap^r	Hoang *et al.*, 1998
pEX18Ap/ΔPA0919	pEX18Ap derivative with 438 bp upstream sequence of orf PA0919, gentamicin resistance cassette of pPS858 (flanked by *BamHI* sites) and 673 bp downstream of orf PA0919, inserted into *KpnI*/*HindIII* site, Ap^r, Gm^r	Groenewold, 2011
pFLP2	source of FLP recombinase, Ap^r	Hoang *et al.*, 1998
pET22b(+)	vector for recombinant protein production in *E. coli*, provides a T7 promoter, a PelB secretion signal sequence and a C-terminal His_6-tag, Ap^r	Merck
pET22b(+)/BAS1375Δaa1-527	pET22b(+) derivative encoding for amino acids 528 – 861 of *B. anthracis* BAS1375, sequence optimized for *E. coli* coding usage, cloned into *NdeI*/*XhoI* site, Ap^r	Jäger, 2011
pET22b(+)PA0919	pET22b(+) derivative encoding for amino acids 35 – 427 of orf PA0919 from *P. aeruginosa*, cloned into *NcoI*/*HindIII* site, employed for expression of PA0919 fused to PelB sequence (N-terminal) and His_6-tag (C-terminal), Ap^r	this work
pET22b(+)Strep	pET22b(+) derivative providing a C-terminal *Strep*-tag II, cloned into *HindIII*/*XhoI* site, Ap^r	T. Nicke, unpublished
pET22b(+)PA0919-Strep	pET22b(+)Strep derivative encoding amino acids 35 – 427 of orf PA0919 from *P. aeruginosa*, cloned into *NcoI*/*HindIII* site, employed for expression of PA0919 fused to PelB sequence (N-terminal) and *Strep*-tag II (C-terminal), Ap^r	this work
pET22b(+)PA0919-S240A-Strep	pET22b(+)PA0919-Strep derivative, amino acid serine 240 changed to alanine, Ap^r	this work
pET22b(+)PA0919-S307A-Strep	pET22b(+)PA0919-Strep derivative, amino acid serine 307 changed to alanine, Ap^r	this work

Plasmid	Description	Reference
pET22b(+)PA0919-H401A-Strep	pET22b(+)PA0919-Strep derivative, amino acid histidine 401 changed to alanine, Ap^r	this work
pET28b(+)PA0903	*E. coli* expression vector pET22b(+) carrying orf PA0903 (*P. aeruginosa* alanyl-tRNA synthetase) cloned into *NdeI*/*BamHI* site, T7 promoter, N-terminal His_6-tag, Kan^r	Hebecker *et al.*, 2011

2.1.4 Oligodeoxynucleotides

Oligodeoxynucleotides employed for cloning are summarized in Table 6, whereas oligodeoxynucleotides used for sequencing purposes are listed in Table 7.

Table 6: Oligodeoxynucleotides for cloning purposes
Restriction sites are indicated by bold letters, nucleotides inserted for reading frame compliance are highlighted gray. Specifically indicated primers were taken from: [1] Jäger, 2011; [2] Groenewold, 2011; [3] T. Nicke, unpublished.
Promoter-terminator construct restriction sites are indicated in bold letters (*SacI*, *SphI*, *BamHI*, *HindIII*; in the given order). Promoter (between *SacI* and *SphI*) and terminator (between *BamHI* and *HindIII*) sequences are italicized and separated by a linker sequence (between *SphI* and *BamHI*).

No.	Name	Sequence (5'-3')
1	Bp4019XhoIfw	GATA**CTCGAG**ATGTCTGACCATCCCCGCTC
2	Bp4019HindIIIrv	TCGTAT**AAGCTT**TCATGAACGCCGGCCCCCTG
3	BthuXhoIfw	CCAGTA**CTCGAG**ATGTCGTTTTCATGG
4	BthuKpnIrv	CGTTGA**GGTACC**CTAAGAATTTAGCTG
5	4555KrSacIfw	GATA**GAGCTC**GTGCTCGGTGACCGGATCCTC
6	4555KrHindIIIrv	TCGTAT**AAGCTT**TCAGCTGTGGACGACCCCGC
7	Mbar2435XhoIfw	GCTAT**CTCGAG**ATGACAGACAAAGGAAG
8	Mbar2435XhoIrv	GCTAT**CTCGAG**TCAGGTGAGTTCTTCGG
9	Paeni1SacIfw	GGAGGT**GAGCTC**ATGAAWTCWAATCACAAACCG
10	Paeni1KpnIrv	GGTTGT**GGTACC**TTAGTCCGAGCGTTTGG
11[1]	BaNdeI22fw	GCGC**CATATG**AATCGTTATCGTAATGAATTTC
12[1]	BaXhoI22rv	GGGG**CTCGAG**GCTATTTTTGCGTTTAC
13[1]	StBamHIGexfwG	GCGC**GGATCC**AGAGTTTTGGCACCTCGTAAG
14[1]	StXhoIGexrv	GGGG**CTCGAG**TTACTTCCAAAGACGTCTTTTC
15[1]	BlBamHIGexfw	GCGC**GGATCC**AACAGGAAAACGAAAGAG
16[1]	BlXhoIGexrv	GGGG**CTCGAG**TCATTTCGTTCTCCTTCC
17	miniSphSafw	CGAGGC**GCATGC**AGATGAATCAGGAAG
18	miniBamSarv	GGCGCC**GGATCC**TTATTTGTGACGTATTACAC
19	miniSphBsfw	CCGGCG**GCATGC**TGATTAAAAAGAATGC
20	miniBamBsrv	CGGCGG**GGATCC**TTAGACGGAGTCTTTTTTGC
21	miniSphEffw	GGGCCC**GCATGC**AGGTGATTTATTTGTTAAAAAATACC
22	miniBamEfrv	GCGCGC**GGATCC**ATACTTTCTTCGTATC
23	miniSphPaflfw	GTTATA**GCATGC**GCACCGACGCTCC
24	miniSphPalfw	GAATTA**GCATGC**GCGCGGCACC

No.	Name	Sequence (5'-3')
25	miniBamPalrv	GCACTG**GGATCC**TCAGCGTTTCACCAATC
26[2]	KoPCR1PA0919Kpn-fw	GCAATG**GGTACC**GCATCGCCATCGTC
27[2]	KoPCR1PA0919Bam-rv	CGTTCA**GGATCC**ATCAGCGTTTCACC
28[2]	KoPCR2PA0919Bam-fw	GGTAAT**GGATCC**TCGCGATCAAGCTCTC
29[2]	KoPCR2PA0919Hind-rv	GGTTGC**AAGCTT**GTCGCGGCTGAC
30	pPA0919SacIfw	GATAAC**GAGCTC**ATCGTCCGCCACCAG
31	PA0919BamHIrv	GCATAA**GGATCC**TCAGGCGTCGGGAGC
32	PA0919SphIfw	CCAAGA**GCATGC**TGATGTCTGTCGTGAAACG
33	pPA0919lacZKpnIfw	CATCAT**GGTACC**ATCGTCCGCCACCAG
34	pPA0919lacZKpnI+35fw	GCATAG**GGTACC**GTTGACCCAGC
35	pPA0919lacZKpnIshortfw	GCATAG**GGTACC**GCGACGCTTCAAG
36[3]	A	AGCTTCTCAGCGCTTGGAGCCACCCGCAGTTCGAAAAATAATAACTGCAGC
37[3]	B	TCGAGCTGCAGTTATTATTTTTCGAACTGCGGGTGGCTCCAAGCGCTGAGA
38	PA0919deltaAS1-34NcoIfw	GAATCA**CCATGG**CGAAACTGGAAGCCCTGGAC
39	PA0919HindIIIrv	GATAGC**AAGCTT**GGCGTCGGGAGCGTTCTC
40	PA0919_S240A_fw	CACCCTGTTCTATGCCGGCGACGGCGG
41	PA0919_S240A_rv	CCGCCGTCGCCGGCATAGAACAGGGTG
42	PA0919_S307A_fw	CCTGGCCGGCTACGCCTTCGGCGCTGAC
43	PA0919_S307A_rv	GTCAGCGCCGAAGGCGTAGCCGGCCAGG
44	PA0919_H401A_fw	CTGCCGGGCGGCGCCCACTTCGACGAG
45	PA0919_H401_rv	CTCGTCGAAGTGGGCGCCGCCCGGCAG
46	pPA0919Kpnlocal-fw	CCTAAG**GGTACC**ATCGTCCGCCACCAGG
47	PA0919StrepII-Bam-rv	GCAAGT**GGATCC**TTATTATTTTTCGAACTGCGGGTGGCTCCAAGCGCTGAGAATCTTGGCGTCGGGAGC
48	1_deltaPA0919AS1-34fw	GGATTGGTGAAACGCTGATATGAAACTGGAAGCCCTGG
49	1_deltaPA0919AS1-34rv	CCAGGGCTTCCAGTTTCATATCAGCGTTTCACCAATCC
promoter-terminator construct		**GAGCTC***GCTGAACCATCGCTGAACGAATACCAGCAAATGGCCTTCGGCCACTTCGCCGACGCAACTCCTGCAAAACCCGGCGGTCTTCTCCCTGTGACAGGACGCCGCCCCGCACAGAAAAAATCTGCTGCGACCACTTGGGAACTCGCCCGAGAGGCCATACTCTGTCGCGCAAATTCCCATGAGGTGGC***GCATGC**GACTATCGGT**GGATCC***TGCCTGGCGGCAGTAGCGCGGTGGTCCCACCTGACCCCATGCCGAACTCAGAAGTGAAACGCCGTAGCGCCGATGGTAGTGTGGGGTCTCCCCATGCGAGAGTAGGGAACTGCCAGGCATCAAATAAAACGAAAGGCTCAGTCGAAAGACTGGGCCTT***AAGCTT*** The construct was employed to integrate the sequences of the P_{PA0920} promoter and the *rrnB* terminator (flanked by designated restriction sites) into the mini-CTX2 vector.

Table 7: Oligodeoxynucleotides employed for sequencing

Specifically indicated primers were taken from: [1] Lorenzo, 2006; [2] Jäger, 2011; [3] Spier, 2007; [4] S. Hebecker, unpublished; [5] primer collection AK Jahn; [6] standard primer from GATC Biotech (Konstanz, Germany).

No.	Name	Sequence (5'-3')
1	pBADfw	GATTAGCGGATCCTACCTG
2[1]	pBAD_r_seq	GATTTAATCTGTATCAGG
3	pBADBthufw	GCGTATATGTCATTGCTGC
4	pBADBthu2fw	CTTATCGGAATATTAGACACGAG
5	pBADBthu3fw	GGAATTGATGTTGAAGAAACG
6	pBADBphyfw	CATCGAGCAGATCCTGCTGG
7	pBADBphy2fw	GCGCTCGTTCTGATGACTG
8	pBADBphy3fw	GACGCTGGGTCTCGCTGTC
9	pBADMbarfw	CCCTGCTTCATGTCCTTGTG
10	pBADPpolyfw	GTGCTGGATGCTCACCCATGG
11	pBADPpolyrv	CCAGCCGAGTGAATATCC
12[2,5]	pGEX-6P-1 fw	CCTCCAAAATCGGATCTG
13[2,5]	pGEX-6P-1 rv	CACCGTCATCACCGAAAC
14[2,6]	pGEX-5 fw	CTGGCAAGCCACGTTTGG
15[2,6]	pGEX-3 rv	GGAGCTGCATGTGTCAGAG
16[2,6]	T7 fw	TAATACGACTCACTATAGGG
17[2]	T7 term rv	CGTTTAGAGGCCCCAAG
18[2]	pET-RP rv	CTAGTTATTGCTCAGCGG
19[3]	oNB-51	CTCAGCCCGAAGCCGGTGTT
20[3]	oNB-53	GAAATCCGGCTGTTGCCCTG
21	SeqSa1fw	GTAGCAATCACATTGTATC
22	SeqSa1rv	GAATAACAAGCGATGCC
23	SeqSa2fw	GGATTGTACTGCACTTTAG
24	SeqSa3fw	GACGGAAATCACTTAACG
25	SeqSa4fw	GCGAGGAGATTATTAATCAG
26	SeqSa5fw	GGCTAGATAATCGTCAG
27	SeqSa6fw	CCGAATTGGGAACCAC
28	SeqBs1fw	GTCATTCAAACGTACGC
29	SeqBs1rv	CGCAGTGAGTACTTCAGGAC
30	SeqBs2fw	CGCATATATTGGAGCTTCAG
31	SeqBs3fw	GTTATACCGCACATTCC
32	SeqBs4fw	GCGTCTTGCTGCGTTTC
33	SeqBs5fw	GAAGGGATTCTCGCTCG
34	SeqBs6fw	GAGTGGCGAGGGAAATAC
35	SeqEf1fw	CCACCTAGGACTGTTC
36	SeqEf1rv	GCATTAGTCCGCTTTTCC
37	SeqEf2fw	CGGCGGTCTATATTTTCC
38	SeqEf3fw	GTACTTTCTGCCACTATCC
39	SeqEf4fw	GGCCATCATCGCTGTTAG
40	SeqEf5fw	GTCTTACAACCACCATTTTC
41	SeqEf6fw	CTGGGTCTCACGTTATAC
42[1]	SPA0920-1850r	GAATTGCCAGATCAGTTC
43[1]	SPA0920-1420r	GAAGGGTACTTCCATCAG
44[1]	SPA0920-950r	ATCAAGCGGTACAAGAGC
45[1]	SPA0920-410r	GGGAATACAGTCGGTAGC

No.	Name	Sequence (5'-3')
46[1]	SPA0920-2360r	CTTGTAGTGGAGGATGAG
47[4]	Sp1MprFHisf	GACGCTTCAAGGACAAGTTC
48[4]	Sp2MprFHisf	CTTCTTCCGCATCGCCATC
49	SeqPafl1rv	GATCAGCCGGATGCGTTGTG
50	miniCTX2rrnBrv	GGCAGTTCCCTACTCTCGC
51	PA0919_2rv	GACCTCGAGTACCGGCAG
52[6]	pET-24a	GGGTTATGCTAGTTATTGCTCAG
53[6]	M13-FP	TGTAAAACGACGGCCAGT
54[6]	M13-RP	CAGGAAACAGCTATGACC

2.2 Sterilization, media and additives

Sterilization conditions, media and additives employed in this study are summarized in the following sections.

2.2.1 Sterilization

Media and subjects were vapor sterilized using 121 °C and 1 bar excess pressure for 20 min. Temperature sensitive solutions were filtrated employing a filter pore width of 0.2 µm.

2.2.2 LB medium

All bacterial strains (except *Streptococcus thermophilus*; see Jäger, 2011) were cultivated in Luria Bertani medium (LB; Sambrook and Russell, 2001) unless indicated otherwise.

LB medium	tryptone	10 g/L
	yeast extract	5 g/L
	NaCl	5 g/L

Solid medium was obtained by adding 15 g/L agar-agar previous to sterilization.

2.2.3 AB medium

AB medium without citrate (Heydorn *et al.*, 2000) supplemented with glucose was employed to cultivate *P. aeruginosa* PAO1, *P. aeruginosa* PA14 and *Pseudomonas putida*. The addition of an appropriate phosphate buffer resulted in modified AB medium adjusted to a specific pH value. The resulting AB medium showed a pH value that was increased by 0.3 units when compared to the employed A10 solution.

AB medium	A10	100 mL/L
	1 M D(+)-glucose	20 mL/L
	14 mg/mL $FeSO_4$ x 7 H_2O	0.5 mL/L
	trace elements	1 mL/L
	1 M $MgCl_2$	1 mL/L
	1 M $CaCl_2$	0.1 mL/L

All components were prepared as stock solutions. A10 solutions, $MgCl_2$ and $CaCl_2$ were sterilized by autoclaving and glucose, $FeSO_4$ and trace elements were filtrated for sterilization.

A10 solution	**pH 7.0**	**pH 6.0**	**pH 5.0**	**pH 4.0**
$(NH_4)_2SO_4$	20 g/L	20 g/L	20 g/L	20 g/L
Na_2HPO_4	300 mM	62.5 mM	20 mM	1 mM
KH_2PO_4	150 mM	387.5 mM	430 mM	449 mM

trace elements	$CaSO_4$ x 2 H_2O	200 mg/L
	$FeSO_4$ x 7 H_2O	200 mg/L
	$MgSO_4$ x H_2O	20 mg/L
	$CuSO_4$ x 5 H_2O	20 mg/L
	$ZnSO_4$ x 5 H_2O	20 mg/L
	Na_2MoO_4 x H_2O	10 mg/L
	H_3BO_3	5 mg/L

2.2.4 SMM

B. subtilis, *Bacillus thuringiensis, Bacillus licheniformis* and *Paenibacillus polymyxa* were cultivated in Spizizen's minimal medium (SMM; Harwood and Cutting, 1990).

SMM medium	SMM basis	880 mL/L
	10x SMM mixture	100 mL/L
	100x SMM trace elements	10 mL/L
	10 % Casamino acids	10 mL/L

The ingredients were prepared and sterilized. SMM basis was prepared with a pH of 7.0. If other pH values were requested, SMM basis was adjusted using 85 % phosphoric acid. SMM basis and Casamino acids solutions were autoclaved, whereas 10x SMM mixture and 100x SMM trace elements were filtrated for sterilization.

SMM basis pH 7.0	$(NH_4)_2SO_4$	17 mM
	K_2HPO_4	91 mM
	KH_2PO_4	50 mM
	trisodium citrate x 2 H_2O	4 mM
	$MgSO_4$ x 7 H_2O	0.9 mM

10x SMM mixture	L-phenylalanine	3 mM
	L-tryptophan	2.5 mM
	thiamine chloride x HCl	15 µM
	D(+)-glucose x H_2O	500 mM
	sodium pyruvate	500 mM
100x SMM trace elements	$CaCl_2$ x 2 H_2O	5.4 mM
	$FeCl_2$ x 4 H_2O	5.75 mM
	$MnCl_2$ x 4 H_2O	0.5 mM
	$ZnCl_2$	1.25 mM
	$CuCl_2$ x 2 H_2O	0.25 mM
	$CoCl_2$ x 6 H_2O	0.25 mM
	Na_2MoO_4 x 2 H_2O	0.25 mM

2.2.5 R2A medium

For the cultivation of *Burkholderia phymatum*, Reasoner's 2A medium (R2A; Reasoner and Geldreich, 1985) was used. If solid medium was needed, 15 g/L agar-agar was added before autoclaving.

R2A medium	yeast extract	0.5 g/L
	Bacto™ Proteose Peptone no. 3	0.5 g/L
	Casamino acids	0.5 g/L
	D(+)-glucose	0.5 g/L
	soluble starch	0.5 g/L
	sodium pyruvate	0.3 g/L
	K_2HPO_4	0.3 g/L
	$MgSO_4$ x 7 H_2O	0.05 g/L

2.2.6 TSB medium

S. thermophilus was cultivated in trypticase soy broth medium (TSB; Yousef and Carlstrom, 2003) supplemented with 0.3 % yeast extract (Jäger, 2011). For the preparation of solid medium, 15 g/L agar-agar was added before vapor sterilization.

TSB medium	yeast extract	3 g/L
	Bacto™ Tryptone	17 g/L
	Bacto™ Soytone	3 g/L
	D(+)-glucose x H_2O	2.5 g/L
	NaCl	5 g/L
	K_2HPO_4	2.5 g/L

2.2.7 Additives

Media additives were prepared as concentrated solutions, sterilized by filtration and stored at –20 °C. For *E. coli* and *P. aeruginosa*, different final concentrations were used. Additives were dissolved in water if no solvent is indicated (Table 8).

Table 8: Media additives

Media additive	Stock solution	Final concentration	
		E. coli	***P. aeruginosa***
5-aminolevulinic acid (ALA)	50 mg/mL	50 µg/mL	–
ampicillin (Ap)	100 mg/mL	100 µg/mL	–
carbenicillin (Cb)	100 mg/mL	100 µg/mL	250 µg/mL
chloramphenicol (Cm)	34 mg/mL (ethanol)	34 µg/mL	–
gentamicin (Gm)	10 mg/mL	10 µg/mL	50 µg/mL
kanamycin (Kan)	30 mg/mL	30 µg/mL	–
tetracycline (Tet)	12.5 mg/mL	12.5 µg/mL	80 µg/mL
isopropyl-β-D-thiogalactopyranoside (IPTG)	0.5 M	25 – 300 µM	–
L(+)-arabinose	20 % (w/v)	0.2 – 2.0 % (w/v)	–
D(+)-sucrose	50 % (w/v)	–	5 % (w/v)

2.3 Microbiological procedures

Bacterial cells were cultivated and stored as summarized in the following chapters.

2.3.1 Cultivation of bacterial cells

Bacterial cells were grown at 37 °C (*B. phymatum*: 30 °C) and 200 rpm (*S. thermophilus*: without shaking, Jäger, 2011). Pre-cultures (5 – 100 mL of the respective medium supplemented with the respective antibiotics, in baffled flasks) were inoculated using a single colony from a plate culture or a glycerol stock culture and cultivated overnight (*S. thermophilus*: for 3 d; Jäger, 2011).

Plate cultures were prepared by plating a bacterial cell suspension (5 – 100 µL) or by streaking cells with an inoculating loop and were incubated overnight (*S. thermophilus*: for 3 – 5 d; Jäger, 2011).

2.3.2 Determination of cell density

For the determination of liquid bacterial cell culture densities, the optical density (OD) at 578 nm was determined photometrically. An OD_{578} of 1 represents a cell culture density of approximately 1 x 10^9 cells per mL (Sambrook and Russell, 2001).

2.3.3 Storage of bacteria

For long term storage, glycerol cultures (20 % (w/v)) were prepared by mixing a bacterial overnight culture with the appropriate amount of 80 % (w/v) sterile glycerol. Cultures were stored at –80 °C (Sambrook and Russell, 2001).

2.3.4 Cultivation of *E. coli* for recombinant protein production

For the production of recombinant protein in *E. coli*, 500 mL LB medium (in baffled flasks) were inoculated (1:100, v/v) employing a pre-culture and incubated at 37 °C and 200 rpm until a specific culture turbidity was reached. Protein production was induced by IPTG or L(+)-arabinose and cells were further incubated (for additive concentrations and cultivation specifications, see the respective method and section 2.2.7).

2.3.5 Determination of *P. aeruginosa* growth phenotypes

Growth phenotypes of *P. aeruginosa* strains were determined using AB medium at pH 7.3 and pH 5.3 (Heydorn *et al.*, 2000). Pre-cultures (AB medium pH 7.3, supplemented with the respective antibiotics) were inoculated using a single colony from a plate culture and incubated at 37 °C and 200 rpm overnight. Main cultures (60 mL AB medium in baffled flasks supplemented with the respective antibiotics) were inoculated to an OD_{578} of 0.05 and cultured at 37 °C and 200 rpm. Growth was monitored by measuring the OD_{578} at distinct time points.

2.4 Molecular biological methods

The molecular biological techniques employed for the preparation of competent *E. coli* cells, transformation as well as DNA extraction, purification, amplification, cloning and manipulation are summarized in the following sections. Moreover, procedures used for *P. aeruginosa* deletion mutant strain construction and complementation techniques are presented.

2.4.1 Preparation of $CaCl_2$ competent *E. coli* cells

100 mL LB medium (in baffled flasks, with additives if required) were inoculated using an overnight pre-culture in a ratio of 1:100 (v/v) and cultured at 37 °C and 200 rpm. When the culture density had reached an OD_{578} of 0.6 – 0.8, cells were harvested by centrifugation (3'000 x g, 10 min, 4 °C). After washing with 10 mL cold $CaCl_2$ solution, the cells were suspended in 1 mL of the same solution and stored at –80 °C in aliquots of 50 – 200 µL (Sambrook and Russell, 2001).

$CaCl_2$ solution	$CaCl_2$	0.1 M
	glycerol	10 % (w/v)

2.4.2 Preparation of RbCl competent *E. coli* cells

RbCl competent *E. coli* cells were prepared according to Engler *et al.*, 2008. After inoculation of 500 mL LB medium (in baffled flasks, with additives if required) in a ratio of 1:100 (v/v) using an overnight pre-culture, the cells were cultivated at 37 °C and 200 rpm to a culture density of OD_{578} = 0.5. The cells were harvested (3'000 x g, 10 min, 4 °C), suspended in cold TFB-I solution and incubated on ice for 5 min. After sedimentation (4'500 x g, 10 min, 4 °C), the cells were suspended in 2 – 3 mL cold TFB-II buffer, incubated on ice for 1 h and stored at –80 °C in aliquots of 50 – 200 µL.

TFB-I	potassium acetate	30 mM
	$CaCl_2$	10 mM
	$MnCl_2$	50 mM
	RbCl	100 mM
	glycerol	15 % (w/v)
	adjusted to pH 5.8 with acetic acid, sterilized by filtration	
TFB-II	piperazine-N,N'-bis(2-ethanesulfonic acid) (PIPES)-HCl pH 6.5	10 mM
	$CaCl_2$	75 mM
	RbCl	10 mM
	glycerol	15 % (w/v)
	adjusted to pH 6.5 with KOH, sterilized by filtration	

2.4.3 Transformation of competent *E. coli* cells by heat shock

50 – 100 µL competent *E. coli* cells were mixed with 1 – 10 µL plasmid solution (50 µg/mL) and incubated on ice for 20 min. The heat shock was performed at 42 °C for 45 sec and subsequently, the cells were incubated on ice for 2 min. After suspending in 250 – 500 µL LB medium, the cells were incubated at 37 °C and 300 rpm for 1 h. For the selection of transformed clones, an appropriate amount of cells was plated on LB agar plates containing the respective antibiotics and incubated at 37 °C overnight (Sambrook and Russell, 2001).

2.4.4 Extraction of plasmid DNA

Two different protocols were used to extract plasmid DNA from bacteria: The first provides highly purified plasmid DNA, whereas the second procedure is time-saving and results in high amounts of plasmid DNA. All centrifugation steps were performed at room temperature (RT) and 11'000 x g unless indicated otherwise.

To obtain highly purified plasmid DNA, plasmid containing *E. coli* cells were grown as overnight cultures in LB medium supplemented with the respective antibiotics. The cells were harvested (4 mL culture, 5 min), suspended in 150 µL GTE buffer and incubated for 2 min. 300 µL NaOH/SDS were added to lyse the cells and the sample was mixed carefully by inverting the tube. After incubation for 5 min, 225 µL sodium acetate were added, the sample was mixed and incubated for 5 min. Denatured proteins and insoluble cell compounds were separated by centrifugation for 5 min and the plasmid DNA was precipitated by adding 600 µL isopropanol to the supernatant. The plasmid DNA was sedimented for 10 min, solved in 200 µL TES buffer containing 3 µL RNase A and incubated at 37 °C for 30 min. For plasmid DNA extraction, the sample was mixed with 200 µL CPI and centrifuged for 3 min. The upper, aqueous phase containing the plasmid DNA was removed, mixed with 400 µL 100 % ethanol and incubated for 5 min. After centrifugation for 15 min, the sedimented DNA was washed with 500 µL 70 % ethanol, dried at 50 °C, dissolved in 50 µL dH_2O and stored at –20 °C (Sambrook and Russell, 2001).

To obtain high amounts of plasmid DNA, 4 mL of an *E. coli* overnight culture were harvested and the cell sediment was suspended in 300 µL buffer P1. 300 µL NaOH/SDS were added and mixed by inverting the tube. Proteins were denatured by the addition of 300 µL potassium acetate and separated together with cell debris by centrifugation for 15 min. The plasmid DNA containing supernatant was mixed with 600 µL isopropanol and precipitated DNA was sedimented at 4 °C for 15 min. The sediment was washed with 400 µL 70 % ethanol at 4 °C, dried at 50 °C, dissolved in 50 µL dH_2O and stored at –20 °C (Sambrook and Russell, 2001).

GTE	D(+)-glucose	50 mM
	tris(hydrolxymethyl)aminomethane (Tris)-HCl pH 8.0	25 mM
	ethylenediaminetetraacetic acid (EDTA)	10 mM
P1	Tris-HCl pH 8.0	50 mM
	EDTA	10 mM
	RNase A	100 µg/mL
NaOH/SDS	NaOH	200 mM
	sodium dodecyl sulfate (SDS)	1 % (w/v)
sodium acetate	sodium acetate adjusted to pH 4.8 with acetic acid	3 M

potassium acetate	potassium acetate adjusted to pH 5.5 with acetic acid	3 M
TES	Tris-HCl pH 8.0	50 mM
	EDTA	10 mM
	NaCl	150 mM
CPI	phenol	50 % (v/v)
	chloroform	49 % (v/v)
	isoamyl alcohol	1 % (v/v)
RNase A	RNase A solved in 50 % glycerol	10 mg/mL

2.4.5 Extraction of genomic DNA

Genomic DNA was extracted using a modified protocol according to Lahiri *et al.*, 1992. Bacterial cells were cultured in 5 mL of the respective medium and grown at 37 °C overnight. 1.5 mL culture were centrifuged (11'000 x g, 5 min, RT), cells were suspended in 200 µL lysis buffer and 66 µL 5 M NaCl were added. After intensive mixing, 1 µL RNase A was added and the sample was incubated at 37 °C for 30 min. Cell debris was separated by centrifugation (11'000 x g, 10 min, 4 °C) and the supernatant was gently mixed with chloroform (1:1, v/v). After an additional centrifugation step (11'000 x g, 3 min, RT), the upper DNA containing aqueous phase was mixed with 100 % ethanol (1:2, v/v) for DNA precipitation. The DNA was sedimented (11'000 x g, 15 min, 4 °C) and washed twice with 200 µL 70 % ethanol (11'000 x g, 5 min, 4 °C). The sediment was dried at 70 °C, the genomic DNA was solved in 50 µL dH_20 and stored at 4 °C.

lysis buffer	EDTA	1 mM
	sodium acetate	20 mM
	SDS	1 % (w/v)
	Tris-acetate pH 7.8	40 mM
RNase A	RNase A solved in 50 % glycerol	10 mg/mL

2.4.6 Determination of DNA concentration

The absorbance of a DNA sample at 260 and 280 nm was determined spectrophotometrically. An absorbance of 1 at 260 nm corresponds to a double-stranded DNA concentration of 50 ng/µL. Protein impurities show a maximum absorption at 280 nm. The quotient A_{260}/A_{280} indicates the DNA sample purity. The DNA sample is supposed to be pure when A_{260}/A_{280} = 1.8 – 2.0 (Sambrook and Russell, 2001).

2.4.7 DNA amplification by polymerase chain reaction (PCR)

DNA fragments were amplified by PCR using the Phusion® High-Fidelity DNA Polymerase or the *Taq* DNA Polymerase. The polymerases, their corresponding buffers and the deoxynucleotide triphosphate (dNTP) mixture were obtained from New England Biolabs (Ipswich, MA, USA). Oligodeoxynucleotides were designed to bind specific target site sequences and provided restriction endonuclease recognition sites, if the fragment was amplified for cloning purposes (for primers used in this study, see Table 6).

PCR reactions (total volume: 20 µL) were composed of a dNTP mixture, the respective primers containing the desired target sites for restriction endonucleases, the DNA polymerase and a polymerase-specific buffer. The template DNA was either provided as an aqueous solution or a bacterial colony was added to the mixture. Colonies of gram positive organisms or of *P. putida* were lysed before subjecting to PCR. For this, a cell colony was suspended in 20 µL lysis buffer and treated at 95 °C for 15 min. Subsequently, 180 µL dH_2O were added and 1 µL of this mixture was used as PCR template. The compositions of reactions using the Phusion® High-Fidelity DNA Polymerase or the *Taq* DNA Polymerase are summarized below.

During PCR, the template DNA was initially denatured (98 °C, 5 – 10 min) and subsequently, DNA amplification took place in 30 cycles consisting of denaturation (98 °C, 10 sec), primer annealing (55 – 75 °C, 15 – 30 sec) and elongation (72 °C, time period depending on the target DNA length and the processivity of the employed polymerase; Phusion®: 30 sec/kb; Taq: 60 sec/kb). After a final elongation step (72 °C, 10 min), PCR samples were stored at 4 °C (Sambrook and Russell, 2001).

compounds	**Phusion® polymerase**	***Taq* polymerase**
template DNA	colony or 0.2 – 5 ng	colony or 0.2 – 5 ng
buffer	4 µL GC (5x) or HF (5x)	2 µL ThermoPol® (10x)
dNTP mixture	0.2 mM	0.2 mM
forward primer	1 µM	1 µM
reverse primer	1 µM	1 µM
polymerase	20 U/mL	20 U/mL
dH_2O	add to 20 µL	add to 20 µL
lysis buffer	NaOH	50 mM
	SDS	0.25 % (w/v)

2.4.8 DNA fragment purification after PCR

After PCR, amplified DNA fragments were purified using the QIAquick PCR Purification Kit (Qiagen, Hilden, Germany) according to the manufacturer's instructions.

2.4.9 Restriction of DNA

DNA fragments amplified by PCR and plasmid DNA were digested by restriction endonucleases (New England Biolabs, Ipswich, MA, USA) according to the manufacturer's instructions.

2.4.10 Agarose gel electrophoresis

DNA fragments of different length obtained by PCR or restriction digest were separated by agarose gel electrophoresis.

DNA samples were mixed with loading dye and loaded onto an agarose gel (1 – 2 % (w/v) agarose in TAE buffer). For DNA fragment size determination, a DNA standard was handled analogously (GeneRuler™ DNA Ladder Mix; Thermo Fisher Scientific, Waltham, MA, USA). Electrophoresis was performed using a voltage of 80 – 100 V and for DNA detection, the gel was incubated with ethidium bromide solution (10 µg/mL) for 20 min or with GelStar™ Nucleic Acid Gel Stain (Lonza, Basel, Switzerland) for at least 30 min. Then, the DNA was visualized using UV light or blue light, respectively (Sambrook and Russell, 2001).

loading dye (6x)	bromophenol blue	350 µM
	xylene cyanol FF	450 µM
	glycerol	50 % (w/v)
TAE buffer	Tris-acetate pH 8.0	40 mM
	EDTA	1 mM

2.4.11 Purification of digested PCR fragments and plasmids

After restriction endonuclease treatment, DNA fragments and vectors were separated by agarose gel electrophoresis and the gel was stained with GelStar™ Nucleic Acid Gel Stain (section 2.4.10). Target DNA fragments were excised and purified employing the QIAquick Gel Extraction Kit (Qiagen, Hilden, Germany) according to the manufacturer's instructions.

2.4.12 Ligation

DNA fragments and vectors were ligated employing the T4 DNA Ligase (New England Biolabs, Ipswich, MA, USA) according to the manufacturer's instructions in varying ratios in a final volume of 20 µL. Samples were incubated at RT for 30 min and the resulting plasmids were transformed into *E. coli* cells (section 2.4.3).

2.4.13 Sequencing

DNA sequence determination was performed by GATC Biotech (Konstanz, Germany) according to Sanger's method (Sanger *et al.*, 1977). Sequence files were analyzed using the Lasergene® software package (DNASTAR, Madison, WI, USA).

2.4.14 Site-directed mutagenesis

Site-directed mutagenesis is a versatile method to exchange single or few base pairs in DNA sequences (Sambrook and Russell, 2001). In this work, the QuikChange® II Site-Directed Mutagenesis Kit (Stratagene, La Jolla, CA, USA) was employed according to the manufacturer's instructions in a final volume of 25 µL. The sequence to be mutated was plasmid encoded and specific primers contained the designated nucleotide sequence mutations. During PCR, the primers annealed to the template DNA and mutated plasmids were synthesized. To eliminate unmodified template plasmids, the obtained PCR samples were incubated with the restriction endonuclease *DpnI* specifically digesting methylated DNA which had been synthesized within a bacterial cell. The mutated plasmids were amplified using *E. coli* DH10B.

2.4.15 Plasmid construction

The plasmids generated in this study were constructed by inserting amplified target sequences into well-established vectors. The respective plasmids are summarized in Table 5 and employed oligodeoxynucleotides are listed in Table 6 and Table 7. Methods employed for the plasmid construction are given in sections 2.4.1 to 2.4.14.

Plasmid construction for recombinant aaPGS activity analysis (full-length enzymes)

Gene sequences of selected putative aaPGSs were cloned into the pBAD-His-A vector designed for recombinant protein expression in *E. coli* TOP10 (Invitrogen, Karlsruhe, Germany). The vector provides the P_{BAD} promoter (of *araBAD*) inducible by L(+)-arabinose in a dose-dependent manner (Guzman *et al.*, 1995).

Orfs Bphy_4019 (*B. phymatum* STM 815), Bthur0008_13400 (*B. thuringiensis* ATCC 10792), Krad_4555 (*K. radiotolerans* SRS 30216) and Mbar_A2435 (*Methanosarcina barkeri* str. Fusaro ATCC 29787) were amplified from genomic DNA by PCR. Since the aaPGS encoding sequence of *P. polymyxa* ATCC 842 was not available, the orf was amplified using random primers designed on the basis of aaPGS homologs from *P. polymyxa* SC2 and E681 (not shown). Plasmids pBAD-His-A/Krad4555, pBAD-His-A/Bp4019 and pBAD-His-A/A2435 were generously provided by S. Hebecker (unpublished). Insert sequences were verified by sequencing using primers 1 – 9 (Table 7). For the *P. polymyxa* ATCC 842 aaPGS, internal

sequencing primers 10 and 11 (Table 7) were designed after successive sequence elucidation. The obtained *P. polymyxa* aaPGS encoding sequence is given the appendix (section 8.1).

orf	primer no. (Table 6)	fragment (bp)	restriction sites	resulting plasmid
Bphy_4019	1, 2	2'595	*XhoI*/*HindIII*	pBAD-His-A/Bp4019
Bthur0008_13400	3, 4	2'589	*XhoI*/*KpnI*	pBAD-His-A/Bthur0008_13400
Krad_4555	5, 6	1'041	*SacI*/*HindIII*	pBAD-His-A/Krad4555
Mbar_A2435	7, 8	2'646	*XhoI*/*XhoI*	pBAD-His-A/A2435
Ppoly_aaPGS	9, 10	2'643	*SacI*/*KpnI*	pBAD-His-A/Ppoly_aaPGS

Plasmid construction for recombinant aaPGS activity analysis (C-terminal domains)

Vectors pGEX-6P-1 (GE Healthcare, Freiburg, Germany) and pET22b(+) (Merck, Darmstadt, Germany) were employed for recombinant production of C-terminal aaPGS domains of *B. licheniformis*, *B. anthracis* and *S. thermophilus*. Both vectors allow for the recombinant expression of proteins in *E. coli* BL21 (λDE3) by providing either a P_{tac} promoter in combination with an N-terminal GST-tag sequence (pGEX-6P-1) or alternatively a T7 promoter and a C-terminal His_6-tag (pET22b(+)). Plasmids pGEX-6P-1/YfiXΔaa1-518, pGEX-6P-1/StMprFΔaa1-503 and pET22b(+)/BAS1375 Δaa1-527 were generously provided by S. Jäger (Jäger, 2011).

Gene sequences encoding C-terminal domains of *B. licheniformis* ATCC 14580 YfiX (amino acid residues 519 – 850; YfiXΔaa1-518) and *S. thermophilus* ATCC 19258 MprF (residues 504 – 851; StMprFΔaa1-503) were amplified by PCR using genomic template DNA and cloned into pGEX-6P-1 yielding pGEX-6P-1/YfiXΔaa1-518 and pGEX-6P-1/StMprFΔaa1-503 (Jäger, 2011). Since the sequenced strain *S. thermophilus* LMG 18311 had not been available, primers were designed based on the sequence of the aaPGS homologous orf STU1256 (from *S. thermophilus* LMG 18311). Sequence analysis revealed that StMprFΔaa1-503 (from *S. thermophilus* ATCC 19258) solely differs from STU1256 in three non-conserved amino acid positions (Jäger, 2011). The sequence encoding amino acid residues 528 – 861 of *B. anthracis* BAS1375 was amplified using a synthetic gene (GENEART, Regensburg, Germany; optimized according to the codon usage of *E. coli*) as template. The resulting PCR fragment was cloned into vector pET22b(+) yielding pET22b(+)/BAS1375Δaa1-527 (Jäger, 2011).

orf	primer no. (Table 6)	fragment (bp)	restriction sites	resulting plasmid
BAS1375Δaa1-527	11, 12	1'005	*NdeI*/*XhoI*	pET22b(+)/BAS1375Δaa1-527
StMprFΔaa1-503	13, 14	1'047	*BamHI*/*XhoI*	pGEX-6P-1/StMprFΔaa1-503
YfiXΔaa1-518	15, 16	999	*BamHI*/*XhoI*	pGEX-6P-1/YfiXΔaa1-518

Construction of the mini-CTX2-PTC vector employed for PAO1 complementation studies

Vector mini-CTX2 was developed for introducing exogenous DNA into the *attB* phage attachment site of the *P. aeruginosa* PAO1 chromosome (Hoang *et al.*, 2000). The vector provides a *tet* (tetracycline resistance) and an *int* (integrase) gene and it can be transferred from *E. coli* to *P. aeruginosa* by conjugation due to the enclosed *oriT*. The multiple cloning site is flanked by FLP recombinase target sites (FRT) allowing for the excision of vector sequences after the integration of exogenous DNA into the *P. aeruginosa* chromosome (Hoang *et al.*, 1998; Hoang *et al.*, 2000).

The mini-CTX2 vector was modified to generate mini-CTX2-PTC. A synthetic DNA sequence (promoter-terminator nconstruct) consisting of the P_{PA0920} promoter encoded upstream of orf PA0920 (187 bp), a linker sequence providing *SphI* and *BamHI* restriction sites and the *rrnB* terminator sequence t_{rrnB} (158 bp; Invitrogen, Darmstadt, Germany) was synthesized by GENEART (Regensburg, Germany; see Table 7 for sequences) and integrated into the *SacI*/*HindIII* site of mini-CTX2. This modified vector was then further modified by the integration of genes employed for the respective complementation of *P. aeruginosa* deletion mutant strains.

Plasmids for the complementation of *P. aeruginosa* PAO1 ΔPA0920

Formerly characterized aaPGS encoding genes were inserted into the *SphI*/*BamHI* site of mini-CTX2-PTC. The resulting plasmids were employed to complement the *P. aeruginosa* deletion mutant strain PAO1 ΔPA0920 (Lorenzo, 2006). The obtained strains allowed for the analysis of the impact of different aaPGS encoding genes under the control of an identical promoter in the gram negative model organism *P. aeruginosa*.

Orfs Sa113 (from *S. aureus* NCTC 8325), BSU08425 (from *B. subtilis* subsp. s*ubtilis* str. 168), aaPGS2 (gi:69249189, from *E. faecium* DO), PA0920 (from *P. aeruginosa* PAO1) and the sequence encoding the C-terminal A-PGS domain (PA0920aa543-881, from *P. aeruginosa* PAO1) were amplified using the respective genomic DNA as template. Since the mini-CTX2-PTC contains two *SphI* restriction sites, the sequence encoding the P_{PA0920} promoter was excised from the mini-CTX2-PTC using *SacI* and *SphI* to yield the 187 bp promoter fragment. This promoter and the amplified aaPGS encoding genes were integrated into the *SacI*/*BamHI* restriction site of mini-CTX2-PTC. Insert sequences were verified using primers 21 – 50 (Table 7). Plasmids were transferred into PAO1 ΔPA0920 by diparental mating.

orf	primer no. (Table 6)	fragment (bp)	restriction sites	resulting plasmid
Sa113	17, 18	2'525	*SphI*/*BamHI*	mini-CTX2-P-SamprF-T
BSU08425	19, 20	2'567	*SphI*/*BamHI*	mini-CTX2-P-BsmprF-T
aaPGS2	21, 22	2'600	*SphI*/*BamHI*	mini-CTX2-P-EfmprF-T
PA0920	23, 24	2'642	*SphI*/*BamHI*	mini-CTX2-P-PA0920-T
PA0920aa543-881	24, 25	1'019	*SphI*/*BamHI*	mini-CTX2-P-PA0920aa543-881-T

Construction of the replacement vector pEX18Ap/ΔPA0919

The gene replacement vector pEX18Ap/ΔPA0919 was constructed to delete the complete orf PA0919 from the PAO1 chromosome resulting in strain PAO1 ΔPA0919 (Groenewold, 2011). The vector encodes genomic sequences flanking the target gene which are separated by a Gm resistance cassette. The vector allows for the homologous recombination with specific genomic sequences resulting in the replacement of orf PA0919 by the Gm resistance cassette.

A 438 bp and a 673 bp fragment representing the genomic sequences directly upstream and downstream of orf PA0919 were amplified by PCR using primers 26 and 27 or 28 and 29, respectively (see Table 6). The Gm resistance cassette was excised out of vector pPS858 employing *BamHI* and ligated together with the two PCR-fragments into the *KpnI*/*HindIII* site of pEX18Ap yielding pEX18Ap/ΔPA0919 (Groenewold, 2011).

Plasmids for the functional complementation of *P. aeruginosa* PAO1 ΔPA0919

Different constructs consisting of orf PA0919 in combination with the putative P_{PA0919} promoter sequence or alternatively with the P_{PA0920} promoter sequence were inserted into vector mini-CTX2-PTC. These plasmids allow for the insertion of the respective construct into the chromosomal *attB* site of PAO1 ΔPA0919 for recovery of the deleted function. For control experiments, mini-CTX2-PTC derivatives containing solely the P_{PA0919} or the P_{PA0920} promoter sequence were constructed.

Orf PA0919 was amplified together with its 430 bp upstream region representing the putative P_{PA0919} promoter using genomic DNA of *P. aeruginosa* PAO1 as template and cloned into mini-CTX2-PTC. Orf PA0919 was amplified (without any promoter sequence) and inserted into mini-CTX2-PTC under the control of the P_{PA0920} promoter as described above (see 'Plasmids for the complementation of *P. aeruginosa* PAO1 ΔPA0920'). For control experiments, the P_{PA0919} promoter was employed without orf PA0919 and mini-CTX2-PTC was used as a control for the P_{PA0920} promoter. Insert sequences were verified using primers 50 and 51 (Table 7) and the employed cloning primers (Table 6). Plasmids were transferred into PAO1 ΔPA0919 by diparental mating.

construct	primer no. (Table 6)	fragment (bp)	restriction sites	resulting plasmid
P_{PA0919}-PA0919	30, 31	1'714	*SacI*/*BamHI*	mini-CTX2-P_{PA0919}-PA0919-T
P_{PA0920}-PA0919	32, 31	1'477	*SphI*/*BamHI*	mini-CTX2-P_{PA0920}-PA0919-T
P_{PA0919}	30, 27	430	*SacI*/*BamHI*	mini-CTX2- P_{PA0919}-T
P_{PA0920}				mini-CTX2-PTC (see above)

Plasmids for the analysis of the P_{PA0919} promoter employing different P_{PA0919}-*lacZ* fusions

For the analysis of the putative promoter sequence located directly upstream of orf PA0919, several promoter fragments of different size were cloned upstream of a *lacZ* gene into vector mini-CTX-*lacZ* (Becher and Schweizer, 2000). This vector was employed for the specific integration of the generated promoter-*lacZ* reporter gene constructs into the *attB* site of the *P. aeruginosa* chromosome allowing for the analysis of the respective promoter activity.

A 430 bp fragment covering the genomic sequence directly upstream of orf PA0919 was amplified by PCR. Truncated fragment versions of 206 bp (containing the proposed –35 and –10 promoter elements) and of 140 bp (devoid of any promoter elements) were also generated by PCR. The obtained fragments were cloned into the vector mini-CTX-*lacZ*. Insert sequences were verified using the respective primers employed for fragment amplification (Table 6). Plasmids were transferred into *P. aeruginosa* PAO1 by diparental mating.

construct	primer no. (Table 6)	fragment (bp)	restriction sites	resulting plasmid
P_{PA0919}-*430*	33, 27	430	*KpnI*/*BamHI*	mini-CTX-P_{PA0919}-*430-lacZ*
P_{PA0920}-*206*	34, 27	206	*KpnI*/*BamHI*	mini-CTX-P_{PA0919}-*206-lacZ*
P_{PA0919}-*140*	35, 27	140	*KpnI*/*BamHI*	mini-CTX-P_{PA0919}-*140-lacZ*

Plasmids for the recombinant production of PA0919 in *E. coli*

For recombinant protein production, orf A0919 was cloned (without its predicted native secretion signal sequence for periplasmic localization encoded by amino acids 1 – 34) into vector pET22b(+) (Merck, Darmstadt, Germany). This vector allows for the production of recombinant PA0919 protein fused to an N-terminal *E. coli* PelB secretion signal peptide for periplasmic localization and a C-terminal His_6-tag. The provided T7 promoter was employed for the IPTG dependent protein expression in *E. coli* BL21 (λDE3) (Studier *et al.*, 1990). In a second approach, the identical PA0919 fragment was cloned into pET22b(+)Strep. This vector had been constructed by inserting the annealed oligonucleotides 36 and 37 (Table 6) into the *HindIII*/*XhoI* site of pET22b(+). Vector pET22b(+)Strep was generously provided by T. Nicke (unpublished). The resulting construct codes for a fusion protein with a C-terminal *Strep*-tag II sequence (Schmidt and Skerra, 2007).

The sequence encoding amino acid residues 35 to 427 of the PA0919 protein was amplified by colony-PCR using PAO1 as template (primers 38 and 39, Table 6) and cloned into the *NcoI*/*HindIII* sites of pET22b(+) and pET22b(+)Strep resulting in pET22b(+)PA0919 and pET22b(+)PA0919-Strep, respectively. Insert sequences were verified by sequencing (primers 16 and 52, Table 7).

Plasmids for the mutagenesis of the PA0919 protein

The PA0919 protein was mutated to study the function of specific amino acid residues. In three individual experiments, serine 240, serine 307 and histidine 401 were changed to alanine.

Plasmid pET22b(+)PA0919-Strep was subjected to site-directed mutagenesis. The mutated plasmids pET22b(+)PA0919-S240A-Strep, pET22b(+)PA0919-S307A-Strep and pET22b(+) PA0919-H401A-Strep were obtained (see section 2.4.14) and verified by sequencing (primers 16 and 52, Table 7).

construct	primer no. (Table 6)	mutation	resulting plasmid
PA0919-S240A-Strep	40, 41	S240A	pET22b(+)PA0919-S240A-Strep
PA0919-S307A-Strep	42, 43	S307A	pET22b(+)PA0919-S307A-Strep
PA0919-H401A-Strep	44, 45	H401A	pET22b(+)PA0919-H401A-Strep

Plasmids for the localization of the PA0919 protein in *P. aeruginosa* PAO1 ΔPA0919

For the localization of PA0919 in *P. aeruginosa*, two different approaches were employed: First, the PA0919 encoding sequence was fused to a C-terminal *Strep*-tag II sequence for detection purposes and cloned into the *E. coli* – *P. aeruginosa* shuttle vector pUCP20T (Schweizer *et al.*, 1996) controlled by the native PA0919 promoter P_{PA0919}. This vector provides a lactose inducible promoter upstream of the multiple cloning site and introduced proteins can be expressed as translational LacZ fusion proteins. The empty vector and a construct lacking the PA0919 leader sequence were employed for control. Second, identical constructs (PA0919 fused to *Strep*-tag II controlled by the P_{PA0919} promoter in the presence or absence of the PA0919 signal sequence) were inserted into mini-CTX-PTC for chromosomal integration.

Orf PA0919 was amplified together with its 430 bp upstream region encoding the P_{PA0919} promoter by PCR using genomic DNA for template and cloned into vectors pUCP20T and mini-CTX2-PTC. The resulting pUCP20T/P_{PA0919}-PA0919-Strep was employed as template for site-directed mutagenesis (compare section 2.4.14) using primers 48 and 49 (Table 6) to delete the PA0919 secretion signal (amino acids 1 – 34) yielding pUCP20T/P_{PA0919}-PA0919-Δaa1-35-Strep. The insert was amplified by PCR and cloned into mini-CTX2-PTC resulting in mini-CTX2-P_{PA0919}-PA0919-Δaa1-35-Strep-T. For control, the empty vector pUCP20T was employed. All insert sequences were verified using the employed cloning primers and additionally primers 50 and 51 (for mini-CTX2-PTC derivatives) or 53 and 54 (for pUCP20T variants) listed in Table 7. Plasmids were transferred into *P. aeruginosa* ΔPA0919 by diparental mating.

construct	primer no. (Table 6)	fragment (bp)	restriction sites	resulting plasmid
P_{PA0919}-PA0919-Strep	46, 47	1'756	*KpnI*/*BamHI*	pUCP20T/P_{PA0919}-PA0919-Strep
P_{PA0919}-PA0919-Δaa1-34-Strep	48, 49	1'657	*KpnI*/*BamHI*	pUCP20T/P_{PA0919}-PA0919-Δaa1-34-Strep
P_{PA0919}-PA0919-Strep-T	30, 47	1'756	*SacI*/*BamHI*	mini-CTX2-P_{PA0919}-PA0919-Strep-T
P_{PA0919}-PA0919 Δaa1-34-Strep-T	30, 47	1'657	*SacI*/*BamHI*	mini-CTX2-P_{PA0919}-PA0919-Δaa1-34-Strep-T

2.4.16 Diparental mating

A diparental mating was performed to transfer *E. coli – P. aeruginosa* shuttle vectors (mini-CTX or pUCP20T derivatives) by conjugation from *E. coli* to *P. aeruginosa* strains.

The *E. coli* donor strain ST18 (Thoma and Schobert, 2009) carrying the respective plasmid and the *P. aeruginosa* target strain were cultivated overnight. 1 mL ST18 culture was gently centrifuged (6'000 x g, 1 min, RT) and cells were suspended using 50 µL of the respective *P. aeruginosa* pre-culture. The suspension drop was dried on a LB agar plate and cultivated at 37 °C for 6 h. Then, the cells were collected in 1 mL LB medium and plated on LB agar plates supplemented with the required antibiotics to select *P. aeruginosa* strains containing the respective extrachromosomal plasmid or the chromosomal integrated plasmid sequences in the *attB* locus (Schweizer *et al.*, 1996; Hoang *et al.*, 2000; Becher and Schweizer, 2000).

2.4.17 Construction of markerless *P. aeruginosa* mutant strains

Mini-CTX vector derivatives were designed to integrate a target sequences into the *attB* locus of the *P. aeruginosa* chromosome (Hoang *et al.*, 2000; Becher and Schweizer, 2000).

First, the mini-CTX vector derivative was transferred into *P. aeruginosa* by diparental mating (section 2.4.16) and integrated into the *attB* phage attachment site of the *P. aeruginosa* chromosome promoted by the vector encoded CTX integrase. Second, vector sequences (e.g. the resistance cassette) encoded between the FRT sites were excised. For this, vector pFLP2 encoding the FLP recombinase (Hoang *et al.*, 1998) was introduced into the mini-CTX modified *P. aeruginosa* strains by diparental mating (section 2.4.16). The FLP recombinase promoted the deletion of mini-CTX vector sequences to generate markerless *P. aeruginosa* strains. Subsequently, the pFLP2 plasmid was removed by plating the generated strains on LB agar plates containing 5 % (w/v) D(+)-sucrose. The pFLP2 vector encoded levansucrase (*sacB*) generates the toxic levan from sucrose and cells devoid of vector pFLP2 were obtained. The chromosomal insertion of the target sequence was verified by PCR (primers 19 and 20, Table 7) and the loss of mini-CTX vector sequences and of the pFLP2 plasmid was

revised by plating the strains on agar plates containing the respective antibiotics (mini-CTX: Tet; pFLP2: Cb).

2.4.18 Construction of the *P. aeruginosa* PAO1 ΔPA0919 deletion mutant

Orf PA0919 was deleted from the *P. aeruginosa* PAO1 chromosome by replacement with a Gm resistance cassette using the well-established protocol of Hoang *et al.*, 1998. To yield a markerless deletion strain, the chromosomally integrated Gm cassette was excised afterwards (section 2.4.17; Groenewold, 2011; Hoang *et al.*, 1998).

The gene replacement vector pEX18Ap/ΔPA0919 was transferred into PAO1 by diparental mating (section 2.4.16). Orf PA0919 was replaced by the Gm resistance cassette by homologous recombination within the upstream and downstream region of orf PA0919 also encoded on the gene replacement vector. Target clones became resistant against Gm and were able to grow on D(+)-sucrose containing media (otherwise the presence of the vector encoded *sacB* gene would result in the toxic levan, see section 2.4.17). The employed Gm resistance cassette was flanked by FRT sites. After transferring vector pFLP2 into the obtained *P. aeruginosa* strain, the Gm resistance cassette was excised from the chromosome by the FLP recombinase (compare section 2.4.17 for details) yielding the markerless deletion mutant strain PAO1 ΔPA0919 (Groenewold, 2011).

2.4.19 Construction of complemented *P. aeruginosa* deletion mutant strains

The deletion mutant strains PAO1 ΔPA0920 and PAO1 ΔPA0920 were complemented with various constructs using mini-CTX2-PTC or pUCP20T derivatives. Mini-CTX-*lacZ* derivatives were transferred into the PAO1 wild-type strain for promoter activity analysis. For plasmids and constructions, see section 2.4.15. The plasmids were transferred into the respective *P. aeruginosa* strain by diparental mating (section 2.4.16) and the mini-CTX derivatives were chromosomally integrated into the *attB* locus. The mini-CTX vector sequences were excised by FLP recombinase (section 2.4.17) to yield markerless *P. aeruginosa* strains. Plasmids and resulting strains are summarized in section 2.1.3. The chromosomal insertion was verified by PCR using primers 19 and 20 (Table 7).

Cross-complementation of PAO1 ΔPA0920 with different aaPGS encoding genes

PAO1 ΔPA0920 was complemented using different mini-CTX2 derivatives (mini-CTX2-P-SamprF-T, mini-CTX2-P-BsmprF-T, mini-CTX2-P-EfmprF-T, mini-CTX2-P-PA0920-T and mini-CTX2-P-PA0920aa543-881-T) to generate PAO1 mutant strains with altered lipid compositions. For this, the mini-CTX2 variants were transferred into *P. aeruginosa* PAO1 ΔPA0920 and complemented markerless PAO1 ΔPA0920 mutant strains were generated. The

resulting strains were the homologously complemented strains harboring orf PA0920 (named ΔPa_{comp}) or the truncated PA0920 variant ($\Delta Pa\text{-}aa543\text{-}881_{comp}$), respectively, and the chimeric strains cross-complemented with aaPGS encoding genes from *S. aureus* (ΔSa_{comp}), from *B. subtilis* (ΔBs_{comp}) or from *E. faecium* (ΔEf_{comp}).

Complementation of PAO1 ΔPA0919 with different constructs for functional analysis

PAO1 ΔPA0919 was complemented using different mini-CTX2 derivatives (mini-CTX2-P_{PA0919}-PA0919-T, mini-CTX2-P_{PA0920}-PA0919-T, mini-CTX2-P_{PA0919}-T and mini-CTX2-PTC) to generate PAO1 mutant strains containing orf PA0919 controlled by the formerly characterized P_{PA0920} promoter (Klein *et al.*, 2009) or by the putative P_{PA0919} promoter. For control, both promoters were inserted into PAO1 ΔPA0919, respectively. The unmarked complemented PAO1 ΔPA0919 mutant strains PAO1 ΔPA0919/P_{PA0920}-PA0919-T (abbreviated Δ19 P_{20}-19), PAO1 ΔPA0919/P_{PA0919}-PA0919-T (Δ19 P_{19}-19), PAO1 ΔPA0919/P_{PA0920}-T (Δ19 P_{20}) and PAO1 ΔPA0919/P_{PA0919}-T (Δ19 P_{19}) were obtained.

Strains containing P_{PA0919}-*lacZ* fusions for the analysis of the PA0919-specific promoter

Plasmids mini-CTX-P_{PA0919}-*430-lacZ*, mini-CTX-P_{PA0919}-*206-lacZ* and mini-CTX-P_{PA0919}-*140-lacZ* carrying P_{PA0919} promoter fragments of different length fused to the *lacZ* reporter gene were introduced into the PAO1 wild-type strain for the chromosomal introduction and analysis of the fusion constructs. After the excision of the mini-CTX vector sequences, strains PAO1 P_{PA0919}-*430-lacZ*, PAO1 P_{PA0919}-*206-lacZ* and PAO1 P_{PA0919}-*140-lacZ* were obtained.

Complementation of PAO1 ΔPA0919 with different constructs for PA0919 localization

PAO1 ΔPA0919 was complemented for PA0919 localization experiments using two mini-CTX2-PTC derivatives (mini-CTX2-P_{PA0919}-PA0919-Strep-T, mini-CTX2-P_{PA0919}-PA0919-Δaa1-34-T) and three pUCP20T variants (pUCP20T empty vector, pUCP20T/P_{PA0919}-PA0919-Strep, pUCP20T/P_{PA0919}-PA0919-Δaa1-34-T) to gain mutant strains containing orf PA0919 fused to a *Strep*-tag II under the control of its native P_{PA0919} promoter. Mutant strains devoid of the PA0919 secretion signal were unable to secrete the PA0919-Strep fusion protein. For control, the empty pUCP20T vector was employed. All plasmids were transferred into *P. aeruginosa* ΔPA0919 by diparental mating (section 2.4.16). Mini-CTX2-PTC derivatives were integrated into the chromosomal *attB* locus and vector sequences were removed by the FLP recombinase (sections 2.4.16 and 2.4.17). Finally, the unmarked complemented PAO1 ΔPA0919 mutant strains PAO1 ΔPA0919 pUCP20T (abbreviated Δ19 pUC), PAO1 ΔPA0919 pUCP20T/P_{PA0919}-PA0919-Strep (Δ19 pUC/19), PAO1 ΔPA0919 pUCP20T/P_{PA0919}-PA0919-Δaa1-34-Strep (Δ19 pUC/$19_{35\text{-}427}$), PAO1 ΔPA0919/P_{PA0919}-PA0919-Strep-T (Δ19 19) and PAO1 ΔPA0919/P_{PA0919}-PA0919-Δaa1-34-Strep-T (Δ19 $19_{35\text{-}427}$) were obtained.

2.5 Lipid analysis

Bacterial polar lipids were extracted employing two different protocols based on the method of Bligh and Dyer, 1959. For most gram negative bacteria (except *P. putida,* but also for *K. radiotolerans*), a time-saving variant was used (Garbus *et al.*, 1963), whereas a protocol with extended incubation times (Klein *et al.*, 2009) was employed for gram positive bacilli and *P. putida*. The extracted lipids were separated by two-dimensional thin-layer chromatography (TLC) and visualized by different methods. Radioactively labeled lipids were analyzed either by scintillation counting or autoradiography.

2.5.1 Lipid extraction from gram negative bacteria

For lipid composition analysis, cells of gram negative bacteria (except *P. putida*) or of the gram positive *K. radiotolerans* were harvested by centrifugation (4'000 x g, 20 min, 4 °C) according to the respective culture turbidity (15 mL were sedimented for OD_{578} = 0.6). Cell sediments were suspended in dH_2O in a final volume of 100 µL and mixed intensively with 375 µL methanol/chloroform (2:1, v/v). After centrifugation (11'000 x g, 3 min, RT), 100 µL dH_2O and 100 µL chloroform were added and samples were mixed intensively. Phase separation was promoted by centrifugation (11'000 x g, 3 min, RT), the lower chloroform phase was isolated and evaporated at 40 °C. Dried lipids were stored at –20 °C (Garbus *et al.*, 1963).

2.5.2 Lipid extraction from gram positive bacteria

After harvesting of 500 mL cell culture of gram positive bacteria (except *K. radiotolerans*) or of the gram negative *P. putida*, the cells were washed with 50 mL 50 mM 4-(2-hydoxyethyl)-1-piperazineethanesulfonic acid-(HEPES)-NaOH pH 7.0. The resulting sediments were freeze-dried and stored at –20 °C. For lipid extraction, 100 mg dried cells were suspended in 9.5 mL extraction solution and stirred at 4 °C for at least 16 h. After centrifugation (3'600 x g, 10 min, 4 °C), the supernatant was intensively mixed with 2.5 mL 0.3 % (w/v) NaCl and 2.5 mL chloroform. Phase separation was achieved by centrifugation (3'600 x g, 5 min, 4 °C) and the lower chloroform phase was isolated. The solvent was evaporated and dried lipids were stored at –20 °C (Klein *et al.*, 2009).

extraction solution	chloroform	2.5 mL
	methanol	5.0 mL
	0.3 % (w/v) NaCl	2.0 mL

2.5.3 Lipid separation by two-dimensional TLC

Lipids extracted from gram negative bacteria were dissolved in 20 µL methanol/chloroform (1:1, v/v) and loaded onto a TLC plate (10 x 10 cm; Macherey-Nagel, Düren, Germany). Lipids from gram positive bacteria (and *P. putida*) were solved in 500 µL methanol/chloroform (2:1, v/v) and equal sample volumes were applied to TLC plates.

Lipid separation was carried out at 25 °C. For the first dimension, chloroform/methanol/ water (65:25:4, v/v/v) were employed and, after drying, chloroform/methanol/acetic acid/water (80:12:15:4, v/v/v/v) were used for the second dimension (Tindall, 1990). TLC plates were sprayed with 5 % (w/v) molybdatophosphoric acid (solved in ethanol; Roth, Karlsruhe, Germany) for detecting reducing compounds (e.g. lipids), with ninhydrin (Merck, Darmstadt, Germany) for visualizing amino group containing compounds or with 1.3 % molybdenum blue (Sigma-Aldrich, St. Louis, MO, USA) for verifying phosphate containing molecules, respectively. TLC plates treated with molybdatophosphoric acid and ninhydrin were incubated at 120 °C until lipid spot development (Klein *et al.*, 2009).

Polar lipids were quantified using Gelscan 6.0 software (BioSciTec, Frankfurt, Germany) based on molybdatophosphoric acid stained TLC plates. Overall amounts of polar lipids and aaPG levels were determined and values were related to appropriate references.

2.5.4 Autoradiography analysis

Samples containing ^{14}C-labeled compounds were analyzed either by X-ray film autoradiography analysis or by scintillation counting.

Autoradiography analysis using an X-ray film

For some experiments, radioactive samples containing ^{14}C-labeled compounds were analyzed by TLC followed by molybdatophosphoric acid or ninhydrin staining (see section 2.5.3). To detect specifically ^{14}C-labeled substances, TLC plates were covered with an X-ray film (Fuji Super RX; BEMA, Pleißenberg, Germany). After incubating for several days, X-ray films were developed using the Optimax® X-ray film processor (Protec®, Oberstenfeld, Germany).

Autoradiography analysis by scintillation counting

For scintillation counting analysis, the target substance was dissolved in 30 – 50 µL chloroform/methanol (1:1, v/v), added to 4 mL scintillation cocktail (OptiPhase HighSafe 2; PerkinElmer, Boston, MA, USA) and analyzed using a Tri-Carb® 2900TR scintillation analyzer (PerkinElmer, Boston, MA, USA).

2.6 Amino acid substrate specificity analysis of aaPGS enzymes

For the elucidation of the aminoacyl-tRNA substrate specificity of aaPGS enzymes, native strains harboring aaPGS homologs or *E. coli* strains overproducing aaPGS full-length enzymes or catalytic domains were employed. For *in vivo* activity analysis, cells were cultured under different conditions and polar lipids were extracted and analyzed by two-dimensional TLC (chapter 2.5). Additionally, aaPGS specificities were analyzed using an *in vitro* activity assay according to Hebecker *et al.*, 2011. For this, *E. coli* cells overproducing the respective aaPGS enzyme were grown and lysed. Crude cellular extracts were mixed with ^{14}C-labeled amino acids and an ATP regenerating system. During incubation, the ^{14}C-labeled amino acids were coupled to their respective tRNAs by aminoacyl-tRNA synthetases present in the crude cellular extract. Subsequently, these activated amino acids were transferred to PG by the respective aaPGS homolog. Afterwards, lipids were analyzed by two-dimensional TLC combined with autoradiography (chapter 2.5).

2.6.1 Specificity determination of aaPGS enzymes using native strains

The native strains were cultivated in their respective medium under neutral and acidic conditions. Subsequently, polar lipids were analyzed for to detect the formation of aminoacylated PG.

Media preparation

For the determination of the bacterial membrane lipid composition under neutral and acidic conditions, the pH of the used media was adjusted (for media formulation, see chapter 2.2): In the case of AB medium and SMM, the respective pH was obtained by the addition of the corresponding buffer (AB medium: A10 solution; SMM: SMM basis). LB and R2A media were adjusted to the respective pH value by the addition of 0.1 – 0.3 M sterile HCl (Uhlig, 2011). After pH adjustment, LB and R2A media were buffered in a ratio of 1:10 (v/v) with the appropriate A10 solution (see section 2.2.3). Media with neutral conditions were supplemented with the respective A10 buffer.

Specificity determination of aaPGS enzymes by analyzing the lipid composition of native strains

Media (60 – 500 mL in baffled flasks) were inoculated to an OD_{578} of 0.05 or in a ratio of 1:100 (v/v) employing an overnight pre-culture (*S. thermophilus*: 3 d; Jäger, 2011) and incubated as specified in Table 9. Growth was monitored by OD_{578} measurement and the pH value was controlled using indicator test stripes (Macherey-Nagel, Düren, Germany). Cells were harvested by centrifugation (3'000 – 4'500 x g, 20 min, 4 °C) at an OD_{578} of at least 0.5

and stored at –20 °C (Uhlig, 2011). Alternatively, cells were cultured for 7 h and then the pH was shifted to the originally intended value. Incubation was continued for an additional hour and comparable amounts of cells were harvested (15 mL for a culture with OD_{578} = 0.6) and stored at –20 °C.

Subsequently, polar lipids of the native strains were extracted, separated by two-dimensional TLC and visualized by molybdatophosphoric acid and ninhydrin staining (sections 2.5.1 to 2.5.3).

Table 9: Bacterial strains and parameters for cultivation under different conditions
Cultures were inoculated using an overnight pre-culture and the bacterial strains were cultivated in their respective medium employing the specified parameters (Uhlig, 2011; Jäger, 2011).

Strain	Medium	Cultivation parameters
P. aeruginosa PAO1 *P. aeruginosa* PA14 *P. putida*	AB medium pH 7.5 and pH 5.3	8 – 24 h 37 °C and 180 – 200 rpm
B. licheniformis *B. thuringiensis* *P. polymyxa*	SMM pH 7 and pH 5	8 – 24 h 37 °C and 180 – 200 rpm
K. radiotolerans	LB medium pH 7 and pH 5	3 h or 8 h with the pH shift 37 °C and 180 – 200 rpm
B. phymatum	R2A medium pH 7 and pH 5	8 h with the pH shift 30 °C and 180 – 200 rpm
S. thermophilus	TSB medium pH 7	3 d 37 °C without agitation

2.6.2 Specificity determination of recombinant aaPGS enzymes

The specificity of several aaPGS enzymes was analyzed by recombinant overproduction in *E. coli*. The lipid composition of the respective *E. coli* strains was analyzed to identify aminoacylated PG variants. Alternatively, *E. coli* cells containing recombinant aaPGS enzymes were lysed and subjected to an *in vitro* activity assay according to Hebecker *et al.*, 2011. For this, crude cellular extracted were mixed with radioactively labeled amino acids. During the assay, the amino acids were activated by binding to the respective tRNA and transferred to PG by the employed aaPGS enzyme. Subsequently, polar lipids were extracted and analyzed.

Analysis of the polar lipid composition of *E. coli* cells harboring recombinant aaPGS enzymes

Sequences encoding the C-terminal aaPGS domains from *B. licheniformis* (YfiXΔaa1-518), *S. thermophilus* (StMprFΔaa1-503) and *B. anthracis* (BAS1375 Δaa1-527) were cloned into the expression vectors pGEX-6P-1 and pET22b(+)providing IPTG inducible expression system (compare 2.4.15 and Jäger, 2011). The resulting plasmids (pGEX-6P-1/YfiXΔaa1-518, pGEX-6P-1/StMprFΔaa1-503 and pET22b(+)/BAS1375 Δaa1-527) were transferred into *E. coli* BL21 (λDE3) (Jäger, 2011).

100 mL LB medium (in baffled flasks, supplemented with Ap) were inoculated (1:100, v/v) using an overnight pre-culture of the respective *E. coli* strain. Cells were grown to an OD_{578} of 0.5 at 37 °C and 200 rpm and protein production was induced employing 50 µM IPTG (300 µM for BL21 (λDE3) pGEX-6P-1/StMprFΔaa1-503). The cultivation was continued for 4 h (BL21 (λDE3) pGEX-6P-1/YfiXΔaa1-518, 37 °C) or overnight (BL21 (λDE3) pET22b(+)/BAS1375 Δaa1-527, 25 °C; BL21 (λDE3) pGEX-6P-1/StMprFΔaa1-503, 17 °C). Cells were harvested by centrifugation (4'500 x g, 15 min, 4 °C) and stored at –20 °C. Lipids were analyzed as presented in sections 2.5.1 and 2.5.3 (Jäger, 2011).

Specificity analysis of recombinant aaPGS enzymes using the *in vitro* activity assay

For the recombinant production of several aaPGS enzymes (*B. phymatum* Bphy_4019, *B. thuringiensis* Bthur0008_13400, *K. radiotolerans* Krad_4555, *M. barkeri* Mbar_A2435, *P. polymyxa* Ppoly_aaPGS), the respective orfs were cloned into the pBAD-His-A vector providing the P_{BAD} promoter inducible by L(+)-arabinose (Guzman *et al.*, 1995; for plasmid construction, see section 2.4.15). The obtained plasmids (pBAD-His-A/Bp4019, pBAD-His-A/ Bthur0008_13400, pBAD-His-A/Krad4555, pBAD-His-A/A2435, pBAD-His-A/Ppoly_aaPGS) were transferred into *E. coli* TOP10. For control experiments, the empty pBAD-His-A vector was employed analogously.

E. coli TOP10 strains carrying a pBAD-His-A derivative were grown in 500 mL LB medium (in baffled flasks, supplemented with Ap). Cultures were inoculated from an overnight pre-culture (1:100, v/v) and cultivated at 37 °C and 200 rpm to an OD_{578} of 0.5. Protein production was induced by the addition of 0.2 % (w/v) L(+)-arabinose (Bp4019, Bthur0008_13400, Ppoly_aaPGS) or 2 % (w/v) L(+)-arabinose (Krad4555, Mbar_A2435) and cultivation was continued for 3 h. Cells were harvested by centrifugation (3'000 x g, 20 min, 4 °C), sediments were washed using 50 mM HEPES-NaOH pH 7.8 (4'000 x g, 20 min, 4 °C) and subjected to the *in vitro* analysis.

After recombinant aaPGS production, the *E. coli* cells were suspended in 50 mM HEPES-NaOH pH 7.8 according to their culture turbidity (10 mL buffer were used for an OD_{578} of 2). Crude cellular extracts were obtained by French® Press passage at 19'200 lb/in² and mixed with ATP, the ATP-regenerating system (creatine phosphate, creatine phosphokinase),

[U-^{14}C]-L-lysine and/or [1-^{14}C]-L-alanine (Moravec Biochemicals, Brea, CA, USA) in a final volume of 500 µL. Sample compositions are indicated below. Samples were incubated at 37 °C and 1'000 rpm for 1 h and stored at –20 °C.

Polar lipids were extracted and analyzed by two-dimensional TLC combined with molybdato-phosphoric acid staining. ^{14}C-labeled phospholipids were detected by autoradiography (chapter 2.5).

stock solutions	**volumes (500 µL)**	**final concentration**
100 mM ATP	10 µL	2 mM
500 mM creatine phosphate	18 µM	18 mM
6.7 U/µL creatine phosphokinase	2.6 µL	35 U/mL
2 mM [1-^{14}C]-L-alanine (51 mCi/mmol)	10 µL	40 µM
0.35 mM [U-^{14}C]-L-lysine (288 mCi/mmol)	10 µL	7 µM
crude cellular extract	add to 500 µL	

2.7 Determination of *P. aeruginosa* resistance phenotypes

Several *P. aeruginosa* strains were analyzed concerning their resistance against antimicrobial compounds. In an initial approach, the Phenotype MicroArray™ system from Biolog (Hayward, CA, USA; Bochner, 2009) providing a wide variety of antimicrobials was employed. The initially obtained results were re-evaluated in an independent experimental setup and the observed phenotypes were quantified by determining the minimal inhibitory concentrations (MIC) of selected compounds.

2.7.1 Phenotype MicroArray™ from Biolog

The PAO1 wild-type strain, the PAO1 ΔPA0920 deletion mutant and the respective complemented variants containing aaPGS encoding genes from different organisms (see 2.4.19 for strain construction) were analyzed using the Phenotype MicroArray™ system (Biolog, Hayward, CA, USA; Bochner, 2009). The employed microplates PM9 – PM20 provide sensitivity tests for a wide variety of antimicrobial compounds, pH conditions and salt stress conditions. The plates were inoculated and an applied tetrazolium dye was reduced to the purple formazan by electrons provided by the cells' metabolism during incubation. The dye formation was measured by the OmniLog® system and data were analyzed using the accessory software (Biolog, Hayward, CA, USA). Media and dye were obtained from Biolog (Hayward, CA, USA).

The cells were cultivated on LB agar plates overnight and suspended in several steps in IF-0 medium to a final culture transmission of 85 %. 21 mL IF-10a medium (per microplate) supplemented with the tetrazolium dye (Redox Dye Mix A; 1:100, v/v) were inoculated with

105 µL of the cell suspension according to the manufacturer's instructions. The prepared cell suspension was transferred into microplates PM9 – PM20 (100 µL/well). The inoculated plates were incubated in the OmniLog® incubator at 37 °C for 48 h and dye formation was observed online. Conditions causing differing phenotypes for the wild-type and the mutant strains were chosen for further investigations.

2.7.2 Re-evaluation of the Phenotype MicroArray™ experiments

The Phenotype MicroArray™ experiments (see section 2.7.1) were re-evaluated in an independent experimental setup. Cells (PAO1 wild-type, ΔPA0920 and the respective complemented strains) were grown in the presence of selected compounds identified in the initial Phenotype MicroArray™ experiments in AB medium pH 5.3 to guarantee elevated aaPG levels (Klein *et al.*, 2009). Due to the fact that the tetrazolium dye system employed for the Phenotype MicroArray™ experiments was not appropriate under acidic conditions (Johno *et al.*, 2010), cell growth was monitored by culture turbidity determination.

Bacterial cells were grown overnight in AB medium pH 7.3 and suspended to a transmission of 85 %. In analogy to the Phenotype MicroArray™ experiments, 17.5 mL AB medium pH 5.3 (per microplate) were inoculated with 100 µL of the cell suspension and 96-well microplates (Sarstedt, Nümbrecht, Germany) prepared with different inhibitory compounds in varying concentrations were inoculated. The plates were covered with a gas permeable membrane (Breathe-Easy™ sealing membrane; Diversified Biotech, Dedham, MA, USA) and incubated without shaking at 37 °C for 18 h. Growth was determined by measuring the culture turbidity in the absence of the membrane at 595 nm employing the Model 680 microplate reader (Bio-Rad, Munich, Germany).

2.7.3 MIC determination

MICs were determined using a modified microdilution method according to Andrews, 2001. Cells were grown to late exponential phase, diluted to a specific OD_{578} and 96-well plates prepared with gradually varying inhibitor concentrations were inoculated. After incubation, the culture turbidity was determined. With this experimental setup, MICs were determined by gradually narrowing the respective antimicrobial compound's concentration.

Strains were grown in AB medium pH 7.3 overnight. 25 mL AB medium pH 5.3 were inoculated to OD_{578} = 0.05 and cultivated at 37 °C and 200 rpm for 4 h to the late exponential growth phase. Cultures were diluted to OD_{578} = 0.2 using AB medium pH 5.3. 96-well plates (Sarstedt, Nümbrecht, Germany) were prepared as follows: each well contained 100 µL of the respective antimicrobial compound in varying concentrations (aqueous solution) mixed with 50 µL of AB medium (pH 5.3, threefold concentrated). For each antimicrobial concentration, identical wells were prepared in quadruplicate. The plates were inoculated

with 50 µL cell suspension, covered with a gas permeable membrane (Breathe-Easy™ sealing membrane; Diversified Biotech, Dedham, MA, USA) and incubated in a plate incubator (PHMP-4; Grant bio, Cambridgeshire, UK) at 37 °C and 350 rpm. After 18 h, the sealing membrane was removed and bacterial growth was monitored by measuring the OD_{595} with a microplate reader (Model 680; Bio-Rad, Munich, Germany).

The lowest antimicrobial compound concentration that resulted in an $OD_{595} < 0.05$ ($OD_{595} < 0.1$ for daptomycin employing the ΔPA0920 complemented strains) was defined as the MIC. For protamine sulfate, the lowest concentration resulting in a constant OD_{595} minimum level was employed. Concentration intervals were successively adjusted to the final MICs of the respective compound.

For determining the relevance of the obtained results, the experiments were reproduced independently for at least three times. Standard deviations were evaluated based on OD_{595}-concentration plots resulting in values of approximately 5 % (10 % for protamine sulfate and daptomycin). Significance analysis was performed employing a paired Student's *t* test (McDonald, 2009).

2.8 Promoter activity analysis

Promoter activities of the P_{PA0920} and the putative P_{PA0919} promoter were performed using promoter-*lacZ* reporter gene fusions chromosomally introduced into the PAO1 wild-type strain. Cells were grown under distinct conditions and the β-galactosidase activity was determined by the method of Miller, 1992.

2.8.1 Promoter activity determination using the β-galactosidase activity assay

Conventionally, promoter activities are determined by the β-galactosidase activity assay employing promoter-*lacZ* fusions. Cells are cultivated under specific conditions, harvested and disrupted. The liberated β-galactosidase cleaves the artificial substrate 2-nitrophenyl-β-D-galactopyranoside (ONPG) into galactose and 2-nitrophenolate which can be determined photometrically and indicates the activity of the promoter of interest (Miller, 1992).

Frozen cell pellets were thawed and suspended in 800 µL Z-buffer. If necessary, 5 µL 10 mg/mL lysozyme were added and samples were incubated at 30 °C for 30 min. 10 – 15 µL 0.1 % SDS and 10 – 15 µL chloroform were added, samples were intensively mixed and incubated at 30 °C for 5 min. 200 µL 4 mg/mL ONPG (Sigma-Aldrich, St. Louis, MO) were added and incubation was continued at 30 °C until the sample became yellow. The reaction was stopped using 500 µL 1 M Na_2CO_3 and cell debris was sedimented for 10 min at

11'000 x g. The absorption of the supernatant was measured at 420 nm. The β-galactosidase activity was calculated in Miller Units (MU) as follows with t representing the incubation time, OD_{578} the culture turbidity and V the sample culture volume (Miller, 1992):

$$\text{β-galactosidase activity [MU]} = \frac{OD_{420}}{t\,[\text{min}] \times OD_{578} \times V\,[\text{mL}]} \times 1000$$

Z-buffer	Na_2HPO_4	60 mM
	NaH_2PO_4	40 mM
	KCl	10 mM
	$MgSO_4$	1 mM
	β-mercaptoethanol	50 mM

2.8.2 Analysis of the P_{PA0920} promoter in the presence of antimicrobial agents

The promoter upstream of orf PA0920 (P_{PA0920}) was analyzed before (Klein *et al.*, 2009) and it was found activated under acidic growth conditions. In this work, the response of the P_{PA0920} promoter to several antimicrobial agents was analyzed. Strain PAO1-P_{PA0920}-*lacZ* containing a transcriptional P_{PA0920}-*lacZ* gene fusion integrated into the *attB* locus of the PAO1 chromosome (Klein *et al.*, 2009) was grown under acidic and neutral conditions and treated with the respective antimicrobials. For control, strain PAO1 KS11 harboring the *lacZ* gene without a controlling promoter in the *attB* site of the PAO1 chromosome was employed (Schreiber *et al.*, 2006). The promoter activity was determined by measuring the β-galactosidase activity (see section 2.8.1).

The presence of antimicrobial agents might influence cell morphologies (Fonseca and Sousa, 2007; Soboh *et al.*, 1995). Therefore, the β-galactosidase activity calculation based on culture turbidity determination (OD_{578}) might provide deviating results. For this, the obtained β-galactosidase activities were also related to the overall bacterial protein content determined by the Bradford method (Irie *et al.*, 2010). All experiments were performed in triplicate.

60 mL AB medium (pH 5.3 and pH 7.3, in baffled flasks) were inoculated to an OD_{578} of 0.05 using an overnight culture (AB medium pH 7.3) and incubated at 37 °C and 200 rpm for 2 h to accustom the cells to the specific pH conditions. Subsequently, the antimicrobial compounds were added and the incubation was continued for additional 4 h. For control, strains were incubated without antimicrobials. 2 h and 4 h after compound application, samples for the determination of the β-galactosidase activity and the protein content were taken in duplicate (11'000 x g, 10 min, RT; pellets were stored at –20 °C) and the cell morphology was investigated. The employed subinhibitory concentrations allowed for an

appropriate growth of the PAO1 derivatives and were chosen as follows: 1/4 of the MIC of the wild-type strain was employed for ampicillin (75 µg/mL), oxacillin (3 mg/mL), cefsulodin (15.25 µg/mL), protamine sulfate (25 µg/mL), poly-L-lysine (4.5 µg/mL) and domiphen bromide (2.48 µg/mL). 1/6 of the MIC was used for polymyxin E (1.33 µg/mL), 1/8 of the MIC for daptomycin (1.5 mg/mL) and 1/12 of the MIC for benzethonium chloride (2.58 µg/mL). The β-galactosidase activity was determined as described above (section 2.8.1).

For the determination of the total protein content, frozen cell pellets were thawed, suspended in 60 – 600 µL 50 mM NaOH and cells were lysed at 95 °C and 1400 rpm for 5 min. Cell debris was sedimented (11'000 x g, 10 min, RT) and 30 µL of the supernatant were mixed with 1 mL Bradford reagent and incubated at RT for 10 min according to the manufacturer's instructions (Sigma-Aldrich, St. Louis, MO). The absorption at 595 nm was measured and the β-galactosidase activity was calculated based on the overall protein content instead of the culture turbidity (see above).

Promoter activities determined for the promoter-less KS11 strain representing the experimental background were subtracted from the respective P_{PA0920} promoter activity. To evaluate the effects of the antimicrobial agents under all employed conditions (pH, antimicrobial agent, growth phase) the promoter activity of strains treated with antibiotics was related to the activity in the absence of any compound resulting in an induction ratio. Standard deviations were calculated according to Taylor, 1997.

To verify if the determined promoter activities resulted in alterations of the lipid composition, the lipid composition of the KS11 control strain was determined under specific conditions using the following antimicrobials: ampicillin and oxacillin (1/4 MIC; pH 7.3, 4 h; pH 5.3, 2 h), protamine sulfate (1/4 MIC; pH 7.3, 2 h; pH 5.3, 2 h) and polymyxin E (1/6 MIC; pH 7.3, 4 h; pH 5.3, 2 h). Lipids were extracted and analyzed as described in sections 2.5.1 and 2.5.3.

2.8.3 P_{PA0919} promoter analysis

The putative P_{PA0919} promoter located upstream of orf PA0919 was analyzed employing several PAO1 strains containing chromosomally integrated transcriptional promoter-reporter gene fusion constructs with varying promoter fragment sizes (PAO1 P_{PA0919}-*430-lacZ*, PAO1 P_{PA0919}-*206-lacZ* and PAO1 P_{PA0919}-*140-lacZ*, compare section 2.4.19). Strain PAO1 KS11 harboring the *lacZ* gene in the absence of any promoter sequence was used for control (Schreiber *et al.*, 2006). All experiments were performed at least in triplicate.

Strains were grown in 60 mL AB medium (pH 7.3 and pH 5.3) in baffled flasks at 37 °C and 200 rpm. Cultures were inoculated out of an overnight culture (AB medium pH 7.3) to OD_{578} = 0.05 and incubated for 24 h. At distinct time points, samples were taken in duplicate and the culture turbidity was measured at 578 nm. The β-galactosidase activity was determined employing the conventional assay (section 2.8.1).

Promoter activities were calculated by subtracting values obtained for the promoter-less control strain KS11 from the respective P_{PA0919} values. Standard deviations were calculated according to Taylor, 1997. Significance was assessed using a paired Student's *t* test (McDonald, 2009).

2.9 PA0919 protein production and purification

The PA0919 protein and its derivatives were recombinantly produced in *E. coli* cells. The protein was synthesized fused to an N-terminal PelB secretion signal sequence and to a C-terminal His_6-tag or *Strep*-tag II. During the recombinant production, the PA0919 fusion protein was secreted into the *E. coli* periplasm (compare section 2.4.15). Cells were treated with polymyxin B to obtain the periplasmic fraction and the protein was isolated by affinity chromatography.

2.9.1 Production of recombinant PA0919 protein

The recombinant PA0919 protein was produced by transferring pET22b(+)PA0919 or pET22b(+)PA0919-Strep derivatives into *E. coli* BL21 (λDE3), protein expression was induced with IPTG and the protein derivatives were secreted into the *E. coli* periplasm (compare section 2.4.15).

500 mL LB medium (in baffled flasks, supplemented with Ap) were inoculated employing an overnight culture in a ratio of 1:100 (v/v). Cultures were incubated at 37 °C and 200 rpm to an OD_{578} of 0.5 to 0.6. After shifting the incubation temperature to 17 °C, protein production was induced by 25 µM IPTG and cultivation was continued overnight. Cells were harvested by centrifugation (3'000 x g, 20 min, 4 °C) and suspended in harvesting buffer containing D(+)-sucrose for spheroblast stabilization (Quan *et al.*, 2013). After sedimentation (4'000 x g, 30 min, 4 °C), the obtained cell pellets were stored at –20 °C (Sambrook and Russell, 2001).

harvesting buffer	HEPES-NaOH pH 8.0	50 mM
	NaCl	150 mM
	D(+)-sucrose	20 % (w/v)

2.9.2 Isolation of the periplasmic fraction

Recombinant PA0919 protein variants were isolated from the *E. coli* periplasm by treating the cells with polymyxin B and by stabilizing the spheroblast with sucrose combining two methods described by Quan *et al.*, 2013.

Frozen *E. coli* pellets containing overexpressed PA0919 protein variants (see section 2.9.1) were thawed on ice for 1 h. Cells were suspended in isolation buffer (twofold pellet volume) and incubated with agitation at 4 °C for 1.5 h. Cell debris was removed by centrifugation (20'000 x g, 1.5 h, 4 °C) and the supernatant representing the isolated soluble periplasmic fraction was separated.

isolation buffer	HEPES-NaOH pH 8.0	50 mM
	NaCl	150 mM
	D(+)-sucrose	20 % (w/v)
	polymyxin B	2 mg/mL

2.9.3 Purification of His_6-tagged PA0919 protein

The isolated periplasmic fraction containing recombinant His_6-tagged PA0919 protein was employed to purify the target protein by chromatography using a Ni-nitrilotriacetic acid (NTA) agarose containing column. The protein was specifically bound to the resin and eluted by imidazole after an extensive washing step (Sambrook and Russell, 2001). Protein purification was performed at 4 °C.

A Poly-Prep chromatography column (BioRad, Munich, Germany) containing 0.5 mL Protino® Ni-NTA agarose (Macherey-Nagel, Düren, Germany) was washed extensively with dH_2O and equilibrated with 10 column volumes (CV) of washing buffer. The isolated periplasmic fraction (section 2.9.2) was mixed carefully with the appropriate amount of 4 M NaCl to increase the NaCl concentration to the optimized value of 300 mM and incubated at 4 °C for 15 min. The periplasmic fraction was loaded onto the Ni-NTA agarose column. After extensive washing (10 CV washing buffer) and a pre-elution step (4 CV pre-elution buffer), the His_6-tagged PA0919 protein was eluted with 5x 2 CV elution buffer and stored at 4 °C.

The Ni-NTA agarose column was regenerated employing 2 CV column buffer followed by 2 CV 6 M guanidine hydrochloride. After extensive washing with 10 CV dH_2O, 2 CV 100 mM $NiSO_4$ were loaded onto the column followed by additional washing with 5 CV dH_2O. The regenerated column was either employed directly or washed with 20 % ethanol and stored at 4 °C (modified according to the manufacturer's instructions and Sambrook and Russell, 2001).

washing buffer	HEPES-NaOH pH 8.0	50 mM
	NaCl	300 mM

pre-elution buffer	HEPES-NaOH pH 8.0	50 mM
	NaCl	300 mM
	imidazole	15 mM
	re-adjusted to pH 8.0 after imidazole application	
elution buffer	HEPES-NaOH pH 8.0	50 mM
	NaCl	300 mM
	imidazole	300 mM
	re-adjusted to pH 8.0 after imidazole application	
column buffer	Tris-HCl pH 8.0	20 mM
	NaCl	500 mM
	EDTA pH 8.0	50 mM

2.9.4 Purification of *Strep*-tagged PA0919 protein

For the purification of *Strep*-tagged PA0919 variant proteins, the isolated periplasmic fraction (section 2.9.2) was mixed with avidin to mask biotinylated proteins. Samples were loaded onto a *Strep*-Tactin® resin containing column and the PA0919 variant proteins were isolated by desthiobiotin-dependent elution according to the manufacturer's instructions. Protein purification was performed at 4 °C.

Poly-Prep chromatography columns (BioRad, Munich, Germany) were prepared with 1 mL *Strep*-Tactin® Superflow® high capacity resin (IBA, Göttingen, Germany) and equilibrated with 2x 5 CV washing buffer. The isolated soluble periplasmic fraction (section 2.9.2) was mixed gently with 0.4 µM avidin (Calbiochem® by Merck, Darmstadt, Germany) and stored at 4 °C for 15 min. The periplasmic fraction was loaded onto the column and after two washing steps (2x 5 CV washing buffer), the protein was eluted with 5x 1 CV elution buffer. The obtained protein was stored at 4 °C.

Columns containing the *Strep*-Tactin® Superflow® high capacity resin were regenerated according to the manufacturer's instructions employing 3x 5 CV regeneration buffer (IBA, Göttingen, Germany) while the color of the column turned from white to yellow. The columns were washed with column washing buffer I until the yellow color was removed. 5 CV column washing buffer II were used to restore pH conditions. *Strep*-Tactin® Superflow® high capacity columns were stored either in regeneration buffer or in column washing buffer II at 4 °C.

washing buffer	HEPES-NaOH pH 8.0	50 mM
	NaCl	100 mM
elution buffer	HEPES-NaOH pH 8.0	50 mM
	NaCl	100 mM
	desthiobiotin	2.5 mM

regeneration buffer	Tris-HCl pH 8.0	100 mM
	NaCl	150 mM
	EDTA	1 mM
	2-(4'-hydroxyl-benzeneazo)benzoic acid (HABA)	1 mM
column washing buffer I	Tris-HCl pH 10.5	100 mM
	NaCl	150 mM
	EDTA	1 mM
column washing buffer II	Tris-HCl pH 8.0	100 mM
	NaCl	150 mM
	EDTA	1 mM

2.9.5 Dialysis

Strep-tagged PA0919 variant proteins were dialyzed to exchange the employed buffer system. Protein containing elution fractions were dialyzed against at least 250 volumes of dialysis buffer employing a dialysis membrane (dialysis tubing membrane visking, molecular weight cutoff of 14 kDa; Roth, Karlsruhe, Germany) at 4 °C for at least 2 h. After dialysis buffer exchange, the procedure was continued at 4 °C for at least 2 h. The obtained protein was stored at 4 °C.

dialysis buffer	HEPES-NaOH pH 6.8	20 mM

2.9.6 Protein concentration

If necessary, protein samples were concentrated up to 3 mg/mL using an Amicon® Ultra-0.5 device exhibiting a nominal molecular weight limit of 10'000 (Merck, Darmstadt, Germany) according to the manufacturer's instructions.

2.10 Protein biochemical methods

Protein biochemical techniques used to characterize the PA0919 protein and its derivatives in this study are summarized in the following sections.

2.10.1 Protein concentration determination

Protein concentrations in solution were determined according to the method of Bradford, 1976. The dye Coomassie Brilliant Blue G250 forms a complex with proteins and its maximal absorption shifts from 465 to 595 nm.

30 µL protein-containing sample were mixed with 1 mL Bradford reagent (Sigma-Aldrich, St. Louis, MO, USA), incubated for 10 – 15 min and the absorbance at 595 nm was determined according to the manufacturer's instructions. Highly concentrated protein samples were diluted employing the respective protein buffer and bovine serum albumin (Roth, Karlsruhe, Germany) dissolved in the corresponding protein buffer was used for calibration.

2.10.2 Discontinuous SDS polyacrylamide gel electrophoresis (SDS-PAGE)

The discontinuous SDS-PAGE was employed to analyze protein samples under denaturing conditions. The proteins were denatured by SDS and β-mercaptoethanol treatment and separated according to their molecular weight (Laemmli, 1970; Sambrook and Russell, 2001).

Cell sediments of 1 mL bacterial culture taken during cultivation to monitor protein expression were suspended in 50 µL dH_2O and mixed with 50 µL SDS loading dye. 20 µL of samples containing soluble proteins were mixed with 20 µL SDS loading dye. All samples were incubated at 95 °C for 10 min for cell disruption and protein denaturation and loaded onto the SDS polyacrylamide gel. Samples from membrane fractions were treated at 40 °C for 30 min to prevent protein aggregation (Klein *et al.*, 2009). The Unstained Protein Molecular Weight Marker was employed as a protein size standard and the PageRuler™ Prestained Protein Ladder was used for gels subjected to Western Blot analysis (Thermo Fisher Scientific, Waltham, MA, USA). Electrophoresis was performed at 45 mA per gel. For protein band visualizing, the gels were treated with staining and de-staining solutions (Laemmli, 1970; Sambrook and Russell, 2001).

running gel, 12 % (w/v)	Rotiphorese® Gel 30	8 mL
	1.5 M Tris-HCl pH 8.8, 0.4 % (w/v) SDS	5 mL
	10 % (w/v) ammonium peroxodisulfate	200 µL
	N,N,N',N'-tetramethylethylenediamine	20 µL
	dH_2O	7 mL
	sufficient for preparing 4 gels	

stacking gel, 6 % (w/v)	Rotiphorese® Gel 30	2 mL
	0.5 M Tris-HCl pH 6.8, 0.4 % (w/v) SDS	2.5 mL
	10 % (w/v) ammonium peroxodisulfate	100 µL
	N,N,N',N'-tetramethylethylenediamine	10 µL
	dH_2O	5.5 mL
	sufficient for preparing 4 gels	
SDS loading dye	Tris-HCl pH 6.8	100 mM
	glycerol	40 % (w/v)
	β-mercaptoethanol	2 % (v/v)
	SDS	3.2 % (w/v)
	bromophenol blue	0.2 % (w/v)
electrophoresis buffer	Tris-HCl pH 8.8	50 mM
	glycine	385 mM
	SDS	0.1 % (w/v)
staining solution	acetic acid	10 % (v/v)
	ethanol	30 % (v/v)
	Coomassie Brilliant Blue G250	0.25 % (w/v)
de-staining solution	acetic acid	10 % (v/v)
	ethanol	30 % (v/v)

2.10.3 Western Blot

The Western Blot procedure was employed to prepare protein samples for N-terminal sequence determination or to detect specific proteins.

Protein samples were separated by SDS-PAGE and unstained gels were equilibrated in Towbin buffer for 15 min. The polyvinylidene difluoride (PVDF) membrane (0.45 µm pore size; Millipore, Merck, Darmstadt, Germany) was washed with methanol for 10 min and equilibrated in Towbin buffer for 15 min. The semi-dry TransBlot® SD system (BioRad, Munich, Germany) was assembled and the proteins were transferred to the membrane at 10 V for 40 min according to the manufacturer's instructions. Alternatively, the Trans-Blot® Turbo™ system (BioRad, Munich, Germany) was employed at 25 V for 17 min. After de-assembly, the membrane was washed with dH_2O.

For protein sequence determination purposes, the blotted proteins were stained with Ponceau S solution and bands of interest were excised from the membrane.

Towbin buffer	Tris-HCl pH 9.5	25 mM
	glycine	192 mM
	methanol	15 % (v/v)

Ponceau S solution	Ponceau S	0.4 % (w/v)
	trichloricacetic acid	3 % (w/v)
	sulfosalicylic acid	3 % (w/v)

2.10.4 Amino acid sequence determination

For the determination of the N-terminal amino acid sequence according to Edman, 1950, the isolated protein was removed from the membrane and the sequence was analyzed step-by-step. During one reaction cycle, phenyl isothiocyanate binds to the N-terminal amino group of the protein under specific reaction conditions. By changing the conditions, the peptide bond linking the first to the second amino acid is cleaved into a phenyl thiohydandoin and the protein lacking its N-terminal amino acid. The protein is removed and the amino acid is released from the phenyl thiohydandoin by changing the reaction conditions and analyzed afterwards (Edman, 1950). This work was kindly performed by Beate Jaschok-Kentner at the Helmholtz Centre for Infection Research, Braunschweig, Germany.

2.10.5 Immunochemical-like detection of *Strep*-tagged PA0919 protein

The PA0919 protein fused to the *Strep*-tag II was detected on the Western Blot membrane using a *Strep*-Tactin® alkaline phosphatase conjugate in an immunochemical-like detection procedure according to the manufacturer's instructions.

The membrane was incubated with agitation in blocking buffer at RT for 1 h or alternatively at 4 °C overnight. After washing with PBST buffer (3x 20 mL, 5 min, RT), the membrane was incubated with agitation with 10 mL PBST buffer supplemented with 10 µL 2 mg/mL avidin (Calbiochem® by Merck, Darmstadt, Germany) at RT for 10 min to mask biotinylated proteins. 2.5 µL *Strep*-Tactin® AP conjugate (IBA, Göttingen, Germany) were added and incubation was continued for 1 h. After washing with PBST buffer (2x 20 mL, 1 min) and with PBS buffer (2x 20 mL, 1 min), the membrane was equilibrated using 15 mL substrate buffer for 10 min. The substrate buffer was exchanged and 49.5 µL of each 5-bromo-4-chloro-3-indolyl phosphate (BCIP) and nitrotetrazolium blue (NBT) were added for dye formation by alkaline phosphatase. The membrane was incubated with gentle agitation until protein bands were visible and the reaction was arrested by transferring the membrane into dH_2O.

PBS buffer	KH_2PO_4	4 mM
	Na_2HPO_4	16 mM
	NaCl	115 mM
	adjusted to pH 7.4 with phosphoric acid	
PBST buffer	Tween® 20	0.1 % (v/v)
	solved in PBS buffer	

blocking buffer	bovine serum albumine	3 % (w/v)
	Tween® 20	0.5 % (v/v)
	solved in PBS buffer	
substrate buffer	Tris-HCl pH 8.8	100 mM
	NaCl	100 mM
	$MgCl_2$	5 mM
BCIP	BCIP	50 mg/mL
	solved in 100 % dimethylformamide	
NBT	NBT	100 mg/mL
	solved in 70 % dimethylformamide	

2.10.6 Determination of the PA0919 native molecular mass

The native molecular mass of the PA0919 protein was determined by analytical gel permeation chromatography. The purified, dialyzed and *Strep*-tagged PA0919 protein and several protein standards employed for calibration (carbonic anhydrase, M_r: 29'000; bovine serum albumin, M_r: 66'000; yeast alcohol dehydrogenase, M_r: 150'000; β-amylase, M_r: 200'000) were analyzed using a Superdex 200 5/150 GL chromatography column (GE Healthcare, Munich, Germany). Approximately 50 µg of protein were loaded onto the column and eluted using a flow rate of 0.45 mL/min. Protein elution was detected *via* the absorption at 280 nm. The native molecular mass of the PA0919 protein was calculated by comparing elution volumes of the sample and the standard proteins.

buffer	Tris-HCl pH 7.5	20 mM
	NaCl	200 mM
	$MgCl_2$	0.5 mM
	glycerol	5 % (w/v)
	dithiotreitol	2 mM

2.10.7 Spectroscopic cofactor analysis

The presence of chromogenic cofactors was analyzed by absorption and fluorescence spectra measurement (Schmid, 2001; Lakowicz, 2006).

The purified, dialyzed and *Strep*-tagged PA0919 protein (approximately 3 mg/mL) was analyzed by UV-visible light spectroscopy (260 – 900 nm) employing a V-650 spectrometer (Jasco, Groß Umstadt, Germany) and by fluorescence spectroscopy (excitation: 250 – 450 nm, emission: 250 – 800 nm) using a LS50B luminescence spectrometer (PerkinElmer, Boston, MA, USA).

2.10.8 Inductively coupled plasma – mass spectrometry (ICP-MS)

For the determination of protein-associated metal ions, the purified, dialyzed and *Strep*-tagged PA0919 protein (8 mg/mL, 180 µM) was analyzed by ICP-MS performed by Currenta (Leverkusen, Germany) concerning the metal ions Cu^{2+}, Fe^{2+}, Mg^{2+}, Mn^{2+}, Ni^{2+} and Zn^{2+}(and others). The detection limit of 0.1 mg/kg was declared by the provider.

2.10.9 Protein lipid overlay assay

The binding of the PA0919 protein to selected membrane lipids was analyzed by performing a protein lipid overlay assay (Dowler *et al.*, 2002). A hydrophobic membrane providing selected membrane lipids was incubated with *Strep*-tagged PA0919 wild-type protein. After extensive washing, bound PA0919 protein was detected *via* its *Strep*-tag II using a protocol differing slightly from the manufacturer's instructions.

For positive control, 10 µg purified, dialyzed and *Strep*-tagged PA0919 wild-type protein was spotted onto the employed Membrane Lipid Strip™ P-6002 (Echelon Biosciences, Salt Lake City, UT, USA). The membrane was dried and incubated with 10 mL PBST buffer (PBS-Tween® tablets; Medicago, Uppsala, Sweden) supplemented with 3 % (w/v) bovine serum albumine at 4 °C overnight. The PA0919 protein (10 µg/mL) was added and incubation was continued to support protein-lipid binding at 4 °C overnight. The membrane was washed with PBS (5x, 10 min) and incubated in 10 mL PBS supplemented with 2.5 µL *Strep*-Tactin® AP conjugate (IBA, Göttingen, Germany) for 1 h. After additional washing with PBS (4x, 10 min), the membrane was equilibrated in 10 mL AP buffer for 10 min. The AP buffer was exchanged and the detection reaction was started by the addition of 33 µL NBT and 66 µL BCIP (see section 2.10.5). After sufficient dye formation, the reaction was arrested by transferring the membrane into dH_2O.

PBS buffer	KH_2PO_4	4 mM
	Na_2HPO_4	16 mM
	NaCl	115 mM
	adjusted to pH 7.4	
AP buffer	Tris-HCl pH 8.0	100 mM
	NaCl	100 mM
	$MgCl_2$	5 mM

2.10.10 Binding of ^{14}C-labeled alanine

For the investigation of the PA0919 alanine binding capacity, purified, dialyzed and *Strep*-tagged protein variants were bound to *Strep*-Tactin® resin and incubated with ^{14}C-labeled alanine. After extensive washing, the protein was eluted and the radioactivity of the obtained samples was determined by scintillation counting.

Portions of 0.1 mL *Strep*-Tactin® Superflow® high capacity resin (IBA, Göttingen, Germany) were equilibrated with column buffer and incubated with 0.1 mL of a solution containing 50 µM PA0919 wild-type or PA0919 S307A mutant protein for 15 min. For control, a sample without protein was handled analogously. Resins were washed using 0.5 mL washing buffer, mixed with 0.1 mL 100 µM [1-^{14}C]-L-alanine (Moravec Biochemicals, Brea, CA, USA) and incubated with gentle agitation for 1 h. After separating the radioactive solution, the resin was washed twice with 0.5 mL washing buffer to remove unbound ^{14}C-labeled alanine. The resin was suspended in 0.2 mL elution buffer and the complete mixture was transferred into 4 mL scintillation solution (OptiPhase HighSafe 2; PerkinElmer, Boston, MA, USA). Samples taken during the loading and washing procedure and the resin samples were analyzed by scintillation counting (TriCarb® 2900TR, PerkinElmer, Boston, MA, USA).

washing buffer	HEPES-NaOH pH 8.0	50 mM
	NaCl	100 mM
elution buffer	HEPES-NaOH pH 8.0	50 mM
	NaCl	100 mM
	desthiobiotin	2.5 mM

2.11 PA0919 *in vitro* activity analyses

The PA0919 protein was analyzed *in vitro* employing various *p*-nitrophenol derivatives to elucidate its substrate specificity. The identified substrate analog was employed to determine the catalytically active amino acids of the PA0919 protein using highly specific inhibitory substances. Finally, the PA0919 *in vitro* activity was analyzed in the presence of the putative native substrate A-PG.

2.11.1 Substrate specificity analysis

For the determination of PA0919 substrate specificity, an *in vitro* activity assay was performed employing artificial chromogenic *p*-nitrophenol derivative substrates. When these substances are hydrolyzed, the product formation of *p*-nitrophenolate can be determined by measuring the absorption at 400 nm (Max *et al.*, 2012). All experiments were performed in triplicate.

The chromogenic substrates Ala-ONp, Gly-ONp, Ac-Gly-ONp, Boc-Ala-ONp, Ala-pNA (Bachem, Bubendorf, Switzerland), 4-nitrophenyl butyrate, 4-nitrophenyl acetate and 4-nitrophenyl phosphate (Sigma-Aldrich, St. Louis, MO, USA) were commercially available. Instead, Lys-ONp was synthesized *de novo* by H. Kuhz and Dr. J. S. Dickschat (Institute for Organic Chemistry, Technische Universität Braunschweig, Braunschweig, Germany) by combining the methods of Ke *et al.*, 2009, and Schnabel, 1964 (compare Figure 5).

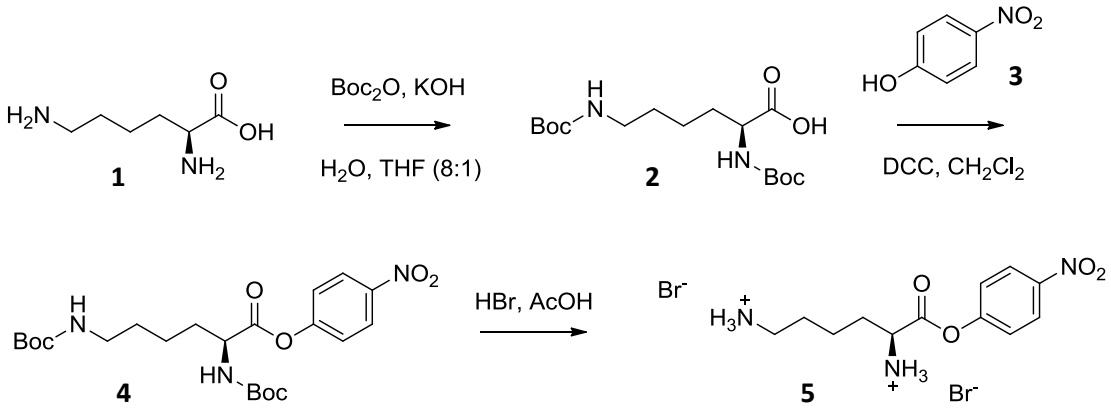

Figure 5: Synthesis of Lys-ONp (kindly provided by J. S. Dickschat)
For the synthesis of Lys-ONp, L-lysine (**1**) was solved with KOH in a mixture of H_2O and THF. Boc_2O was added carefully and the mixture was stirred at 50 °C for 14 h. For product isolation, the mixture was acidified with HCl and extracted with EtOAc. Extracts were pooled, dried by $MgSO_4$ and concentrated *in vacuo*. After column chromatography (silica gel, hexane/EtOAc 2:1; v/v), the product *N*,*N'*-di-(*tert*-butyloxycarbonyl)-L-lysine (**2**) was obtained. The product was solved in CH_2Cl_2, *p*-nitrophenol (**3**) and DCC were added and the mixture was stirred at RT overnight. The precipitate was isolated and washed with CH_2Cl_2 and, after solvent removal, the *p*-nitrophenyl ester of *N*,*N'*-di-(*tert*-butyloxycarbonyl)-L-lysine (**4**) was obtained. After adding a mixture of HBr and acetic acid and stirring at RT for 2 h, the precipitated product L-lysine *p*-nitrophenylester dihydrobromide (**5**, Lys-ONp) was isolated, washed with EtOAc and dried.
Figure and information were generously provided by Dr. J. S. Dickschat.
THF: tetrahydrofuran, Boc_2O: di-*tert*-butyl dicarbonate, DCC: dicyclohexylcarbodiimide.

The amino groups of the basic compound L-lysine (**1**) were protected by the addition of *tert*-butyloxycarbonyl (Boc) groups. The resulting *N*,*N*'-di-(*tert*-butyloxycarbonyl)-L-lysine (**2**) was esterified with *p*-nitrophenol (**3**) under carboxylic acid activation by dicyclohexylcarbodiimide (DCC). The protecting Boc groups were removed by hydrobromic acid treatment yielding Lys-ONp dihydrobromide (**5**).

For the *in vitro* activity assay, the chromogenic substrates were dissolved in dimethyl sulfoxide (DMSO) and dialysis buffer was employed for 4-nitrophenol phosphate. Purified, dialyzed and *Strep*-tagged PA0919 protein was diluted using dialysis buffer and mixed with the respective chromogenic *p*-nitrophenol derivative at RT in a final volume of 300 µL to start the *in vitro* activity assay. Immediately after mixing, the *p*-nitrophenolate formation was monitored by measuring the absorption at 400 nm (V-650 spectrometer; Jasco, Groß Umstadt, Germany) for at least 2 min. Analogous experiments were performed without the respective PA0919 protein to determine the spontaneous hydrolysis of the respective chromogenic substrate. Initial slopes of the obtained *p*-nitrophenolate formation curves were calculated and for protein activity determination, the rate of spontaneous hydrolysis was subtracted from the corresponding experiment in the presence of the PA0919 protein. All experiments were independently performed at least in triplicate.

dialysis buffer	HEPES-NaOH pH 6.8	20 mM
sample composition	HEPES-NaOH pH 6.8	20 mM
	PA0919 derivative	3 – 12 µM
	DMSO	2 % (v/v)
	chromogenic *p*-nitrophenol derivative	50 µM

2.11.2 PA0919 inactivation by inhibitory substances

Purified, dialyzed and *Strep*-tagged PA0919 protein was incubated with the inhibiting compounds phenylmethylsulfonyl fluoride (PMSF), N_{α}-tosyl-L-lysine chloromethyl ketone (TLCK) and EDTA and the residual enzyme activity was analyzed using the well-established *in vitro* assay (see section 2.11.1).

Stock solutions of PMSF (in DMSO), TLCK (in 50 mM sodium acetate pH 4.8) and EDTA (in dH_2O, pH 8.0) were prepared. Purified, dialyzed and *Strep*-tagged PA0919 wild-type protein was pre-incubated with PMSF, TLCK and EDTA at 4 °C for 30 min, respectively. 60 µL of the prepared mixture were subjected to the *in vitro* activity assay using Ala-ONp as the substrate in a final volume of 300 µL. The assay was performed and monitored as described in section 2.11.1. Control experiments were prepared without the inhibiting compound. Values obtained for samples without protein were treated analogously and employed to determine the spontaneous hydrolysis of the substrate Ala-ONp in the presence of the specific inhibitor. Values for the spontaneous hydrolysis were subtracted from the corresponding experiment in the presence of PA0919 protein (in analogy to section 2.11.1). All experiments were performed in duplicate and the whole study was repeated in triplicate independently.

compound	**stock solution**	**pre-incubation**	**final concentration**
PMSF	150 mM	5 mM	1 mM
TLCK	9 mM, 150 mM	0.3 mM, 5 mM	60 µM, 1 mM
EDTA	150 mM	5 mM	1 mM
DMSO			2 % (v/v)
PA0919 protein		30 µM	6 µM
Ala-ONp	10 mM		50 µM

2.11.3 PA0919 protein *in vitro* activity assay in the presence of ^{14}C-labeled A-PG

The activity of the PA0919 protein in the presence of the putative native substrate A-PG was investigated. Since A-PG was not commercially available, the radioactively labeled substrate was synthesized using the well-established A-PGS *in vitro* assay (compare Hebecker *et al.*, 2011). The ^{14}C-labeled A-PG was extracted and solubilized for the subsequent PA0919 *in vitro* activity assay.

A-PGS *in vitro* assay for the synthesis of [1-^{14}C]-A-PG

The A-PGS *in vitro* assay was employed to synthesize sufficient amounts of A-PG for the analysis of the PA0919 activity according to Hebecker *et al.*, 2011. The A-PGS enzyme of *P. aeruginosa* transfers an alanine moiety form its corresponding $tRNA^{Ala}$ to the 3' or 2' hydroxyl group of PG (Hebecker *et al.*, 2011). During the employed assay, the $tRNA^{Ala}$ can be re-used by its corresponding Ala-$tRNA^{Ala}$ synthetase (PA0903). To provide sufficient ATP molecules, an ATP regenerating system (consisting of creatine phosphate and creatine phosphokinase) was added to the reaction mixture (Hebecker *et al.*, 2011). The recombinantly produced and purified catalytic A-PGS domain from *P. aeruginosa* (A-$PGS_{543-881}$; all tags were removed after purification) used in this assay was generously provided by S. Hebecker. The application of [1-^{14}C]-L-alanine allowed for the detection of synthesized [1-^{14}C]-A-PG, but also for product detection after the PA0919 *in vitro* assay (see below).

E. coli Rosetta (λDE3) pLysS pET28b(+)PA0903 was grown in 500 mL cultures (LB medium supplemented with Kan and Cm) at 37 °C and 180 rpm. At OD_{578} = 0.5, the cultures were shifted to 30 °C and 180 rpm for 10 min. Protein production was induced with 200 µM IPTG and cultivation was continued at 30 °C and 180 rpm for 4 h. The cultures were harvested (3'000 x g, 20 min, 4 °C), washed with 50 mM HEPES-NaOH pH 7.8 (4'000 x g, 20 min, 4 °C) and suspended according to the culture turbidity (10 mL buffer were used for an OD_{578} of 2) using the same buffer. Crude cellular extracts were obtained by French® Press passage at 19'200 lb/in².

The assay was performed in reaction volumes of 1 mL containing purified A-$PGS_{543-881}$, ATP and an ATP regenerating system (creatine phosphokinase, creatine phosphate) in 50 mM HEPES-NaOH pH 7.8 and [1-^{14}C]-L-alanine (Moravec Biochemicals, Brea, CA, USA) in a final volume of 300 µL. The reaction was started by the addition of 700 µL crude cellular extract and mixtures were incubated at 37 °C and 1'000 rpm for 1 h. Samples were taken at distinct time points to monitor A-PG synthesis by scintillation counting after lipid extraction (see chapter 2.5). The reaction was stopped by adding 10 µL 10 mg/mL RNase A (Invitrogen by Life Technologies, Darmstadt, Germany) and mixtures were incubated at 37 °C for 15 min. Samples were stored at –20 °C in 200 µL portions.

stock solutions	**volumes (1000 µL)**	**final concentration**
100 mM ATP	10 µL	2 mM
500 mM creatine phosphate	18 µM	18 mM
6.7 U/µL creatine phosphokinase	2.6 µL	35 U/mL
2 mM [1-^{14}C]-L-alanine (51 mCi/mmol)	10 µL	20 µM
purified A-$PGS_{543-881}$		10 µM
50 mM HEPES-NaOH pH 7.8	add to 300 µL	
crude cellular extract	700 µL	

Preparation of [1-^{14}C]-A-PG for the PA0919 *in vitro* activity assay

The synthesized [1-^{14}C]-A-PG was isolated from the reaction mixture to prevent contamination of the PA0919 *in vitro* activity assay with ^{14}C-labeled alanine and the isolated lipids were solubilized by Triton^{TM} X-100 treatment.

The polar lipids were extracted from the 200 µL portions as described in section 2.5.1. After chloroform evaporation, isolated lipids were solved in 190 µL dialysis buffer (section 2.9.5) supplemented with 3.2 mg/mL Triton^{TM} X-100 (Sigma-Aldrich, St. Louis, MO, USA) and incubated under vigorous shaking at 37 °C for 15 min. Unsolved lipids were removed by centrifugation (11'000 x g, 10 min, RT) and solubilized lipids were subjected to the PA0919 *in vitro* activity assay.

PA0919 *in vitro* activity assay employing [1-^{14}C]-A-PG

Strep-tagged PA0919 variant proteins were mixed with solubilized lipids containing [1-^{14}C]-A-PG. After incubation, samples were subjected to TLC analysis for product detection. All experiments were reproduced at least three times independently.

80 µL of 80 µM purified, dialyzed and *Strep*-tagged PA0919 variant protein was mixed with 80 µL solubilized lipid mixture and incubated at 37 °C and 1'000 rpm for 30 min. For control, a sample without protein was handled analogously. The reactions were stopped by heat at 60 °C for 5 min.

For product formation analysis, 12 µL of the individual samples were loaded onto a TLC plate (Macherey-Nagel, Düren, Germany). 1 µL 10 mM L-alanine (Sigma-Aldrich, St. Louis, MO, USA) was used as a reference. Lipids were separated from amino acids at 25 °C on TLC plates using a solvent mixture of *n*-butanol, acetic acid and water (5:3:2, v/v/v; Qiu *et al.*, 2010). Amino group carrying molecules were detected by ninhydrin (Merck, Darmstadt, Germany) and incubation at 100 °C (Klein *et al.*, 2009). Plates were subjected to autoradiography analysis (section 2.5.4) to specifically detect ^{14}C-labeled spots.

2.12 Localization of PA0919 in *P. aeruginosa*

The PA0919 protein was localized in *P. aeruginosa* using strain Δ19 pUC/19 (compare section 2.4.19) carrying a PA0919-Strep fusion protein. The strain was cultivated under acidic growth conditions and cells were fractionated by different methods into periplasm, cytoplasm, outer and inner membrane fractions. The PA0919 protein was detected within these fractions after SDS-PAGE and Western Blot *via* its C-terminal *Strep*-tag II.

2.12.1 Cultivation of *P. aeruginosa* strains for PA0919 protein localization

P. aeruginosa Δ19 pUC/19 was cultivated under acidic conditions and harvested before subjecting the cells to fractionation procedures.

500 mL AB medium pH 5.3 (in baffled flasks, supplemented with Cb) were inoculated to an OD_{578} of 0.05 using an overnight *P. aeruginosa* Δ19 pUC/19 culture and incubated at 37 °C and 200 rpm for 6 h. Cells of 1 L culture were harvested by centrifugation (3'000 x g, 15 min, 4 °C) and washed with 50 mL buffer (4'000 x g, 20 min, 4 °C). The harvesting buffer containing D(+)-sucrose for spheroblast stabilization (Quan *et al.*, 2013) was employed for the isolation of the periplasmic (section 2.9.1) and the cytoplasmic fraction, whereas the Tris buffer was used for cells subjected to the total membrane isolation procedure. Cells designated for periplasm/cytoplasm isolation were directly employed, whereas sediments for membrane preparation were stored at –20 °C.

harvesting buffer	HEPES-NaOH pH 8.0	50 mM
	NaCl	150 mM
	D(+)-sucrose	20 % (w/v)
Tris buffer	Tris-HCl pH 8.0	50 mM

2.12.2 Isolation of the periplasmic and cytoplasmic fraction

For the localization of the PA0919 protein, periplasmic and cytoplasmic fractions were isolated from *P. aeruginosa* Δ19 pUC/19 cells. First, the periplasmic fraction was isolated by polymyxin B treatment in analogy to section 2.9.2 and the obtained spheroblasts were employed for the cytoplasm isolation (Jensch and Fricke, 1997).

After harvesting (section 2.12.1), the cell sediments of 1 L culture were suspended carefully in isolation buffer (compare section 2.9.2; using 2 buffer volumes for 1 sediment volume) and incubated with gentle agitation at 4 °C for 3 h. The spheroblasts were separated by centrifugation (10'000 – 20'000 x g, 15 min, 4 °C) and the periplasmic fraction was obtained as the supernatant. The spheroblast sediment was stored at –20 °C.

The frozen spheroblasts were thawed and suspended in cytoplasm buffer using 4 buffer volumes for 1 pellet volume. 250 mg glass beads were added to 750 µL cell suspension and cells were disrupted by FastPrep® treatment (3x at 5.5 m/s and 45 sec; MP Biomedicals, Eschwege, Germany). The cytoplasmic fraction was obtained as the supernatant after cell debris removal (20'000 x g, 1 h, 4 °C).

isolation buffer	HEPES-NaOH pH 8.0	50 mM
	NaCl	150 mM
	D(+)-sucrose	20 % (w/v)
	polymyxin B	2 mg/mL

cytoplasm buffer	HEPES-NaOH pH 8.0	50 mM
	NaCl	100 mM

2.12.3 Isolation of total membrane protein fractions

Total membrane fractions were obtained by lysing the cells and removing cell debris. The membrane fraction sediment was obtained after high-speed centrifugation according to Strugatsky *et al.*, 2013.

After cell harvesting (section 2.12.1), 50 mM Tris-HCl pH 8.0 was added to the thawed cell sediment of 1 L culture to a final volume of 15 mL. Cells were lysed by French® Press passage at 19'200 lb/in² and cell debris was removed by low-speed centrifugation (2'000 x g, 25 min, 4 °C). The supernatant was subjected to a high-speed centrifugation (110'000 x g, 65 min, 4 °C) and the sedimented membrane fraction was carefully washed (3x 500 µL). Membrane proteins were solubilized with gentle agitation using 5 mL solubilization buffer at 4 °C for 2 h and subjected to a second high-speed centrifugation (110'000 x g, 65 min, 4 °C) to sediment lipids. Solubilized membrane proteins were obtained in the supernatant.

washing buffer	Tris-HCl pH 8.0	50 mM
	$MgCl_2$	20 mM
solubilization buffer	Tris-HCl pH 8.0	50 mM
	$MgCl_2$	20 mM
	Triton™ X-100	2 % (v/v)

2.12.4 Separation of membranes by isopycnic sucrose gradient centrifugation

After cell lysis and removal of cell debris, the inner and the outer membrane of *P. aeruginosa* Δ19 pUC/19 were obtained by centrifugation employing an isopycnic sucrose gradient according to Magnowska, 2010.

After thawing, the sediment of 3 L cell culture was suspended in cell disruption buffer in a final volume of 15 mL. Cells were disrupted by French® Press passage at 19'200 lb/in² and cell debris was removed by low-speed centrifugation (20'000 x g, 25 min, 4 °C). 4 – 4.5 mL of the supernatant was loaded on top of the isopycnic sucrose gradient (3 mL of 2.0 M, 1.5 M and 0.5 M D(+)-sucrose solutions) and high-speed centrifugation was performed (100'000 x g, 65 min, 4 °C) using the swing-out-rotor SW 40 Ti (Beckman Coulter, Brea, CA, USA). The visible membrane fractions (upper: inner membrane; lower: outer membrane) were carefully isolated from the gradient.

cell disruption buffer	potassium acetate	100 mM
	magnesium acetate	5 mM
	HEPES-NaOH pH 8.0	50 mM
	β-mercaptoethanol	0.05 % (v/v)
	cOmplete protease inhibitor cocktail	1 tablet/50 mL

2.12.5 Isolation of the outer membrane by sarcosyl treatment

After cell disruption and cell debris removal, the total membrane fraction was sedimented and the outer membrane fraction was separated from the inner one by sarcosyl treatment combining different methods (Eitel and Dersch, 2002; Bölin *et al.*, 1982; Filip *et al.*, 1973).

Frozen *P. aeruginosa* Δ19 pUC/19 cells sediments of 2 L cell culture were thawed and mixed with TEM buffer in a final volume of 20 mL. Cells were disrupted by twofold French® Press passage at 19'200 lb/in² and cell debris was removed by low-speed centrifugation (2'800 x g, 10 min, 4 °C). The total membrane fraction was isolated by high-speed centrifugation (110'000 x g, 65 min, 4 °C) and suspended with gentle agitation using 20 mL sarcosyl solution at 4 °C overnight. The suspension was additionally centrifuged (110'000 x g, 65 min, 4 °C). The supernatant containing the inner membrane fraction was removed and concentrated for protein analysis (compare section 2.9.6). The sedimented outer membrane fraction was resolved (20 mL sarcosyl solution, gentle agitation, 4 °C for 2 h) and subjected to high-speed centrifugation for improving the purity. The obtained outer membrane sediment was solubilized with gentle agitation in 1 mL sample buffer I at 4 °C for 1 h and 333 µL sample buffer II were added subsequently.

TEM buffer	Tris-HCl pH 8.0	10 mM
	EDTA pH 8.0	5 mM
	β-mercaptoethanol	1 mM
	DNase I	6 µg/mL
	cOmplete protease inhibitor cocktail	1 tablet/50 mL
sarcosyl solution	sodium *N*-laurylsarcosinate	0.5 % (w/v)
	β-mercaptoethanol	1 mM
sample buffer I	Tris-HCl pH 8.0	10 mM
	lysozyme	2 mg/mL
sample buffer II	Tris-HCl pH 6.8	62.5 mM
	SDS	1 % (w/v)
	glycerol	10 % (w/v)
	β-mercaptoethanol	0.5 % (v/v)

2.12.6 Sample preparation for localization studies

Samples of the cellular fractions obtained by different isolation methods (sections 2.12.2 to 2.12.5) were mixed with SDS sample buffer (1:1 or 1:2, v/v) and subjected to SDS-PAGE as described in section 2.10.2. Proteins were transferred to a membrane by performing a Western Blot (section 2.10.3) and the *Strep*-tagged PA0919 protein was detected *via* the employed *Strep*-tag-II (section 2.10.5) in the respective cellular fractions.

2.13 Bioinformatic tools

Several bioinformatic tools were used for the generation of amino acid sequence alignments, for phylogenetic tree construction, for operon and promoter analysis and for protein topology prediction.

2.13.1 Sequence alignment

The basic local alignment search tool (BLAST) was employed for the identification of homologous sequences using amino acid sequences of PA0920 and PA0919 for query (Altschul *et al.*, 1990). C-terminal domains of aaPGS enzymes were defined based on a sequence alignment with the C-terminal domain of the A-PGS of *P. aeruginosa* (Hebecker *et al.*, 2011) using ClustalW2 (Larkin *et al.*, 2007). Identified homologous sequences were aligned by ClustalW2 and sequence logos were created with WebLogo (Crooks *et al.*, 2004). The Lasergene® software package (DNASTAR, Madison, WI, USA) was employed for sequence identity analysis and vector design for cloning purposes.

2.13.2 Phylogenetic tree construction

The interactive Tree Of Life (iTOL) software provided by the European Molecular Biotechnology Laboratory (EMBL; Heidelberg, Germany; www.itol.embl.de) was employed for the construction of a phylogenetic tree (Letunic and Bork, 2007). Therefore, representative members were selected and the presence of aaPGS homologs was individually verified by using the C-terminal domain of *P. aeruginosa* A-PGS for query in BLAST analysis (Altschul *et al.*, 1990). AaPGS absence was defined by an E-value > e^{-40} and for *Mycobacteria* (containing fusion proteins of aaPGS and tRNA synthetase; Maloney *et al.*, 2009), an E-value > e^{-20} was used.

2.13.3 Operon prediction and cluster analysis

Orfs PA0920 and PA0919 were employed as query for the DOOR database (Mao *et al.*, 2009) and cluster analysis was performed using the microbial genome database MBGD for comparative analysis (Uchiyama *et al.*, 2010) to identify orthologous PA0920/PA0919 groups. Both databases were used according to the provider's instructions, respectively.

2.13.4 Prediction of promoter elements and ribosome binding site

The 430 bp sequence located upstream of orf PA0919 on the PAO1 chromosome was analyzed employing the online tool BPROM (SoftBerry, Mount Kisco, NY, USA; www.softberry.com) according to the provider's instructions. This tool was developed to identify putative promoter elements recognized by sigma factor σ^{70}.

The ribosome binding site (RBS, also termed Shine-Dalgarno sequence) is located within 20 bp upstream of the translation start of the gene. This sequence traditionally consists of adenines and guanines in slightly varying order and is recognized by the anti-Shine-Dalgarno sequence provided by the ribosomal 16 S rRNA during the translation initiation process (Ma *et al.*, 2002). The RBS upstream of orf PA0919 was identified due to its similarity to the *E. coli* RBS consensus sequence (Schneider and Stephens, 1990) and by comparison to the *P. aeruginosa* anti-Shine-Dalgarno sequence (Ma *et al.*, 2002).

2.13.5 Secretion signal and transmembrane helices prediction

The PA0919 amino acid sequence was analyzed using the online tool SignalP 4.1 (Petersen *et al.*, 2011) allowing for the identification of N-terminal secretion signal sequences and developed especially for discriminating signal sequences from membrane helices. The online tool TMHMM (Krogh *et al.*, 2001) was employed to predict transmembrane helices within the PA0919 protein.

3 Results

The aminoacyl-tRNA substrate specificity of nine as yet uncharacterized aaPGS enzymes was investigated. The determinants for the aaPGS substrate specificity were analyzed and the phylogenetic distribution of bacteria containing aaPGS enzymes was investigated to identify evolutionary correlations.

Furthermore, the functional roles of different aaPG variants were analyzed by introducing different aaPGS enzymes into the gram negative model organism *P. aeruginosa*. The lipid composition and the susceptibility to antimicrobial compounds of the obtained strains were analyzed. Additionally, the response of the A-PGS specific promoter to antimicrobial compounds was investigated under neutral and acidic conditions in *P. aeruginosa*.

Orf PA0919 which is clustered together with the A-PGS encoding orf PA0920 is analyzed *in vivo* in the model organism *P. aeruginosa* and the PA0919 specific promoter was identified. Furthermore, the PA0919 protein was recombinantly produced and characterized *in vitro*. Finally, the PA0919 protein was localized in the native host *P. aeruginosa*.

3.1 Substrate specificity of aaPGS enzymes

For several bacterial pathogens, the synthesis of aminoacylated PG was found to result in the resistance against several antimicrobial compounds and in some cases also in reduced virulence (Klein *et al.*, 2009; Maloney *et al.*, 2009; Peschel *et al.*, 2001; Thedieck *et al.*, 2006; Samant *et al.*, 2009). Therefore, the development of an aaPGS specific inhibitor had been proposed as promising strategy to overcome infections of aaPGS harboring bacteria (Roy, 2009). For this, aaPGS enzymes had to be classified according to their aminoacyl-tRNA substrate specificity. To date, eight L-PG and two A-PG specific enzymes had been elucidated (compare Table 10).

Table 10: Overview of annotated aaPGS enzymes from the literature

Strain	Enzyme/orf	Specificity	Reference
Agrobacterium tumefaciens	LpiA	L-PG	Roy and Ibba, 2009
Bacillus anthracis	BAS1375	L-PG	Samant *et al.*, 2009
Bacillus subtilis	MprF	L-PG, A-PG	Roy and Ibba, 2009 Roy and Ibba, 2008a Sohlenkamp *et al.*, 2007
Caulobacter crescentus	CC_2047	L-PG	Contreras *et al.*, 1978 Jones and Smith, 1979
Clostridium perfringens	CPR_1564	A-PG	Roy and Ibba, 2009 Roy and Ibba, 2008b
	CPR_1258	L-PG	Roy and Ibba, 2008b
Enterococcus faecalis	EF_1027	L-PG, A-PG, R-PG	Bao *et al.*, 2012
Enterococcus faecium	ZP_000604896	L-PG, A-PG, R-PG	Roy and Ibba, 2009
Listeria monocytogenes	Lmo1695	L-PG, L-DPG	Thedieck *et al.*, 2006
Mycobacterium smegmatis	LysX	L-PG	Maloney *et al.*, 2011
Mycobacterium tuberculosis	LysX	L-PG	Maloney *et al.*, 2009
Pseudomonas aeruginosa PAO1	A-PGS (PA0920)	A-PG	Hebecker *et al.*, 2011 Klein *et al.*, 2009
Rhizobium tropici	LpiA	L-PG	Sohlenkamp *et al.*, 2007
Staphylococcus aureus	MprF	L-PG	Ernst *et al.*, 2009 Staubitz *et al.*, 2004 Peschel *et al.*, 2001

Since the number of as yet characterized A-PG specific enzymes was limited (compare Table 10), the bioinformatic annotation of L-PGS and A-PGS enzymes was not possible. Furthermore, the observed broadened specificity for the employed aminoacyl-tRNA substrate of three aaPGS enzymes (Table 10) indicates a high diversity for this class of enzymes. In the present study, the mechanism responsible for the development of different aminoacyl-tRNA substrate specificities of aaPGS enzymes was investigated. Therefore, the specificity of nine as yet uncharacterized aaPGS homologs was elucidated to identify additional A-PGS enzymes. For this, selected aaPGS harboring bacteria and *E. coli* strains producing recombinant aaPGS enzymes were analyzed concerning their lipid composition using well-established techniques (chapter 2.6). The initial results were verified using *in vitro* activity assays in the presence of radioactively labeled amino acids (section 2.6.2). Finally, the determinants for the aaPGS substrate specificity were investigated based on an amino acid sequence analysis. The phylogenetic distribution of bacteria containing aaPGS enzymes was analyzed to identify evolutionary correlations.

3.1.1 Substrate specificity determination of selected aaPGS enzymes

Recombinant aaPGS enzymes or C-terminal catalytic aaPGS domains were overproduced and the *E. coli* lipid composition was analyzed (section 2.6.2). Since the *E. coli* host does not provide an aaPGS homolog, the overproduction of recombinant aaPGS enzymes resulted in the formation of an additional phospholipid. This can be observed after lipid extraction by two-dimensional TLC combined with molybdatophosphoric acid or ninhydrin staining (Staubitz *et al.*, 2004; Klein *et al.*, 2009).

Furthermore, the substrate specificity of the aaPGS enzymes was verified using an *in vitro* activity assay: For this, aaPGS overproducing *E. coli* cells were lysed and incubated in the presence of radioactively labeled amino acids. During incubation, ^{14}C-labeled amino acids were transferred to their respective tRNA by aminoacyl-tRNA synthetases. The activated amino acids were coupled to PG by the respective aaPGS enzyme. PG, tRNAs and aminoacyl-tRNA synthetases were provided by the crude cellular extracts. Subsequently, the synthesized radioactively labeled aaPG was identified after lipid extraction by two-dimensional TLC in combination with autoradiography (section 2.6.2).

Additionally, the lipid composition of aaPGS harboring native strains was analyzed under neutral and acidic growth conditions and their aaPG amount was quantified (sections 2.6.1 and 2.5.3).

The results of all analyses are summarized and presented in Figure 6 (page 91).

L-PG formation was observed for the aaPGS enzymes of *B. anthracis*, *B. licheniformis*, *B. thuringiensis* and *S. thermophilus*

The human pathogen *B. anthracis* causes the serious anthrax disease (Koehler, 2009). To elucidate the substrate specificity of the aaPGS of *B. anthracis*, the C-terminal catalytic enzyme domain (BAS1375Δaa1-527) was overproduced in *E. coli* and the specific formation of L-PG was observed (Figure 6, A), when compared to the *E. coli* lipid composition in the absence of any aaPGS enzyme (Figure 6, A: negative control). The observed synthesis of L-PG by the *B. anthracis* C-terminal domain corresponds to a previous study reporting an overall

amount of 10 % L-PG for the native *B. anthracis* in the presence of the aaPGS homologous orf BAS1375 (Samant *et al.*, 2009).

B. licheniformis is used for the industrial production of several exoenzymes like amylases and proteases and also for the synthesis of the polypeptide antibiotic bacitracin (Veith *et al.*, 2004). The formation of L-PG was observed for the *E. coli* strain producing the recombinant C-terminal aaPGS domain of *B. licheniformis* (YfiXΔaa1-518; Figure 6). The analysis of lipid composition of the native *B. licheniformis* strain identified an amount of 3 % L-PG under all conditions when compared to the overall polar lipid content (Figure 6, B).

B. thuringiensis is employed in agriculture due to its production of insecticidal proteins (Ibrahim *et al.*, 2010). The overproduction of the full-length aaPGS enzyme of *B. thuringiensis* (Bthu_13400) in *E. coli* resulted in the formation of L-PG (Figure 6, A). The observed L-PG specificity was verified by the *in vitro* activity assay in the presence of radioactively labeled amino acids (compare Figure 6, A). Furthermore, 10 % L-PG (compared to the overall polar lipid content) were determined for the native *B. thuringiensis* strain under all employed conditions (Figure 6, B).

S. thermophilus is able to ferment lactose to lactic acid and is therefore employed in dairy industry (Delorme, 2008). The C-terminal aaPGS domain of *S. thermophilus* (StMprf Δaa1-503) was recombinantly overproduced in *E. coli*. However, the overproduction did not result in the observation of an additional phospholipid in *E. coli* (Jäger, 2011). It seems reasonable that the recombinant C-terminal domain lacks any catalytic activity as it was observed previously for the C-terminal domain of the *S. aureus* L-PGS (Ernst *et al.*, 2009). However, for the native *S. thermophilus* strain, an amount of 10 % L-PG compared to the overall polar lipid content was observed (Figure 6, B; Jäger, 2011). Due to the fact that a single aaPGS homologous orf was identified by BLAST analysis in *S. thermophilus* LMG 18311, it was concluded that orf STU1256 encodes for an L-PGS enzyme (Jäger, 2011).

Under acidic conditions, highly increased aaPG amounts were observed in several bacteria (e.g. Houtsmuller and van Deenen, 1965; Klein *et al.*, 2009; Sohlenkamp *et al.*, 2007). However, the amount of L-PG was found identical for *B. thuringiensis* and *B. licheniformis* under acidic (pH 5) and neutral conditions (pH 7) (not shown). Therefore, it was concluded that the adaptation of these strains to acidic growth condition is not facilitated by elevated aaPG levels which might indicate that the synthesis of L-PG is not a general cellular

mechanism for the adaptation to acidic conditions. Since *S. aureus* does not contain any PE (Peschel *et al.*, 2001), it seems reasonable that L-PG can substitute the function of this phospholipid to some extend.

The observed amounts of 3 to 10 % L-PG for the investigated bacteria (compare Figure 6, B) clearly indicate that L-PG is a standard membrane component under the employed growth conditions. Interestingly, a high amount of 10 % L-PG was observed for *S. thermophilus* which produces high concentrations of lactate from lactose (Delorme, 2008). In *P. aeruginosa*, the synthesis of A-PG resulted in an increased resistance against sodium lactate (Klein *et al.*, 2009). It was concluded that L-PG synthesis is not generally related to the antimicrobial resistance or pathogenicity of specific organisms. Instead, it might be a mechanism for the adaptation of bacterial membranes to various environmental requirements.

High levels of A-PG are synthesized in *Pseudomonads* under acidic growth conditions

A-PG synthesis had been described for *P. aeruginosa* PAO1 under acidic conditions (Klein *et al.*, 2009). Here, the non-pathogenic *P. putida* often used in biotechnological processes (Nelson *et al.*, 2002) and the highly virulent pathogen *P. aeruginosa* PA14 strain (Lee *et al.*, 2006) were analyzed concerning their lipid composition (section 2.6.1). For both strains, a minor A-PG amount of 0.5 % was observed under neutral conditions (pH 7.3; not shown), whereas A-PG levels of 5 % (*P. putida*) and 4 % (*P. aeruginosa* PA14) compared to the overall polar lipid content were detected under acidic growth conditions (pH 5.3; compare Figure 6, B). The lipid composition analysis did not reveal the synthesis of L-PG. Since BLAST analysis identified only a single aaPGS homologous gene in both organisms and since both enzymes share a high sequence identity with the A-PGS of *P. aeruginosa* PAO1 (at least 79 % for the full-length enzymes), it was concluded that orf PP_1202 from *P. putida* and orf PA14_52350 from *P. aeruginosa* PA14 encode A-PG specific enzymes. Due to the newly and previously observed A-PG synthesis in *Pseudomonads* under acidic conditions, one might speculate that the formation of A-PG represents a general mechanism to adapt membranes of *Pseudomonads* to acidic growth conditions.

A-PG formation was observed for the aaPGS enzymes of *B. phymatum*, *K. radiotolerans* and *P. polymyxa*

For the gram negative β-proteobacterium *B. phymatum* which is able to fix nitrogen (Elliott *et al.*, 2007), an amount of 0.5 % A-PG compared to the polar lipid content was determined for the native strain (see Figure 6, B). This result was confirmed by the *in vitro* analysis of the recombinantly overproduced aaPGS homolog, for which solely the synthesis of A-PG was observed (see Figure 6, A).

The gram positive bacterium *K. radiotolerans* had been found to tolerate high levels of γ-radiation (Bagwell *et al.*, 2008). For the native *K. radiotolerans* strain, an amount of 0.5 % A-PG compared to the overall polar lipid content was detected (Figure 6, B) and for the respective recombinant enzyme, the formation of A-PG was observed using the *in vitro* assay (Figure 6, A).

For the gram positive diazotrophic bacterium *P. polymyxa*, the synthesis of antimicrobial polymyxins and fusaricidins had been observed (Raza *et al.*, 2008). The analysis of the phospholipid composition of the native *P. polymyxa* strain revealed an amount of 4 % A-PG (compared to the overall polar lipid content; Figure 6, B). For the recombinant aaPGS enzyme of *P. polymyxa*, solely the formation of A-PG was observed using the *in vitro* assay in the presence of radioactively labeled alanine and lysine (Figure 6, A). Since a level of 4 % A-PG was observed under all employed conditions, one might propose that the formation of A-PG is important for the resistance of *P. polymyxa* against cationic antimicrobial polymyxins produced by this bacterium.

For these three bacteria, the formation of A-PG was detected under acidic and neutral growth conditions (pH 5 and pH 7). It is concluded that these organisms employ a different adaption strategy compared to the *Pseudomonads* described above. Although *B. phymatum* is phylogenetically related to *Pseudomonads*, the observed A-PG content was not found increased under acidic growth conditions. This indicates that an increased A-PG formation is not a general principle to adapt bacterial membranes to acidic stress conditions.

A-PG synthesis was also observed for the aaPGS enzyme from the archaeon *M. barkeri*

The archaeon *M. barkeri* is highly oxygen-sensitive and synthesizes methane using different pathways (Maeder *et al.*, 2006). Archaeal phospholipids differ in their structure from bacterial phospholipids (compare 1.3.2). Archaeal phospholipids contain diether phospholipid molecules and their hydrophobic isoprene residues are bound to a glycerol-1-posphate backbone. Interestingly, the polar lipid head groups were found identical in archaea and bacteria (compare section 1.3.2; Koga, 2011). AaPGS homologous enzymes were identified in the archaeal kingdom solely in the *Methanosarcinacae* (Roy and Ibba, 2008b).

Since *M. barkeri* is highly sensitive to oxygen, the substrate specificity of the respective aaPGS homolog was analyzed by recombinant production in *E. coli*. The analysis of the lipid composition of the *E. coli* strain overproducing the aaPGS enzyme of *M. barkeri* revealed the formation of A-PG, which was confirmed by the *in vitro* activity assay in the presence of radioactively labeled amino acids (Figure 6, A).

Figure 6: Substrate specificity determination of aaPGS enzymes (see next page)

A. The recombinant C-terminal aaPGS domains of *B. anthracis* (BAS1375Δaa1-527) and *B. licheniformis* (YfiXΔ1-518) were overproduced in *E. coli* BL21 (λDE3). After cultivation, the polar lipids were extracted and analyzed by two-dimensional TLC combined with molybdatophosphoric acid staining (section 2.6.2) (Jäger, 2011).
The recombinant full-length enzymes of *B. thuringiensis* (Bthur_134000), *B. phymatum* (Bphy_4019), *K. radiotolerans* (Krad_4555), *P. polymyxa* (Ppoly_aaPGS) and *M. barkeri* (Mbar_A2435) were overproduced in *E. coli* TOP10. After cell lysis, crude cellular extracts were subjected to the *in vitro* activity assay in the presence of ^{14}C-labeled L-alanine and/or L-lysine. Subsequently, polar lipids were extracted, separated and analyzed by two-dimensional TLC and molybdatophosphoric acid staining. ^{14}C-labeled phospholipids were visualized by autoradiography which revealed the formation of 2' and 3' A-PG as partially overlapping lipid spots (2' A-PG: lower spot, 3' A-PG: upper spot; Hebecker *et al.*, 2011).
For experimental details, see section 2.6.2.

B. Native strains harboring aaPGS enzymes were cultivated, polar lipids were extracted, analyzed by two-dimensional TLC and lipids were visualized by molybdatophos-phoric acid and ninhydrin staining (section 2.6.1).

Presented TLC plates were stained with molybdatophosphoric acid. L-PG position is indicated by a rectangle and A-PG position is given by a circle. Identical sections of the TLC plate after autoradiography analysis (dotted frames) or after ninhydrin staining (dashed frames) are presented in the upper left of the respective TLC plate. TLC plates and X-ray films of Bphy_4019, Krad_4555 and Mbar_A2435 were generously provided by S. Hebecker. Results for *S. thermophilus* strain the C-terminal aaPGS domain of *B. licheniformis* were taken from Jäger, 2011.
Phospholipids were named according to Kämpfer *et al.*, 2006, Thedieck *et al.*, 2006 and Klein *et al.*, 2009: A-PG: alanyl-phosphatidylglycerol, DGDG: diglucosyl diacylglycerol, DPG: diphosphatidylglycerol, L-PG: lysyl-phosphatidylglycerol, PE: phosphatidylethanolamine, PG: phosphatidylglycerol.

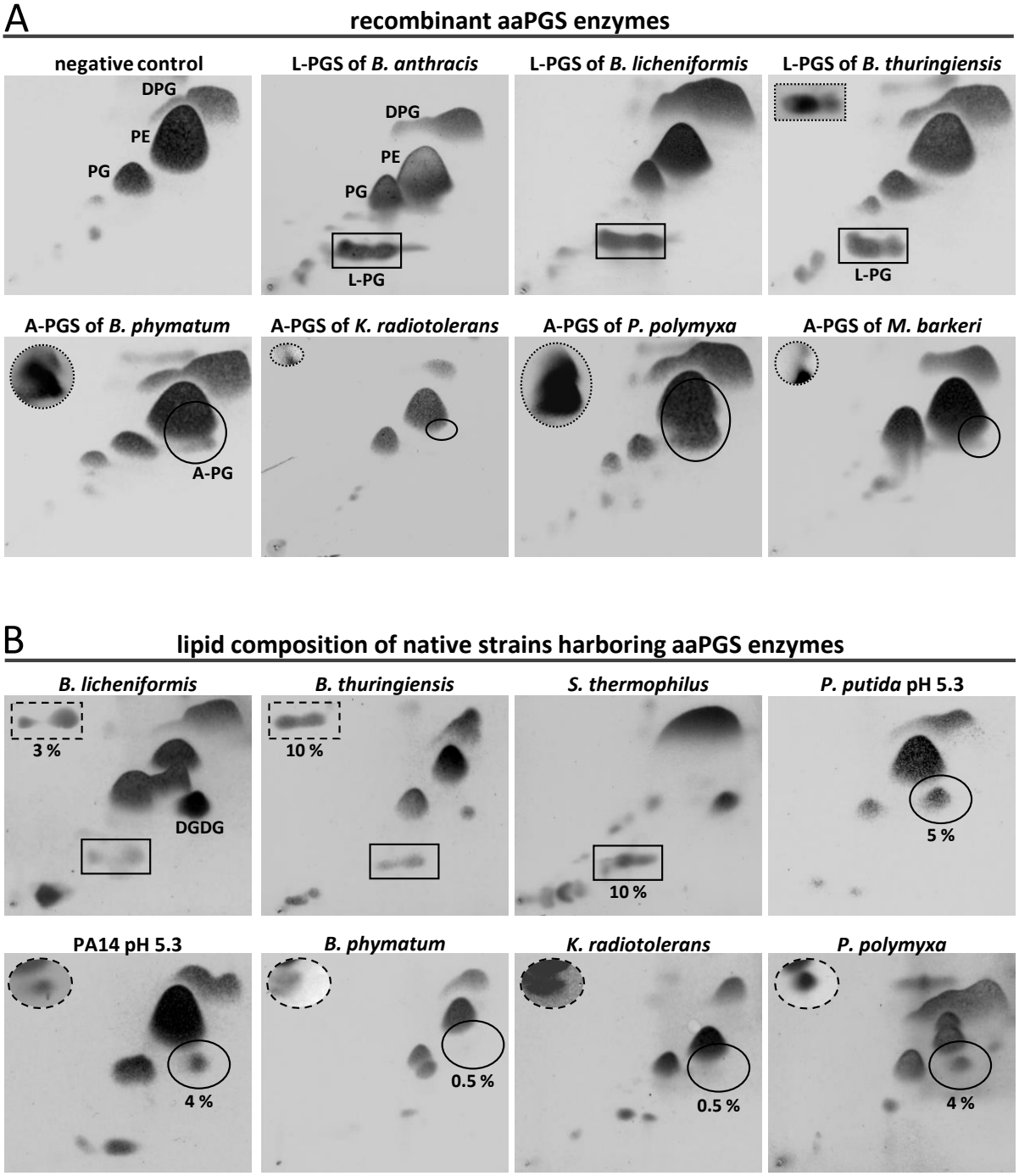

It is worth noting that the *M. barkeri* aaPGS enzyme is able to modify the PG substrate of *E. coli* which differs in structure from the corresponding archaeal phospholipid archaetidyl-glycerol (isoprenoid ether of *sn*-glycerol-1-phosphate, compare section 1.3.2; Koga, 2011). This is in good agreement with a study elucidating the determinants of the PG substrate for recognition by the *P. aeruginosa* A-PGS using various substrate derivatives (Hebecker *et al.*,

2011): It had been reported that the hydrophilic rather than the hydrophobic part of PG is of importance for substrate recognition. Importantly, an 'archaeal-like' substrate derivative (1,2-diphytanoyl-*sn*-glycero-3-phospho-(1´rac-glycerol)) with two isoprenoid-like fatty acid ester side chains was also utilized by the *P. aeruginosa* A-PGS (Hebecker *et al.*, 2011). Therefore, it might be concluded that the aaPGS enzyme of *M. barkeri* is able to synthesize A-PG in the native strain. For several *Methanosarcina* genes, the lateral transfer of these genes from bacteria had been described (Deppenmeier *et al.*, 2002; Maeder *et al.*, 2006). Because BLAST analyses of archaeal genomes detected aaPGS homologs only in *Methanosarcinaceae* and indicated a high sequence identity to the *P. aeruginosa* A-PGS, a comparable transfer of the *M. barkeri* A-PGS encoding gene donated by a bacterium seems reasonable.

The specificities of the investigated aaPGS enzymes determined in this study are summarized in Table 11.

Table 11: Identified substrate specificities of aaPGS enzymes
*BAS1375 full-length L-PGS activity had been elucidated previously by Samant *et al.*, 2009, and the lipid content had been determined based on TLC plates presented in the same publication.
n.d.: not determined, - : no increase of cellular aaPG concentration, + : aaPG concentration increased, † : aaPG content [%] at pH 7.3 / pH 5.3.

Strain	Enzyme/orf	Specificity	AaPG amount of overall lipid content [%]	Acidic induction
Bacillus anthracis str. *Sterne*	BAS1375	L-PG*	10*	n.d.
Bacillus licheniformis ATCC 14580	YfiX	L-PG	3	-
Bacillus thuringiensis ATCC 10792	Bthur0008_13400	L-PG	10	-
Streptococcus thermophilus ATCC 19258	STU1256	L-PG	10	n.d.
Pseudomonas aeruginosa UCBPP-PA14	PA14_52350	A-PG	0.5 / 4†	+
Pseudomonas putida KT2440	PP_1202	A-PG	0.5 / 5†	+
Burkholderia phymatum STM 815	Bphy_4019	A-PG	0.5	-
Kineococcus radiotolerans SRS 30216	Krad_4555	A-PG	0.5	-
Paenibacillus polymyxa ATCC 842	aaPGS	A-PG	4	-
Methanosarcina barkeri ATCC 29787	Mbar_A2435	A-PG	n.d.	n.d.

3.1.2 Determinants for aaPGS substrate specificity

An overall amount of 23 aaPGS enzymes has been characterized yet (see Table 10 and Table 11). This amount allows for an amino acid-based sequence analysis to identify the determinants for the aaPGS substrate specificity.

Former analyses revealed that the N-terminal domains of aaPGS enzymes, which anchor the aaPGS enzyme to the cell membrane and translocate aaPG molecules to the outer membrane leaflet, are highly variable and show very low sequence identity values (Peschel *et al.*, 2001; Hebecker *et al.*, 2011; Ernst *et al.*, 2009; Slavetinsky *et al.*, 2012). In contrast, the C-terminal aaPGS domains are more conserved and share a considerable sequence identity value (at least 16 %; compare appendix, Figure 33). Several previous experiments located the catalytic active site to the C-terminal aaPGS domain and it was found responsible for substrate recognition and amino acid transfer to PG (Hebecker *et al.*, 2011; Ernst *et al.*, 2009; Roy and Ibba, 2009). Consequently, C-terminal catalytic domains of aaPGS enzymes with elucidated aminoacyl-tRNA substrate specificity (summarized in Table 10 and Table 11) were defined by comparison of their respective sequence to the amino acid sequence of the C-terminal domain of the *P. aeruginosa* A-PGS according to Hebecker *et al.*, 2011. The sequence identity values for the C-terminal aaPGS sequences were calculated using the Lasergene® software package (DNASTAR, Madison, WI, USA) and are given in the appendix, Figure 33. The sequence identity analysis demonstrated that the employed L-PGS enzyme sequences indicated a sequence identity value of at least 16 % (Figure 33, light gray), whereas a value of 31 % was obtained for the A-PGS enzymes (dark gray). Interestingly, the minimal sequence identity of 17 % was calculated for the cross-comparison of L-PGS and A-PGS sequences (black). This result might indicate that the substrate specificity of A-PG and L-PG synthesizing enzymes is not determined by characteristic sequence motifs.

This assumption was verified by employing the defined C-terminal aaPGS enzyme domains to generate several sequence alignments using ClustalW2 (Larkin *et al.*, 2007). These alignments were grouped according to the aaPGS specificity (Figure 7). Based on the sequence alignments of A-PGSs, of L-PGSs and of all aaPGS enzymes, sequence logos indicating the amino acid conservation were generated by WebLogo (Crooks *et al.*, 2004) and arranged together with the formerly aligned aaPGS sequences in Figure 7.

The analysis of the sequence logos did not result in the identification of an amino acid position that is characteristic for L-PGS enzymes or alternatively for A-PGS enzymes (compare Figure 7). Instead, an almost identical distribution of conserved positions was observed for both sequence logos, as verified by the logo for the overall aaPGS sequences. In consequence, C-terminal sequences of *B. subtilis*, *E. faecium* and *E. faecalis* exhibiting broadened aminoacyl-tRNA substrate specificities (Roy and Ibba, 2009; Bao *et al.*, 2012) can be related to both the A-PGS and the L-PGS enzyme group. Interestingly, the C-terminal *Bacillus* aaPGS sequences share an identity of at least 63 % (see appendix, Figure 33), although the aaPGS homologs of *B. anthracis* (Samant *et al.*, 2009), *B. licheniformis* and *B. thuringiensis* are specific for lysine, whereas the *B. subtilis* enzyme makes use of both alanine and lysine *in vitro* (Roy and Ibba, 2009).

In a previous study, 15 amino acid residues with relevance for PG modification had been identified within the C-terminal A-PGS domain of *P. aeruginosa* (Hebecker *et al.*, 2011; see Figure 7). These key residues and also their neighboring amino acid residues were found conserved within the sequence logos of A-PGS and also of L-PGS enzyme sequences. One might conclude that these residues are important for the general transesterification process but do not directly determine the aminoacyl-tRNA substrate specificity.

Taken together, these results indicate that the specificity of aaPGS enzymes for Ala-tRNA^{Ala} or Lys-tRNA^{Lys} cannot be predicted based on the C-terminal aaPGS amino acid sequence, since no determinants for the respective specificity were identified. Instead, a diverse evolutionary origin for the individual specificity is proposed.

Figure 7: Sequence alignments and logos for aaPGS C-terminal catalytic domains (see next page)
The C-terminal domains of aaPGS enzymes were defined based on a sequence alignment with the C-terminal A-PGS domain of *P. aeruginosa* (Hebecker *et al.*, 2011). Defined C-terminal sequences were aligned by ClustalW2 (Larkin *et al.*, 2007) generating sequence alignments grouped according to the aaPGS aminoacyl-tRNA substrate specificity (A-PGS group (above), L-PGS group (below), aaPGSs with relaxed specificity (middle)). Sequence logos were calculated by WebLogo (Crooks *et al.*, 2004) employing the overall aaPGS sequences, the A-PGS group and the L-PGS group, respectively. All amino acid residues from *P. aeruginosa* A-PGS (A_PAO1) analyzed in a previous study (Hebecker *et al.*, 2011) are indicated within the sequence (key residues for enzymatic catalysis are highlighted yellow).
PAO1: *P. aeruginosa* PAO1, Bph: *B. phymatum*, Cpe: *C. perfringens*, Kra: *K. radiotolerans*, Mba: *M. barkeri*, PA14: *P. aeruginosa* PA14, Ppoly: *P. polymyxa*, Pput: *P. putida*, Bsu: *B. subtilis*, Efm: *E. faecium*, Efs: *E. faecalis*, Atu: *A. tumefaciens*, Ban: *B. anthracis*, Bli: *B. licheniformis*, Bthu: *B. thuringiensis*, Ccre: *C. crescentus*, Lmo: *L. monocytogenes*, Rtr: *R. tropici*, Sa: *S. aureus*, Sth: *S. thermophilus*, Msm: *M. smegmatis*, Mtb: *M. tuberculosis*.

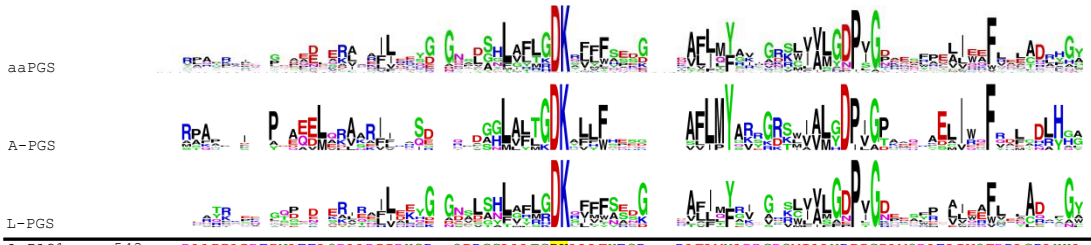


```
A_PAO1      543----RAAPPAIREPNAEELQRAARIIRHSD--QPDGGLALTGDKALLFHESD---DAFLMYARRGRSMIALYDPIGPAMQRAELIWQFRDLCDLHHA 630
A_Bph       531----RPAAGRFVKPAQQDLADAARIFRAQE--RSDAGLALMGDKSFLFSESR---QAFLMYAKYGRTWAALHDPVGPRAEWADLIRKFVALAHAHGG 618
A_Cpe       228----MPKIEDDERYMDADLEKVSKFFKEIDYGTIFSHLVYLKDKKVFWANEG---ESLIMYSKYKDKIIVLGDPIATKENLYSCIEEFQAFTNLYGY 317
A_Kra         8----ASAALGPQVACEQVMARVSAVVARSR--RCTAHLAFTGDKRFHFSPSG---AAFLMYQVEGRSWVVMGDPVGDPADFPELVRSFVGEIDRHGG  95
A_Mba       521----SPFSRDIHMPGAEEMELAKRIINQSE--ETAGNLVFTGDKYLLFDDEK---KAFLMYGVSGKTWVAMGDIVGTSNQAKELIWDFYEMSKLHQG 608
A_PA14      543----RAAPPAIREPDAEELQRAARIIRHSD--QPDGGLALTGDKALLFHEGD---DAFLMYARRGRSMIALYDPIGPAMQRAELIWQFRDLCDLHHA 630
A_Ppoly     546----RPQRSISNLPDAQELVKLKEFLERQG-GNLVSHMLFLGDKYLYWTKDE---QVVLPYARSRDKLIVLGDPLGPKERVSEAIQEFQRFADRYAL 634
A_Pput      542----RTAPPVIHLPDEEELQRANRILQASD--QPDGGLALTGDKALLFHPRG---NAFLMYARRGRSLVALYDPIGPAQERAEMIWQFRDLCDLHHA 629
AL_Bsu      520----VYHKRTKPIGEKADPERLAAFLNEKG-GNALSHLGFLGDKRFYFSSDG---NALLLFGKIARRLVVLGDPSGQRESFPLVLEEFLNEAHQKGF 608
ALR_Efm     510---HFLQGEKKQIGEAFNEEKALKILTTYG-GNSDSQLIFLKDKRMFAYEKDGEPTVLLQFACFNNKCIVMGDPSGKKEDFPEAIEAFIEETDRLCY 602
ALR_Efs     506---RYLQGKKHQVGEFPEDSILHNILTTYG-GNIDSELVFLHDKQVFLYPKE-EPTVFLQFNTINNKCVVMGNPSGNKEDFPAAIDAFLKETDRFGY 597
L_Atu       528----RPVTFKPDSIQPEDVERATDIVMRQD--SADANLVRMGDKHVMFSESG---NAFIMYGIQGRSWIAFADPVGDEEDFPDLVWQFVEAARGAGA 615
L_Ban       528-----NRYRNEFPGQPANDKRLQNFLDEHG-GNVLSHLGFLGDKQFFFSSDG---KALLLFSITGKRLVVLGDPIGDPSSYRTVLQEFLAEADRFGY 615
L_Bli       519------NRKTKEIGEEPDPEKLEAFLEEKG-GNALSHLGFLGDKRFFYSSDG---NALIQFAKVGQRLVVLGDPSGREDSFPLVIKEFLHAADQKGY 605
L_Bthu      526-----NRYRNEFPGQPANDKRLQNFLDEHG-GNVLSHLGFLGDKQFFFSSDG---KALILFSITGKRLIVLGDPIGDPSSYRTVLQEFLAEADRFGY 613
L_Ccre      187----TAATPPVVDDTDPEFDRVRAILAKAEGAEPSANLALLGDKRFLFSASG---ETFLMFGVRGRSWIALGPPVGKREERMELFWRFRELADAHAA 276
L_Cpe       503----NIRRKIPVKTFDQCSEYIEKIIEEYK-GDSLTHLVFLKDKYIYLNEDK---DLFIQYEVYGDKLFVLGNPVGNNENLFREIEKFCEYADNYGY 591
L_Lmo       510----YLSTTKEKLGSPFEAVKVREHLAKWG-GNEVSHTMFLRDKLLFWAAEG---EVLFSYRIIADKMVIMGEPTGNMDKMEAAIEEVMMNADRFGY 598
L_Rtr       530----RPATKRPEPVSDDAVARAVEIVRKQG--VADANLVRMGDKSIMFSEKG---DAFIMYGKQGRSWIALFDPVGPAQALPDLIWRFVETARAAGC 617
L_Sa        510-----FDYQFSKVRISSKIEDCEEIINQYG-GNYLSHLIYSGDKQFFTNENK---TAFLMYRYKASSLVVLGDPLGDENAFDELLEAFYNYAEYLGY 597
L_Sth       504---RVLAPRKH-FGQSMDNERFTALLEKYG-GASESALAYLHDKRLFWYRVDGQDQVVFQFAQISNKCVVMGNPIGNEKYYRPAWEAFLKNLSDWNL 595
L_Msm       217-------QRASNALTGEDESAIRGLLELYGKNDSLGYFATRRDKSVVFAPNG---RAAITYRVEVGVCLASGDPVGDPKSWPQAIAAWLQLCQAYGW 303
L_Mtb       293-------QRADNALTGEDESAIRGLLDLYGKDDSLGYFATRRDKSVVFASSG---RACITYRVEVGVCLASGDPVGDHRAWPQAVDAWLRLCQTYGW 379
```

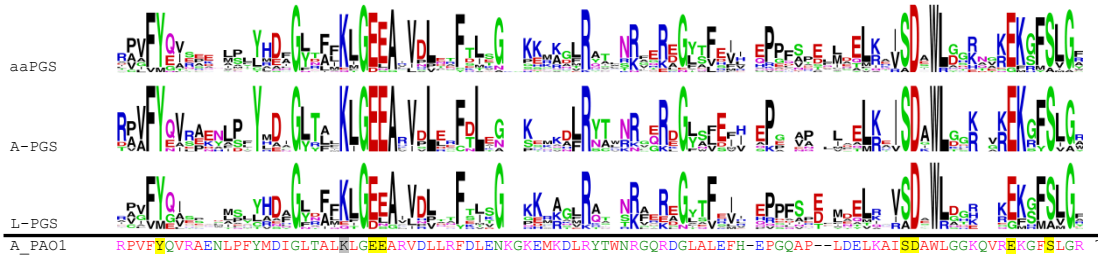


```
A_PAO1      RPVFYQVRAENLPFYMDIGLTALKLGEEARVDLLRFDLENKGKEMKDLRYTWNRGQRDGLALEFH-EPGQAP--LDELKAISDAWLGGKQVREKGFSLGR 727
A_Bph       RAAFYQVRANALPLYLDAGLTLMKLGEEAHVVLDEFDLKG--PHRAHLRYALKRCERDGFSVEVI-EPARVPESIATLRTISDGWLDSRDAREKSFSVAA 715
A_Cpe       DVVFYEIEEKNFSTYHDAGYYFFKLGEEARIDLEEFNLIG--SKKSAFRNTLRRVEREGYNFSII-EPPFNNEVVSQLKEISDKWLGDR--KEKGFSLGW 412
A_Kra       RPVFYNVLPDHADLYRACGLTLAKLGEEAVVPLEGFTLAG--KSKVNLRNCRNKSQRLGLSVDFV-APEDVAPLLPALREVSDAWLTHRNGKEKRFSLGA 192
A_Mba       RAAFYEVSEKYIPVYLDLGLTLIKIGEEAKVSLEAFTLEG--STGKDFRYTVRNVEKKGYWFEIV-SKEEVQSLMPELKKISDAWLKLKAGKEKRFSIGY 705
A_PA14      RPVFYQVRAENLPFYMDIGLTALKLGEEARVDLLRFDLENKGKEMKDLRYTWNRGQRDGLALEFH-EPGQAP--LDELKAISDAWLGGKQVREKGFSLGR 727
A_Ppoly     TAVFYQASPEYLSIYHENGYRFFKLGEEALVPLESCTLTG--KSNQALRSAKNRLGREGYSFEMI-QPPLEASLIEEMRHISDIWLDGR--KEKGYSLGW 729
A_Pput      RPVFYQVRAENLPFYMDIGLTALKLGEEARVDLRRFDLEAKGKEMKDLRYTWNRGGRDGLSLEIH-EPGHAP--LAELKEISDAWLGGKNVREKGFSLGR 726
AL_Bsu      SVLFYQIEREDMALYHDFGYNFFKLGEEAYVDLNTFTLTG--KKKAGLRAINNRFEREEYTFHVD-HPPFSDAFLEELKQISDEWLGSK--KEKGFSLGF 703
ALR_Efm     LPVFYETSEEIVMILHEFGYDFIKMGEEAYVDLNSFTTSG--KKMKGTRAVLNRIEREGFTFDVL-QPPFSTEQMSTFKNISDNWLGSR--KEKGFSLGF 697
ALR_Efs     VPVFYETNEDSVMLLHEFGYEFIKMGEEALVNLETFTMSG--KKFKGTRAVFNKITKAGYSFDVL-QPPFSTEQMHELKAISDSWLDNR--KEKGFSLGF 692
L_Atu       RAAFYQISPFLLSHCADAGLRAFKLGLEALVDLTAFELKG--GKLATLRQSLSRGARDGLTFEVV-EQSQVPDIMDELQQVSDGWLAHHNTREKRFSLGA 712
L_Ban       ICVFYQIESKWMSLYHDFGYNFFKLGEEAVVDLNTFTITG--KKRAGMRATFNRFEREGYTFSIH-QPPFSNELFEELRKVSDAWLGGK--KEKSFSLGY 710
L_Bli       LVIFYQIEREDMALYHDFGYRFFKLGEEAIVDLDTFTISG--KKRAGLRAIYNRFEREGYTFHVE-QPPFSREFLNELRQVSDEWLGRK--KEKGFSLGF 700
L_Bthu      ICVFYQIESKWMSLYHDFGYNFFKLGEEAVVDLNTFTITG--KKRAGMRATFNRFEREGYTFSIH-EPPFSDELYEELRKVSDAWLGGK--KEKGFSLGY 708
L_Ccre      RAGFYGLGPDDLPDTVDLGLAIQKTGESAAVPLEAFSLVGRRREV--LRRNWRKAGEGGAAFEVL-PVGAAPTMMDELKSISDSWLSHHAGGEKSFSMGG 373
L_Cpe       TPVFYQVNEEMISYLHSNGYDFMKIGEEAKVDVKEFKVVG--NKMKSLKTSRSKVTKEGYTFHMV-EPPFSREFLDYLKEISDEWLDGR--KEKGFSVGF 686
L_Lmo       RPVFYEVRGTMIPYLHDHGFDFIKLGEEGFVDVQNFTMSG--KKKKGERALMNKLEREGYTFEII-EPPFNHDTWTTLRAVSDEWLDGR--EEKGFSLGF 693
L_Rtr       RVVFYQISPALLSYCADAGLRAFKLGELAVVNLANFELKG--GKWANLRQTASRAVRDGLEFAVI-EPQDIPDVLDQLAHVSDTWLADHNAKEKSFSLGA 714
L_Sa        DVIFYQVTDQHMPLYHNFGNQFFKLGEEAIIDLTQFSTSG--KKRRGFRATLNKFDELNISFEII-EPPFSTEFINELQHVSDLWLDNR--QEMHFSVGE 692
L_Sth       QALFYEADERVTLMLHDYGFDFMKFGENAMVDLTTYSIDG--KHGKKFRKPTNRVEKAGFQFKLL-NPPFSETQMQEMKAVSDIWLNGR--KEKGFSLGF 690
L_Msm       APGVMGASLAGAEAYRAAGLNALQLGDEAILHPDRFRLSG--PDMRAVRQAVTRARRAGTSVRIRRHRELSPEEMAAVIRRADAWRDTETERGFSMALGR 401
L_Mtb       APGVMGASSQGAQTYREAGLTALELGDEAILRPADFKLSG--PEMRGVRQAVTRARRAGLTVRIRRHRDIAEDEMAQTITRADSWRDTETERGFSMALGR 477
```

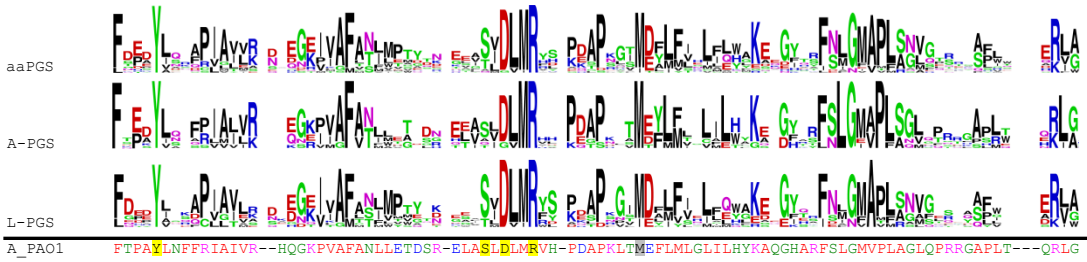


```
A_PAO1      FTPAYLNFFRIAIVR--HQGKPVAFANLLETDSR-ELASLDLMRVH-PDAPKLTMEFLMLGLILHYKAQGHARFSLGMVPLAGLQPRRGAPLT---QRLG 820
A_Bph       FTEDYLAAQSVMLVR--QKGEPVAFVTFMTTDLN-TEATVGVMRHV-PQASPYAMEYLFTQLALHLKQADFRSLSLGIAPFSGMSPTPLASRW---HRLA 808
A_Cpe       FSEDYIQRSPIAILKNEEENKIMGFVTIMDANDGGETVAIDLMRID-KDAPNASMDYLMLNLFLTFKEKGYKYFSLGEAPLSNVGFNTHSHLQ---EKLA 508
A_Kra       FDEDYVSRFPLVVVR--QEGRIIAFATLWVGGDG-HEVQVDLMRRL-PDGPRTVMTYLFVECILWAGENGFTSFNLGMAPLSGLRTGTGPSLW---NRLG 285
A_Mba       FNEKYLSNFPIALVR--NESEIVAFANIWTGADN-EEISVDLMRHS-PDAPDRTMEYLFVKLMLWGKEKGYRRFSLGMAPLSGLETRQFAPMW---HKIG 798
A_PA14      FTPAYLNFFRIAIVR--HQGKPVAFANLLETDSR-ELASLDLMRVH-PEAPKLTMEFLMLGLILHYKAQGHARFSLGMVPLAGLQPRRGAPLT---QRLG 820
A_Ppoly     FKESYLQLAPIALLK-DSEGKVIAFATMAPAYDHGQTVSIDLMRHL-PDTPNGTMDYLFTRVIEWAKESGYTTFNLGMAPLSQVGQSEKALRE---EKLA 824
A_Pput      FSPDYLQHFRIALIR--FQGRPVAFANLLETHGN-ELASLDLMRAH-PEAPKLTMEFMMIGLILHYKSHDYGRFSLGMVPLSGLQPRRGAPLT---QRLG 819
AL_Bsu      FDPSYLQKAPIAYMK-NAEGEIVAFANVMPMYQE-GEISVDLMRYR-GDAPNGIMDALFIRMFLWAKEEGCTSFNMGMAPLANVGTAFTSFWS---ERFA 797
ALR_Efm     FSEDYLQRAPIAVVK-NTQEEIVAFATIMPTYTNNKVGTIDLMRYDSKKAPSGSMDFLFLHLFAYMKEEHIQWFNLGMAPLSNVGTSRKSFLQ---ERIA 793
ALR_Efs     FDEAYLQRNPIAVVR-NAEGEMVSFANIIPSYTN-EVGTIDLMRHHKEKAPSGSMDFLFIHLFEYMKTENIHYFNLGMAPLANVGQSRKSFIQ---ERIA 787
L_Atu       FEPDYILSQPVAVLR--KDGKITAFANLMVTETK-KEATIDLMRFS-ADAPRGSMDFLFVSIMQHLREAGYESFNLGMAPMSGMSKRDAAPVW---DRIG 805
L_Ban       FDHEYISRAPIATLS-DADGKIIAFTTFMPVYQD-GSLSVDLMRYY-PDAPSGIMDAIFIHLFQWAKENEYHSFNIGMAPLSNVGLSTQSFWS---ERVA 804
L_Bli       FQEDYLQKAPIAVLK-SEEGEIVAFMNIMPMYRE-GEISIDLMRYS-KKAPKGIMDALFIYLFQWGKEQGYTAFNMGMAPLSNVGTTFQSFWT---ERLA 794
L_Bthu      FDREYISRAPIATLS-DADGKIIAFTTFMPVYQN-GSLSVDLMRYY-PDAPSGIMDAIFIHLFQWAKENEYHSFNIGMAPLSNVGLSTQSFWS---ERVA 802
L_Ccre      FDPRYVAEFPVAVVR--SEGKIVAFATLWTTAAK-TAFSMDLMRYS-DEAPKNVMDYLFVELLQWGKDEGYSAFEFGVAPLAGLQDRPLAPIM---SRVG 466
L_Cpe       FDEDYLNKAPIAILR-DREGEIKAFANIMYMYDD-ESFSVDLMRFS-KNTPRGVMDFMFINLIEYGKEKGYEIFNMGMAPLANVGLSKYAFWN---EKLA 780
L_Lmo       FDTYYLEQAPIAIAK-NGEGTIVGFASMMPSYTD-EMTSIDLMRYS-KEAPSGIMDFLFINLFEKAKEDGFQTFNAGMAPLANVGESKYAFLG---ERLA 787
L_Rtr       FDPDYVCSQPVGVLK--KDGKIVAFANILMTETK-EEGSVDLMRFS-PDAPKVSMDFLFVQILEYLKGEGFQRFNLGMAPLSGMSRRESAPVW---DRVG 807
L_Sa        FNEEYLSKAPIGVMR-NEENEVIAFCSLMPTYFN-DAISVDLIRWL-PELDLPLMDGLYLHMLLWSKEQGYTKFNMGMATLSNVGQLHYSYLR---ERLA 786
L_Sth       FDEAYLQQAPIAIVE-SKEGEIVAFANIMPTQNK-RVATIDLMRYDFKKAPEGIMDYLFVKLFQYFKAEGKQYFDMGMAPLANVGTEEDSFIE---EKVA 785
L_Msm       LGDP-ADDDCLLVEAVQ-GDEVVAMLSLVPWGSN--GVSLDVMRRS-PRSPNGTIELMVSELCMQAEDIGISRISLNFAMFRSAFEQGAQLGAGPVARLW 496
L_Mtb       LGDP-ADSDCLLVEAIDPHNQVLAMLSLVPWGTT--GVSLDLMRRS-PQSPNGTIELMVSELALHAESLGITRISLNFAVFRAAFEQGAQLGAGPVARLW 573
```

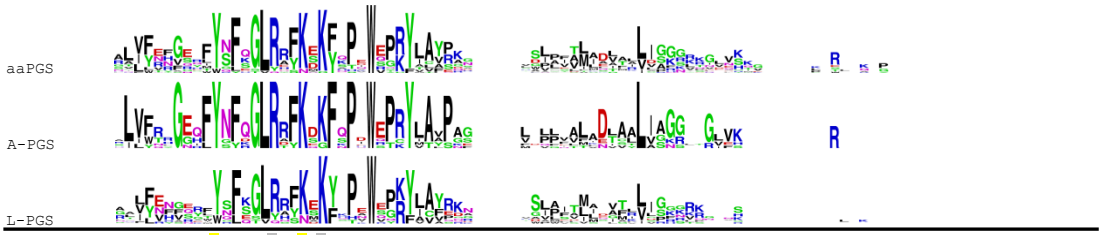


```
A_PAO1      ALVFRRGEQFYNFQGLRRFKDKFQPDWEPRYLAVPAG-----LDPLVALADTAALIAGGLTGLVK---------R---------------------- 881
A_Bph       NIVWRFGGRFYNFRGLRAFKSKFQPHWEPRYLAASGS-----VGVFFTLADLSLLAGGRRS---------------------------------- 864
A_Cpe       RLVYNSGNIFYSFDGLRRYKSKFSPIWQPRYLAYPKF-----MSLPEVFINLCLLIANSKERVEKK---------------------------- 569
A_Kra       HLLWTHGEQFYNFQGLRTFKQGFSPEWRTCYVAAPGE-----LALPNAMVDVATLVGGGIRGVVHS---------------------------- 346
A_Mba       SLIFTHGEHFYNYKGLRDFKEKFNPIWSPKYITLPNG-----FKQGFVLKDIAALISGGVKGIFSKENKRPASRRGNQLPEKPSEELT--------- 881
A_PA14      ALVFRRGEQFYNFQGLRRFKDKFQPDWEPRYLAVPAG-----LDPLVALADTAALIAGGLTGLVK---------R---------------------- 881
A_Ppoly     RLVFQYGGHFYGFQGLRRFKDKFKPQWEPRYLAYPAS-----VFLPILTLELVYLVSKRSD--------------------------------- 880
A_Pput      SLVFRRGEQLYNFQGLRRFKDKFQPDWEPRYMAVPAG-----LDPLVALADTAALIAGGLTGLVK---------R---------------------- 880
AL_Bsu      AVIFNNVRYMYSFSGLRAFKEKYKPEWRGKYLAYRKN-----RSLSVTMFLVTRLIGKSKKDSV---------------------------------- 856
ALR_Efm     YLVYEFGSHFYSFHGLREYKSKYATNWVSRYTLYSRD-----SWIAYVMIALLIID--NAPVEQTQGRISGLKKWIRRKY---------------- 866
ALR_Efs     ALIYEFGSEIYSFQGLREYKEKFASKWQPRYTLYSKS-----SWIVYVMIALLIVD--QKNID------------------------------- 843
L_Atu       STLFEHGERFYNFKGLRAFKAKFHPKWEPRYLAVQNG-----ADAALALMDATVLISGGVRGVIGK---------------------------- 866
L_Ban       AAIFNNVRYTYSFSGLRHFKEKYKPAWSGKYLAFRKN-----HSLPITMLSVTKLIGKRK---NS---------------------------- 861
L_Bli       AVIFNNVSYMYSFSGLRSFKEKYKPVWRGKYLAYRKN-----RSLPVTMILVTRLIGRRTK--------------------------------- 850
L_Bthu      AAIFNNVRYTYSFSGLRHFKEKYKPAWSGKYLAFRKN-----HSLPITMLSVTKLIGKKKQLNS------------------------------ 862
L_Ccre      RLLYERGEEIYNFQGVRRYKDKYDPVWQPRYIAAPQK-----WAIPFLLADIGLLSSGGVSGLAK---------RPKKLPEKAAT---------- 537
L_Cpe       LQFYENGQALYSFKGLRRFKEKFSHNWEYKYIAYRRN-----TSILITVIQAAIVCSRNRNVDESIVVRN--LKSLIK---------------- 851
L_Lmo       GLVYRYSQGFYGFKGLRNFKSKYVTEWEQKFVAFRKR-----SSIAFTMLQLMILVGKKRPLANSQVVLDFPLEEETKKPDSE---------- 865
L_Rtr       GTVFEHGERFYNFKGLRAFKSKFHPEWQPRYLAVSGG-----VSPMIALMDATFLIGGGLKGVVRK---------------------------- 868
L_Sa        GRVFEHFNGLYRFQGLRRYKSKYNPNWEPRFLVYRKD-----NSLWESLSKVMRVIRHK---------------------------------- 840
L_Sth       NLVYVFAQRFYSFSGLQRYKEKFSPIWSPKYIVYPKR-----TWLLFDMIAIFRID--NRKIEDKMKKRRLWK---------------------- 851
L_Msm       RALLVFFSKWWQLESLYRSNMKYQPEWVPRYACYEDARLVPRVGVASVIAEGFLVLPFSRRNKQHTGEHIAAPDTLVQSGRLHRDGSAPDVTGLQGE 593
L_Mtb       RGLLVFFSRWWQLETLYRSNMKYQPEWVPRYACYEDARVIPRVGVASVIAEGFLVLPFSRRNRVHTGHHPAVPERLAATGLLHHDGSAPDVSGLRQV 670
```

3.1.3 Phylogenetic distribution of aaPGS enzymes

The formerly described results might indicate a diverse evolutionary origin for aaPGS enzyme sequences with different specificities. A-PGSs might exhibit a smaller amino acid binding pocket than L-PGSs. Due to the lack of a characteristic amino acid conservation pattern distinguishing both enzyme variants from each other, minor amino acid substitutions in spatial positions might result in the tuning of the respective amino acid binding pocket and in the evolution of the respective aminoacyl-tRNA specificity. Thus, the aaPGS homologs of *B. subtilis*, *E. faecium* and *E. faecalis* showing a broadened amino acid substrate specificity (Roy and Ibba, 2009; Bao *et al.*, 2012) might represent evolutionary intermediate states. Different aaPG variants might enable the respective organism to fine-tune its membrane composition and lipid homeostasis. As mentioned before, C-terminal *Bacillus* aaPGS enzyme domains share a high sequence identity (see appendix, Figure 33), which might indicate that the broadening of *B. subtilis* MprF substrate specificity has occurred recently and therefore cannot be observed in related species.

To investigate the diverse evolution of aaPGS sequences, a phylogenetic tree consisting of representative prokaryotes was generated using the iTOL program (section 2.13.2; Letunic and Bork, 2007) and is presented in Figure 8. Within this tree, organisms carrying an aaPGS homolog identified by BLAST analysis (Altschul *et al.*, 1990; highlighted gray) and aaPGS enzymes with characterized substrate specificity are indicated (A-PGS: yellow; L-PGS: blue; broadened substrate specificity: orange). From this representation it becomes clear that A-PGS and L-PGS enzymes are detected within the *Bacilli* and the *Actinobacteria* and that enzymes with broadened specificity are only found in the *Bacilli* group. However, for none of the specificity groups, a phylogenetic clustering was observed and – *vice versa* – organisms of the same phylogenetic branch do not share the same aaPGS dependent lipid homeostasis.

Figure 8: Phylogenetic distribution of aaPGS enzymes in prokaryotes (see next page)
The pylogenetic tree of representative prokaryotes was generated using iTOL (Letunic and Bork, 2007). Organisms with aaPGS homologs identified by BLAST analysis are indicated (dark gray). Microbes with characterized A-PGS (yellow) and L-PGS enzymes (blue) are highlighted. *B. subtilis*, *E. faecalis* and *E. faecium* enzymes (orange) exhibit a broadened substrate specificity.
* *C. perfringens* possesses both an A-PGS and an L-PGS. # The corresponding activity has been newly elucidated (compare Table 11). ‡ Data are taken from the literature (compare Table 10).

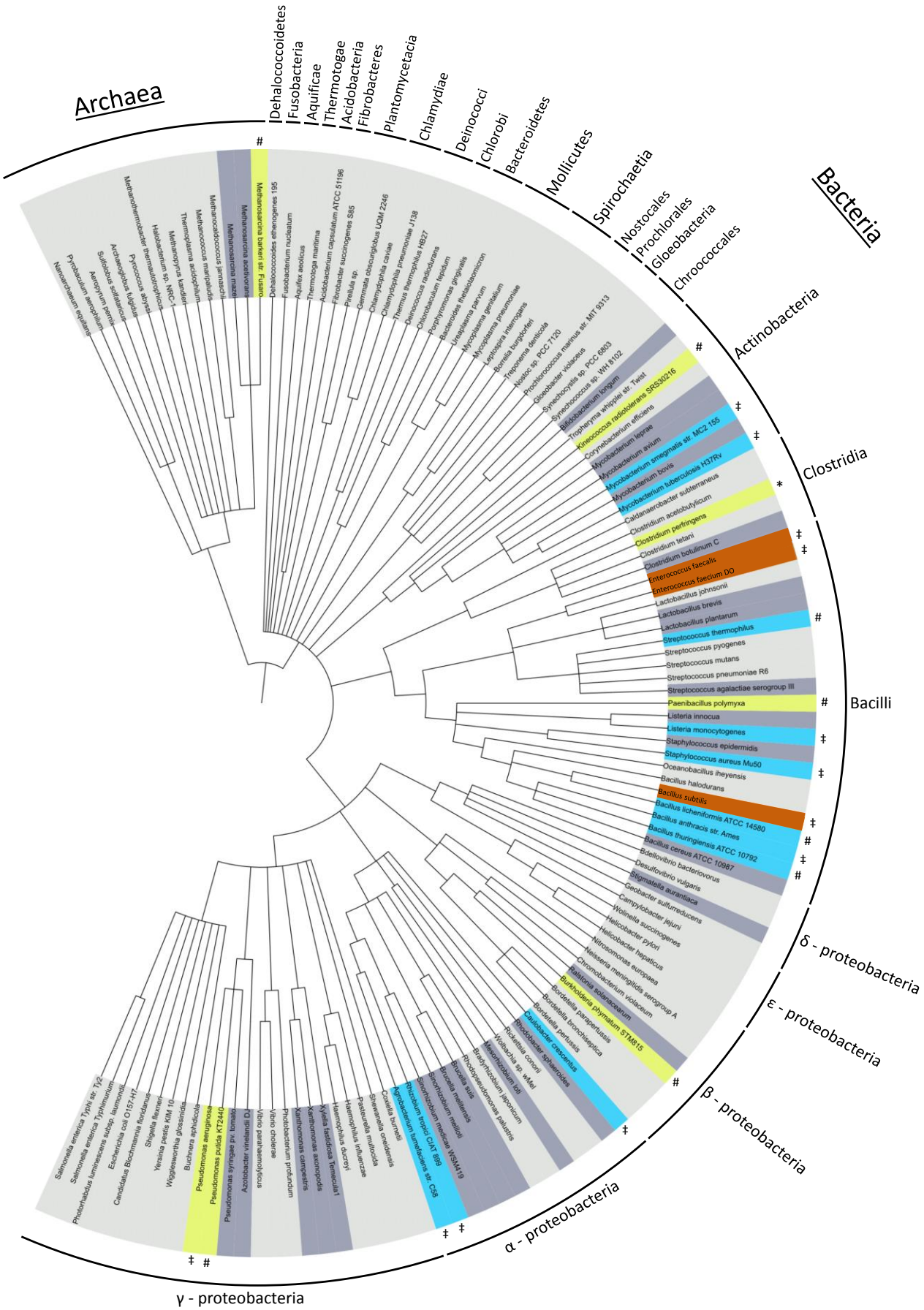
Archaea
Bacteria
Dehalococcoidetes
Fusobacteria
Aquificae
Thermotogae
Acidobacteria
Fibrobacteres
Plantomycetacia
Chlamydiae
Deinococci
Chlorobi
Bacteroidetes
Mollicutes
Spirochaetia
Nostocales
Prochlorales
Gloeobacteria
Chroococcales
Actinobacteria
Clostridia
Bacilli
δ - proteobacteria
ε - proteobacteria
β - proteobacteria
α - proteobacteria
γ - proteobacteria
Methanosarcina barkeri str. Fusaro
Methanosarcina acetivorans
Methanosarcina mazei
Methanococcoides burtonii DSM 6242
Methanococcus maripaludis
Methanococcus jannaschii
Methanothermobacter thermautotrophicus
Halobacterium sp. NRC-1
Methanopyrus kandleri
Thermoplasma acidophilum
Pyrococcus abyssi
Pyrococcus furiosus
Archaeoglobus fulgidus
Sulfolobus solfataricus
Aeropyrum pernix
Pyrobaculum aerophilum
Nanoarchaeum equitans
Dehalococcoides ethenogenes 195
Fusobacterium nucleatum
Aquifex aeolicus
Thermotoga maritima
Acidobacterium capsulatum ATCC 51196
Fibrobacter succinogenes S85
Pirellula sp.
Gemmata obscuriglobus UQM 2246
Chlamydophila caviae
Chlamydophila pneumoniae J138
Thermus thermophilus HB27
Deinococcus radiodurans
Chlorobaculum tepidum
Porphyromonas gingivalis
Bacteroides thetaiotaomicron
Ureaplasma parvum
Mycoplasma genitalium
Mycoplasma pneumoniae
Leptospira interrogans
Borrelia burgdorferi
Treponema denticola
Nostoc sp. PCC 7120
Prochlorococcus marinus str. MIT 9313
Gloeobacter violaceus
Synechocystis sp. PCC 6803
Synechococcus sp. WH 8102
Bifidobacterium longum
Tropheryma whipplei str. Twist
Kineococcus radiotolerans SRS30216
Corynebacterium efficiens
Mycobacterium leprae
Mycobacterium avium
Mycobacterium smegmatis str. MC2 155
Mycobacterium bovis
Mycobacterium tuberculosis H37Rv
Mycobacterium tuberculosis
Caldanaerobacter subterraneus
Clostridium acetobutylicum
Clostridium perfringens
Clostridium tetani
Clostridium botulinum C
Enterococcus faecalis
Enterococcus faecium DO
Lactobacillus johnsonii
Lactobacillus brevis
Lactobacillus plantarum
Streptococcus thermophilus
Streptococcus pyogenes
Streptococcus mutans
Streptococcus pneumoniae R6
Streptococcus agalactiae serogroup III
Paenibacillus polymyxa
Listeria innocua
Listeria monocytogenes
Staphylococcus epidermidis
Staphylococcus aureus Mu50
Oceanobacillus iheyensis
Bacillus halodurans
Bacillus subtilis
Bacillus licheniformis ATCC 14580
Bacillus anthracis str. Ames
Bacillus thuringiensis ATCC 10792
Bacillus cereus ATCC 10987
Bdellovibrio bacteriovorus
Desulfovibrio vulgaris
Stigmatella aurantiaca
Geobacter sulfurreducens
Campylobacter jejuni
Wolinella succinogenes
Helicobacter pylori
Helicobacter hepaticus
Nitrosomonas europaea
Neisseria meningitidis serogroup A
Chromobacterium violaceum
Ralstonia solanacearum
Burkholderia phymatum STM815
Bordetella parapertussis
Bordetella bronchiseptica
Bordetella pertussis
Caulobacter crescentus
Rickettsia conorii
Wolbachia sp. wMel
Brucella melitensis
Brucella suis
Rhodopseudomonas palustris
Bradyrhizobium japonicum
Mesorhizobium loti
Sinorhizobium meliloti
Sinorhizobium medicae WSM419
Rhizobium tropici CIAT 899
Agrobacterium tumefaciens str. C58
Silvereamella oneidensis
Cockella burmeli
Pasteurella multocida
Haemophilus influenzae
Haemophilus ducreyi
Xylella fastidiosa Temecula1
Xanthomonas axonopodis
Xanthomonas campestris
Photobacterium profundum
Vibrio cholerae
Vibrio parahaemolyticus
Azotobacter vinelandii DJ
Pseudomonas syringae pv. tomato
Pseudomonas putida KT2440
Pseudomonas aeruginosa
Buchnera aphidicola
Wigglesworthia glossinidia
Yersinia pestis KIM 10
Shigella flexneri
Escherichia coli O157:H7
Candidatus Blochmannia floridanus
Salmonella enterica Typhi str. Ty2
Salmonella enterica Typhimurium
Photorhabdus luminescens subsp. laumondii

3.2 Impact of different aaPGs on *P. aeruginosa* resistance phenotypes

The aminoacylation of PG with alanine and lysine was related to the resistance against several antimicrobial compounds for different bacteria (e.g. Peschel *et al.*, 2001; Klein *et al.*, 2009). It is not clear, if the observed resistance phenotypes resulted from a comparable mechanism of A-PG and L-PG or if the aaPG variants have different effects in different bacteria. For this, the well-established gram negative model organism *P. aeruginosa* PAO1 was chromosomally modified to synthesize different aaPG variants in the same genetic background. The constructed strains were employed to study the impact of specifically altered aaPG contents in the bacterial membrane on the resistance against a set of antimicrobial compounds.

3.2.1 Construction of *P. aeruginosa* mutant strains with altered aaPG content

To elucidate the role of the respective aaPG in *P. aeruginosa*, the PAO1 wild-type and the A-PGS deficient PAO1 ΔPA0920 deletion mutant strain (Lorenzo, 2006) were employed. Additionally, mutant strains synthesizing aaPG variants were constructed based on the PAO1 ΔPA0920 deletion mutant strain. All constructs consisted of the native PA0920 promoter P_{PA0920}, an aaPGS encoding gene and the t_{rrnB} terminator and were chromosomally integrated into the specific chromosomal *attB* locus for ΔPA0920 complementation (see Figure 9). The resulting strains were devoid of any resistance marker genes (see section 2.4.19). This mutant design guaranteed for a consistent transcriptional response in all complemented strains.

Orf PA0920 encoding the *P. aeruginosa* A-PGS was introduced into the *attB* locus which results in the homologous complementation variant of the ΔPA0920 deletion mutant strain (ΔPa_{comp}). The truncated version of orf PA0920 (PA0920aa543-881) encoding the C-terminal catalytic A-PGS domain (Hebecker *et al.*, 2011) was also employed yielding strain ΔPa-aa543-881_{comp}. For the synthesis of L-PG in *P. aeruginosa*, strain ΔPA0920 was cross-complemented using the *S. aureus mprF* gene (Sa113; Peschel *et al.*, 2001) and for the simultaneous production of L-PG and A-PG, the *B. subtilis mprF* gene (BSU08425; Roy and Ibba, 2009) was employed resulting in strains ΔSa_{comp} and ΔBs_{comp}. For the *E. faecium* aaPGS2, the modification of PG with alanine, lysine and arginine was observed *in vitro* (Roy and Ibba,

2009). The respective gene was also selected for the cross-complementation of the ΔPA0920 deletion mutant to yield strain ΔEf_{comp} (for details, see section 2.4.19).

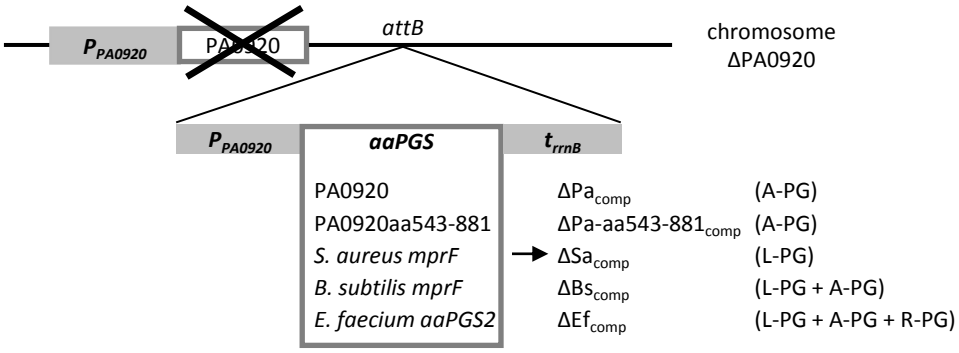

Figure 9: Complementation variants of the PAO1 ΔPA0920 deletion mutant strain
The *P. aeruginosa* PAO1 ΔPA0920 deletion mutant strain was chromosomally complemented with orf PA0920 (strain ΔPa_{comp}) or with a truncated PA0920 variant (PA0920aa543-881, yielding strain $\Delta Pa\text{-}aa543\text{-}881_{comp}$) at the *attB* locus. Analogously, ΔPA0920 was cross-complemented employing the aaPGS enconding genes from *S. aureus* (ΔSa_{comp}), *B. subtilis* (ΔBs_{comp}) and *E. faecium* (ΔEf_{comp}). For details, see section 2.4.19.
The specificity of the respective aaPGS enzyme is indicated. A-PG: alanyl-phosphatidylglycerol, L-PG: lysyl-phosphatidylglycerol, R-PG: arginyl-phosphatidylglycerol, P_{PA0920}: native promoter of orf PA0920, t_{rrnB}: *rrnB* terminator sequence, *attB*: attachment site B locus.

3.2.2 Lipid composition and growth behavior of complemented *P. aeruginosa* PAO1 ΔPA0920 mutant strains

The induction of the A-PGS promoter P_{PA0920} under acidic growth conditions (pH 5.3) resulted in the formation of 6 % A-PG compared to the overall polar lipid content for the PAO1 wild-type (Klein *et al.*, 2009). To investigate if the various complemented mutants of PAO1 ΔPA0920 synthesize the expected PG variants in *P. aeruginosa*, strains were grown under acidic conditions (pH 5.3; section 2.3.5) and their lipids were separated by two-dimensional TLC and visualized using molybdatophosphoric acid (sections 2.5.1 and 2.5.3). The resulting TLC plates are presented in Figure 10. For all complemented mutant strains, no variations in the amounts of the *P. aeruginosa* standard phospholipids PG, PE and DPG were observed (compare Figure 10). The A-PG content of the PAO1 wild-type was defined as 100 % and the aaPG amounts of the complemented strains were related to this value.

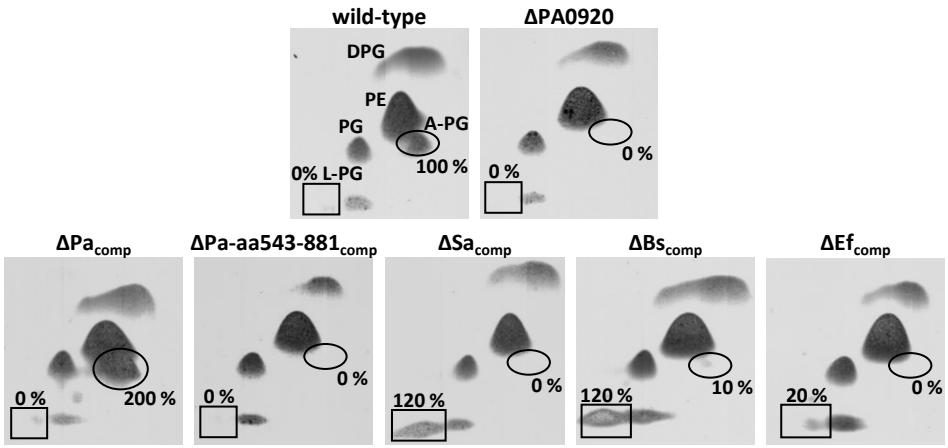

Figure 10: Lipid composition of *P. aeruginosa* PAO1 ΔPA0920 complementation variants
P. aeruginosa mutant strains were cultured in AB medium pH 5.3 at 37 °C for 24 h (section 2.3.5). After harvesting, polar lipids were extracted, analyzed by two-dimensional TLC and stained with molybdatophosphoric acid (sections 2.5.1 and 2.5.3). A-PG and L-PG positions are indicated by a circle or a rectangle, respectively. Relative aaPG amounts were quantified and related to the wild-type strain A-PG level defined as 100 % (section 2.5.3).
A-PG: alanyl-phosphatidylglycerol, DPG: diphosphatidylglycerol, L-PG: lysyl-phosphatidylglycerol, PE: phosphatidylethanolamine, PG: phosphatidylglycerol.

For the homologous complemented ΔPa$_{comp}$ strain, an increased amount of 200 % A-PG compared to the wild-type strain was determined. This elevated A-PG level might be a consequence of the integration of the respective construct into the *attB* locus site which provided an artificial chromosomal context compared to the wild-type strain (compare section 3.2.1). Due to the elevated A-PG content of the ΔPa$_{comp}$ mutant, this strain allowed for the determination of resistance phenotypes under artificially raised A-PG amounts in *P. aeruginosa*.

No A-PG was detected in the polar lipids of strain ΔPa-aa543-881$_{comp}$ containing the C-terminal soluble A-PGS domain catalyzing the alanylation of PG *in vitro* (Hebecker *et al.*, 2011). This observation might be a result of the deletion of the transmembrane domain anchoring the catalytic A-PGS domain to the cytoplasmic membrane. The ΔPa-aa543-881$_{comp}$ strain was excluded from further investigation because of its ΔPA0920 deletion mutant phenotype.

Strain ΔSa_{comp} was cross-complemented with the gene encoding the well-characterized L-PGS (MprF) from *S. aureus* (Peschel *et al.*, 2001; Staubitz *et al.*, 2004). As expected from previous studies, L-PG was detected for strain ΔSa_{comp} and the amount was quantified to 120 % compared to the PAO1 wild-type. The artificial synthesis of the positively charged L-PG instead of the zwitterionic A-PG in almost comparable amounts in *P. aeruginosa* provided a versatile tool to elucidate the validity of the 'charge repulsion' model originally proposed for the gram positive *S. aureus* (see section 1.4.3; Peschel *et al.*, 2001) in the context of the gram negative model organism *P. aeruginosa*.

For strain ΔBs_{comp} harboring the *B. subtilis mprF* gene, the formation of A-PG and L-PG was observed. In former studies, the synthesis of both aaPG variants had been reported with the dominant formation of L-PG and minor amounts of A-PG (Roy and Ibba, 2009). Therefore, the observed lipid levels of 120 % L-PG and 10 % A-PG were in good agreement with the previous *in vitro* characterization. Because of the concomitant synthesis of both L-PG and A-PG, strain ΔBs_{comp} was an appropriate tool to analyze resistance phenotypes in the presence of two aaPGs in *P. aeruginosa*.

20 % L-PG was detected for the ΔEf_{comp} strain cross-complemented with the aaPGS2 from *E. faecium*. The aaPGS2 had been characterized to synthesize predominantly L-PG together with minor amounts of R-PG and A-PG before (Roy and Ibba, 2009). Due to the low L-PG amount detected in ΔEf_{comp}, it seems reasonable that the levels of A-PG and R-PG were below the detection limit of the employed method. Therefore, strain ΔEf_{comp} was not subjected to further investigations.

Importantly, for the chimeric mutant strains ΔSa_{comp}, ΔBs_{comp} and ΔEf_{comp}, the observed aaPG formation resulted from the utilization of the specific *P. aeruginosa* aminoacyl-tRNAs as amino acid substrate donors. These results were in good agreement with a previous study elucidating that the individual tRNA sequence is of minor importance for the aminoacyl-tRNA recognition. Instead, the amino acid moiety of the aminoacyl-tRNA substrate was identified as the major determinant (Hebecker *et al.*, 2011).

To further characterize the complemented PAO1 ΔPA0920 variants, their growth behavior was analyzed under neutral and acidic growth conditions (pH 7.3 and pH 5.3). The resulting growth curves are presented in Figure 11.

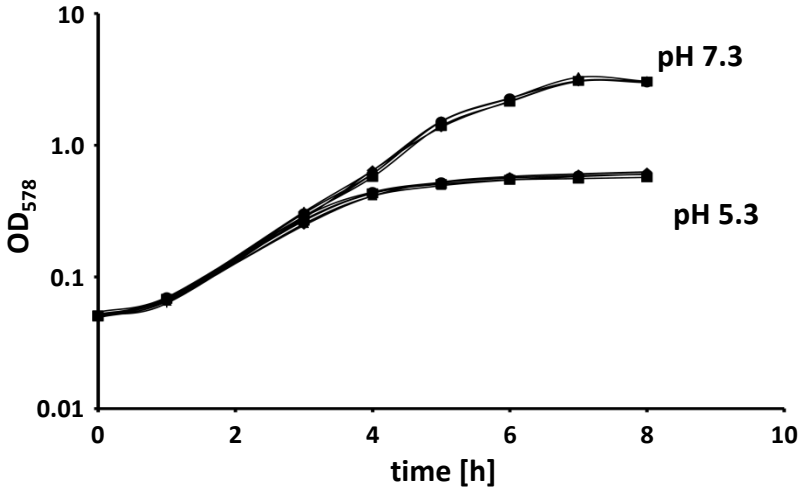

Figure 11: Growth curves of *P. aeruginosa* PAO1 ΔPA0920 complementation variants
P. aeruginosa mutant strains were cultured in AB medium pH 7.3 and pH 5.3 at 37 °C and 200 rpm (section 2.3.5). Culture turbidity was measured at 578 nm.
Rhombus: PAO1 wild-type, square: PAO1 ΔPA0920, triangle: ΔPa_{comp}, dot: ΔSa_{comp}, plus: ΔBs_{comp}.

The growth of the ΔPA0920 deletion mutant strain was identical to the behavior of the PAO1 wild-type strain under acidic and neutral growth conditions. This was also observed for the constructed complemented strains (Figure 11).

3.2.3 AaPGS dependent resistance phenotypes of *P. aeruginosa*

In several bacterial pathogens, the aminoacylation of PG had been related to a reduced susceptibility to antimicrobial agents (e.g. *S. aureus*, *M. tuberculosis*, *P. aeruginosa*; Peschel *et al.*, 2001; Maloney *et al.*, 2009; Klein *et al.*, 2009). To analyze the impact of different aaPGs, *P. aeruginosa* strains producing elevated A-PG amounts, L-PG or A-PG and L-PG simultaneously (compare sections 3.2.1 and 3.2.2) were analyzed concerning their resistance phenotypes in the presence of antimicrobial compounds.

In an initial approach, the PAO1 wild-type, the PAO1 ΔPA0920 deletion mutant and the complemented strains were cultivated under 1152 different conditions employing the Phenotype MicroArray™ system (Biolog, Hayward, CA, USA) at neutral pH conditions (section 2.7.1). This system allows for a high-throughput investigation of a wide variety of antimicrobial substances (Bochner, 2009). The strains were cultivated in 96-well plates

providing the substances to be analyzed. During incubation, an applied tetrazolium dye was reduced by electrons provided by the respiratory chain of the bacteria. The resulting purple formazan was detected to determine the survival of the bacteria under the specifically employed conditions (section 2.7.1). This initial analysis revealed a set of around 30 conditions with different phenotypes for the applied mutant strains compared to the wild-type strain (data not shown). Compounds resulting in diverse phenotypes for the wild-type and the mutant strains were subjected to further analyses.

The initial results were verified in a second independent experimental setup (see section 2.7.2). The employed *P. aeruginosa* strains were diluted in AB medium pH 5.3 according the Phenotype MicroArray™ protocol and 96-well plates were individually prepared with inhibitory compounds in varying concentrations. The plates were inoculated with the prepared cell suspensions, covered with a gas permeable membrane and incubated without shaking at 37 °C for 18 h. Cell growth was monitored by measuring the culture turbidity in the absence of the membrane. The employed acidic conditions ensured maximal cellular aaPG content due to the employed P_{PA0920} promoter (Klein *et al.*, 2009). For the present study, antimicrobial compounds were selected based on the initial Phenotype MicroArray™ experiments. Compounds further reported to result in resistance phenotypes mediated by aaPGS enzymes (daptomycin, oxacillin, methicillin, polymyxins, nisin), to have a direct influence on the integrity of bacterial membranes (poly-L-lysine) or to be of special clinical interest (vancomycin) were also employed (Hachmann *et al.*, 2009; Komatsuzawa *et al.*, 2001; Nishi *et al.*, 2004; Hartmann and Galla, 1978; Rossetti *et al.*, 2004; Mogi and Kita, 2009; Bao *et al.*, 2012).

Growth differences observed for the respective strains resulted in the utilization of the antimicrobials ampicillin, oxacillin, cefsulodin, daptomycin, protamine sulfate, poly-L-lysine, polymyxin E, benzethonium chloride, domiphen bromide and vancomycin for further investigations (for chemical structures of antimicrobial compounds, see appendix, Figure 34). Resistance phenotypes mediated by aaPG synthesis in the presence of daptomycin and several β-lactam antibiotics had been described before for *S. aureus* and *B. subtilis* (Hachmann *et al.*, 2009; Komatsuzawa *et al.*, 2001; Nishi *et al.*, 2004; Jones *et al.*, 2008) and a reduced susceptibility of *P. aeruginosa* synthesizing A-PG was observed for protamine sulfate and cefsulodin (Klein *et al.*, 2009).

To quantify the observed growth differences of the employed *P. aeruginosa* mutant strains in the presence of the selected antimicrobial compounds, a modified microdilution method for MIC determination was employed (see section 2.7.3). Cells were grown under acidic conditions to induce aaPG synthesis (compare 3.2.2; Klein *et al.*, 2009) and mixed with antimicrobial compounds in gradually varying concentrations in 96-well plates. After incubation, the culture turbidity of each well was measured and the lowest concentration with an $OD_{595} < 0.05$ was defined as the MIC ($OD_{595} < 0.1$ for daptomycin; the lowest concentration resulting in a constant OD_{595} minimum level was employed for protamine sulfate). Each value employed for MIC determination was averaged from four parallel growth experiments in different wells. MIC determination experiments were reproduced independently at least in triplicate. This system allows for the efficient determination of resistance phenotypes in the presence of gradually varying concentrations. The MICs obtained for the complemented ΔPA0920 mutant strains are summarized in Table 12.

Table 12: MICs (µg/mL) of *P. aeruginosa* strains with different aaPG contents
For MIC determination, strains were treated with gradually varying concentrations of the antimicrobials in AB medium pH 5.3 (section 2.7.3). The relative standard deviation was approximately 5 % (10 % for protamine sulfate and daptomycin). P values were calculated by significance analysis and are indicated: P ≤ 0.1 (*), P ≤ 0.05 (**) and P ≤ 0.01 (***). Lipid amounts are indicated as determined in section 3.2.2. All concentrations are given in µg/mL. Experiments were performed at least in triplicate.
aaPG: aminoacyl-phosphatidylglycerol, A-PG: alanyl-phosphatidylglycerol, L-PG: lysyl-phosphatidylglycerol.

	wild-type 100 % A-PG	**ΔPA0920** 0 % aaPG	**ΔPa$_{comp}$** 200 % A-PG	**ΔSa$_{comp}$** 120 % L-PG	**ΔBs$_{comp}$** 120 % L-PG 10 % A-PG
ampicillin	300 ± 15	60*** ± 3	300 ± 15	90*** ± 5	60*** ± 3
oxacillin	12‘000 ± 600	10‘000 ± 500	12‘000 ± 600	5‘000*** ± 250	5‘000*** ± 250
cefsulodin	61 ± 3	28*** ± 2	44** ± 2	44** ± 2	28*** ± 2
daptomycin	12‘000 ± 1200	6‘000** ± 600	9‘000* ± 900	3‘000** ± 300	6‘000** ± 600
protamine sulfate	100 ± 10	40* ± 4	40* ± 4	40* ± 4	40* ± 4
poly-L-lysine	18 ± 1	9*** ± 0.5	9*** ± 0.5	6*** ± 0.5	9*** ± 0.5
polymyxin E	8 ± 0.5	5** ± 0.3	4** ± 0.3	5** ± 0.3	5** ± 0.3
benzethonium chloride	31 ± 1.6	25*** ±1.3	16*** ± 0.8	16*** ± 0.8	25** ± 1.3
domiphen bromide	9.9 ± 0.5	8.7 ± 0.4	8.7 ± 0.4	8.7 ± 0.4	8.7 ± 0.4
vancomycin	17‘800 ± 900	15‘600 ± 800	15‘600 ± 800	17‘800 ± 900	15‘600 ± 800

Of note, the MICs determined for oxacillin, daptomycin and vancomycin are at least three orders of magnitude higher than employed for clinical application (Enoch *et al.*, 2007; Wright, 1999; Truong *et al.*, 2012). The observed changes of MIC due to the presence or absence of aaPGS encoding genes are comparable to alterations reported for multiresistant *P. aeruginosa* clinical isolates (Strateva and Yordanov, 2009; Riou *et al.*, 2010).

Phenotypes in the presence of β-lactam antibiotics

P. aeruginosa strains possess a high intrinsic resistance against β-lactam antibiotics due to their low outer membrane permeability and their chromosomally encoded detoxification systems like antibiotic inactivating enzymes and multidrug efflux pumps (section 1.2.1; Hancock and Speert, 2000). In a former study, the susceptibility of *P. aeruginosa* to the cephalosporin cefsulodin had been related additionally to the presence of A-PG in cellular membranes (Klein *et al.*, 2009). In this work, the presence of modified A-PG levels (strains ΔPA0920 and ΔPa_{comp}), of L-PG (ΔSa_{comp}) or of L-PG and A-PG concomitantly (ΔBs_{comp}) resulted in MIC reductions when compared to the PAO1 wild-type (see Table 12).

Ampicillin

The deletion of orf PA0920 from the PAO1 genome resulted in a MIC reduction from 300 µg/mL to 60 µg/mL in the presence of ampicillin. For the homologously complemented ΔPa_{comp} strain, a MIC of 300 µg/mL was observed representing the wild-type phenotype. This result indicated that the elevated A-PG level of ΔPa_{comp} had no influence on the susceptibility to ampicillin. A MIC of 90 µg/mL was observed for the ΔSa_{comp} strain. Obviously, the synthesis of 120 % L-PG resulted in an only partially restored phenotype. However, for the ΔBs_{comp} strain, exhibiting 10 % A-PG and 120 % L-PG, a MIC of 60 µg/mL was determined representing the deletion mutant strain resistance phenotype. Thus, the ampicillin resistance in *P. aeruginosa* depends on the incorporation of sufficient amounts of A-PG into the cellular membranes.

Oxacillin

For the PAO1 wild-type, a MIC of 12 mg/mL oxacillin was observed, whereas a reduced value of 10 mg/mL was determined for the deletion mutant strain indicating the influence of A-PG on the susceptibility of *P. aeruginosa* to the employed β-lactam. A MIC of 12 mg/mL was also detected for strain ΔPa_{comp}. Apparently, the synthesis of 200 % A-PG restored the wild-type phenotype as it was also observed for ampicillin. However, the MICs of strains ΔSa_{comp} and ΔBs_{comp} were determined to 5 mg/mL meaning that these strains were more susceptible to oxacillin than the ΔPA0920 deletion mutant strain devoid of any aaPG. Obviously, the artificially altered membrane lipid composition with 120 % L-PG (ΔSa_{comp}) or with 120 % L-PG and 10 % A-PG (ΔBs_{comp}) has deleterious effects on the oxacillin resistance of *P. aeruginosa*.

By comparing the chemical structures of ampicillin and oxacillin (see appendix, Figure 34), it becomes clear that minor structural alterations discriminating these compounds have important consequences for the resistance of *P. aeruginosa* represented by a 40-fold increased MIC for oxacillin (12 mg/mL) compared to ampicillin (300 µg/mL). Studies of the *E. coli* outer membrane protein OmpF indicated a selective transport for zwitterionic β-lactam antibiotics (ampicillin). Instead, mono- or dianionic β-lactams (oxacillin) were transported with significantly lower rates (Yoshimura and Nikaido, 1985; Nestorovich *et al.*, 2002; Vidal *et al.*, 2005). A comparable selective uptake mechanism might also be present in *P. aeruginosa* judging from the highly increased resistance to oxacillin compared to ampicillin. However, three decades ago, it was shown that phospholipid bilayers are permeable for β-lactams with varying rates depending presumably on the β-lactam charge characteristic (Yamaguchi *et al.*, 1982). According to the differing MICs obtained for the cross-complemented strains in the presence of ampicillin and oxacillin compared to the wild-type and the ΔPA0920 deletion mutant strain in this study, other membrane parameters like fluidity or polarity might also be involved in the observed susceptibility phenotypes.

Cefsulodin

The MIC for the ΔPA0920 deletion mutant (28 µg/mL) was found reduced compared to the wild-type strain (61 µg/mL) in the presence of the cephalosporin cefsulodin. Interestingly, in contrast to the results for ampicillin and oxacillin, a reduced MIC of 44 µg/mL was observed

for strain ΔPa_{comp}, restoring the wild-type phenotype only partially. It seems reasonable that the *P. aeruginosa* cefsulodin resistance depends on a specific A-PG level. For the cross-complemented strains, MICs of 44 µg/mL (ΔSa_{comp}) and 28 µg/mL (ΔBs_{comp}) were obtained confirming the hypothesis of an accurate lipid homeostasis. Interestingly, the relative amount of 120 % L-PG (ΔSa_{comp}) resulted in the same partially restored phenotype as it was observed for 200 % A-PG (ΔPa_{comp}).

Phenotypes in the presence of daptomycin

Daptomycin is a new lipopeptide antibiotic employed for the treatment of serious infections with gram positive bacteria being resistant to several antimicrobial compounds (Enoch *et al.*, 2007). The specific mechanism of action was proposed: The lipopeptide interacts with PG molecules of the membrane in a Ca^{2+}-dependent manner and pores are formed within the membrane by aggregating oligomers. Consequently, the membrane becomes depolarized, the membrane potential collapses and subsequently, the cells die (Muraih *et al.*, 2011; Pogliano *et al.*, 2012).

As became clear from the present study (compare Table 12), *P. aeruginosa* is highly resistant to daptomycin presumably due to the low outer membrane permeability (Hancock and Speert, 2000). MICs of 12 mg/mL and 6 mg/mL were obtained for the wild-type strain and the ΔPA0920 deletion mutant, respectively. A MIC of 9 mg/mL observed for strain ΔPa_{comp} indicated a partially restored wild-type phenotype due to the elevated A-PG level of 200 % present in this strain. In contrast, MICs of 3 mg/mL and 6 mg/mL were determined for strains ΔSa_{comp} and ΔBs_{comp}, respectively. The synthesis of 120 % L-PG in strain ΔSa_{comp} increased the susceptibility of the cells to daptomycin, whereas the presence of 10 % A-PG and 120 % L-PG resulted in a deletion mutant phenotype for strain ΔBs_{comp}. From this it might be concluded that the incorporation of A-PG into *P. aeruginosa* membranes is important for daptomycin resistance, whereas the formation of L-PG increases the susceptibility to this lipopeptide antibiotic. In several previous studies, daptomycin resistance phenotypes had been related to L-PG formation in *S. aureus* and *B. subtilis* (Friedman *et al.*, 2006; Hachmann *et al.*, 2009; Julian *et al.*, 2007; Mishra *et al.*, 2009; Rubio *et al.*, 2011). In a recently published study, the daptomycin resistance of *S. aureus* strains synthesizing different aaPG variants had been compared. Interestingly, the phenotypes of

strains incorporating A-PG or L-PG into the cytoplasmic membrane did not differ from each other (Slavetinsky *et al.*, 2012). The diverging results obtained for the gram positive model organism *S. aureus* by Slavetinsky *et al.*, 2012, and for the gram negative model organism *P. aeruginosa* in this study might indicate that different mechanisms are responsible for daptomycin resistance. Interestingly, other studies indicated that daptomycin resistance in *Enterococci* and *B. subtilis* depends on the level of PG rather than on the L-PG content (Mishra *et al.*, 2012a; Hachmann *et al.*, 2011) but might also be influenced by membrane fluidity (Mishra *et al.*, 2012b). Since the PG content of the employed *P. aeruginosa* strains was identical, the 'PG reduction' hypothesis does not explain the observed phenotypes.

Phenotypes in the presence of CAMPs

Cationic antimicrobial compounds are widely used by various organisms for the defense of competing species. Most CAMPs consist of two domains: a cationic part interacting with negatively charged bacterial membrane surfaces and a hydrophobic part putatively mediating the integration and pore formation into the membranes (Zasloff, 2002; Peschel and Sahl, 2006). To escape CAMPs produced by competing organisms, several resistance mechanisms have evolved in bacteria like the alteration of the membrane surface charge, e.g. by the formation of L-PG (Koprivnjak and Peschel, 2011; Peschel and Sahl, 2006). The 'charge repulsion' model postulated by Peschel *et al.*, 2001, was developed based on increased susceptibilities to CAMPs for L-PG deficient *S. aureus* strains. In the present study, the CAMPs protamine sulfate, poly-L-lysine and polymyxin E were employed to analyze the impact of different aaPGs in *P. aeruginosa*. For several organisms, an interaction of these CAMPs with membrane components was described as the antimicrobial action mechanism (Aspedon and Groisman, 1996; Conte *et al.*, 2007; Epand *et al.*, 2010; Johansen *et al.*, 1997; Koo *et al.*, 2001; Lim *et al.*, 2010; Zhang *et al.*, 2000). For complemented *S. aureus* strains analyzed by CAMP treatment, restored wild-type MICs had been observed (Peschel *et al.*, 2001).

For the ΔPA0920 deletion mutant strain, an increased susceptibility to protamine sulfate indicated by a MIC of 40 µg/mL compared to the wild-type strain (100 µg/mL) was observed (see Table 12). Likewise, for all complemented strain variants, a MIC of 40 µg/mL was obtained in the presence of protamine sulfate. The results for poly-L-lysine exhibited an

identical tendency: A MIC of 18 µg/mL was detected for the wild-type strain, which was reduced to 9 µg/mL for strains ΔPA0920, ΔPa_{comp} and ΔBs_{comp}. For ΔSa_{comp}, a MIC of 6 µg/mL indicated an increased susceptibility to poly-L-lysine in the absence of A-PG. The treatment of the various *P. aeruginosa* strains with polymyxin E resulted in reduced MICs of 5 µg/mL for the ΔPA0920 deletion mutant and for the ΔSa_{comp} and ΔBs_{comp} strains compared to a MIC of 8 µg/mL determined for the wild-type. The susceptibility of the homologously complemented strain ΔPa_{comp} to polymyxin E was slightly increased (4 µg/mL) compared to the other mutant strains.

In summary, the wild-type resistance phenotype for CAMP molecules was not restored by any of the complemented strains possessing elevated A-PG levels (ΔPa_{comp}), L-PG (ΔSa_{comp}) or L-PG together with A-PG (ΔBs_{comp}). In conclusion, it is proposed that the membrane lipid homeostasis is of high importance for CAMP resistance in the employed gram negative model organism *P. aeruginosa*. Neither the 'charge repulsion' mechanism, as it was proposed for the resistance of L-PG synthesizing *S. aureus* strains against CAMPs (Peschel *et al.*, 2001), nor the 'PG reduction' hypothesis, as it was proposed based on studies analyzing the resistance of *Enterococci* and *B. subtilis* to daptomycin (Mishra *et al.*, 2012a; Hachmann *et al.*, 2011), do explain the results for the *P. aeruginosa* mutant strains observed in this study.

Phenotypes in the presence of cationic surfactants

Cationic surfactants possess an antimicrobial activity against a wide variety of bacteria and are therefore used as disinfectant components and for liquid drug conservation (Hegstad *et al.*, 2010). Because *P. aeruginosa* possesses a high intrinsic resistance (Hancock and Speert, 2000), disinfectants must be selected with caution. Remarkably, *P. aeruginosa* strains can grow in the presence of disinfectants and have been isolated out of disinfectants previously (Bullard *et al.*, 2011; Lanini *et al.*, 2011). In this study, the quaternary ammonium compounds benzethonium chloride and domiphen bromide were employed to treat *P. aeruginosa* strains with artificially altered membrane compositions (see Table 12). These compounds are proposed to interact with bacterial membranes in a detergent-like mode of action because of their amphiphilic structure (Gilbert and Moore, 2005).

The MIC of the ΔPA0920 deletion mutant strain was reduced to 25 µg/mL in the presence of benzethonium chloride compared to 31 µg/mL observed for the wild-type strain. Interestingly, for strain ΔPa_{comp} synthesizing elevated A-PG levels and for the L-PG producing ΔSa_{comp} strain, an increased susceptibility of 16 µg/mL was detected. A deletion mutant-like phenotype (25 µg/mL) was observed for the ΔBs_{comp} strain incorporating both L-PG and A-PG into its membrane. Domiphen bromide treatment resulted in MICs of 9.9 µg/mL for the wild-type strain and of 8.7 µg/mL for all mutant strains.

Due to these results obtained for all complemented strains which provide an altered membrane composition resulting in a more positively charged membrane surface, the resistance of *P. aeruginosa* to the quaternary ammonium surfactants cannot be related directly to the membrane surface charge. Thus, the formerly postulated 'charge repulsion' mechanism (Peschel *et al.*, 2001) is inapplicable for the *P. aeruginosa* model organism used in this study. Instead, the characteristics of the present lipids and a fine-tuning of membrane lipid homeostasis are proposed to be of high importance.

Phenotypes in the presence of vancomycin

The glycopeptide antibiotic vancomycin has been used to treat infections caused by gram positive bacteria since more than 20 years. It binds to peptidoglycan precursors and prevents the transpeptidation reaction cross-linking specific amino acid residues (Courvalin, 2006).

In this study, *P. aeruginosa* strains with artificial aaPG levels were incubated with vancomycin (see Table 12). The vancomycin treatment of the wild-type strain resulted in a MIC of 17.8 mg/mL, whereas the value was slightly reduced to 15.6 mg/mL for the ΔPA0920 deletion mutant and the complemented mutant strains ΔPa_{comp} (200 % A-PG) and ΔBs_{comp} (120 % L-PG, 10 % A-PG). Importantly, for the ΔSa_{comp} strain (120 % L-PG), a wild-type-like MIC of 17.8 mg/mL was observed. These observations are consistent with previous results obtained by vancomycin treatment of gram positive *S. aureus* strains. These results indicated that the resistance of both pathogens to vancomycin does not depend directly on the synthesis of aaPG (Komatsuzawa *et al.*, 2001; Julian *et al.*, 2007).

3.3 Cellular response of *P. aeruginosa* in the presence of selected antimicrobial agents

The bacterial membrane lipid composition can be adapted to various environmental conditions (Hazel and Williams, 1990). Former studies reported the alteration of transcriptional and translational profiles of a wide variety of genes and proteins in response to several antimicrobials. The altered profiles resulted in the adaptation of the cells to the respective stress condition (Brazas and Hancock, 2005; Wenzel and Bandow, 2011; Davies *et al.*, 2006). In this work, the influence of selected antimicrobial agents on the transcriptional regulation of the A-PG synthesizing A-PGS of *P. aeruginosa* was investigated. For this, the formerly constructed PAO1-P_{PA0920}-*lacZ* strain was employed harboring the P_{PA0920} promoter upstream of the *lacZ* reporter gene within the *attB* integration site of the PAO1 chromosome (Klein *et al.*, 2009). In a previous study, the P_{PA0920} promoter was identified to be activated under acidic growth conditions (Klein *et al.*, 2009). Hence, P_{PA0920} promoter activity was analyzed under neutral and acidic growth conditions (pH 7.3 and pH 5.3) in the presence of selected antimicrobials in subinhibitory concentrations (0.08- to 0.25-fold MIC of the PAO1 wild-type) to allow for appropriate growth (compare section 2.8.2). During incubation, samples were taken and the β-galactosidase activity was determined. The obtained values were related to the culture turbidity and the overall bacterial protein content to eliminate deviations in the promoter activity determination due to cell morphology alterations induced by the antimicrobial agents (for details, see section 2.8.2). Notably, the β-galactosidase activities calculated on the basis of the overall protein content were consistent with the values conventionally calculated on the basis of the culture turbidity (data not shown).

In all cases, a significant promoter activity induction was obtained under acidic growth conditions compared to neutral conditions. Exemplary results for daptomycin and polymyxin E are displayed in Figure 12.

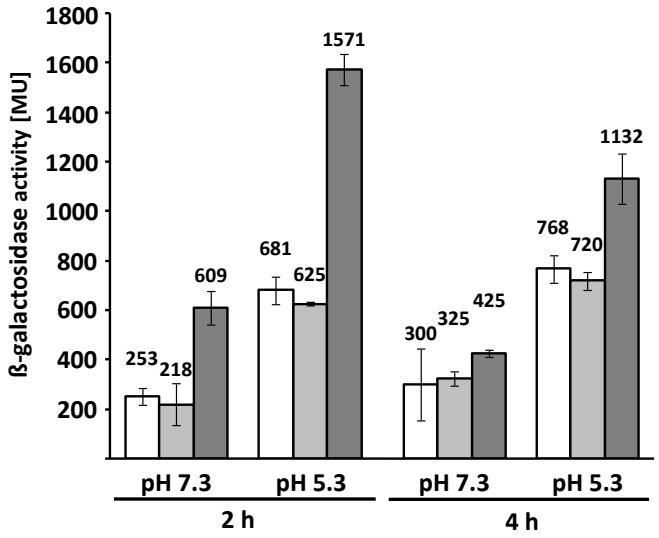

Figure 12: P_{PA0920} promoter activity in the presence of daptomycin and polymyxin E
The P_{PA0920} promoter activity was analyzed employing strain PAO1-P_{PA0920}-*lacZ* harboring the transcriptional P_{PA0920}-*lacZ* promoter-reporter gene fusion. The cells were cultivated in AB medium (pH 5.3 and pH 7.3) in the presence of daptomycin and polymyxin E in subinhibitory concentrations. The β-galactosidase activity was determined 2 h and 4 h after antimicrobial application (section 2.8.2).
White: untreated cultures, light gray: cultures treated with 1.5 mg/mL daptomycin, dark gray: cultures treated with 1.33 µg/mL polymyxin E.

For the experiment in the absence of antimicrobials, an induction of the promoter activity under acidic growth conditions (pH 5.3) from 253 to 681 MU (2 h) and from 300 to 768 MU (4 h) was observed compared to the values obtained at pH 7.3. Daptomycin treatment resulted in comparable values under all observed conditions (2 h: 218 MU (pH 7.3), 625 MU (pH 5.3); 4 h: 325 MU (pH 7.3), 720 MU (pH 5.3)) indicating that the transcript level of the A-PGS was not altered in the presence of this lipopeptide antibiotic. Interestingly, the application of polymyxin E resulted in increased β-galactosidase activities under both pH conditions after 2 h (pH 7.3: 609 MU; pH 5.3: 1571 MU) representing induction ratios of 2.4 (pH 7.3) and 2.3 (pH 5.3). After 4 h of polymyxin E treatment, the induction ratios were reduced but were still present as indicated by values of 425 MU (pH 7.3: ratio 1.4) and 1132 MU (pH 5.3: ratio 1.5).

In general, the β-galactosidase activity was increased under acidic conditions in comparable ranges in the presence of all employed antimicrobials, respectively, indicating the dominant influence of the acidic pH on the P_{PA0920} promoter activity. Interestingly, the overall extent of

the promoter activity was additionally modulated by some of the applied antimicrobials as exemplified for polymyxin E above (Figure 12) and it depends on the growth phase of the bacteria. In order to quantify the promoter activity modulation caused by the individual compound, induction ratios were calculated relating promoter activities in the presence of the respective compound to values obtained without any antimicrobial compound. The results are presented in Table 13.

Table 13: P_{PA0920} promoter induction by several antimicrobial compounds
The P_{PA0920} promoter induction was analyzed employing the PAO1-P_{PA0920}-*lacZ* strain harboring a transcriptional P_{PA0920}-*lacZ* promoter-reporter gene fusion inserted into the *attB* locus of the PAO1 chromosome. Cells were cultured in AB medium (pH 5.3 and pH 7.3) for 2 h. The respective antimicrobials were added in subinhibitory concentrations and the β-galactosidase activity was determined 2 h and 4 h after compound application. The promoter activity modulation by the individual compound was calculated as the induction ratio representing the promoter activity in the presence of the respective antimicrobial agent related to the control experiment in the absence of any antimicrobial compound. A ratio > 1 represents an increased induction of the P_{PA0920} promoter caused by the individual compound. Modulation maxima and minima are indicated by bold letters. Experiments were performed at least threefold.

	pH 5.3		**pH 7.3**	
	2 h	**4 h**	**2 h**	**4 h**
ampicillin	1.2 ± 0.1	0.8 ± 0.2	1.2 ± 0.1	**1.9 ± 0.2**
oxacillin	1.2 ± 0.3	0.9 ± 0.3	1.0 ± 0.3	**1.6 ± 0.3**
cefsulodin	1.1 ± 0.2	0.8 ± 0.1	0.9 ± 0.1	0.9 ± 0.1
daptomycin	0.9 ± 0.0	0.9 ± 0.1	0.9 ± 0.3	1.1 ± 0.2
protamine sulfate	**1.6 ± 0.4**	1.2 ± 0.3	**1.9 ± 0.6**	1.5 ± 0.2
poly-L-lysine	**0.6 ± 0.1**	0.7 ± 0.1	1.1 ± 0.2	1.1 ± 0.1
polymyxin E	**2.3 ± 0.5**	1.5 ± 0.2	**2.4 ± 0.4**	1.4 ± 0.2
benzethonium chloride	0.8 ± 0.1	**0.7 ± 0.0**	1.2 ± 0.1	1.0 ± 0.1
domiphen bromide	1.0 ± 0.4	0.8 ± 0.2	1.0 ± 0.1	0.9 ± 0.1

The treatment of the PAO1-P_{PA0920}-*lacZ* strain with the β-lactam antibiotics ampicillin and oxacillin resulted in increased P_{PA0920} promoter activities (induction ratios of 1.9 and 1.6) under neutral conditions after 4 h, whereas the activity was almost unaffected under all other conditions. In contrast, in the presence of the cephalosporin cefsulodin and the lipopeptide daptomycin, no promoter activity alteration was observed under all employed conditions (see above, Figure 12).

For the employed CAMP molecules, a modulated promoter activity was observed for each compound: Whereas an increased promoter activity was obtained under all employed conditions after the application of protamine sulfate (ratios of 1.2 to 1.9) and polymyxin E

(ratios of 1.4 to 2.4; see also Figure 12), a reduced promoter induction was determined when poly-L-lysine was applied under acidic conditions (ratios of 0.6 and 0.7). Poly-L-lysine treatment had almost no effect on the promoter induction under neutral conditions.

The utilization of the cationic surfactant benzethonium chloride resulted in a clearly reduced promoter induction under acidic growth conditions after for 4 h (ratio of 0.7), whereas no modulation of the promoter activity was observed under the all other conditions. The presence of domiphen bromide did not affect the P_{PA0920} promoter activity.

The obtained results indicate that the A-PGS expression is modulated in response to some but not all antimicrobial agents for which a resistance phenotype according to the synthesis of A-PG was observed (compare section 3.2.3). Interestingly, even for the functionally related CAMP molecules protamine sulfate, polymyxin E and poly-L-lysine, the transcription of the A-PGS was differently modulated (Table 13). These results indicate a diverse function of A-PG in the presence of various environmental stresses reflected by the individual regulation of the P_{PA0920} promoter in response to several antimicrobials, acidic or neutral growth conditions and in distinct growth phases.

Consequently, it was analyzed if the observed promoter activity modulations resulted in altered lipid compositions. For this, the membrane lipids of the control strain *P. aeruginosa* KS11 (Schreiber *et al.*, 2006) were extracted and separated by two-dimensional TLC after 2 h and 4 h treatment with the respective compound (compare section 2.8.2). However, only after oxacillin application, a slight increase of the A-PG content was observed at pH 7.3 (data not shown). Hence, it was concluded that the cellular A-PGS amount and consequently, the A-PG content are fine-tuned by the applied antimicrobials as indicated by the observed transcriptional modulation. In conclusion, the acidic pH condition was identified as the dominant effector increasing the P_{PA0920} promoter activity and the A-PG amount. Additionally, the P_{PA0920} activity can be modulated by specific antimicrobial compounds.

3.4 PA0920 is clustered together with PA0919 in gram negative bacteria

The A-PGS (orf PA0920) is encoded together with orf PA0919 on the *P. aeruginosa* PAO1 chromosome. Both orfs are separated by one single base pair. Therefore, they are predicted to form an operon according to the DOOR database (Mao *et al.*, 2009; data not shown). The MBGD database (Uchiyama *et al.*, 2010) was also employed to analyze the clustering of PA0920 and PA0919 homologous orfs in other aaPG synthesizing bacteria. PA0919 homologous genes were detected downstream of aaPGS encoding genes e.g. in *A. tumefaciens* (AcvB, 61 % sequence identity compared to PA0919), *R. tropici* (AtvA, 38 %), *Ralstonia pickettii* (Rpic_3994, 60 %) and *B. phymatum* (Bphy_4018, 36 %). In some organisms, at least two copies of PA0919 homologs were detected with at least one orf located distantly in the genome (e.g. in *Xanthomonas axonopodis, Pedobacter heparinus*, *Xylella fastidiosa* or *Sinorhizobium meliloti*). In contrast, the PA0919 homologous gene *virJ* is encoded on octopine-type Ti-plasmids of *A. tumefaciens* (VirJ encoded on the pTiA6 plasmid, 33 %) clustered together with virulence genes for plant infection (Pan *et al.*, 1995; Kalogeraki and Winans, 1995). Only in *Cellvibrio japonicus*, a potential PA0919 homolog (CJA_1309, 31 %) was detected in the absence of any aaPGS encoding gene.

Interestingly, the MBGD analysis did not identify any PA0919 homologous genes in gram positive bacteria. This result is in good agreement with a former study locating PA0919 to the periplasm of *P. aeruginosa* employing a translational PA0919-PhoA fusion construct (Lewenza *et al.*, 2005). Although PA0919 has not been analyzed biochemically yet, the predicted operon structure of PA0920 and PA0919 might indicate a function of the PA0919 protein in A-PG homeostasis.

3.5 PA0919 deletion results in various phenotypes

The first hints towards the function of PA0919 were obtained by analyzing mutant strains with transposon insertion sites within orf PA0919. These results were verified by generating a ΔPA0919 deletion mutant and several complemented strain variants and analyzing their growth behavior, lipid composition and antibiotic resistance phenotypes.

3.5.1 PA0919 transposon mutant strains provided increased A-PG levels

To get initial evidence towards the function of PA0919, two mutant strains with different transposon insertion sites within orf PA0919 were characterized (MPAO1 17368 and 53595, see Table 4 for details; strains were generously provided by Prof. Dr. S. Häußler from the Helmholtz Centre for Infection Research, Braunschweig, Germany; Jacobs *et al.*, 2002). The mutant strains and their corresponding wild-type strain MPAO1 were grown under neutral and acidic conditions (pH 7.3 and pH 5.3) to late stationary phase. Subsequently, polar lipids were extracted and analyzed by two-dimensional TLC (sections 2.3.5, 2.5.1 and 2.5.3).

Growth behavior and lipid patterns of both mutant strains were not affected under neutral conditions compared to the wild-type strain (data not shown). In contrast, bacterial growth of both mutant strains was reduced in acidified medium and A-PG levels were highly increased compared to the MPAO1 wild-type (data not shown).

3.5.2 Construction of the ΔPA0919 deletion mutant and complemented variants

To substantiate the results of the transposon mutant analysis, orf PA0919 was deleted from the PAO1 wild-type strain by homologous recombination (section 2.4.18) employing the method of Hoang *et al.*, 1998, yielding the markerless deletion mutant strain PAO1 ΔPA0919 (Groenewold, 2011). For detailed phenotype analyses, this strain was specifically complemented with different constructs as presented in Figure 13.

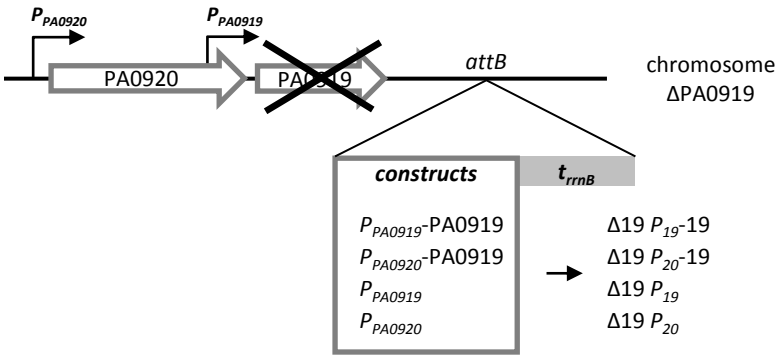

Figure 13: Complementation variants of PAO1 ΔPA0919 for functional analysis of PA0919
Strain PAO1 ΔPA0919 was chromosomally complemented with the orf PA0919 controlled by its own putative promoter (strain Δ19 P_{19}-19) or under the control of the P_{PA0920} promoter (Δ19 P_{20}-19), respectively. For control, both promoters were solely inserted into the ΔPA0919 chromosome (Δ19 P_{19} and Δ19 P_{20}). Construction details are presented in section 2.4.19.
attB: attachment site B locus, P_{PA0919}: putative native promoter of orf PA0919, P_{PA0920}: native promoter of orf PA0920, t_{rrnB}: *rrnB* terminator sequence.

First, a fragment covering orf PA0919 together with its 430 bp upstream region (carrying the putative P_{PA0919} promoter region) was inserted at the *attB* locus of the PAO1 ΔPA0919 chromosome resulting in strain Δ19 P_{19}-19. Interestingly, the putative P_{PA0919} promoter region is located within orf PA0920 (A-PGS) encoded upstream of orf PA0919. Second, orf PA0919 was cloned under the control of the P_{PA0920} promoter which had been shown to be induced under acidic conditions (see chapter 3.3 and Klein *et al.*, 2009) yielding strain Δ19 P_{20}-19. For control, the deletion mutant strain was complemented solely with each of the promoters, resulting in strains Δ19 P_{19} and Δ19 P_{20}. For strain construction details, see section 2.4.19.

3.5.3 PA0919 deficient strains exhibit a stationary growth phenotype and an increased A-PG content

For initial analysis, the PAO1 wild-type, the ΔPA0919 deletion mutant and the different ΔPA0919 complemented strains were grown under acidic and neutral conditions (pH 5.3 and pH 7.3) to the late stationary growth phase. Growth was monitored by measuring the culture turbidity. An identical growth behavior was observed for all strains under neutral conditions (see appendix, Figure 35), whereas growth was reduced for mutant strains devoid

of orf PA0919 compared to PA0919 harboring strains. Growth curves obtained under acidic growth conditions are presented in Figure 14.

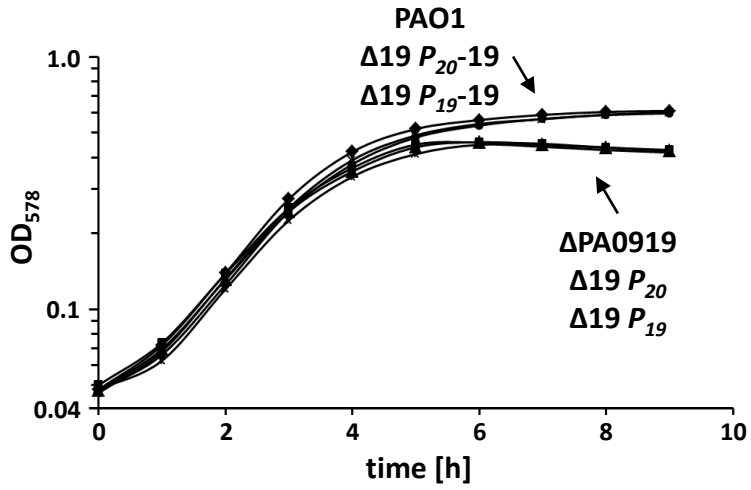

Figure 14: Stationary growth phenotype observed for *P. aeruginosa* strains devoid of orf PA0919

Different *P. aeruginosa* mutant strains were cultured in AB medium pH 5.3 at 37 °C and 200 rpm (section 2.3.5). Culture turbidity was measured at 578 nm.
Rhombus: PAO1 wild-type, square: PAO1 ΔPA0919, triangle: Δ19 P_{20}, cross: Δ19 P_{20}-19, star: Δ19 P_{19}, dot: Δ19 P_{19}-19.

Cultivation of strains devoid of orf PA0919 (ΔPA0919, Δ19 P_{20} and Δ19 P_{19}) under acidic conditions resulted in a stationary growth phase phenotype when compared to strains possessing a copy of orf PA0919 (PAO1 wild-type, Δ19 P_{20}-19 and Δ19 P_{19}-19). The observed phenotype was in good agreement with the results initially obtained by the transposon mutant strain investigation (section 3.5.1). Interestingly, reduced generation times obtained under acidic growth conditions had been reported before for *R. tropici* and *A. tumefaciens* mutant strains lacking the respective PA0919 homolog AtvA or AcvB, whereas the generation times had not been found affected significantly under neutral conditions (Vinuesa *et al.*, 2003). It was concluded that PA0919 is important for the growth of *P. aeruginosa* under acidic growth conditions.

The analysis of *P. aeruginosa* transposon mutant strains devoid of a functional PA0919 protein indicated an increased A-PG level under acidic conditions (section 3.5.1). Therefore, the employed PAO1 wild-type and the corresponding ΔPA0919 mutant strain variants were cultivated to late stationary phase under acidic conditions (compare section 2.3.5), when the

P_{PA0920} promoter was activated (Klein *et al.*, 2009). Polar lipids were extracted, analyzed by two-dimensional TLC and visualized by molybdatophosphoric acid staining (sections 2.5.1 and 2.5.3). The resulting TLC plates are displayed in Figure 15.

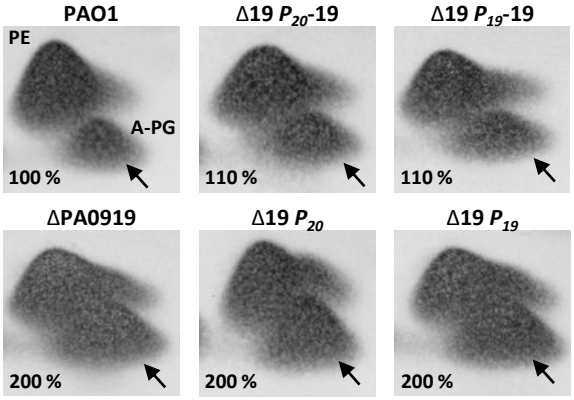

Figure 15: Lipid composition of *P. aeruginosa* PAO1 ΔPA0919 complemented strains
Various *P. aeruginosa* mutant strains were cultured in AB medium pH 5.3 for 24 h (section 2.3.5). After harvesting, polar lipids were extracted, analyzed by two-dimensional TLC and stained with molybdatophosphoric acid (sections 2.5.1 and 2.5.3). Relative A-PG amounts were quantified (section 2.5.3) and related to the wild-type strain A-PG level defined as 100 %. The position of A-PG position is indicated by an arrow.
A-PG: alanyl-phosphatidylglycerol, PE: phosphatidylethanolamine.

For the PAO1 wild-type strain, the formerly reported amount of 6 % of the overall lipid content was observed under acidic growth conditions (Klein *et al.*, 2009). This A-PG level was defined as 100 % and the values obtained for the various mutant strains were related to this. For the ΔPA0919 deletion mutant strain, a significantly increased A-PG level of 200 % was observed indicating the relevance of orf PA0919 for A-PG lipid homeostasis in *P. aeruginosa*. For both complemented strains containing orf PA0919 (Δ19 P_{20}-19 and Δ19 P_{19}-19), the A-PG amount was approximately 110 %. This value is comparable to the wild-type situation. In contrast, the control strains solely harboring the promoters (Δ19 P_{20} and Δ19 P_{19}), the elevated A-PG level characteristic for the deletion mutant strain was observed (200 % A-PG). The cellular content of the *P. aeruginosa* standard phospholipids PE, PG and DPG was identical in all mutant strains (not shown). Under neutral growth conditions, no significant A-PG amounts were detected (see appendix, Figure 35) which might be attributed to absence of the A-PGS whose expression is not induced under neutral conditions (Klein *et al.*, 2009).

In summary, the growth experiments and the lipid analyses clearly indicate the relevance of PA0919 for A-PG lipid homeostasis in *P. aeruginosa*. Besides, these results indicate the presence of a specific P_{PA0919} promoter upstream of orf PA0919.

3.5.4 Resistance phenotypes of ΔPA0919 derivative strains

Previously, alterations of the A-PG content were related to an increased susceptibility of *P. aeruginosa* to several antimicrobial agents (section 3.2.3). To elucidate the influence of PA0919 on the antimicrobial susceptibility of *P. aeruginosa*, the ΔPA0919 deletion mutant and the respective complemented variants were treated with selected compounds.

The strains were subjected to the modified microdilution method for MIC determination established in this study (section 2.7.3). The cells were cultured under acidic conditions and treated with antimicrobials at varying concentrations. The culture turbidity was determined and the MIC value was defined as the lowest antimicrobial concentration with $OD_{595} < 0.5$. The results are summarized in Table 14.

Table 14: MICs (µg/mL) of *P. aeruginosa* ΔPA0919 related strains
The various strains were treated with gradually varying concentrations of the respective antimicrobial in AB medium pH 5.3 (section 2.7.3). The relative standard deviation was approximately 5 % (10 % for daptomycin). A-PG amounts are determined in section 3.5.3. P values were calculated by significance analysis and are indicated: P ≤ 0.1 (*), P ≤ 0.05 (**) and P ≤ 0.01 (***). For experimental details, see section 2.7.3.
All concentrations are given in µg/mL. Experiments were performed at least in triplicate.
A-PG: alanyl-phosphatidylglycerol.

	wild-type 100 % A-PG	**ΔPA0919** 200 % A-PG	**Δ19 P_{20}** 200 % A-PG	**Δ19 P_{20}-19** 110 % A-PG	**Δ19 P_{19}** 200 % A-PG	**Δ19 P_{19}-19** 110 % A-PG
ampicillin	360 ± 18	180** ± 9	150** ± 8	360 ± 18	150*** ± 8	360 ± 18
cefsulodin	61 ± 3	55 ± 3	33** ± 2	44* ± 2	39*** ± 2	44* ± 2
daptomycin	> 15’000	9’000* ± 900	9’000* ± 900	> 15’000	9’000** ± 900	> 15’000
poly-L-lysine	8 ± 0.4	6* ± 0.3	6* ± 0.3	8 ± 0.4	6* ± 0.3	8 ± 0.4
polymyxin E	4 ± 0.2	2* ± 0.1	2* ± 0.1	4 ± 0.2	2* ± 0.1	4 ± 0.2
polymyxin B	2.4 ± 0.1	1.7* ± 0.1	1.7* ± 0.1	2.4 ± 0.1	1.7* ± 0.1	2.4 ± 0.1
benzethonium chloride	22 ± 1.1	11*** ± 0.6	11*** ± 0.6	18** ± 0.9	11*** ± 0.6	18** ± 0.9
domiphen bromide	6.8 ± 0.3	5.0*** ± 0.3	5.0* ± 0.3	6.2 ± 0.3	5.0** ± 0.3	6.2 ± 0.3
vancomycin	23’800 ± 1200	20’800*** ± 1000	20’800*** ± 1000	23’800 ± 1200	20’800*** ± 1000	23’800 ± 1200

The MICs observed for the PAO1 wild-type strain were in a comparable range as the previously obtained results (compare Table 12).

The ΔPA0919 deletion mutant containing an A-PG level of 200 % was found more susceptible to all employed antimicrobial compounds as indicated by MIC reduction when compared to the wild-type strain. The presence of the β-lactams ampicillin and cefsulodin resulted in MICs of 180 µg/mL and 55 µg/mL compared to 360 µg/mL and 61 µg/mL for the wild-type strain, respectively. For the lipopeptide daptomycin, a MIC of 9 mg/mL was determined (compared to > 15 mg/mL for the wild-type). Treatment of the ΔPA0919 deletion mutant with the CAMPs poly-L-lysine, polymyxin E and polymyxin B resulted in reduced MICs of 6 µg/mL (wild-type: 8 µg/mL), 2 µg/mL (wild-type: 4 µg/mL) and 1.7 µg/mL (wild-type: 2.4 µg/mL). In the presence of the cationic surfactants benzethonium chloride and domiphen bromide, reduced values of 11 µg/mL (wild-type: 22 µg/mL) and 5.0 µg/mL (wild-type: 6.8 µg/mL) were determined. The presence of vancomycin resulted in a slightly increased susceptibility of ΔPA0919 as represented by a MIC of 20.8 mg/mL compared to 23.8 mg/mL observed for the wild-type strain.

For the ΔPA0919 derivative strains complemented with orf PA0919 under the control of the well-known P_{PA0920} promoter (Δ19 P_{20}-19) or of the putative P_{PA0919} promoter (Δ19 P_{19}-19), MICs comparable to the wild-type strain values were obtained for most antimicrobials (ampicillin, daptomycin, poly-L-lysine, polymyxin E, polymyxin B, domiphen bromide and vancomycin). For the control strains containing solely the respective promoter (Δ19 P_{20} and Δ19 P_{19}), MIC values identical to the deletion mutant strain were observed for these compounds.

In the presence of benzethonium chloride, the wild-type phenotype was only partially restored by PA0919 (strains Δ19 P_{20}-19 and Δ19 P_{19}-19) and the control strains exhibited resistance phenotypes identical to the deletion mutant strain. After cefsulodin treatment, a different situation was observed: MICs for the control strains devoid of PA0919 (Δ19 P_{20} and Δ19 P_{19}) were reduced in comparison to the deletion mutant strain (33 µg/mL and 39 µg/mL *versus* 55 µg/mL, compare Table 14). The presence of PA0919 resulted in a reduced susceptibility indicated by increased MICs (44 µg/mL for both strains), when compared to the respective control strain. Nevertheless, this value was not as high as the MIC for the ΔPA0919 deletion mutant strain (55 µg/mL) and was significantly reduced when compared

to the wild-type strain result (61 µg/mL). The deviating results for strains Δ19 P_{20}-19 and Δ19 P_{19}-19 in the presence of benzethonium chloride and cefsulodin (compared to the other compounds) might be ascribed to the slightly increased amount of 110 % A-PG in these strains.

From these results it becomes clear that the reduction of the A-PG amount depending on the presence of PA0919 is of relevance for the fine-tuning of the cellular membrane lipid composition and for the resistance of *P. aeruginosa* against several antimicrobial agents. Furthermore, the complementation variant experiments supported the idea of the presence of a PA0919 specific promoter.

3.6 Analysis of the P_{PA0919} promoter

Orfs PA0920 and PA0919 are separated by one single base pair and were predicted to form an operon. In contrast, the abovementioned experiments employing the ΔPA0919 complemented strain Δ19 P_{19}-19 indicated that PA0919 might be controlled by a specific P_{PA0919} promoter (compare chapter 3.5). Here, the putative promoter sequence was analyzed in detail.

3.6.1 Predicted promoter elements are located upstream of orf PA0919

The formerly employed 430 bp promoter fragment located directly upstream of orf PA0919 on the PAO1 chromosome was analyzed to identify potential promoter elements and the RBS controlling PA0919 expression (section 2.13.4). The theoretically determined elements are summarized in Figure 16.

A –35 promoter region (TTCCGG) and a –10 element also designated as Pribnov box (TTCTACAAT) were identified by the BPROM software (SoftBerry, Mount Kisco, NY, USA) in an appropriate distance upstream of the PA0919 translation start site in the PAO1 chromosome. A potential RBS also termed Shine-Dalgarno sequence was identified (TGGTGAAA) due to its similarity with the *E. coli* consensus sequence motif (Schneider and

Stephens, 1990) and according to the ribosomal anti-Shine-Dalgarno sequence (section 2.13.4; Ma *et al.*, 2002).

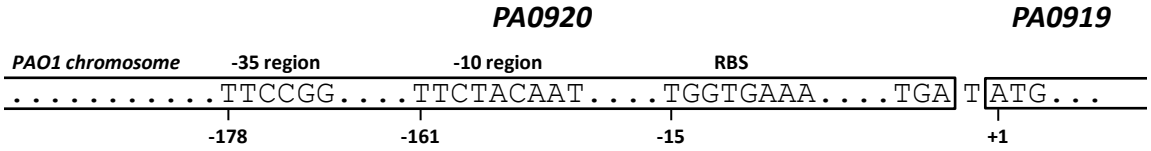

Figure 16: Localization of the hypothetical P_{PA0919} promoter
Orfs PA0920 and PA0919 are separated by one single base in the PAO1 chromosome. –35 and –10 region promoter elements identified by the BPROM software (SoftBerry, Mount Kisco, NY, USA) are indicated. The RBS was identified by comparison to the *E. coli* RBS consensus sequence motif and to the *P. aeruginosa* anti-Shine-Dalgarno sequence (section 2.13.4). Positions are indicated related to the PA0919 translation start site.
RBS: ribosome binding site (Shine-Dalgarno sequence).

3.6.2 P_{PA0919} analysis by transcriptional promoter-reporter gene fusions

For the detailed investigation of the proposed P_{PA0919} promoter, a set of P_{PA0919} promoter-reporter gene (*lacZ*) fusions were introduced into the PAO1 wild-type strain chromosome. Specific promoter fragments were designed according to the bioinformatically determined promoter elements (compare section 3.6.1). The employed constructs are displayed in Figure 17.

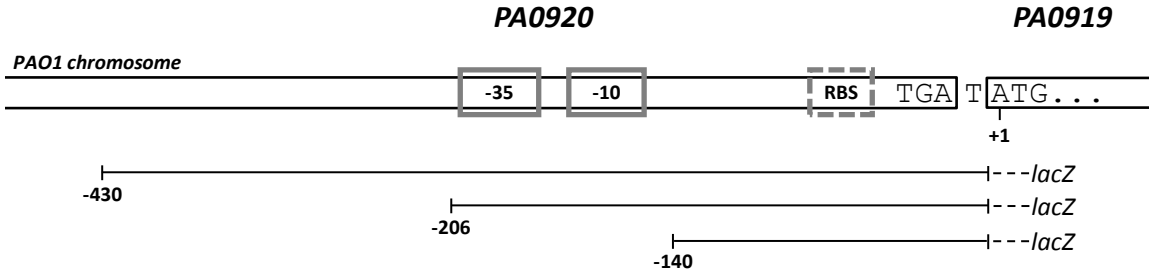

Figure 17: Construction of P_{PA0919} promoter fragment-reporter gene fusions
Promoter fragments of 430 bp, 206 bp and 140 bp covering the genomic region upstream of orf PA0919 were fused to the reporter gene *lacZ* and introduced into the PAO1 wild-type chromosome. Bioinformatically identified –35 and –10 promoter regions, the detected RBS and the genomic organization of orfs PA0920 and PA0919 are indicated. Positions are indicated related to the PA0919 translation start site.
RBS: ribosome binding site (Shine-Dalgarno sequence).

Three different constructs were generated: First, the formerly employed P_{PA0919} fragment covering 430 bp upstream of orf PA0919 on the PAO1 chromosome was employed. Second, a 206 bp promoter fragment representing the minimal promoter containing predicted –35 and –10 regions was constructed. Third, a 140 bp fragment without any determined promoter elements was employed for control (compare section 2.4.19). The obtained strains (PAO1 P_{PA0919}-*430-lacZ*, PAO1 P_{PA0919}-*206-lacZ* and PAO1 P_{PA0919}-*140-lacZ*) were grown under neutral and acidic conditions (pH 7.3 and pH 5.3; see section 2.8.3). The promoter-less strain KS11 (Schreiber *et al.*, 2006) was used for background activity determination. Samples were subjected to the β-galactosidase activity assay to quantify the induction of the respective promoter fragment under the employed conditions (section 2.8.1). The calculated promoter activities are displayed in Figure 18.

Under neutral pH conditions, an almost constant promoter activity of approximately 80 MU was obtained for the 430 bp P_{PA0919} promoter fragment. In contrast, the analysis of the same promoter fragment indicated an induction from 80 MU (early logarithmic phase) to 170 MU (stationary phase) under acidic conditions. The activity determination of the minimal P_{PA0919} promoter (206 bp fragment) resulted in an almost constant level of 55 MU under acidic growth conditions and results ranging from 25 to 60 MU were obtained under neutral conditions. The 140 bp fragment not containing any promoter elements resulted in promoter activities between 0 and 20 MU. These values represent the background activity of the 140 bp sequence. From these results it becomes clear that the specific P_{PA0919} promoter is located upstream of orf PA0919. Due to the fact that the minimal promoter fragment of 206 bp showed an almost constant activity under acidic conditions, whereas the activity of the 430 bp promoter fragment was significantly induced ($P < 0.001$), the presence of at least one additional promoter element is proposed. This element, which is presumably a transcription factor binding site, is located in the position between 430 bp and 206 bp upstream of the PA0919 transcription start site and might be responsible for the upregulation of the transcription under acidic conditions in the stationary phase. Instead, the presence of a repressor binding site is improbable since the transcription of orf PA0920 would be affected by a bound repressor molecule. However, one might expect that the P_{PA0919} promoter activity is additionally modulated by other stimuli not analyzed in this study.

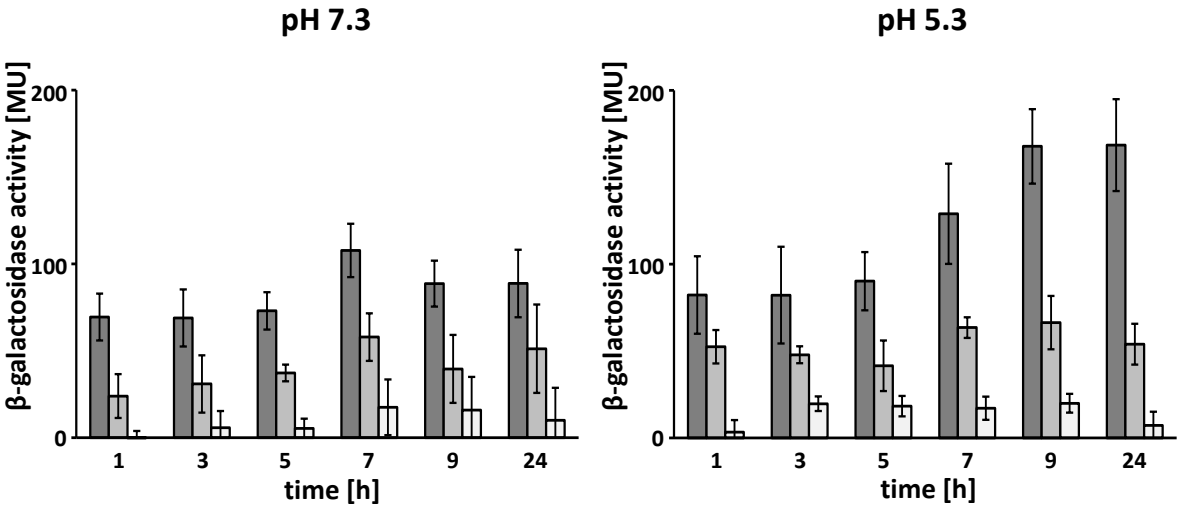

Figure 18: Analysis of the P_{PA0919} promoter
PAO1 derivative strains harboring P_{PA0919} promoter fragments of different length fused to the reporter gene *lacZ* were incubated in AB medium pH 7.3 or pH 5.3 for 24 h. The promoter activity was determined by measuring the β-galactosidase activity (sections 2.8.1 and 2.8.3). Values of the promoter-less reference strain KS11 representing the background activity were subtracted. Results and standard deviations of at least three independent experiments are indicated.
Dark gray: P_{PA0919}-*430-lacZ*, middle gray: P_{PA0919}-*206-lacZ*, light gray: P_{PA0919}-*140-lacZ*.

3.7 Characterization of the PA0919 protein

Initially, the PA0919 protein was theoretically analyzed concerning potential active site amino acid residues. Furthermore, the PA0919 protein and mutated variants were recombinantly produced and purified from the periplasm of the *E. coli* host. The PA0919 protein substrate specificity and the enzyme activity were analyzed *in vitro*. Specific inhibitory compounds were employed to identify potential active site amino acid residues and the activity of the PA0919 protein for the hydrolysis of the potential native substrate was investigated.

3.7.1 Identification of potential active site amino acid residues

Earlier studies of the PA0919 homolog AtvA of *R. tropici* had revealed that this protein contains a conserved amino acid sequence pattern named LIPASE_SER motif (accession number: PS00120, PROSITE; Sigrist *et al.*, 2013) originally identified in lipases (Vinuesa *et al.*, 2003). Within this motif, a serine residue is highly conserved and an exchange to alanine in AtvA of *R. tropici* had resulted a phenotype characteristic for the Δ*atvA* deletion mutant strain (Vinuesa *et al.*, 2003). Based on these results and due to the presence of further amino acid residues characteristic for catalytic diads/triads it had been proposed that AtvA and its homologs might represent a new class of lipolytic enzymes, although neither the substrate nor the products of this reaction had been identified (Vinuesa *et al.*, 2003).

In this work, the sequence alignment analysis of several PA0919 homologs indicated the presence of the abovementioned LIPASE_SER motif, a second conserved serine and additionally, a conserved histidine residue. Excerpts of the sequence alignment are given in Figure 19 (for the entire alignment, see appendix, Figure 36).

These theoretical investigations suggested a catalytic function of the PA0919 protein. Since the reduction of the A-PG level had been related to the presence of PA0919 (section 3.5.3) and since the LIPASE-SER motif was identified in the PA0919 protein, it is reasonable that the PA0919 protein might hydrolyze A-PG. Taken into account that PA0919 but also PA0920 expression is induced under acidic growth conditions (compare chapter 3.6 and Klein *et al.*, 2009), PA0919 might fine-tune the cellular A-PG level in *P. aeruginosa* under acidic stress conditions.

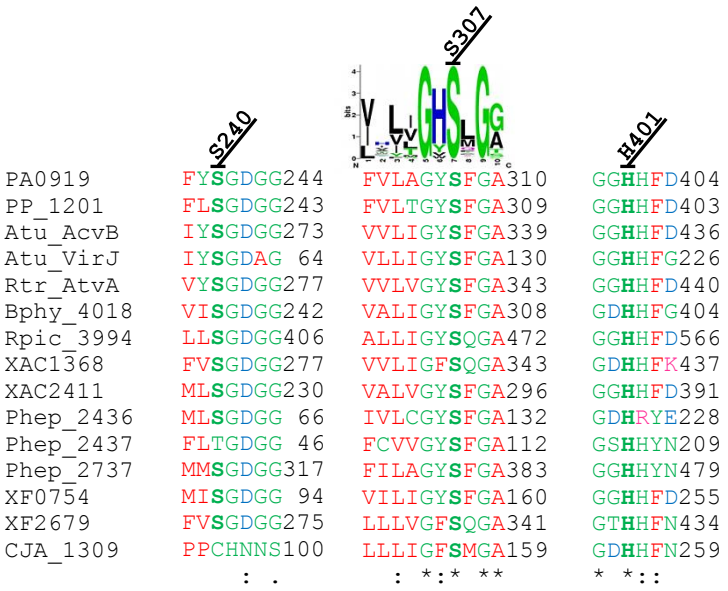

Figure 19: Excerpts of a sequence alignment of PA0919 homologous proteins
Selected PA0919 homologous proteins identified by BLAST analysis were aligned by ClustalW2 (section 2.13.1). Partial alignments are given with the respective amino acid position within the specific protein. The LIPASE_SER motif (Vinuesa *et al.*, 2003) is indicated above the corresponding alignment part. Conserved serines and a conserved histidine are indicated in bold letters and amino acid positions are numbered according to PA0919. Conservation degrees are indicated in increasing order by a period (.), a colon (:) or an asterisk (*).
Gene names/locus tags: PA0919: *P. aeruginosa* PAO1, PP_1202: *P. putida* KT2440, Atu_AcvB: *A. tumefaciens* C58, Atu_VirJ: *A. tumefaciens* octopine-type Ti-plasmid pTiA6, Rtr_AtvA: *R. tropici* CIAT 899, Bphy_4018: *B. phymatum* STM815, Rpic_3994: *R. pickettii* 12J, XAC1368 and XAC2411: *X. axonopodis* 306, Phep_2436, Phep_2437 and Phep_2737: *P. heparinus* DSM2366, XF0754 and XF2679: *X. fastidiosa* 9a5c, CJA_1309: *C. japonicus* Ueda107.

3.7.2 Heterologous production of recombinant PA0919 protein variants

PA0919 was proposed to be located in the periplasm of *P. aeruginosa* by bioinformatic analysis and by a PA0919-PhoA fusion protein screening in a former study (Lewenza *et al.*, 2005). The secretion signal for periplasmic localization was predicted to consist of amino acids 1 – 34 of the entire PA0919 amino acid sequence by several bioinformatic programs (Lewenza *et al.*, 2005). Therefore, PA0919 was cloned without its native secretion signal (amino acids 35 to 427) into the pET22b(+) vector. It was N-terminally fused to the *E. coli* PelB secretion signal encoding sequence and C-terminally linked to a His_6-tag (compare section 2.4.15). In a second approach, a *Strep*-tag II (Schmidt and Skerra, 2007) was employed instead of the His_6-tag. The fusion protein was overproduced in *E. coli* BL21 (λDE3)

cells (section 2.9.1). Samples of *Strep*-tagged PA0919 protein overproducing *E. coli* cells were subjected to SDS-PAGE analysis and the resulting gel is presented in Figure 20.

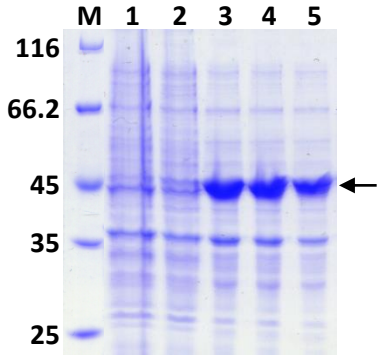

Figure 20: Heterologous production of recombinant PA0919 protein
E. coli BL21 (λDE3) containing pET22b(+)PA0919-Strep was incubated at 37 °C and 200 rpm to an OD_{578} of 0.5 to 0.6. Cultures were shifted to 17 °C, protein expression was induced by 25 µM IPTG and incubation was continued overnight. Samples were subjected to SDS-PAGE analysis according to their OD_{578}. The gel was stained with Coomassie Brilliant Blue (sections 2.9.1 and 2.10.2). The calculated molecular weight of the PA0919 protein (44.6 kDa) is indicated by an arrow (fused to the *Strep*-tag II, PelB leader sequence removed).
M: Unstained Protein Molecular Weight Marker, relative molecular masses (*1000) are indicated; 1: cells prior to induction; cells after induction: 2 (2 h), 3 (16 h), 4 (18 h) and 5 (20 h).

The production of *Strep*-tagged PA0919 was not detectable 2 h after the induction of the protein production (compare lanes 1 and 2). After 16 h of incubation, high amounts of protein were observed (lane 3). A prolonged cultivation up to 18 h or 20 h did not result in increased protein amounts (lanes 4 and 5).

After recombinant protein production, the periplasmic fraction was isolated from the *E. coli* cells by an optimized polymyxin B treatment protocol (section 2.9.2). The His_6-tagged PA0919 protein was purified employing a Ni-NTA agarose chromatography column (section 2.9.3) and for the *Strep*-tagged variant, a *Strep*-Tactin® resin was used (section 2.9.4). Due to the fact that the isolated His_6-tagged PA0919 variant protein was contaminated by co-purified proteins (data not shown), the *Strep*-tagged PA0919 protein was employed for all investigations.

For detailed enzyme activity studies, the PA0919-Strep protein was mutated (section 2.4.15) by exchanging three conserved amino acids using site-directed mutagenesis (compare section 3.7.1): The amino acid residue serine 307 (located within the LIPASE_SER motif and predicted to represent the catalytically active amino acid) and the highly conserved amino acid residues serine 240 and histidine 401 were replaced by alanine resulting in the mutant proteins S307A, S240A and H401A. The respective plasmids were transferred into *E. coli* BL21 (λDE3) and the *Strep*-tagged protein variants were produced and isolated from the *E. coli* periplasm by polymyxin B treatment. For protein purification, the soluble periplasmic fractions were loaded onto *Strep*-Tactin® affinity chromatography columns and extensively washed. The protein variants were eluted by desthiobiotin and dialyzed for buffer exchange (chapter 2.9). The SDS-PAGE of a representative *Strep*-tagged PA0919 wild-type protein purification and the samples of the corresponding mutant proteins are presented in Figure 21.

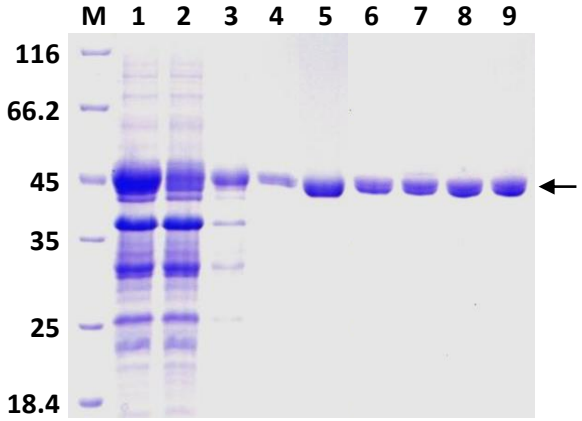

Figure 21: Purification of *Strep*-tagged PA0919 protein
E. coli BL21 (λDE3) containing pET22b(+)PA0919-Strep was incubated at 37 °C and 200 rpm to an OD_{578} of 0.5 to 0.6. Cultures were shifted to 17 °C, protein expression was induced by 25 µM IPTG and incubation was continued overnight (section 2.9.1). The periplasmic fraction was isolated (section 2.9.2), *Strep*-tagged PA0919 protein was purified using a *Strep*-Tactin® chromatography column (section 2.9.4) and subsequently dialyzed (section 2.9.5). Protein variants S240A, S307A and H401A were purified analogously. Samples were subjected to SDS-PAGE analysis (lanes 1 – 4: 2 µL; lanes 5 – 9: 10 µL). The gel was stained with Coomassie Brilliant Blue (section 2.10.2). The calculated molecular weight of the PA0919 wild-type protein (44.6 kDa) is indicated by an arrow (fused to the *Strep*-tag II, PelB leader sequence removed).
M: Unstained Protein Molecular Weight Marker, relative molecular masses (*1000) are indicated; *Strep*-tagged PA0919 wild-type protein: 1: periplasmic fraction, 2: column flow-through, 3: washing step 1, 4: washing step 2, 5: elution fraction, 6: dialyzed protein.
Variant proteins after dialysis: 7: S240A, 8: S307A, 9: H401A.

The periplasmic fraction of PA0919 wild-type protein expressing cells was obtained after polymyxin B treatment (lane 1) and loaded onto the *Strep*-Tactin® column. Considerable amounts of *Strep*-tagged PA0919 protein were bound to the resin as indicated by a reduction of the respective band in the flow-through fraction (lane 2). Contaminating proteins were removed by two washing steps (lanes 3 and 4) and the pure protein was eluted (lane 5). Approximately 3 mg were obtained from 1 L *E. coli* culture. To change the employed buffer system, a dialysis was performed (lane 6). *Strep*-tagged PA0919 variant proteins S240A, S307A and H401A were isolated using the same protocol and are presented in lanes 7 to 9. All PA0919 proteins were purified to apparent homogeneity as judged from SDS-PAGE analysis.

To unambiguously identify the isolated protein and to verify the loss of the PelB secretion signal, the N-terminal amino acid sequence of the PA0919-Strep protein was determined according to the method of Edman, 1950 (section 2.10.4). The observed N-terminal amino acid sequence (MA$\underline{K_{35}LEALDLDDGGHA_{47}}$, PA0919 amino acids underlined) indicated the efficient cleavage of the signal sequence and also verified the PA0919 protein. This result indicates the efficient secretion of the recombinant PA0919 protein in the periplasm of *E. coli*.

3.7.3 Initial characterization of the PA0919 protein

The recombinant PA0919-Strep protein was initially characterized by native molecular weight determination and by absorption and fluorescence spectral analysis.

The native molecular mass of the PA0919-Strep protein was determined by analytical gel permeation chromatography (section 2.10.6). The protein and a number of standard proteins employed for calibration were loaded onto the Superdex 200 5/150 GL chromatography column (GE Healthcare, Munich, Germany) using a flow rate of 0.45 mL/min. By comparing the specific elution volumes, the native molecular mass of PA0919-Strep was calculated to 57 kDa (see appendix, Figure 37). By comparison with the calculated molecular weight of PA0919-Strep after the cleavage of the PelB leader sequence (44’626 Da), it was concluded that PA0919 possesses a monomeric architecture under the employed conditions.

In some cases, proteins contain organic and/or metal cofactors which might be co-purified with the target proteins (Schmid, 2001; Lakowicz, 2006; Waldron *et al.*, 2009). To determine if PA0919 provides an organic cofactor like NADH/NADPH (nicotinamide adenine dinucleotide/nicotinamide adenine dinucleotide phosphate), $FADH_2$ (flavine adenine dinucleotide) or heme, the protein was analyzed by absorption and fluorescence spectroscopy (section 2.10.7). The obtained spectra did not indicate the presence of any cofactor (data not shown). For the identification of metal cofactors, an ICP-MS analysis was performed (section 2.10.8) and no metal cofactor was detected.

Since PA0919 influences the overall A-PG content in *P. aeruginosa* (see chapter 3.5), an interaction of the enzyme with membrane lipids was assumed. In an initial approach, a protein lipid overlay assay was performed employing a Membrane Lipid Strip™ (Echelon Biosciences, Salt Lake City, UT, USA) providing several standard membrane lipids like PG, PE and DPG immobilized on a hydrophobic membrane. The membrane was incubated with purified PA0919-Strep wild-type protein and after extensive washing, the lipid bound protein was detected *via* its *Strep*-tag II (section 2.10.9). However, an interaction between the PA0919 protein and the provided membrane lipids was not detectable (data not shown). Of note, the Membrane Lipid Strip™ did not provide any aaPG derivatives and consequently, an interaction with this class of phospholipids was not investigated.

It was suggested that PA0919 hydrolyzes A-PG to alanine and PG (section 3.7.1). For this, PA0919 might have the ability to bind alanine. To analyze this, purified *Strep*-tagged PA0919 protein was immobilized on the *Strep*-Tactin® affinity chromatography matrix and incubated with ^{14}C-labeled alanine. After extensive washing, the protein was eluted and analyzed by scintillation counting. For control, the PA0919 S307A variant protein mutated within the potential active site and a sample treated in the absence of any protein were employed (section 2.10.10). With this experimental setup, identical radioactivity values were obtained for all samples (data not shown). This result indicated that PA0919 does not bind to alanine.

3.7.4 PA0919 substrate specificity using artificial *p*-nitrophenol ester derivatives

For the analysis of the PA0919 substrate specificity, an *in vitro* activity assay using artificial *p*-nitrophenol derivatives as substrates was performed. During the assay, the substrates were hydrolyzed by the purified PA0919-Strep protein and product formation was monitored by measuring the *p*-nitrophenolate absorption at 400 nm. For control, the spontaneous hydrolysis of the respective substrate was quantified in the absence of the PA0919 wild-type protein (section 2.11.1).

The employed artificial chromogenic substrates mainly representing *p*-nitrophenol esters of amino acid derivatives or aliphatic acid compounds are displayed in Figure 22. Most of them were commercially available, whereas Lys-ONp was synthesized *de novo* and kindly provided by Dr. J. S. Dickschat (compare section 2.11.1).

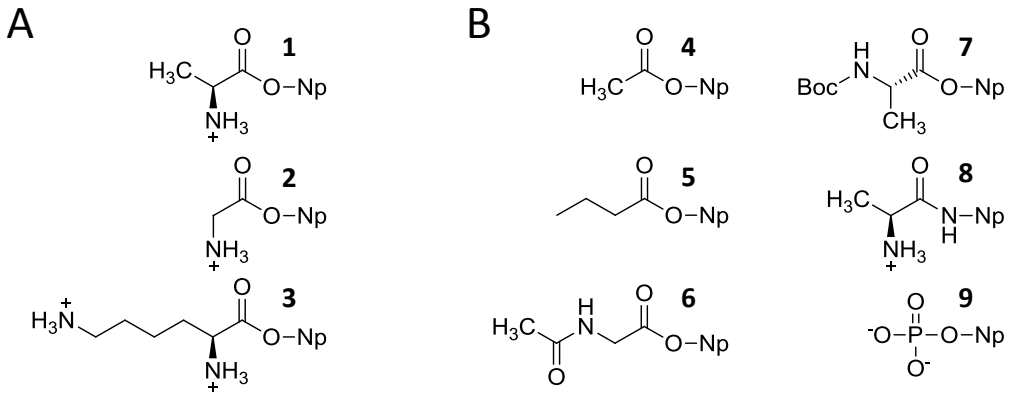

Figure 22: Chromogenic compounds employed for the PA0919 substrate specificity analysis
A. Amino acid *p*-nitrophenyl ester compounds hydrolyzed by PA0919.
B. *p*-Nitrophenyl derivatives not hydrolyzed by PA0919.
1: Ala-ONp (L-alanine 4-nitrophenyl ester), **2**: Gly-ONp (glycine 4-nitrophenyl ester), **3**: Lys-ONp (L-lysine 4-nitrophenyl ester), **4**: 4-NP acetate (4-nitrophenyl acetate), **5**: 4-NP butyrate (4-nitrophenyl butyrate), **6**: Ac-Gly-ONp (acetyl-glycine 4-nitrophenyl ester), **7**: Boc-Ala-ONp (*tert*-butyloxycarbonyl alanine 4-nitrophenyl ester), **8**: Ala-pNA (alanine *p*-nitroanilide), **9**: 4-NP phosphate (4-nitrophenyl phosphate).

The specificity analysis of the PA0919-Strep protein revealed that the employed amino acid *p*-nitrophenyl esters Ala-ONp, Gly-ONp and Lys-ONp (**1** – **3**) were accepted as substrates. The specific activity of PA0919 for each compound was calculated (spontaneous autohydrolysis subtracted): for Ala-ONp (**1**) a specific activity of 11 ± 3 nmol/(min*mg) was determined and

13 ± 4 nmol/(min*mg) were obtained for Gly-ONp (**2**). Additionally, a specific activity of 16 ± 4 nmol/(min*mg) was calculated for Lys-ONp (**3**). These values are in the same order of magnitude and might indicate a minor importance of the respective amino acid side chain.

Interestingly, artificial substrates lacking the amino group like 4-NP acetate or 4-NP butyrate (**4** and **5**) were hydrolyzed by PA0919. Amino acid derivatives with amino groups bound to acetyl or Boc residues like Ac-Gly-ONp or Boc-Ala-ONp (**6** and **7**) were not accepted as substrates. These results indicate that the amino group of the artificial substrates is highly important for the substrate recognition. Furthermore, compounds like Ala-pNA (**8**) carrying an amide instead of an ester bond or 4-NP phosphate (**9**) were not hydrolyzed and therefore not accepted by the PA0919 protein.

In summary, these *in vitro* assay results indicate that the PA0919 protein does neither cleave the ester bonds linking the fatty acids to the glycerol backbone of the putative native substrate A-PG nor the phosphodiester linkages between the glyceroldiester moiety and glycerol (see Figure 23). Instead, it was proposed that PA0919 cleaves the aminoacyl bond linking alanine to PG in the native substrate A-PG by recognizing the amino group of the alanine moiety.

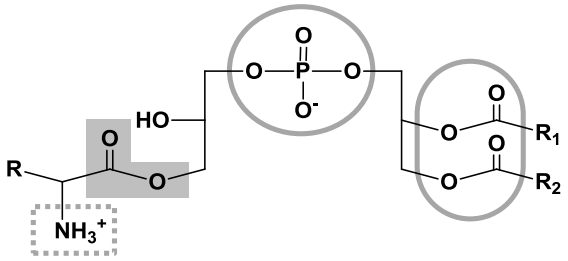

Figure 23: Structural formula of aminoacylated PG
The results obtained by the PA0919 substrate specificity analysis using chromogenic compounds are indicated: The aminoacyl ester bond linking the amino acid to PG (highlighted gray) is hydrolyzed. The amino group (dotted rectangle) is important for substrate recognition, whereas the amino acid side chain (R) is of minor importance for the PA0919 substrate specificity. The fatty acyl ester bonds and the phosphodiester linkage might not be hydrolyzed (gray circles) by PA0919.
aaPG: aminoacyl-phosphatidylglycerol, PG phosphatidylglycerol.

The *in vitro* activity assay was also employed to analyze the specific activity of the PA0919 variant proteins S240A, S301A and H401A. Due to the assumption that A-PG is the native PA0919 substrate, Ala-ONp was employed as substrate.

For the active site mutant S307A and for the H401A variant protein, no Ala-ONp hydrolysis was detectable. Instead, a reduced activity of 45 % (± 15 % standard deviation) was obtained for the S240A variant when compared to the wild-type protein. Thus, this *in vitro* activity assay indicates that the amino acid residues serine 307 and histidine 401 are important for PA0919 catalysis.

3.7.5 PA0919 activity is reduced by PMSF and TLCK

The well-established *in vitro* activity assay was employed to analyze the inhibition of the PA0919 protein by specific compounds. PMSF is known to inhibit serine proteases (Gold and Fahrney, 1964; Gold, 1965) and TLCK specifically inactivates trypsin-like proteases by exclusively binding to active site histidines (Shaw and Springhorn, 1967). The metal ion chelating EDTA (Diermayr *et al.*, 1987) was employed to investigate the PA0919 activity dependency of metal ions. The experiments in the presence of inhibitory substances were performed to initially characterize main principles of the PA0919 catalysis. The purified PA0919-Strep protein (chapter 2.9) was pre-incubated with the respective inhibitor and subsequently, the PA0919 activity was determined using the *in vitro* activity assay employing Ala-ONp as the substrate (section 2.11.2; see Groenewold, 2013).

The utilization of 1 mM PMSF did not result in any detectable PA0919 activity indicating a serine dependent catalytic mechanism. Interestingly, experiments in the presence of 60 µM and 1 mM of the histidine-specific TLCK revealed reduced PA0919 activities of 90 % and 10 % compared to the enzyme activity in the absence of TLCK. Therefore, the involvement of an active site histidine residue in the catalytic mechanism must be taken into account. Instead, in the presence of the metal chelating agent EDTA, no reduction of PA0919 enzyme activity was observed (Groenewold, 2013). This result is in good agreement with the previously described ICP-MS analysis by which no metal ions were detected in the purified PA0919-Strep protein (see sections 2.10.8 and 3.7.3).

In conclusion, the results of the inhibitor study indicate a serine and/or histidine dependent PA0919 catalysis in the absence of any metal ion cofactor.

3.7.6 PA0919 *in vitro* activity analysis using the putative native A-PG substrate

The PA0919 protein was analyzed employing an *in vitro* activity assay in the presence of the putative native substrate A-PG. Since A-PG was not commercially available, a coupled PA0919 *in vitro* activity assay was established (section 2.11.3) which is based on the previously described A-PGS *in vitro* activity assay (Hebecker *et al.*, 2011). The principles of the employed *in vitro* procedure are summarized in Figure 24.

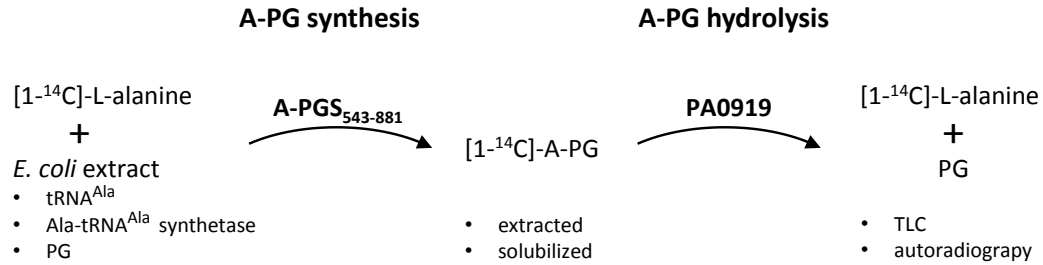

Figure 24: Basic principle of A-PG synthesis and the PA0919 protein *in vitro* activity assay
For A-PG synthesis, [1-^{14}C]-L-alanine was mixed with crude cellular extracts of *E. coli* Rosetta (λDE3) pLysS pET28b(+)PA0903 overproducing the recombinant *P. aeruginosa* Ala-tRNA^{Ala} synthetase (PA0903) and providing tRNA^{Ala} and PG. During incubation, the synthetase transferred the ^{14}C-labeled alanine to its tRNA^{Ala}. [1-^{14}C]-A-PG was synthesized by the purified *P. aeruginosa* A-PGS$_{543-881}$ (catalytic A-PGS domain, compare Hebecker *et al.*, 2011) by transferring the activated [1-^{14}C]-L-alanine from its tRNA^{Ala} to PG.
Polar lipids containing [1-^{14}C]-A-PG were extracted, solubilized by Triton^{TM} X-100 and subjected to the PA0919 *in vitro* assay. Lipid mixtures were mixed with PA0919 proteins and incubated. Product formation was observed by TLC and autoradiography analysis.
For detailed protocol, see section 2.11.3.
A-PG: alanyl-phosphatidylglycerol, PG phosphatidylglycerol, TLC: thin-layer chromatography.

For the synthesis of ^{14}C-labeled A-PG, the [1-^{14}C]-L-alanine substrate was mixed with an *E. coli* crude cellular extract providing the PG substrate, the alanine-specific tRNA^{Ala} and the recombinantly overproduced Ala-tRNA^{Ala} synthetase (PA0903 from *P. aeruginosa* PAO1) coupling alanine to the tRNA^{Ala}. During the A-PGS assay, the purified A-PGS$_{543-881}$ (from *P. aeruginosa*; see Hebecker *et al.*, 2011) transferred the [1-^{14}C]-L-alanine from its tRNA to an hydroxyl group of PG yielding [1-^{14}C]-A-PG (compare section 1.4.2). The polar lipid fraction containing [1-^{14}C]-A-PG was isolated from reaction mixtures and the lipids were solubilized by Triton^{TM} X-100. Purified PA0919-Strep protein variants were mixed with solubilized lipids and the reaction products PG and [1-^{14}C]-L-alanine were detected by one-dimensional TLC and autoradiography (section 2.11.3). The obtained results are presented in Figure 25.

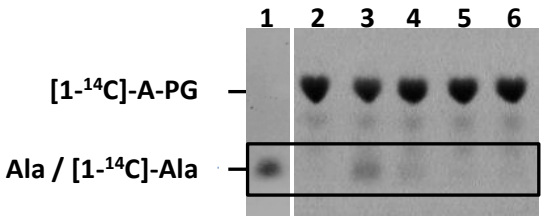

Figure 25: Autoradiography analysis of the PA0919 *in vitro* activity using ^{14}C-labeled A-PG
The synthesized substrate [1-^{14}C]-A-PG (section 2.11.3) was solubilized by Triton™ X-100 treatment and mixed with 40 µM of PA0919 variant proteins. A sample without protein was prepared for control. Samples were incubated at 37 °C under vigorous shaking for 30 min. A-PG hydrolysis was observed by separating amino acids and lipids by one-dimensional TLC using *n*-butanol, acetic acid and water (5:3:2, v/v/v; Qiu *et al.*, 2010). 1 µL 10 mM L-alanine was loaded onto the TLC plate for reference. TLC plates were stained with ninhydrin and radioactive spots were detected by autoradiography analysis (section 2.5.4).
1: L-alanine reference, stained with ninhydrin; lanes 2 to 6 present autoradiography results: 2: negative control in the absence of protein, 3: PA0919 wild-type protein, 4: S240A mutant, 5: S307A mutant, 6: H401A mutant.
A-PG: alanyl-phosphatidylglycerol, Ala: alanine.

In the absence of any PA0919 protein, a dominant spot with an R_f of 0.7 was observed by autoradiography analysis (lane 2) representing the ^{14}C-labeled A-PG substrate. This spot was also detected by ninhydrin staining (data not shown) indicating the presence of an amino group containing compound. For assays containing the PA0919 wild-type protein, a second radioactively labeled spot with an R_f of 0.46 was detected (lane 3). This spot exhibited identical migration characteristics to the L-alanine reference spot visualized by ninhydrin staining (lane 1). Hence, the hydrolysis of A-PG to alanine and PG by PA0919 was concluded.

Likewise, the PA0919 variant proteins S240A, S307A and H401A were also subjected to the [1-^{14}C]-A-PG *in vitro* activity assay. The exchange of the conserved serine 240 to alanine did result in a reduced hydrolysis as indicated by a minor spot with alanine migration characterristics (lane 4). Instead, no A-PG hydrolysis was observed for the S307A mutant protein representing the active site mutant (lane 5). Analogously, in experiments performed with the H401A mutant protein (highly conserved histidine 401 changed to alanine), no alanine was determined (lane 6). These results indicate that serine 307 and histidine 401 are key residues for the enzymatic hydrolyzation of A-PG by PA0919.

3.8 Localization of the PA0919 protein in *P. aeruginosa*

The previously presented results of the PA0919 *in vitro* characterization were obtained using a recombinant *Strep*-tagged PA0919 protein fused to an N-terminal PelB secretion signal that had been heterologously produced in *E. coli* cells. After protein production, the mature protein was secreted and the PelB leader sequence was removed yielding a soluble PA0919-Strep fusion protein localized in the *E. coli* periplasm.

Previous studies indicated a periplasmic localization of PA0919 in *P. aeruginosa* by a screening approach using PhoA-fusion proteins (compare Lewenza *et al.*, 2005). Of note, the updated version of the secretion signal prediction program SignalP specifically developed to distinguish between N-terminal secretion signal sequences and transmembrane domains (SignalP 4.1 used with SignalP-TM networks; Petersen *et al.*, 2011) did not identify a secretion signal sequence at the N-terminus of PA0919 (see appendix, Figure 38). Instead, the transmembrane protein topology prediction program TMHMM (Krogh *et al.*, 2001) identified a transmembrane helix formed by amino acids 12 – 31 and predicted an periplasmic localization of the C-terminus represented by amino acids 32 – 427 (see appendix, Figure 39). Although the PA0919 protein had been predicted previously to contain an N-terminal secretion signal by several bioinformatics programs (Lewenza *et al.*, 2005), these newly obtained prediction results indicate that PA0919 is anchored to the cytoplasmic membrane of *P. aeruginosa* by the N-terminal transmembrane helix. Nevertheless, the predicted periplasmic direction of the soluble protein part had been proven by the PhoA fusion experiment before (Lewenza *et al.*, 2005).

To identify the cellular localization of the PA0919 protein in its native host *P. aeruginosa*, the PA0919 encoding sequence was C-terminally fused to a *Strep*-tag II sequence. This construct was introduced into the *P. aeruginosa* PAO1 ΔPA0919 deletion mutant strain for complementation either by chromosomal integration or by employing an appropriate plasmid. For control, a construct devoid of the proposed N-terminal PA0919 secretory signal (encoded by amino acids 1 to 34) was designed and employed analogously. Since a stationary growth phase phenotype and an elevated A-PG content were observed for the ΔPA0919 deletion mutant strain under acidic conditions, the obtained strains were analyzed concerning their growth behavior and lipid composition.

After establishing an appropriate strain expressing the PA0919-Strep fusion protein, this strain was employed for PA0919 localization. For this, the respective cells were fractionated using different strategies and the PA0919 protein was detected within these fractions *via* its C-terminal *Strep*-tag II.

3.8.1 Complemented ΔPA0919 mutant strains for PA0919 localization

To unambiguously localize the PA0919 protein in *P. aeruginosa*, variants of the PA0919 encoding sequence were fused to a C-terminal *Strep*-tag II and transferred into the PAO1 ΔPA0919 deletion mutant strain (sections 2.4.15 and 2.4.19). The constructs employed for the complementation of the ΔPA0919 strain are summarized in Figure 26.

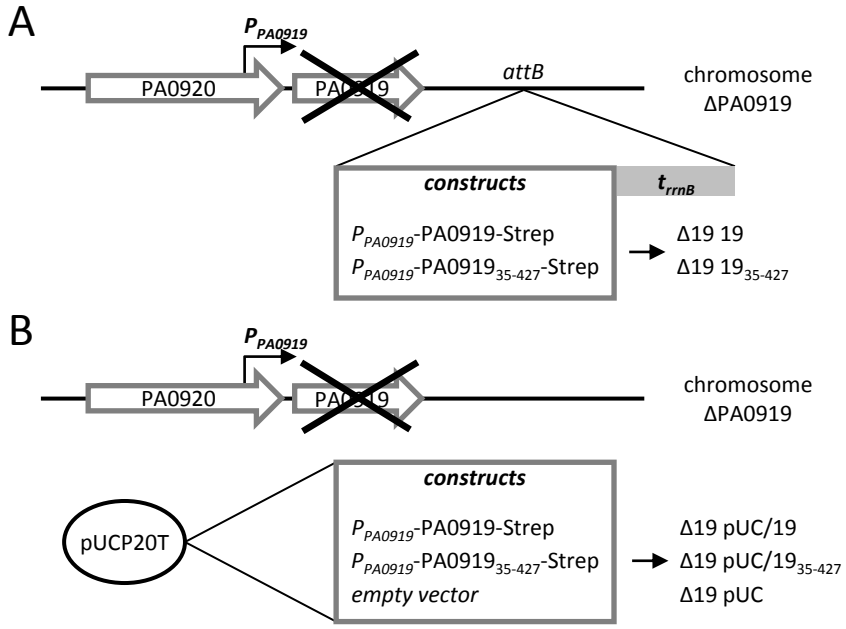

Figure 26: Complementation variants of PAO1 ΔPA0919 for PA0919 localization

A. Chromosomal complementation of PAO1 ΔPA0919. A construct consisting of the P_{PA0919} promoter and the PA0919-Strep fusion protein (P_{PA0919}-PA0919-Strep) was inserted into the *attB* locus of the PAO1 ΔPA0919 chromosome. A second construct devoid of the PA0919 secretory signal sequence (P_{PA0919}-PA0919$_{35-427}$-Strep) was employed analogously.

B. pUCP20T-based complementation of PAO1 ΔPA0919. The previously designed constructs P_{PA0919}-PA0919-Strep and P_{PA0919}-PA0919$_{35-427}$-Strep were cloned into the pUCP20T plasmid (*E. coli – P. aeruginosa* shuttle vector) and transferred into PAO1 ΔPA0919, respectively. The empty pUCP20T vector was used for control.

Construction details are presented in sections 2.4.15 and 2.4.19.

attB: attachment site B locus, P_{PA0919}: native promoter of orf PA0919, t_{rrnB}: *rrnB* terminator sequence, Strep: *Strep*-tag II.

The PAO1 ΔPA0919 deletion mutant strain was complemented by *Strep*-tagged PA0919 variant proteins controlled by its native promoter P_{PA0919} using two different approaches (Figure 26, A and B): First (A), the complementing construct was inserted into the chromosomal *attB* locus of PAO1 ΔPA0919 using the well-established mini-CTX2 technique (section 2.4.19; Hoang *et al.*, 2000) resulting in a markerless complemented mutant strain (named Δ19 19). For control, a construct devoid of the PA0919 secretion signal sequence (amino acids 1 – 34) was applied equally (strain Δ19 $19_{35\text{-}427}$). Second (B), a complementation strategy based on the *E. coli – P. aeruginosa* shuttle vector pUCP20T (Schweizer *et al.*, 1996) was employed. The complementing construct consisting of the P_{PA0919} promoter and the PA0919-Strep fusion protein encoding sequence was cloned into pUCP20T and transferred into PAO1 ΔPA0919 (strain Δ19 pUC/19). A construct lacking the PA0919 secretion signal sequence was employed in analogy to the chromosomal complementation strategy (Δ19 pUC/$19_{35\text{-}427}$). For control, the empty pUCP20T vector was introduced into PAO1 ΔPA0919 (Δ19 pUC). The resulting five complemented variant strains were subjected to further analyses.

3.8.2 The PA0919 secretion signal peptide is essential for A-PG dependent lipid homeostasis

The PAO1 ΔPA0919 strain showed a specific late stationary phase growth phenotype and an increased A-PG level of 200 % under acidic conditions when compared to the PAO1 wild-type. In contrast, neither a growth nor an A-PG associated phenotype was observed under neutral pH conditions. Complementation experiments clearly attributed the observed phenotypes to the presence of PA0919 (compare section 3.5.3).

The strains generated for PA0919 localization (section 3.8.1) were analyzed concerning their growth and A-PG content to investigate the effects of the employed *Strep*-tag II on PA0919 function. Phenotype analyses of strains Δ19 19 and Δ19 pUC/19 were expected to indicate the secretion of PA0919 into the periplasm. In contrast, strains Δ19 $19_{35\text{-}427}$ and Δ19 pUC/$19_{35\text{-}427}$ were expected to show a ΔPA0919 deletion mutant phenotype since the putative N-terminal secretion signal sequence was absent in the respective complementing construct.

The growth analysis revealed an almost identical growth behavior for all strains under neutral conditions (pH 7.3; see appendix, Figure 40) as observed before for other complemented ΔPA0919 variant strains (compare section 3.5.3). The growth curves obtained by cultivating the strains under acidic conditions (pH 5.3) are presented in Figure 27.

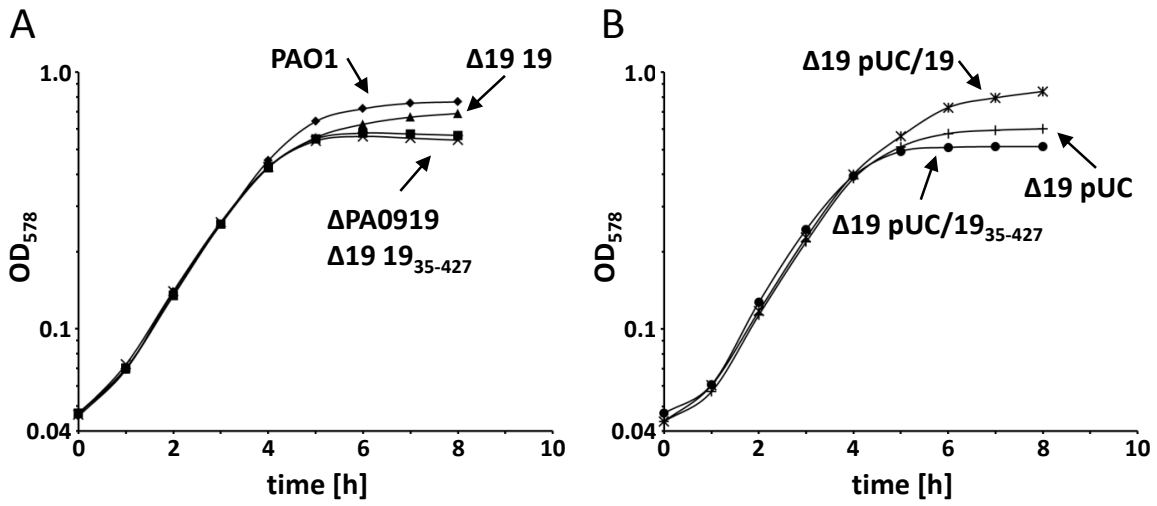

Figure 27: Growth of complemented PAO1 ΔPA0919 strains for PA0919 localization
PAO1 ΔPA0919 variant strains were grown in AB medium pH 5.3 (supplemented with Cb for pUCP20T harboring strains) at 37 °C and 200 rpm. Growth was monitored by measuring the OD_{578} (section 2.3.5). For strain designation and construction details, see Figure 26 and section 2.4.19.

A. Chromosomally complemented PAO1 ΔPA0919 variant strains. Rhombus: PAO1 wild-type, square: PAO1 ΔPA0919 deletion mutant, triangle: Δ19 19, cross: Δ19 19_{35-427}.

B. PAO1 ΔPA0919 variant strains complemented with pUCP20T derivative plasmids. Star: Δ19 pUC/19, dot: Δ19 pUC/19_{35-427}, plus: Δ19 pUC.

The chromosomally complemented strain Δ19 19 encoding a full-length PA0919-Strep fusion protein showed a growth behavior almost identical to the wild-type (Figure 27, A) indicating the expression of a functional secreted PA0919 protein. Instead, for the corresponding Δ19 19_{35-427} strain lacking the putative PA0919 N-terminal secretion sequence, the deletion mutant phenotype was obtained. It was concluded that the *Strep*-tagged $PA0919_{35-427}$ protein is not secreted.

The PAO1 ΔPA0919 variant strains carrying a pUCP20T derivative exhibited an extended lag phase which might be attributed to the application of Cb for vector maintenance (Figure 27, B). The observed growth phenotypes of the plasmid-based complemented strains were in good agreement with the results obtained for the chromosomally complemented mutants:

Strain Δ19 pUC/19 showed a phenotype identical to the PAO1 wild-type and the Δ19 19 strain. In analogy to the ΔPA0919 deletion mutant and to strain Δ19 $19_{35\text{-}427}$, a stationary growth phase phenotype was observed for strain Δ19 pUC/$19_{35\text{-}427}$ devoid of the PA0919 secretion signal and for strain Δ19 pUC harboring the empty vector.

Lipid compositions of the employed PAO1 ΔPA0919 derivative strains were analyzed by extracting and separating the polar lipid fractions of the cells (sections 2.3.5, 2.5.1 and 2.5.3). Under neutral growth conditions, no A-PG was detected for all strains (see appendix, Figure 41). TLC plates obtained after cultivation in under acidic conditions (pH 5.3) are summarized in Figure 28.

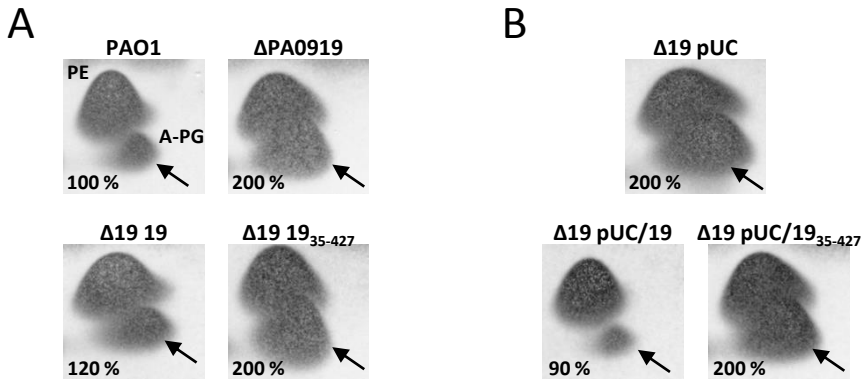

Figure 28: Lipid composition of complemented PAO1 ΔPA0919 variants for PA0919 localization
Various *P. aeruginosa* mutant strains were cultured in AB medium pH 5.3 (supplemented with Cb for pUCP20T carrying strains) at 37 °C for 24 h (section 2.3.5). After harvesting, polar lipids were extracted, analyzed by two-dimensional TLC and stained with molybdatophosphoric acid (sections 2.5.1 and 2.5.3). Relative A-PG amounts were quantified and related to the wild-type strain A-PG level (defined as 100 %). For strain designation and construction details, compare Figure 26 and section 2.4.19. A-PG position is indicated by an arrow.
A-PG: alanyl-phosphatidylglycerol, PE: phosphatidylethanolamine.
A. Chromosomal complementation variants of PAO1 ΔPA0919.
B. pUCP20T-based PAO1 ΔPA0919 complementation strains.

For strain Δ19 19 expressing the full-length PA0919-Strep protein, an A-PG level of 120 % was observed almost reflecting the wild-type A-PG content of 100 %. An increased A-PG level of 200 % was determined for the Δ19 $19_{35\text{-}427}$ strain harboring the truncated PA0919-Strep protein which is comparable to the A-PG content observed for the ΔPA0919 deletion mutant (Figure 28, A). The complementation of the ΔPA0919 deletion mutant strain employing the pUCP20T-based constructs resulted in analogous lipid phenotypes: For strain Δ19 pUC/19,

an A-PG amount of 90 % was observed which reflects almost the A-PG level of the wild-type strain. Furthermore, the introduction of the PA0919-Strep protein devoid of the secretory signal sequence (strain Δ19 $19_{35\text{-}427}$) or the empty pUCP20T vector (strain Δ19 pUC) resulted in an elevated A-PG level of 200 % also observed for the ΔPA0919 deletion mutant.

In conclusion, the growth analysis and the determination of the A-PG content of the various complemented strains revealed that the constructs encoding the full-length *Strep*-tagged PA0919 protein were able to complement the deletion mutant and almost restore the wild-type phenotype. Hence, the PA0919 protein was expressed, secreted and the employed C-terminal *Strep*-tag II did not influence the activity of the protein *in vivo*. In contrast, strains harboring the PA0919-Strep fusion protein lacking the predicted N-terminal PA0919 secretion signal sequence exhibited phenotypes characteristic for the ΔPA0919 deletion mutant strain. These results indicate that the N-terminal secretion signal peptide consisting of amino acids 1 – 34 of the entire PA0919 protein is necessary for the localization and function of the PA0919 protein in *P. aeruginosa*.

3.8.3 Localization of the PA0919 protein in cellular fractions of *P. aeruginosa*

The PA0919 protein was localized in *P. aeruginosa* using the Δ19 pUC/19 strain expressing a PA0919-Strep fusion protein (compare sections 3.8.1 and 3.8.2). Cells were grown under acidic conditions, when PA0919 expression was induced by the P_{PA0919} promoter (compare section 3.6). After harvesting, different cellular fractions (periplasm, cytoplasm, total membrane fraction, inner and outer membrane fractions) were isolated by various methods (chapter 2.12). SDS-PAGE and Western Blot analyses were performed and the PA0919 protein was detected within the obtained fractions *via* its *Strep*-tag II (Groenewold, 2013).

The *P. aeruginosa* strain Δ19 pUC/19 was selected for the PA0919 localization study based on several initial experiments (M. Groenewold, not shown). The cells were grown under acidic conditions (pH 5.3) to the early stationary growth phase. After harvesting, the cells were subjected to different fractionating procedures. To isolate periplasmic and cytoplasmic fractions (section 2.12.2), the cells were treated with polymyxin B for outer membrane permeabilization. After removing the periplasmic fraction by centrifugation, the spheroblasts were lysed, cell debris was sedimented and the cytoplasmic fraction was received.

The total membrane protein fraction of Δ19 pUC/19 cells was isolated by disrupting harvested cells, removing cell debris and sedimenting the total membrane fraction by high-speed centrifugation. Additionally, the membrane proteins were solubilized by Triton™ X-100 treatment and lipids were removed by a second high-speed centrifugation step (section 2.12.3).

To specifically locate the PA0919-Strep fusion protein to the inner or the outer membrane of *P. aeruginosa*, the respective membrane fractions were isolated by two different methods: First, the isopycnic sucrose gradient procedure according to Magnowska, 2010, was employed (section 2.12.4). After harvesting, cells lysis and cell debris removal, the membrane containing supernatant was loaded onto an isopycnic three-step sucrose gradient and subjected to ultracentrifugation. The inner and the outer membrane fractions were enriched at the interphases of the sucrose layers and were carefully isolated. The second protocol (section 2.12.5) employed for the isolation of *P. aeruginosa* membranes made use of the selective solubilization of the inner membrane by sarcosyl (Filip *et al.*, 1973). For this, the employed cells were lysed and cell debris was removed. The total membrane fraction was sedimented by high-speed centrifugation and suspended in a sarcosyl-containing solution. After an additional ultracentrifugation step, the inner membrane proteins resided in the supernatant while the outer membrane fraction was sedimented. The inner membrane fraction proteins were concentrated to increase the protein concentration. The outer membrane sediment was purified by a second sarcosyl solubilization and a subsequent ultracentrifugation. The obtained purified outer membrane sediment was suspended for further analysis.

Samples of the isolated protein fractions were analyzed by SDS-PAGE (section 2.10.2) and Western Blot (section 2.10.3). The PA0919 protein was detected within the samples *via* its *Strep*-tag II employing a Strep-Tactin® alkaline phosphatase conjugate (section 2.10.5). The obtained membrane is presented in Figure 29 (Groenewold, 2013).

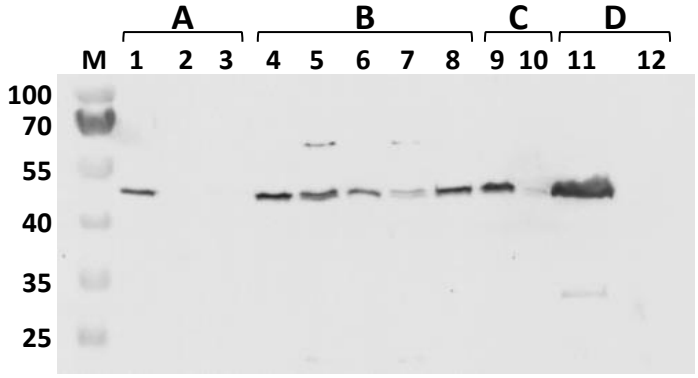

Figure 29: PA0919 protein localization in *P. aeruginosa*
Strain *P. aeruginosa* Δ19 pUC/19 expressing the *Strep*-tagged PA0919 protein was grown in AB medium pH 5.3 for 6 h (early stationary phase). After harvesting, the cells were fractionated into the periplasm, the cytoplasm and the inner and the outer membrane fractions. Samples were analyzed by SDS-PAGE and transferred to the PVDF membrane by Western Blot procedure. The PA0919 protein was detected *via* its C-terminal *Strep*-tag II (for details, see chapter 2.12).
M: PageRuler™ Prestained Protein Ladder, relative molecular masses (*1000) as indicated.

A. Periplasm and cytoplasm isolation. 1: whole cells, 2: soluble periplasmic fraction, 3: soluble cytoplasmic fraction.
B. Total membrane protein preparation. 4: whole cells, 5: supernatant after cell debris removal, 6: cell debris and unbroken cells, 7: supernatant after membrane sedimentation, 8: Triton™ X-100 solubilized total membrane fraction.
C. Separation of the inner and the outer membrane by isopycnic sucrose gradient centrifugation. 9: inner membrane fraction, 10: outer membrane fraction.
D. Separation of the inner and the outer membrane by sarcosyl solubilisation. 11: inner membrane proteins, 12: outer membrane proteins.

The PA0919 protein was detected in the whole cell fraction prior to the isolation of the periplasm and cytoplasm (A, lane 1). After polymyxin B treatment, soluble periplasmic and cytosolic proteins were isolated. However, the PA0919-Strep fusion protein was neither detected in the periplasmic nor in the cytoplasmic fraction (A, lanes 2 and 3).

The total membrane protein fraction was isolated to identify a general membrane association of PA0919 (B). PA0919 was detected in the whole cell fraction (B, lane 4). After cell lysis, the PA0919-Strep fusion protein was present in the membrane containing supernatant (B, lane 5) and residual amounts were observed in sedimented cell debris and unbroken cells (B, lane 6). The membrane containing supernatant was centrifuged to sediment the total membrane fraction. Minor amounts of PA0919 were observed in the supernatant after high-speed centrifugation (B, lane 7), whereas most of the protein was sedimented in the total membrane fraction (B, lane 8).

The separation of the inner and the outer membrane employing the isopycnic sucrose gradient method (C) indicated that PA0919 is associated to the inner membrane of *P. aeruginosa* as demonstrated by the detection of major amounts of the PA0919-Strep fusion protein in the inner membrane fraction (C, lane 9) compared to the outer membrane sample (C, lane 10). This result was verified by the second technique employing sarcosyl for membrane fraction separation (D). Here, the PA0919-Strep protein was detected exclusively in the inner membrane (D, lane 11), whereas no PA0919 was detectable in the outer membrane fraction (D, lane 12).

This investigation clearly localized the PA0919 protein to the inner membrane of *P. aeruginosa*. Interestingly, the recombinant *Strep*-tagged PA0919 protein heterologously produced as a soluble variant protein in the *E. coli* periplasm was enzymatically active in several *in vitro* analyses (compare chapter 3.7). Therefore, it was concluded that PA0919 is associated to the inner *P. aeruginosa* membrane by an N-terminal transmembrane helix and the C-terminal part of the protein is directed into the periplasmic space as indicated by the previous study (Lewenza *et al.*, 2005). This orientation would allow for the specific interaction with the hydrophilic alanine residue of the A-PG substrate present within the outer leaflet of the inner membrane of *P. aeruginosa*.

4 Discussion

4.1 A diverse evolution is responsible for the aaPGS substrate specificity

Prior to this work, the amino acid substrate specificity of 14 aaPGS enzymes had been investigated (compare Table 10). Due to the limited number of A-PGS enzymes, the identification of determinants responsible for the amino acid substrate specificity was not possible. In this study, the amino acid specificity of three L-PGS and six A-PGS enzymes was elucidated (compare Table 11) resulting in an overall number of 23 characterized aaPGS enzymes. The amino acid sequence comparison of enzymes specific for alanine or lysine did not result in the identification of determinants characteristic for the employed amino acid substrates Ala-tRNA^{Ala} and Lys-tRNA^{Lys}. In a phylogenetic study, A-PG or L-PG synthesizing organisms do not cluster together. Instead, the utilization of alanine or alternatively of lysine is widely distributed in prokaryotes (compare Figure 8).

A previous study analyzing the determinants for the Ala-tRNA^{Ala} recognition by the *P. aeruginosa* A-PGS enzyme had revealed that only five terminal base pairs of the tRNA acceptor stem are recognized by the enzyme (Hebecker *et al.*, 2011). Another study dealing with the tRNA substrate recognition by *C. perfringens* aaPGS enzymes had identified the tRNA acceptor stem as necessary for PG aminoacylation (Roy and Ibba, 2008b). Interestingly, both studies had revealed that the amino acid moiety is the most important determinant for the aaPGS substrate recognition (Hebecker *et al.*, 2011; Roy and Ibba, 2008b).

Due to the results obtained in the present study, a diverse evolution of the respective alanine or lysine specific enzyme was proposed. It seems reasonable that the aminoacyl-tRNA substrate specificity is determined by the architecture of the substrate binding pocket. The successive exchange of minor conserved amino acid residues forming the binding pocket might have slightly altered the pocket architecture leading to a successive change of the substrate specificity of the individual aaPGS. AaPGS enzymes with broadened substrate specificity may represent intermediate stages of such processes and it was proposed that they enable the respective bacterial host to effectively fine-tune their membrane lipid homeostasis by the simultaneous incorporation of different aaPG molecules.

Taken together, these considerations imply that even the application of an increased number of aaPGS enzymes might not result in the identification of determinants for aminoacyl-tRNA recognition. Moreover, the amino acid sequence of an aaPGS enzyme might not be sufficient for the prediction of its substrate specificity. Perhaps, the structural analysis of several aaPGS enzymes might provide further insights into the aminoacyl-tRNA substrate specificity determination.

4.2 Bacterial adaptation strategies by A-PG and L-PG synthesis

In this study, the formation of A-PG in *P. aeruginosa* was correlated with increased resistances against selected antimicrobial compounds like β-lactams, CAMPs, cationic disinfectants and the lipopeptide daptomycin (see Table 12). The complementation of the A-PGS deficient deletion mutant strain PAO1 ΔPA0920 with aaPGS homologs from different organisms resulted in the synthesis of A-PG, L-PG or L-PG together with A-PG in the identical genetic background. This experimental setup allowed for the *in vivo* analysis of the physiological impact of aminoacylated PG in the gram negative model organism *P. aeruginosa*. The formation of altered aaPG levels resulted in increased susceptibilities to most antimicrobials compared to the deletion mutant (compare Table 12).

Previous studies analyzing the resistance of *S. aureus* against several positively charged antimicrobials had resulted in the 'charge repulsion' mechanism hypothesis which relates the resistance against several CAMP molecules to the synthesis of the positively charged L-PG (see section 1.4.3; Peschel *et al.*, 2001). A previous study dealing with the synthesis of A-PG and L-PG in the gram positive model organism *S. aureus* clearly indicated that the formation of both aaPG variants resulted in comparable resistance phenotypes in the presence of the lipopeptide daptomycin (Slavetinsky *et al.*, 2012). Based on these and further results, the susceptibility of bacteria to CAMPs was correlated rather to the content of PG than L-PG (compare section 1.4.3; Bayer *et al.*, 2013). It was concluded that the type of amino acid employed for PG modification is of minor importance for antimicrobial resistance but might be relevant for membrane fluidity or lipid homeostasis in *S. aureus* synthesizing high levels of aaPG (Slavetinsky *et al.*, 2012; Bayer *et al.*, 2013).

Based on the 'charge repulsion' hypothesis, an increased resistance against positively charged antimicrobial compounds was expected for the *P. aeruginosa* strains synthesizing L-PG and therefore providing an altered membrane surface charge in this study. Additionally, elevated amounts of the zwitterionic A-PG resulted in slightly altered membrane surface charges. However, for these strains, increased susceptibilities were obtained for all applied cationic antimicrobial compounds (protamine sulfate, poly-L-lysine, polymyxin E, benzethonium chloride and domiphen bromide) with phenotypes comparable rather to the aaPG deficient ΔPA0920 deletion mutant than to the A-PG synthesizing PAO1 wild-type strain. In certain cases, the complemented variant exhibited an increased susceptibility when compared to the deletion mutant strain (e.g. ΔSa_{comp} for poly-L-lysine or ΔPa_{comp} for polymyxin E; compare Table 12). The PG levels of all employed mutant strains synthesizing artificial aaPGs were found constant and comparable to the wild-type amount (compare Figure 10) and therefore the obtained phenotypes cannot be related to the PG level. Furthermore, the transcription level of the P_{PA0920} promoter was found mainly determined by the environmental pH value but was modulated in the presence of specific antimicrobials indicating a fine-tuning of the membrane lipid composition in response to specific compounds.

These observations clearly elucidate that neither the postulated 'charge repulsion' mechanism nor the 'PG reduction' hypothesis can explain the aaPG mediated antibiotic resistance observed for the gram negative model organism *P. aeruginosa* in this study. Instead, it seems reasonable that the aaPG mediated resistance mechanisms differ from each other in gram positive and gram negative organisms and might depend on the overall aaPG amount. Other physical aspects like hydrophobic interactions of cationic compounds with membranes (Pogliano *et al.*, 2012; Zasloff, 2002) have to be considered beside the electrostatic effects described by the 'charge repulsion' and 'PG reduction' mechanisms. Additionally, membrane characteristics like homeostasis, permeability, fluidity and potential might be responsible for the observed phenotypes (Klein *et al.*, 2009; Roy *et al.*, 2009; Ernst and Peschel, 2011). The formation of microdomains might dramatically change local membrane characteristics and the activity and conformation of membrane proteins might be influenced by alterations in their lipid environment (Dowhan and Bogdanov, 2002; Matsumoto *et al.*, 2006; Barák and Muchová, 2013).

It seems reasonable that the resistance against different antimicrobial compounds, which is correlated to the synthesis of aaPG molecules, is mediated by different mechanisms in one organism. In this study, such a variety of mechanisms might be responsible for the susceptibility of *P. aeruginosa* to ampicillin and to oxacillin. Additionally, the specific cell envelope architecture of gram positive and gram negative bacteria might also result in different aaPG-dependent resistance mechanisms. However, the present study does not allow for the elucidation of the molecular mode of antimicrobial resistance.

Taken together, the analysis of A-PG and L-PG formation in *P. aeruginosa* and the P_{PA0920} promoter activity study revealed that the amino acid employed for PG modification and, additionally, the level of modified PG within the membrane maintaining the membrane lipid homeostasis are important for the susceptibility of *P. aeruginosa* to antimicrobial compounds. However, the precise molecular mechanism remains to be identified.

4.3 PA0919 is an alanyl-phosphatidylglycerol hydrolase (A-PGH)

AaPGS homologs are often chromosomally encoded together with an AcvB/PA0919 homologous protein in gram negative organisms. To elucidate the function of orf PA0919 located directly downstream of the A-PGS encoding gene in *P. aeruginosa*, orf PA0919 was deleted. The resulting PAO1 ΔPA0919 deletion mutant strain showed a stationary growth phase phenotype, an elevated A-PG level and was found susceptible to several antibiotic compounds (compare Table 14). In complemented variants of strain ΔPA0919 expressing orf PA0919, the wild-type resistance phenotype was restored. These results clearly indicate that the accurate fine-tuning of the cellular A-PG content and therefore the maintenance of membrane homeostasis are of prime importance for the resistance of *P. aeruginosa* to several antimicrobial compounds.

Due to the elevated A-PG content of the ΔPA0919 mutant strain and the identified LIPASE_SER motif in the PA0919 amino acid sequence, it was assumed that the PA0919 protein hydrolyzes A-PG (compare section 3.7.1). To analyze the protein *in vitro*, it was recombinantly produced in *E. coli* and the substrate specificity of the purified protein was investigated using artificial *p*-nitrophenol derivative substrates. The PA0919 protein was found to hydrolyze ester bonds linking amino acids to *p*-nitrophenol depending on the

presence of the amino group. Taken into account that PA0919 homologous proteins are also detected in L-PG synthesizing organisms, these findings might indicate that PA0919 homologs are generally involved in aaPG dependent lipid homeostasis in gram negative bacteria. The hydrolysis of the artificial lysine substrate by PA0919 *in vitro* might either be a general feature of PA0919 homologs or an evolutionary relict. The future analysis of PA0919 homologous proteins might confirm this hypothesis.

In a second *in vitro* approach, the PA0919 activity was analyzed in the presence of radioactively labeled A-PG representing the putative native substrate. The observed hydrolysis of A-PG into alanine and PG indicated first, that A-PG represents the native PA0919 substrate and second, that PA0919 modulates the A-PG content in *P. aeruginosa* membranes. Consequently, the PA0919 protein was named alanyl-phosphatidylglycerol hydrolase (A-PGH).

The enzymatic hydrolysis of ester bonds is catalyzed by three key amino acid residues (serine, aspartate/glutamate and histidine) forming a catalytic triade e.g. in esterases, lipases or phospholipases (Jaeger *et al.*, 1999; Aloulou *et al.*, 2012). After binding of the ester substrate, the active site serine is activated by a histidine (promoted by an aspartate/ glutamate) located in an appropriate position. Subsequently, the serine nucleophile attacks the substrate ester bond and a covalent enzyme-substrate intermediate is obtained while the alcoholic moiety of the ester substrate is liberated. Finally, the carboxylic residue of the ester substrate is released from the serine residue (Jaeger *et al.*, 1999; Aloulou *et al.*, 2012). An analogous mechanism and active site architecture are proposed for the A-PGH due to the identified LIPASE_SER motif. For the analysis of the enzymatic mechanism of A-PGH, the protein was treated with serine- and histidine-specific inhibitors and the protein activity was found reduced in the presence of the respective compound. This indicates the involvement of a serine and a histidine residue in the enzymatic mechanism. To substantiate this hypothesis, the A-PGH protein was analyzed by site-directed mutagenesis. The *in vitro* activity analysis of the obtained A-PGH mutant proteins S307A (putative active site serine mutated) and H401A (conserved histidine mutated) clearly indicated the importance of these amino acid residues for the enzymatic mechanism due to the lack of enzyme activity of both mutant proteins. Instead, the third A-PGH mutant protein S240A (conserved serine mutated) exhibited a residual activity in all *in vitro* analyses and therefore, it was concluded

that serine 240 is not essential for PA0919 catalysis. To unambiguously elucidate the enzymatic mechanism, the PA0919 protein and its derivatives should be analyzed by X-ray crystallography in the presence and absence of inhibitory compounds.

Bioinformatic and experimental analyses performed in a previous study had predicted the presence of an N-terminal secretion signal for the A-PGH enzyme and identified the A-PGH protein in the periplasm of *P. aeruginosa* using a PhoA fusion protein (Lewenza *et al.*, 2005). To unambiguously localize the A-PGH in its native host in this study, the full-length A-PGH protein was fused to a *Strep*-tag II and produced in an A-PGH deficient *P. aeruginosa* strain. The bacterial cells were fractionated and the A-PGH fusion protein was localized within the cytoplasmic membrane fraction by two different experimental approaches.

Based on all obtained results, an A-PGH topology and reaction mechanism model is proposed (Figure 30).

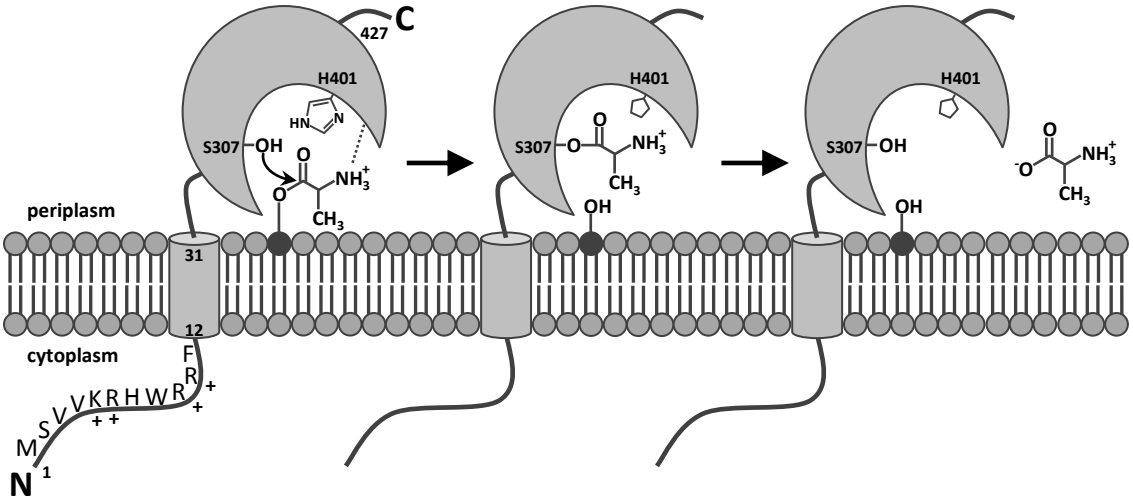

Figure 30: Model of the topology and the proposed enzymatic mechanism of the A-PGH
The domain structure model was developed based on bioinformatic and experimental results presented in this study. It is proposed that the A-PGH is anchored to the inner membrane of *P. aeruginosa* by one transmembrane helix located near the N-terminus (amino acids 12 to 31). The N-terminus providing several positively charged amino acid residues faces the cytoplasm and the active site containing C-terminal protein domain (characterized by serine 307 and histidine 401) is directed to the periplasm.
For the reaction, the alanine residue of A-PG is recognized by the membrane anchored A-PGH enzyme based on its ester linkage and its amino group. The active site serine attacks the aminoacyl bond between alanine and PG (dark gray lipid head group) and promoted by the active site histidine, a covalent enzyme-alanine intermediate is obtained and PG is liberated. In the second step, alanine is released into the periplasm.

It is concluded that the A-PGH is anchored to the inner membrane of *P. aeruginosa* by its uncleaved N-terminal sequence and that the catalytic active site containing domain is located in the periplasmic space. Four N-terminal located amino acids, which are proposed to be located at the cytoplasmic surface of the inner membrane, provide positively charged amino acid side chains (compare Figure 30). This is in good agreement with the 'positive inside rule' describing membrane protein topologies (see section 1.3.3; Dalbey *et al.*, 2011; Bogdanov *et al.*, 2009). The membrane spanning helix formed by amino acids 12 to 31 was predicted using TMHMM (compare appendix, Figure 39). Due to this proposed A-PGH topology, the catalytic active site containing the identified key amino acid residues serine 307 and histidine 401 would be positioned at the membrane surface next to the alanine residue of the A-PG substrate located in the outer leaflet of the inner membrane of *P. aeruginosa*. The catalytic mechanism of the A-PGH is proposed based on the enzymatic mechanism of lipases (Jaeger *et al.*, 1999): The A-PG substrate is recognized by the A-PGH enzyme due to its ester bond and the amino group provided by alanine. The A-PG ester bond linking the alanine moiety to PG is attacked by the nucleophilic hydroxyl group of serine 307 resulting in a covalent enzyme-substrate intermediate while the PG residue is liberated. Subsequently, alanine is released from the active site serine completing the A-PG hydrolysis. The active site histidine 401 is proposed to be involved in both reaction steps.

The functions of the A-PGH homologous enzymes AcvB and VirJ from *A. tumefaciens* and AtvA from *R. tropici* had been analyzed in previous studies: The respective A-PGH homolog deficient strains had shown an increased acid sensitivity (Vinuesa *et al.*, 2003) and *A. tumefaciens* virulence had been reduced in the absence of AcvB/VirJ (Wirawan *et al.*, 1993; Pan *et al.*, 1995). Based on the identified LIPASE_SER motif in AtvA, Vinuesa and coworkers had proposed a lipolytic activity of AtvA homologs (Vinuesa *et al.*, 2003). After the characterization of several aaPGS enzymes had been published, Sohlenkamp and coworkers speculated that AtvA hydrolyzes L-PG in *R. tropici* (Sohlenkamp *et al.*, 2007). However, this present work represents the first characterization of an A-PGH-type enzyme hydrolyzing A-PG, thus mediating the aaPG membrane lipid homeostasis in gram negative bacteria.

4.4 A-PG-dependent lipid homeostasis in *P. aeruginosa*

In former studies, the A-PG synthesis in *P. aeruginosa* had been elucidated and first hints concerning the role of A-PG in antibacterial resistance had been obtained (Klein *et al.*, 2009; Hebecker *et al.*, 2011). The present study provides new insights into the A-PG homeostasis of *P. aeruginosa*, summarized in Figure 31.

The A-PG homeostasis in *P. aeruginosa* is mediated by the A-PGS and the A-PGH located in or at the inner membrane. An alanine residue is transferred from its corresponding tRNA to a hydroxyl group of the phospholipid PG by the C-terminal catalytic A-PGS domain (Hebecker *et al.*, 2011). The N-terminal A-PGS transmembrane domain is proposed to translocate the synthesized A-PG to the outer leaflet of the inner membrane as it had been described for homologous enzymes (Slavetinsky *et al.*, 2012). Subsequently, the cellular A-PG level, which was identified to be of relevance for antimicrobial resistance in this study, is fine-tuned by the A-PGH enzyme identified and characterized in this work. A-PG is transferred to the inner leaflet of the outer membrane (Klein *et al.*, 2009) by an as yet unidentified mechanism. Although the molecular basis remains unclear, the accurate A-PG level seems to be responsible for the resistance of *P. aeruginosa* against a wide variety of antimicrobial compounds (this work; Klein *et al.*, 2009). Furthermore, the A-PG level is controlled by regulating the transcription of the A-PGS and the A-PGH: The formerly identified promoter P_{PA0920} induces the A-PGS transcription under acidic conditions (Klein *et al.*, 2009), but the overall induction level was found modulated in the presence of specific compounds (this work). Additionally, the P_{PA0920} promoter is induced under neutral conditions by certain antimicrobials (this work). The A-PGH regulating P_{PA0919} promoter newly identified in this study induces the transcription of the A-PGH enzyme under acidic conditions.

From these results it becomes clear that the inhibition of the A-PGS and/or the A-PGH might be a promising strategy to overcome the high resistance of *P. aeruginosa* against several antibiotics of clinical relevance. This is of special interest considering the presence of aaPGS enzymes (in some gram negatives in combination with A-PGH homologous enzymes) in many pathogens causing serious infections.

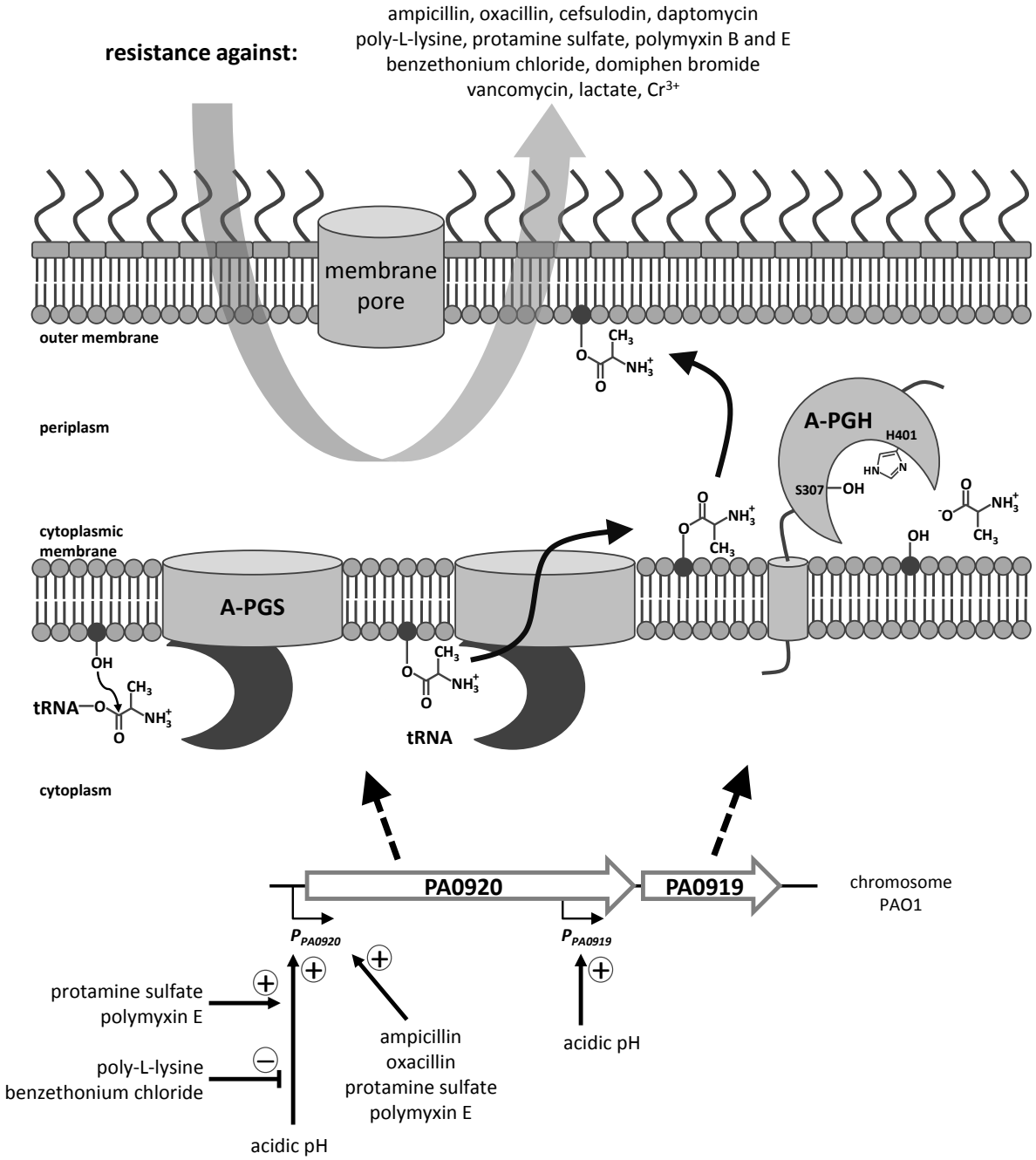

Figure 31: A-PG homeostasis in *P. aeruginosa*

A-PG is synthesized by the C-terminal A-PGS domain (dark gray) located in the cytoplasm of *P. aeruginosa*. An alanine residue is transferred from its tRNA to a hydroxyl group of the phospholipid PG (dark gray lipid). The product A-PG proposed to be translocated to the outer leaflet of the inner membrane by the A-PGS transmembrane domain (light gray) exhibiting a potential flippase activity. A-PG is transported to the inner leaflet of the outer membrane by an as yet unidentified pathway. The A-PGH enzyme hydrolyzes A-PG to maintain A-PG homeostasis mediating antimicrobial resistance against a wide variety of compounds.

The cellular A-PG level is also influenced by regulating the expression of the A-PGS and the A-PGH enzymes: Both promoters are induced under acidic conditions and A-PGS expression is additionally modulated by several antimicrobial compounds.

A-PG: alanyl-phosphatidylglycerol, A-PGH: A-PG hydrolase, A-PGS: A-PG synthase, PG: phosphatidylglycerol, P_{PA0919}: promoter upstream of orf PA0919, P_{PA0920}: promoter upstream of orf PA0920.

5 Summary

Bacteria are able to adapt their cell envelope to changing environmental conditions. Several bacterial pathogens modify their membrane lipid component phosphatidylglycerol (PG) by the addition of lysine or alanine. This modification is mediated by aminoacyl-phosphatidylglycerol (aaPG) synthases and confers resistance against several antimicrobial compounds. The inhibition of aaPG synthases was proposed as a promising strategy to defend bacterial infections. At the beginning of this work, it was not clear how the aminoacyl-tRNA substrate specificity of the synthases is determined. In this work, the specificity of nine aaPG synthesizing enzymes was elucidated. The subsequent analysis of the phylogenetic distribution and the amino acid sequence-based comparison of all as yet characterized aaPG synthases indicate a diverse evolution for the aminoacyl-tRNA substrate specificity of the respective enzymes.

Most aaPG synthases are specific either for the lysyl-tRNA or the alanine-tRNA substrate. Up to now, only three enzymes with broadened substrate specificity have been identified resulting in the concomitant synthesis of at least two aaPG variants in the same organism. Furthermore, the observed aaPG amount in the bacterial membranes was found to vary in a wide range. To date, it is not clear if alanyl-PG and lysyl-PG provide complementary or differing functions in different bacteria. To address this question, strains of the gram negative model organism *Pseudomonas aeruginosa* with artificially altered aaPG contents were generated and analyzed phenotypically. It was shown that the amino acid employed for PG modification but also the overall level of aaPG incorporated into the membrane are of importance for the antimicrobial resistance of *P. aeruginosa*. Furthermore, the adaptation of the alanyl-PG content to antimicrobial stresses in *P. aeruginosa* was investigated. For this, the P_{PA0920} promoter which is located upstream of the aaPG synthase in *P. aeruginosa* was analyzed. The pH value was identified as the prominent determinant for aaPG synthase expression in *P. aeruginosa*. Besides this, the overall induction level of the P_{PA0920} promoter is modulated in the presence of specific antimicrobial compounds.

In several gram negatives, aaPG synthases are encoded in an operon with a second protein. The function of this PA0919 protein from *P. aeruginosa* was investigated in this study *in vivo* and *in vitro*. A PA0919 deficient *P. aeruginosa* strain exhibited an increased alanyl-PG

content, a stationary growth phase phenotype and an increased susceptibility to specific antimicrobial compounds. The PA0919 protein expression was found upregulated under acidic conditions by the PA0919 specific promoter P_{PA0919}.

The PA0919 protein was recombinantly produced in *Escherichia coli* and characterized concerning its substrate specificity *in vitro*. It accepts *p*-nitrophenol esters of several amino acids as artificial substrates. The *in vitro* hydrolysis of the native substrate alanyl-PG was observed and consequently, PA0919 was termed A-PGH for alanyl-phosphatidylglycerol hydrolase. The analysis of site-directed mutant proteins and an inhibitor study indicated that the hydrolysis of alanyl-PG depends on the active site amino acid residues serine 307 and histidine 401 of the A-PGH in a lipase-like mechanism. A localization study identified the A-PGH in the inner membrane of *P. aeruginosa*. Based on theoretical observations it is proposed that the A-PGH is anchored to the cytoplasmic membrane by one N-terminal transmembrane helix and its catalytic domain is directed to the periplasmic space of *P. aeruginosa*. This investigation elucidated the regulatory circuit that maintains the alanyl-PG dependent membrane lipid homeostasis in *P. aeruginosa*.

6 Outlook

- Elucidation of the three-dimensional structure of the A-PGS
- Analysis of A-PG function using artificial membrane models

- Organic synthesis of A-PG
- Direct *in vitro* A-PGH activity measurement using A-PG containing liposomes

- Elucidation of the three-dimensional structure of A-PGH in the presence of a substrate molecule
- Characterization of A-PGH homologous enzymes

7 References

Aloulou, A., Ali, Y. B., Bezzine, S., Gargouri, Y. and Gelb, M. H. (2012) Phospholipases: an overview. *Methods Mol Biol* **861**: 63-85.

Altschul, S. F., Gish, W., Miller, W., Myers, E. W. and Lipman, D. J. (1990) Basic local alignment search tool. *J Mol Biol* **215**: 403-410.

Andrews, J. M. (2001) Determination of minimum inhibitory concentrations. *J Antimicrob Chemother* **48 Suppl 1**: 5-16.

Aspedon, A. and Groisman, E. A. (1996) The antibacterial action of protamine: evidence for disruption of cytoplasmic membrane energization in *Salmonella typhimurium*. *Microbiology* **142**: 3389-3397.

Bagwell, C. E., Bhat, S., Hawkins, G. M., Smith, B. W., Biswas, T., Hoover, T. R., Saunders, E., Han, C. S., Tsodikov, O. V. and Shimkets, L. J. (2008) Survival in nuclear waste, extreme resistance, and potential applications gleaned from the genome sequence of *Kineococcus radiotolerans* SRS30216. *PLoS One* **3**: e3878.

Baltz, R. H. (2009) Daptomycin: mechanisms of action and resistance, and biosynthetic engineering. *Curr Opin Chem Biol* **13**: 144-151.

Bao, Y., Sakinc, T., Laverde, D., Wobser, D., Benachour, A., Theilacker, C., Hartke, A. and Huebner, J. (2012) Role of *mprF1* and *mprF2* in the pathogenicity of *Enterococcus faecalis*. *PLoS One* **7**: e38458.

Barák, I. and Muchová, K. (2013) The role of lipid domains in bacterial cell processes. *Int J Mol Sci* **14**: 4050-4065.

Bayer, A. S., Schneider, T. and Sahl, H. G. (2013) Mechanisms of daptomycin resistance in *Staphylococcus aureus*: role of the cell membrane and cell wall. *Ann N Y Acad Sci* **1277**: 139-158.

Becher, A. and Schweizer, H. P. (2000) Integration-proficient *Pseudomonas aeruginosa* vectors for isolation of single-copy chromosomal *lacZ* and *lux* gene fusions. *Biotechniques* **29**: 948-950, 952.

Bleves, S., Viarre, V., Salacha, R., Michel, G. P., Filloux, A. and Voulhoux, R. (2010) Protein secretion systems in *Pseudomonas aeruginosa*: A wealth of pathogenic weapons. *Int J Med Microbiol* **300**: 534-543.

Bligh, E. G. and Dyer, W. J. (1959) A rapid method of total lipid extraction and purification. *Can J Biochem Physiol* **37**: 911-917.

Bochner, B. R. (2009) Global phenotypic characterization of bacteria. *FEMS Microbiol Rev* **33**: 191-205.

Bogdanov, M., Xie, J. and Dowhan, W. (2009) Lipid-protein interactions drive membrane protein topogenesis in accordance with the positive inside rule. *J Biol Chem* **284**: 9637-9641.

Bölin, I., Norlander, L. and Wolf-Watz, H. (1982) Temperature-inducible outer membrane protein of *Yersinia pseudotuberculosis* and *Yersinia enterocolitica* is associated with the virulence plasmid. *Infect Immun* **37**: 506-512.

Bradford, M. M. (1976) A rapid and sensitive method for the quantitation of microgram quantities of protein utilizing the principle of protein-dye binding. *Anal Biochem* **72**: 248-254.

Brazas, M. D. and Hancock, R. E. (2005) Using microarray gene signatures to elucidate mechanisms of antibiotic action and resistance. *Drug Discov Today* **10**: 1245-1252.

Breidenstein, E. B., de la Fuente-Nunez, C. and Hancock, R. E. (2011) *Pseudomonas aeruginosa*: all roads lead to resistance. *Trends Microbiol* **19**: 419-426.

Bullard, J. W., Champlin, F. R., Burkus, J., Millar, S. Y. and Conrad, R. S. (2011) Triclosan-induced modification of unsaturated fatty acid metabolism and growth in *Pseudomonas aeruginosa* PAO1. *Curr Microbiol* **62**: 697-702.

Byarugaba, D. K. (2004) A view on antimicrobial resistance in developing countries and responsible risk factors. *Int J Antimicrob Agents* **24**: 105-110.

Callaghan, M. and McClean, S. (2012) Bacterial host interactions in cystic fibrosis. *Curr Opin Microbiol* **15**: 71-77.

Coakley, R. D., Grubb, B. R., Paradiso, A. M., Gatzy, J. T., Johnson, L. G., Kreda, S. M., O'Neal, W. K. and Boucher, R. C. (2003) Abnormal surface liquid pH regulation by cultured cystic fibrosis bronchial epithelium. *Proc Natl Acad Sci U S A* **100**: 16083-16088.

Conrad, R. S. and Gilleland, H. E., Jr. (1981) Lipid alterations in cell envelopes of polymyxin-resistant *Pseudomonas aeruginosa* isolates. *J Bacteriol* **148**: 487-497.

Conte, M., Aliberti, F., Fucci, L. and Piscopo, M. (2007) Antimicrobial activity of various cationic molecules on foodborne pathogens. *World J Microbiol Biotechnol* **23**: 1679-1683.

Contreras, I., Shapiro, L. and Henry, S. (1978) Membrane phospholipid composition of *Caulobacter crescentus*. *J Bacteriol* **135**: 1130-1136.

Cosgrove, S. E. (2006) The relationship between antimicrobial resistance and patient outcomes: mortality, length of hospital stay, and health care costs. *Clin Infect Dis* **42 Suppl 2**: S82-89.

Courvalin, P. (2006) Vancomycin resistance in gram-positive cocci. *Clin Infect Dis* **42 Suppl 1**: S25-34.

Cronan, J. E. (2003) Bacterial membrane lipids: where do we stand? *Annu Rev Microbiol* **57**: 203-224.

Crooks, G. E., Hon, G., Chandonia, J. M. and Brenner, S. E. (2004) WebLogo: a sequence logo generator. *Genome Res* **14**: 1188-1190.

Cutler, D. M., Deaton, A. S. and Lleras-Muney, A. (2006) The Determinants of Mortality. *J Econ Perspect* **20**: 97-120.

Dalbey, R. E., Wang, P. and Kuhn, A. (2011) Assembly of bacterial inner membrane proteins. *Annu Rev Biochem* **80**: 161-187.

Dare, K. and Ibba, M. (2012) Roles of tRNA in cell wall biosynthesis. *Wiley Interdiscip Rev RNA* **3**: 247-264.

Davies, J. and Davies, D. (2010) Origins and evolution of antibiotic resistance. *Microbiol Mol Biol Rev* **74**: 417-433.

Davies, J., Spiegelman, G. B. and Yim, G. (2006) The world of subinhibitory antibiotic concentrations. *Curr Opin Microbiol* **9**: 445-453.

Delorme, C. (2008) Safety assessment of dairy microorganisms: *Streptococcus thermophilus*. *Int J Food Microbiol* **126**: 274-277.

Deppenmeier, U., Johann, A., Hartsch, T., Merkl, R., Schmitz, R. A., Martinez-Arias, R., Henne, A., Wiezer, A., Baumer, S., Jacobi, C., Bruggemann, H., Lienard, T., Christmann, A., Bomeke, M., Steckel, S., Bhattacharyya, A., Lykidis, A., Overbeek, R., Klenk, H. P., Gunsalus, R. P., Fritz, H. J. and Gottschalk, G. (2002) The genome of *Methanosarcina mazei*: evidence for lateral gene transfer between bacteria and archaea. *J Mol Microbiol Biotechnol* **4**: 453-461.

Deurenberg, R. H. and Stobberingh, E. E. (2008) The evolution of *Staphylococcus aureus*. *Infect Genet Evol* **8**: 747-763.

Diermayr, P., Kroll, S. and Klostermeyer, H. (1987) Influence of EDTA and metal ions on a metalloproteinase from *Pseudomonas fluorescens* biotype I. *Biol Chem Hoppe Seyler* **368**: 57-61.

Dobson, A. P. and Carper, E. R. (1996) Infectious Diseases and Human Population History. *BioScience* **46**: 115-126.

Dowhan, W. (1997) Molecular basis for membrane phospholipid diversity: why are there so many lipids? *Annu Rev Biochem* **66**: 199-232.

Dowhan, W. and Bogdanov, M. (2002) Functional roles of lipids in membranes. In: Biochemistry of Lipids, Lipoproteins and Membranes. D. E. Vance & J. E. Vance (eds). Elsevier Science B. V., pp. 1-35.

Dowhan, W. and Bogdanov, M. (2009) Lipid-dependent membrane protein topogenesis. *Annu Rev Biochem* **78**: 515-540.

Dowler, S., Kular, G. and Alessi, D. R. (2002) Protein lipid overlay assay. *Sci STKE* **2002**: pl6.

Edman, P. (1950) Method for determination of the amino acid sequence in peptides. *Acta Chem Scand*: 283-293.

Eitel, J. and Dersch, P. (2002) The YadA protein of *Yersinia pseudotuberculosis* mediates high-efficiency uptake into human cells under environmental conditions in which invasin is repressed. *Infect Immun* **70**: 4880-4891.

Elliott, G. N., Chen, W.-M., Chou, J.-H., Wang, H.-C., Sheu, S.-Y., Perin, L., Reis, V. M., Moulin, L., Simon, M. F., Bontemps, C., Sutherland, J. M., Bessi, R., De Faria, S. M., Trinick, M. J., Prescott, A. R., Sprent, J. I. and James, E. K. (2007) *Burkholderia phymatum* is a highly effective nitrogen-fixing symbiont of *Mimosa* spp. and fixes nitrogen *ex planta*. *New Phytol* **173**: 168-180.

Engler, C., Kandzia, R. and Marillonnet, S. (2008) A one pot, one step, precision cloning method with high throughput capability. *PLoS One* **3**: e3647.

Enoch, D. A., Bygott, J. M., Daly, M. L. and Karas, J. A. (2007) Daptomycin. *J Infect* **55**: 205-213.

Epand, R. F., Maloy, L., Ramamoorthy, A. and Epand, R. M. (2010) Amphipathic helical cationic antimicrobial peptides promote rapid formation of crystalline states in the presence of phosphatidylglycerol: lipid clustering in anionic membranes. *Biophys J* **98**: 2564-2573.

Ernst, C. M. and Peschel, A. (2011) Broad-spectrum antimicrobial peptide resistance by MprF-mediated aminoacylation and flipping of phospholipids. *Mol Microbiol* **80**: 290-299.

Ernst, C. M., Staubitz, P., Mishra, N. N., Yang, S. J., Hornig, G., Kalbacher, H., Bayer, A. S., Kraus, D. and Peschel, A. (2009) The bacterial defensin resistance protein MprF consists of separable domains for lipid lysinylation and antimicrobial peptide repulsion. *PLoS Pathog* **5**: e1000660.

Filip, C., Fletcher, G., Wulff, J. L. and Earhart, C. F. (1973) Solubilization of the cytoplasmic membrane of *Escherichia coli* by the ionic detergent sodium-lauryl sarcosinate. *J Bacteriol* **115**: 717-722.

Filloux, A. (2011) Protein Secretion Systems in *Pseudomonas aeruginosa*: An Essay on Diversity, Evolution, and Function. *Front Microbiol* **2**: 155.

Friedman, L., Alder, J. D. and Silverman, J. A. (2006) Genetic changes that correlate with reduced susceptibility to daptomycin in *Staphylococcus aureus*. *Antimicrob Agents Chemother* **50**: 2137-2145.

Garbus, J., Deluca, H. F., Loomans, M. E. and Strong, F. M. (1963) The rapid incorporation of phosphate into mitochondrial lipids. *J Biol Chem* **238**: 59-63.

Gaspar, M. C., Couet, W., Olivier, J. C., Pais, A. A. and Sousa, J. J. (2013) *Pseudomonas aeruginosa* infection in cystic fibrosis lung disease and new perspectives of treatment: a review. *Eur J Clin Microbiol Infect Dis*: DOI 10.1007/s10096-10013-11876-y.

Geiger, O., Gonzalez-Silva, N., Lopez-Lara, I. M. and Sohlenkamp, C. (2010a) Amino acid-containing membrane lipids in bacteria. *Prog Lipid Res* **49**: 46-60.

Geiger, O., Sohlenkamp, C. and López-Lara, I. M. (2010b) Formation of Bacterial Membrane Lipids: Pathways, Enzymes, Reactions. In: Handbook of Hydrocarbon and Lipid Microbiology. K. Timmis (ed). Springer Berlin Heidelberg, pp. 395-407.

Gilbert, P. and Moore, L. E. (2005) Cationic antiseptics: diversity of action under a common epithet. *J Appl Microbiol* **99**: 703-715.

Gold, A. M. (1965) Sulfonyl Fluorides as Inhibitors of Esterases. 3. Identification of Serine as the Site of Sulfonylation in Phenylmethanesulfonyl α-Chymotrypsin. *Biochemistry* **4**: 897-901.

Gold, A. M. and Fahrney, D. (1964) Sulfonyl Fluorides as Inhibitors of Esterases. II. Formation and Reactions of Phenylmethanesulfonyl α-Chymotrypsin. *Biochemistry* **3**: 783-791.

Goossens, H. and Sprenger, M. J. (1998) Community acquired infections and bacterial resistance. *Bmj* **317**: 654-657.

Grant, S. G., Jessee, J., Bloom, F. R. and Hanahan, D. (1990) Differential plasmid rescue from transgenic mouse DNAs into *Escherichia coli* methylation-restriction mutants. *Proc Natl Acad Sci U S A* **87**: 4645-4649.

Groenewold, M. K. (2011) Deletion Lipid modifizierender Enzyme aus *Pseudomonas putida* KT2440. Bachelor thesis. Technische Universität Braunschweig, Braunschweig, Germany.

Groenewold, M. K. (2013) Aminoacyl-Phosphatidylglycerol Hydrolase aus *Pseudomonas aeruginosa* PAO1. Master thesis. Technische Universität Braunschweig, Braunschweig, Germany.

Guzman, L. M., Belin, D., Carson, M. J. and Beckwith, J. (1995) Tight regulation, modulation, and high-level expression by vectors containing the arabinose P_{BAD} promoter. *J Bacteriol* **177**: 4121-4130.

Hachmann, A. B., Angert, E. R. and Helmann, J. D. (2009) Genetic analysis of factors affecting susceptibility of *Bacillus subtilis* to daptomycin. *Antimicrob Agents Chemother* **53**: 1598-1609.

Hachmann, A. B., Sevim, E., Gaballa, A., Popham, D. L., Antelmann, H. and Helmann, J. D. (2011) Reduction in membrane phosphatidylglycerol content leads to daptomycin resistance in *Bacillus subtilis*. *Antimicrob Agents Chemother* **55**: 4326-4337.

Hancock, R. E. (1998) Resistance mechanisms in *Pseudomonas aeruginosa* and other nonfermentative gram-negative bacteria. *Clin Infect Dis* **27 Suppl 1**: S93-99.

Hancock, R. E. and Speert, D. P. (2000) Antibiotic resistance in *Pseudomonas aeruginosa*: mechanisms and impact on treatment. *Drug Resist Updat* **3**: 247-255.

Hartmann, W. and Galla, H. J. (1978) Binding of polylysine to charged bilayer membranes: molecular organization of a lipid-peptide complex. *Biochim Biophys Acta* **509**: 474-490.

Harwood, C. R. and Cutting, S. M. (1990) Molecular biological method for *Bacillus*. Wiley, Chichester.

Hazel, J. R. and Williams, E. E. (1990) The role of alterations in membrane lipid composition in enabling physiological adaptation of organisms to their physical environment. *Prog Lipid Res* **29**: 167-227.

Hebecker, S., Arendt, W., Heinemann, I. U., Tiefenau, J. H., Nimtz, M., Rohde, M., Söll, D. and Moser, J. (2011) Alanyl-phosphatidylglycerol synthase: mechanism of substrate recognition during tRNA-dependent lipid modification in *Pseudomonas aeruginosa*. *Mol Microbiol* **80**: 935-950.

Hegstad, K., Langsrud, S., Lunestad, B. T., Scheie, A. A., Sunde, M. and Yazdankhah, S. P. (2010) Does the wide use of quaternary ammonium compounds enhance the selection and spread of antimicrobial resistance and thus threaten our health? *Microb Drug Resist* **16**: 91-104.

Heydorn, A., Nielsen, A. T., Hentzer, M., Sternberg, C., Givskov, M., Ersboll, B. K. and Molin, S. (2000) Quantification of biofilm structures by the novel computer program COMSTAT. *Microbiology* **146**: 2395-2407.

Hoang, T. T., Karkhoff-Schweizer, R. R., Kutchma, A. J. and Schweizer, H. P. (1998) A broad-host-range Flp-FRT recombination system for site-specific excision of chromosomally-located DNA sequences: application for isolation of unmarked *Pseudomonas aeruginosa* mutants. *Gene* **212**: 77-86.

Hoang, T. T., Kutchma, A. J., Becher, A. and Schweizer, H. P. (2000) Integration-proficient plasmids for *Pseudomonas aeruginosa*: site-specific integration and use for engineering of reporter and expression strains. *Plasmid* **43**: 59-72.

Holland, I. B. (2004) Translocation of bacterial proteins-an overview. *Biochim Biophys Acta* **1694**: 5-16.

Houtsmuller, U. M. and van Deenen, L. L. (1965) On the amino acid esters of phosphatidyl glycerol from bacteria. *Biochim Biophys Acta* **106**: 564-576.

Huijbregts, R. P., de Kroon, A. I. and de Kruijff, B. (2000) Topology and transport of membrane lipids in bacteria. *Biochim Biophys Acta* **1469**: 43-61.

Ibrahim, M. A., Griko, N., Junker, M. and Bulla, L. A. (2010) *Bacillus thuringiensis*: a genomics and proteomics perspective. *Bioeng Bugs* **1**: 31-50.

Jacobs, M. A., Alwood, A., Thaipisuttikul, I., Spencer, D., Haugen, E., Ernst, S., Will, O., Kaul, R., Raymond, C., Levy, R., Chun-Rong, L., Guenthner, D., Bovee, D., Olson, M. V. and Manoil, C. (2003) Comprehensive transposon mutant library of *Pseudomonas aeruginosa*. *Proc Natl Acad Sci U S A* **100**: 14339-14344.

Jaeger, K. E., Dijkstra, B. W. and Reetz, M. T. (1999) Bacterial biocatalysts: molecular biology, three-dimensional structures, and biotechnological applications of lipases. *Annu Rev Microbiol* **53**: 315-351.

Jäger, S. (2011) Klonierung, Überproduktion und Reinigung der löslichen Domäne von Aminoacyl-Phosphatidylglycerol Synthasen zur Kristallisation. Master thesis. Technische Universität Braunschweig, Braunschweig, Germany.

Jensch, T. and Fricke, B. (1997) Localization of alanyl aminopeptidase and leucyl aminopeptidase in cells of *Pseudomonas aeruginosa* by application of different methods for periplasm release. *J Basic Microbiol* **37**: 115-128.

Jeong, H., Park, S. Y., Chung, W. H., Kim, S. H., Kim, N., Park, S. H. and Kim, J. F. (2011) Draft Genome Sequence of the *Paenibacillus polymyxa* Type Strain (ATCC 842^T), a Plant Growth-Promoting Bacterium. *J Bacteriol* **193**: 5026-5027.

Johansen, C., Verheul, A., Gram, L., Gill, T. and Abee, T. (1997) Protamine-induced permeabilization of cell envelopes of gram-positive and gram-negative bacteria. *Appl Environ Microbiol* **63**: 1155-1159.

Johno, H., Takahashi, S. and Kitamura, M. (2010) Influences of acidic conditions on formazan assay: a cautionary note. *Appl Biochem Biotechnol* **162**: 1529-1535.

Jones, D. E. and Smith, J. D. (1979) Phospholipids of the differentiating bacterium *Caulobacter crescentus*. *Can J Biochem* **57**: 424-428.

Jones, T., Yeaman, M. R., Sakoulas, G., Yang, S. J., Proctor, R. A., Sahl, H. G., Schrenzel, J., Xiong, Y. Q. and Bayer, A. S. (2008) Failures in clinical treatment of *Staphylococcus aureus* Infection with daptomycin are associated with alterations in surface charge, membrane phospholipid asymmetry, and drug binding. *Antimicrob Agents Chemother* **52**: 269-278.

Julian, K., Kosowska-Shick, K., Whitener, C., Roos, M., Labischinski, H., Rubio, A., Parent, L., Ednie, L., Koeth, L., Bogdanovich, T. and Appelbaum, P. C. (2007) Characterization of a daptomycin-nonsusceptible vancomycin-intermediate *Staphylococcus aureus* strain in a patient with endocarditis. *Antimicrob Agents Chemother* **51**: 3445-3448.

Kadokura, H. and Beckwith, J. (2010) Mechanisms of oxidative protein folding in the bacterial cell envelope. *Antioxid Redox Signal* **13**: 1231-1246.

Kalogeraki, V. S. and Winans, S. C. (1995) The octopine-type Ti plasmid pTiA6 of *Agrobacterium tumefaciens* contains a gene homologous to the chromosomal virulence gene *acvB*. *J Bacteriol* **177**: 892-897.

Kämpfer, P., Rossello-Mora, R., Falsen, E., Busse, H. J. and Tindall, B. J. (2006) *Cohnella thermotolerans* gen. nov., sp. nov., and classification of '*Paenibacillus hongkongensis*' as *Cohnella hongkongensis* sp. nov. *Int J Syst Ecol Microbiol* **56**: 781-786.

Kang, H. W., Wirawan, I. G. and Kojima, M. (1994) Cellular localization and functional analysis of the protein encoded by the chromosomal virulence gene (*acvB*) of *Agrobacterium tumefaciens*. *Biosci Biotechnol Biochem* **58**: 2024-2032.

Ke, D., Zhan, C., Li, X., Li, A. D. Q. and Yao, J. (2009) The urea-dipeptides show stronger H-bonding propensity to nucleate β-sheetlike assembly than natural sequence. *Tetrahedron* **65**: 8269-8276.

Kingston, W. (2000) Antibiotics, invention and innovation. *Research Policy* **29**: 679-710.

Klein, S., Lorenzo, C., Hoffmann, S., Walther, J. M., Storbeck, S., Piekarski, T., Tindall, B. J., Wray, V., Nimtz, M. and Moser, J. (2009) Adaptation of *Pseudomonas aeruginosa* to various conditions includes tRNA-dependent formation of alanyl-phosphatidylglycerol. *Mol Microbiol* **71**: 551-565.

Koehler, T. M. (2009) *Bacillus anthracis* physiology and genetics. *Mol Aspects Med* **30**: 386-396.

Koga, Y. (2010) The Biosynthesis and Evolution of Archaeal Membranes and Ether Phospholipids. In: Handbook of Hydrocarbon and Lipid Microbiology. K. Timmis (ed). Springer Berlin Heidelberg, pp. 451-458.

Koga, Y. (2011) Early evolution of membrane lipids: how did the lipid divide occur? *J Mol Evol* **72**: 274-282.

Komatsuzawa, H., Ohta, K., Fujiwara, T., Choi, G. H., Labischinski, H. and Sugai, M. (2001) Cloning and sequencing of the gene, fmtC, which affects oxacillin resistance in methicillin-resistant Staphylococcus aureus. *FEMS Microbiol Lett* **203**: 49-54.

Koo, S. P., Bayer, A. S. and Yeaman, M. R. (2001) Diversity in antistaphylococcal mechanisms among membrane-targeting antimicrobial peptides. *Infect Immun* **69**: 4916-4922.

Koprivnjak, T. and Peschel, A. (2011) Bacterial resistance mechanisms against host defense peptides. *Cell Mol Life Sci* **68**: 2243-2254.

Krogh, A., Larsson, B., von Heijne, G. and Sonnhammer, E. L. (2001) Predicting transmembrane protein topology with a hidden Markov model: application to complete genomes. *J Mol Biol* **305**: 567-580.

Kunst, F., Ogasawara, N., Moszer, I., Albertini, A. M., Alloni, G., Azevedo, V., Bertero, M. G., Bessieres, P., Bolotin, A., Borchert, S., Borriss, R., Boursier, L., Brans, A., Braun, M., Brignell, S. C., Bron, S., Brouillet, S., Bruschi, C. V., Caldwell, B., Capuano, V., Carter, N. M., Choi, S. K., Codani, J. J., Connerton, I. F., Danchin, A. and et al. (1997) The complete genome sequence of the gram-positive bacterium *Bacillus subtilis*. *Nature* **390**: 249-256.

Laemmli, U. K. (1970) Cleavage of structural proteins during the assembly of the head of bacteriophage T4. *Nature* **227**: 680-685.

Lahiri, D. K., Bye, S., Nurnberger, J. I., Jr., Hodes, M. E. and Crisp, M. (1992) A non-organic and non-enzymatic extraction method gives higher yields of genomic DNA from whole-blood samples than do nine other methods tested. *J Biochem Biophys Methods* **25**: 193-205.

Lakowicz, J. R. (2006) Principles of Fluorescence Spectroscopy. Springer, Baltimore, Maryland, USA.

Lanini, S., D'Arezzo, S., Puro, V., Martini, L., Imperi, F., Piselli, P., Montanaro, M., Paoletti, S., Visca, P. and Ippolito, G. (2011) Molecular epidemiology of a *Pseudomonas aeruginosa* hospital outbreak driven by a contaminated disinfectant-soap dispenser. *PLoS One* **6**: e17064.

Larkin, M. A., Blackshields, G., Brown, N. P., Chenna, R., McGettigan, P. A., McWilliam, H., Valentin, F., Wallace, I. M., Wilm, A., Lopez, R., Thompson, J. D., Gibson, T. J. and Higgins, D. G. (2007) Clustal W and Clustal X version 2.0. *Bioinformatics* **23**: 2947-2948.

Lederberg, J. (2000) Infectious history. *Science* **288**: 287-293.

Lee, D. G., Urbach, J. M., Wu, G., Liberati, N. T., Feinbaum, R. L., Miyata, S., Diggins, L. T., He, J., Saucier, M., Deziel, E., Friedman, L., Li, L., Grills, G., Montgomery, K., Kucherlapati, R., Rahme, L. G. and Ausubel, F. M. (2006) Genomic analysis reveals that *Pseudomonas aeruginosa* virulence is combinatorial. *Genome Biol* **7**: R90.

Lennarz, W. J., Nesbitt, J. A., III. and Reiss, J. (1966) The participation of sRNA in the enzymatic synthesis of *O*-L-lysyl phosphatidylgylcerol in *Staphylococcus aureus*. *Proc Natl Acad Sci U S A* **55**: 934-941.

Letunic, I. and Bork, P. (2007) Interactive Tree Of Life (iTOL): an online tool for phylogenetic tree display and annotation. *Bioinformatics* **23**: 127-128.

Lewenza, S., Gardy, J. L., Brinkman, F. S. and Hancock, R. E. (2005) Genome-wide identification of *Pseudomonas aeruginosa* exported proteins using a consensus computational strategy combined with a laboratory-based PhoA fusion screen. *Genome Res* **15**: 321-329.

Lim, L. M., Ly, N., Anderson, D., Yang, J. C., Macander, L., Jarkowski, A., III., Forrest, A., Bulitta, J. B. and Tsuji, B. T. (2010) Resurgence of colistin: a review of resistance, toxicity, pharmacodynamics, and dosing. *Pharmacotherapy* **30**: 1279-1291.

Lorenzo, C. (2006) Funktionsanalyse des potentiellen *mprF*-Gens Orf PA0920 aus *Pseudomonas aeruginosa*. Diploma thesis. Technische Universität Braunschweig, Braunschweig, Germany.

Ma, J., Campbell, A. and Karlin, S. (2002) Correlations between Shine-Dalgarno sequences and gene features such as predicted expression levels and operon structures. *J Bacteriol* **184**: 5733-5745.

MacFarlane, M. G. (1962) Characterization of lipoamino-acids as *O*-amino-acid esters of phosphatidyl-glycerol. *Nature* **196**: 136-138.

Madigan, M. T. and Martinko, J. M. (2009) Brock Mikrobiologie. Pearson Education, Munich, Germany.

Maeder, D. L., Anderson, I., Brettin, T. S., Bruce, D. C., Gilna, P., Han, C. S., Lapidus, A., Metcalf, W. W., Saunders, E., Tapia, R. and Sowers, K. R. (2006) The *Methanosarcina barkeri* genome: comparative analysis with *Methanosarcina acetivorans* and *Methanosarcina mazei* reveals extensive rearrangement within methanosarcinal genomes. *J Bacteriol* **188**: 7922-7931.

Magnowska, Z. (2010) Membranes Provide New Insight into the Pathogenicity of *Pseudomonas aeruginosa* in Cystic Fibrosis. PhD thesis. Helmholtz Centre for Infection Research, Braunschweig, Germany.

Maloney, E., Lun, S., Stankowska, D., Guo, H., Rajagoapalan, M., Bishai, W. R. and Madiraju, M. V. (2011) Alterations in phospholipid catabolism in *Mycobacterium tuberculosis lysX* mutant. *Front Microbiol* **2**: 19.

Maloney, E., Stankowska, D., Zhang, J., Fol, M., Cheng, Q. J., Lun, S., Bishai, W. R., Rajagopalan, M., Chatterjee, D. and Madiraju, M. V. (2009) The two-domain LysX protein of *Mycobacterium tuberculosis* is required for production of lysinylated phosphatidylglycerol and resistance to cationic antimicrobial peptides. *PLoS Pathog* **5**: e1000534.

Manring, M. M., Hawk, A., Calhoun, J. H. and Andersen, R. C. (2009) Treatment of war wounds: a historical review. *Clin Orthop Relat Res* **467**: 2168-2191.

Mao, F., Dam, P., Chou, J., Olman, V. and Xu, Y. (2009) DOOR: a database for prokaryotic operons. *Nucleic Acids Res* **37**: D459-463.

Martinez, M. A., Schujman, G. E., Gramajo, H. C. and de Mendoza, D. (2010) Regulation of Membrane Lipid Homeostasis in Bacteria. In: Handbook of Hydrocarbon and Lipid Microbiology. K. Timmis (ed). Springer Berlin Heidelberg, pp. 509-517.

Matsumoto, K., Kusaka, J., Nishibori, A. and Hara, H. (2006) Lipid domains in bacterial membranes. *Mol Microbiol* **61**: 1110-1117.

Max, J. J., Meddeb-Mouelhi, F., Beauregard, M. and Chapados, C. (2012) Multi-wavelength dye concentration determination for enzymatic assays: evaluation of chromogenic *para*-nitrophenol over a wide pH range. *Appl Spectrosc* **66**: 1433-1441.

McDonald, J. H. (2009) Handbook of Biological statistics. SPARKY HOUSE PUBLISHING, Baltimore, Maryland, USA.

Miller, J. M. (1992) A short course in bacterial genetics. A Laboratory Manual and Handbook for *Escherichia coli* and related bacteria. Cold Spring Harbor Laboratory, Cold Spring Harbor, NY.

Minnikin, D. E. and Abdolrahimzadeh, H. (1974) Effect of pH on the proportions of polar lipids, in chemostat cultures of *Bacillus subtilis*. *J Bacteriol* **120**: 999-1003.

Mishra, N. N., Bayer, A. S., Tran, T. T., Shamoo, Y., Mileykovskaya, E., Dowhan, W., Guan, Z. and Arias, C. A. (2012a) Daptomycin resistance in enterococci is associated with distinct alterations of cell membrane phospholipid content. *PLoS One* **7**: e43958.

Mishra, N. N., Rubio, A., Nast, C. C. and Bayer, A. S. (2012b) Differential Adaptations of Methicillin-Resistant *Staphylococcus aureus* to Serial *In Vitro* Passage in Daptomycin: Evolution of Daptomycin Resistance and Role of Membrane Carotenoid Content and Fluidity. *Int J Microbiol* **2012**: 683450.

Mishra, N. N., Yang, S. J., Sawa, A., Rubio, A., Nast, C. C., Yeaman, M. R. and Bayer, A. S. (2009) Analysis of cell membrane characteristics of *in vitro*-selected daptomycin-resistant strains of methicillin-resistant *Staphylococcus aureus*. *Antimicrob Agents Chemother* **53**: 2312-2318.

Mogi, T. and Kita, K. (2009) Gramicidin S and polymyxins: the revival of cationic cyclic peptide antibiotics. *Cell Mol Life Sci* **66**: 3821-3826.

Muraih, J. K., Pearson, A., Silverman, J. and Palmer, M. (2011) Oligomerization of daptomycin on membranes. *Biochim Biophys Acta* **1808**: 1154-1160.

Natale, P., Bruser, T. and Driessen, A. J. (2008) Sec- and Tat-mediated protein secretion across the bacterial cytoplasmic membrane-distinct translocases and mechanisms. *Biochim Biophys Acta* **1778**: 1735-1756.

Nelson, K. E., Weinel, C., Paulsen, I. T., Dodson, R. J., Hilbert, H., Martins dos Santos, V. A., Fouts, D. E., Gill, S. R., Pop, M., Holmes, M., Brinkac, L., Beanan, M., DeBoy, R. T., Daugherty, S., Kolonay, J., Madupu, R., Nelson, W., White, O., Peterson, J., Khouri, H., Hance, I., Chris Lee, P., Holtzapple, E., Scanlan, D., Tran, K., Moazzez, A., Utterback, T., Rizzo, M., Lee, K., Kosack, D., Moestl, D., Wedler, H., Lauber, J., Stjepandic, D., Hoheisel, J., Straetz, M., Heim, S., Kiewitz, C., Eisen, J. A., Timmis, K. N., Dusterhoft, A., Tummler, B. and Fraser, C. M. (2002) Complete genome sequence and comparative analysis of the metabolically versatile *Pseudomonas putida* KT2440. *Environ Microbiol* **4**: 799-808.

Nesbitt, J. A., III. and Lennarz, W. J. (1968) Participation of aminoacyl transfer ribonucleic acid in aminoacyl phosphatidylglycerol synthesis. I. Specificity of lysyl phosphatidylglycerol synthetase. *J Biol Chem* **243**: 3088-3095.

Nestorovich, E. M., Danelon, C., Winterhalter, M. and Bezrukov, S. M. (2002) Designed to penetrate: time-resolved interaction of single antibiotic molecules with bacterial pores. *Proc Natl Acad Sci U S A* **99**: 9789-9794.

Nishi, H., Komatsuzawa, H., Fujiwara, T., McCallum, N. and Sugai, M. (2004) Reduced content of lysyl-phosphatidylglycerol in the cytoplasmic membrane affects susceptibility to moenomycin, as well as vancomycin, gentamicin, and antimicrobial peptides, in *Staphylococcus aureus*. *Antimicrob Agents Chemother* **48**: 4800-4807.

Oberhardt, M. A., Puchalka, J., Fryer, K. E., Martins dos Santos, V. A. and Papin, J. A. (2008) Genome-scale metabolic network analysis of the opportunistic pathogen *Pseudomonas aeruginosa* PAO1. *J Bacteriol* **190**: 2790-2803.

op den Kamp, J. A., Redai, I. and van Deenen, L. L. M. (1969) Phospholipid composition of *Bacillus subtilis*. *J Bacteriol* **99**: 298-303.

Pan, S. Q., Jin, S., Boulton, M. I., Hawes, M., Gordon, M. P. and Nester, E. W. (1995) An *Agrobacterium* virulence factor encoded by a Ti plasmid gene or a chromosomal gene is required for T-DNA transfer into plants. *Mol Microbiol* **17**: 259-269.

Pantoja, M., Chen, L., Chen, Y. and Nester, E. W. (2002) *Agrobacterium* type IV secretion is a two-step process in which export substrates associate with the virulence protein VirJ in the periplasm. *Mol Microbiol* **45**: 1325-1335.

Peschel, A., Jack, R. W., Otto, M., Collins, L. V., Staubitz, P., Nicholson, G., Kalbacher, H., Nieuwenhuizen, W. F., Jung, G., Tarkowski, A., van Kessel, K. P. and van Strijp, J. A. (2001) *Staphylococcus aureus* resistance to human defensins and evasion of neutrophil killing *via* the novel virulence factor MprF is based on modification of membrane lipids with L-lysine. *J Exp Med* **193**: 1067-1076.

Peschel, A. and Sahl, H. G. (2006) The co-evolution of host cationic antimicrobial peptides and microbial resistance. *Nat Rev Microbiol* **4**: 529-536.

Petersen, T. N., Brunak, S., von Heijne, G. and Nielsen, H. (2011) SignalP 4.0: discriminating signal peptides from transmembrane regions. *Nat Methods* **8**: 785-786.

Phillips, R. W., Wiegel, J., Berry, C. J., Fliermans, C., Peacock, A. D., White, D. C. and Shimkets, L. J. (2002) *Kineococcus radiotolerans* sp. nov., a radiation-resistant, gram-positive bacterium. *Int J Syst Ecol Microbiol* **52**: 933-938.

Pogliano, J., Pogliano, N. and Silverman, J. A. (2012) Daptomycin-mediated reorganization of membrane architecture causes mislocalization of essential cell division proteins. *J Bacteriol* **194**: 4494-4504.

Qiu, T., Li, H. and Cao, Y. (2010) Pre-staining thin layer chromatography method for amino acid detection. *Afr. J. Biotechnol.* **9**: 8679-8681.

Quan, S., Hiniker, A., Collet, J. F. and Bardwell, J. C. (2013) Isolation of bacteria envelope proteins. *Methods Mol Biol* **966**: 359-366.

Ramrakhiani, L. and Chand, S. (2011) Recent progress on phospholipases: different sources, assay methods, industrial potential and pathogenicity. *Appl Biochem Biotechnol* **164**: 991-1022.

Raza, W., Xang, W. and Shen, Q.-R. (2008) *Paenibacillus polymyxa*: antibiotics, hydrolytic enzymes and hazard assessment. *J Plant Pathol* **90**: 419-430.

Reasoner, D. J. and Geldreich, E. E. (1985) A new medium for the enumeration and subculture of bacteria from potable water. *Appl Environ Microbiol* **49**: 1-7.

Rossetti, F. F., Reviakine, I., Csucs, G., Assi, F., Voros, J. and Textor, M. (2004) Interaction of poly(L-lysine)-g-poly(ethylene glycol) with supported phospholipid bilayers. *Biophys J* **87**: 1711-1721.

Roy, H. (2009) Tuning the properties of the bacterial membrane with aminoacylated phosphatidylglycerol. *IUBMB Life* **61**: 940-953.

Roy, H., Dare, K. and Ibba, M. (2009) Adaptation of the bacterial membrane to changing environments using aminoacylated phospholipids. *Mol Microbiol* **71**: 547-550.

Roy, H. and Ibba, M. (2008a) Monitoring Lys-tRNA^{Lys} phosphatidylglycerol transferase activity. *Methods* **44**: 164-169.

Roy, H. and Ibba, M. (2008b) RNA-dependent lipid remodeling by bacterial multiple peptide resistance factors. *Proc Natl Acad Sci U S A* **105**: 4667-4672.

Roy, H. and Ibba, M. (2009) Broad range amino acid specificity of RNA-dependent lipid remodeling by multiple peptide resistance factors. *J Biol Chem* **284**: 29677-29683.

Rubio, A., Conrad, M., Haselbeck, R. J., G, C. K., Brown-Driver, V., Finn, J. and Silverman, J. A. (2011) Regulation of *mprF* by antisense RNA restores daptomycin susceptibility to daptomycin-resistant isolates of *Staphylococcus aureus*. *Antimicrob Agents Chemother* **55**: 364-367.

Sacre, M. M., El Mashak, E. M. and Tocanne, J. F. (1977) A monolayer (π,ΔV) study of the ionic properties of alanylphosphatidylglycerol: effects of pH and ions. *Chem Phys Lipids* **20**: 305-318.

Samant, S., Hsu, F. F., Neyfakh, A. A. and Lee, H. (2009) The *Bacillus anthracis* protein MprF is required for synthesis of lysylphosphatidylglycerols and for resistance to cationic antimicrobial peptides. *J Bacteriol* **191**: 1311-1319.

Sambrook, J. and Russell, D. W. (2001) Molecular cloning: a laboratory manual. Cold Spring Harbor Laboratory Press, Cold Spring Harbor.

Sanger, F., Nicklen, S. and Coulson, A. R. (1977) DNA sequencing with chain-terminating inhibitors. *Proc Natl Acad Sci U S A* **74**: 5463-5467.

Schmid, F.-X. (2001) Biological Macromolecules: UV-visible Spectrophotometry. Macmillan Publishers Ltd, Nature Publishing Group.

Schmidt, T. G. and Skerra, A. (2007) The *Strep*-tag system for one-step purification and high-affinity detection or capturing of proteins. *Nat Protoc* **2**: 1528-1535.

Schmiel, D. H. and Miller, V. L. (1999) Bacterial phospholipases and pathogenesis. *Microbes Infect* **1**: 1103-1112.

Schnabel, E. (1964) Eine weitere Synthese der Insulinsequenz B 21–30. *Liebigs Ann. Chem.* **674**: 218-225.

Schneider, T. D. and Stephens, R. M. (1990) Sequence logos: a new way to display consensus sequences. *Nucleic Acids Res* **18**: 6097-6100.

Schobert, M. and Jahn, D. (2010) Anaerobic physiology of *Pseudomonas aeruginosa* in the cystic fibrosis lung. *Int J Med Microbiol* **300**: 549-556.

Schreiber, K., Boes, N., Eschbach, M., Jaensch, L., Wehland, J., Bjarnsholt, T., Givskov, M., Hentzer, M. and Schobert, M. (2006) Anaerobic survival of *Pseudomonas aeruginosa* by pyruvate fermentation requires an Usp-type stress protein. *J Bacteriol* **188**: 659-668.

Schweizer, H. P., Klassen, T. and Hoang, T. (1996) Improved Methods for Gene Analysis and Expression in *Pseudomonas* spp. In: Molecular Biology of *Pseudomonads.* T. Nakazawa, K. Furukawa, D. Haas & S. Silver (eds). Washington DC: ASM Press, pp. 229-237.

Shaw, E. and Springhorn, S. (1967) Identification of the histidine residue at the active center of trypsin labelled by TLCK. *Biochem Biophys Res Commun* **27**: 391-397.

Sievers, S., Ernst, C. M., Geiger, T., Hecker, M., Wolz, C., Becher, D. and Peschel, A. (2010) Changing the phospholipid composition of Staphylococcus aureus causes distinct changes in membrane proteome and membrane-sensory regulators. *Proteomics* **10**: 1685-1693.

Sigrist, C. J., de Castro, E., Cerutti, L., Cuche, B. A., Hulo, N., Bridge, A., Bougueleret, L. and Xenarios, I. (2013) New and continuing developments at PROSITE. *Nucleic Acids Res* **41**: D344-347.

Simmen, H. P., Battaglia, H., Giovanoli, P. and Blaser, J. (1994) Analysis of pH, pO2 and pCO2 in drainage fluid allows for rapid detection of infectious complications during the follow-up period after abdominal surgery. *Infection* **22**: 386-389.

Slavetinsky, C. J., Peschel, A. and Ernst, C. M. (2012) Alanyl-Phosphatidylglycerol and Lysyl-Phosphatidylglycerol Are Translocated by the Same MprF Flippases and Have Similar Capacities To Protect against the Antibiotic Daptomycin in *Staphylococcus aureus*. *Antimicrob Agents Chemother* **56**: 3492-3497.

Sohlenkamp, C., Galindo-Lagunas, K. A., Guan, Z., Vinuesa, P., Robinson, S., Thomas-Oates, J., Raetz, C. R. and Geiger, O. (2007) The lipid lysyl-phosphatidylglycerol is present in membranes of *Rhizobium tropici* CIAT899 and confers increased resistance to polymyxin B under acidic growth conditions. *Mol Plant Microbe Interact* **20**: 1421-1430.

Spier, S. (2007) Charakterisierung der Aminoacyl-Phosphatidylglycerol-Synthase Lmo1695 aus *Listeria monocytogenes*. Diploma thesis. Technische Universität Braunschweig, Braunschweig, Germany.

Staubitz, P., Neumann, H., Schneider, T., Wiedemann, I. and Peschel, A. (2004) MprF-mediated biosynthesis of lysylphosphatidylglycerol, an important determinant in staphylococcal defensin resistance. *FEMS Microbiol Lett* **231**: 67-71.

Stover, C. K., Pham, X. Q., Erwin, A. L., Mizoguchi, S. D., Warrener, P., Hickey, M. J., Brinkman, F. S., Hufnagle, W. O., Kowalik, D. J., Lagrou, M., Garber, R. L., Goltry, L., Tolentino, E., Westbrock-Wadman, S., Yuan, Y., Brody, L. L., Coulter, S. N., Folger, K. R., Kas, A., Larbig, K., Lim, R., Smith, K., Spencer, D., Wong, G. K., Wu, Z., Paulsen, I. T., Reizer, J., Saier, M. H., Hancock, R. E., Lory, S. and Olson, M. V. (2000) Complete genome sequence of *Pseudomonas aeruginosa* PAO1, an opportunistic pathogen. *Nature* **406**: 959-964.

Strateva, T. and Yordanov, D. (2009) *Pseudomonas aeruginosa* - a phenomenon of bacterial resistance. *J Med Microbiol* **58**: 1133-1148.

Strugatsky, D., McNulty, R., Munson, K., Chen, C. K., Soltis, S. M., Sachs, G. and Luecke, H. (2013) Structure of the proton-gated urea channel from the gastric pathogen *Helicobacter pylori*. *Nature* **493**: 255-258.

Studier, F. W., Rosenberg, A. H., Dunn, J. J. and Dubendorff, J. W. (1990) Use of T7 RNA polymerase to direct expression of cloned genes. *Methods Enzymol* **185**: 60-89.

Taylor, J. R. (1997) An introduction to error analysis: the study of uncertainties in physical measurements. University Science Books, Sausalito, USA.

Thedieck, K., Hain, T., Mohamed, W., Tindall, B. J., Nimtz, M., Chakraborty, T., Wehland, J. and Jänsch, L. (2006) The MprF protein is required for lysinylation of phospholipids in listerial membranes and confers resistance to cationic antimicrobial peptides (CAMPs) on *Listeria monocytogenes*. *Mol Microbiol* **62**: 1325-1339.

Thoma, S. and Schobert, M. (2009) An improved *Escherichia coli* donor strain for diparental mating. *FEMS Microbiol Lett* **294**: 127-132.

Tindall, B. J. (1990) Lipid composition of *Halobacterium lacusprofundi*. *FEMS Microbiol Lett* **66**: 199-202.

Tocanne, J. F., Verheij, H. M., op den Kamp, J. A. F. and Van Deenen, L. L. M. (1974a) Chemical and physicochemical studies of lysylphosphatidylglycerol derivatives. Occurrence of A2' → 3' lysyl migration. *Chem Phys Lipids* **13**: 389-403.

Tocanne, J. F., Ververgaert, P. H. J. T., Verkleij, A. J. and van Deenen, L. L. M. (1974b) A monolayer and freeze-etching study of charged phospholipids I. Effects of ions and pH on the ionic properties of phosphatidylglycerol and lysylphosphatidylglycerol. *Chem Phys Lipids* **12**: 201-219.

Tocanne, J. F., Ververgaert, P. H. J. T., Verkleij, A. J. and van Deenen, L. L. M. (1974c) A monolayer and freeze-etching study of charged phospholipids. II. Ionic properties of mixtures of phosphatidylglycerol and lysylphosphatidylglycerol. *Chem Phys Lipids* **12**: 220-231.

Truong, J., Levkovich, B. J. and Padiglione, A. A. (2012) Simple approach to improving vancomycin dosing in intensive care: a standardised loading dose results in earlier therapeutic levels. *Intern Med J* **42**: 23-29.

Uchiyama, I., Higuchi, T. and Kawai, M. (2010) MBGD update 2010: toward a comprehensive resource for exploring microbial genome diversity. *Nucleic Acids Res* **38**: D361-365.

Uhlig, C. M. (2011) Säureinduzierte Lipidmodifikation in unterschiedlichen Mikroorganismen. Bachelor thesis. Technische Universität Braunschweig, Braunschweig, Germany.

van Delden, C. and Iglewski, B. H. (1998) Cell-to-cell signaling and *Pseudomonas aeruginosa* infections. *Emerg Infect Dis* **4**: 551-560.

Veith, B., Herzberg, C., Steckel, S., Feesche, J., Maurer, K. H., Ehrenreich, P., Baumer, S., Henne, A., Liesegang, H., Merkl, R., Ehrenreich, A. and Gottschalk, G. (2004) The complete genome sequence of *Bacillus licheniformis* DSM13, an organism with great industrial potential. *J Mol Microbiol Biotechnol* **7**: 204-211.

Vidal, S., Bredin, J., Pages, J. M. and Barbe, J. (2005) Beta-lactam screening by specific residues of the OmpF eyelet. *J Med Chem* **48**: 1395-1400.

Vinuesa, P., Neumann-Silkow, F., Pacios-Bras, C., Spaink, H. P., Martinez-Romero, E. and Werner, D. (2003) Genetic analysis of a pH-regulated operon from *Rhizobium tropici* CIAT899 involved in acid tolerance and nodulation competitiveness. *Mol Plant Microbe Interact* **16**: 159-168.

von Heijne, G. (2006) Membrane-protein topology. *Nat Rev Mol Cell Biol* **7**: 909-918.

Waldron, K. J., Rutherford, J. C., Ford, D. and Robinson, N. J. (2009) Metalloproteins and metal sensing. *Nature* **460**: 823-830.

Wenzel, M. and Bandow, J. E. (2011) Proteomic signatures in antibiotic research. *Proteomics* **11**: 3256-3268.

Wilson, M. E. (1995) Infectious diseases: an ecological perspective. *Bmj* **311**: 1681-1684.

Wirawan, I. G., Kang, H. W. and Kojima, M. (1993) Isolation and characterization of a new chromosomal virulence gene of *Agrobacterium tumefaciens*. *J Bacteriol* **175**: 3208-3212.

Wood, L. F. and Ohman, D. E. (2012) Identification of genes in the σ^{22} regulon of *Pseudomonas aeruginosa* required for cell envelope homeostasis in either the planktonic or the sessile mode of growth. *MBio* **3**: e00094-00012.

Yamaguchi, A., Hiruma, R. and Sawai, T. (1982) Phospholipid bilayer permeability of beta-lactam antibiotics. *J Antibiot (Tokyo)* **35**: 1692-1699.

Yang, S. J., Bayer, A. S., Mishra, N. N., Meehl, M., Ledala, N., Yeaman, M. R., Xiong, Y. Q. and Cheung, A. L. (2012) The *Staphylococcus aureus* two-component regulatory system, GraRS, senses and confers resistance to selected cationic antimicrobial peptides. *Infect Immun* **80**: 74-81.

Yoshimura, F. and Nikaido, H. (1985) Diffusion of beta-lactam antibiotics through the porin channels of *Escherichia coli* K-12. *Antimicrob Agents Chemother* **27**: 84-92.

Yousef, A. E. and Carlstrom, C. (2003) Food microbiology: a laboratory manual. John Wiley & Sons, Hoboken, New Jersey.

Zasloff, M. (2002) Antimicrobial peptides of multicellular organisms. *Nature* **415**: 389-395.

Zhang, L., Dhillon, P., Yan, H., Farmer, S. and Hancock, R. E. (2000) Interactions of bacterial cationic peptide antibiotics with outer and cytoplasmic membranes of *Pseudomonas aeruginosa*. *Antimicrob Agents Chemother* **44**: 3317-3321.

Zhang, Y. M. and Rock, C. O. (2008) Membrane lipid homeostasis in bacteria. *Nat Rev Microbiol* **6**: 222-233.

8 Appendix

8.1 *P. polymyxa* aaPGS encoding nucleotide sequence

The aaPGS encoding gene of *P. polymyxa* ATCC 842 was amplified using random primers since the genome sequence of this specific strain was not available (compare section 2.4.15). The elucidated nucleotide sequence is presented in Figure 32.

```
ATGAATTCAA ATCACAAACC GATCCAATCC TTTAAAATCG TACAGTACAT CATGACCATC TATAGGCAGC   70
GATTAACGCG TATTTTGCTA CCGCTGGCTG TACTGGCTTT TATTATATGG GAGGCTGGAC GAGAGCTAAA  140
AGACTTTAAT CTGGCACGGA TGCTTCATGA GCTGCGGCGA ATGGATGCCA CGTTTCTCAT CGAAATTGGC  210
TTGTTCTCAC TGGTAGCCGT AGCTGCTATG AGTGCTTACG ATTATGTAAT CAGGCATCAT TTCAAGCTTC  280
AGGTTATGCC TGGAACGACA TTCCGGTACG CCTGGATCTC CAATACCTTC AATAATGTCT TCGGCTTCGC  350
CGGCTTTACA GGAGCTGGAC TGCGCACTGT GCTGTATAAA AAGAGCGGTG TGCCATTGGG TGTCATTACC  420
TCGGCAGTCG TATTTCTTTC GCCTGTCGTC ATTACCGGAC TATCTTTGCT AGCTTGGGGT GCTATTGTCC  490
ATCTGTATCC GGTGCAGCCT GTGCTGGATG CTCACCCATG GCTTCATTGG GCGCTATGGG GAATGGCACT  560
TTACCTGCCT CTATTTCTGA TCATGCAGCG CTCCAAAAGG TATGCCACAT GGTTCAACAA GGGAGAAGGA  630
CAGCTCTCCT GGTTCACCAT CTCTGCCTCC ATTGGCGCCT CTCTGCTGGA ATGGCTGCTG GCTGGTCTTA  700
CCTTTGCATG GATCGGCTCG CACTTGCTCC ATGAGCTGCC GCTCCATGCT GTGTTCGGTA TTTATGTAAT  770
AGCCGCAATT GCGGGGTTAA TCAGTCTTGC ACCCGGAGGC GTCGGCGCAT TCGATATTAT CGCCCTGCTC  840
GGGCTGCAAA TGGCAGGAGC CAACTCGGAC CGGGCGCTGG CTGTGCTGCT GGTCTTTCGC GTCTTTTATT  910
ACATCATTCC GTGGCTCATC GGCTTGGTAT TAGCGGCGCT GGAAATGATT CCGCGTAATG AGCGCTTGAG  980
CCAGCTCGCT GAGACAGGCT GGGATTACTC CCTTAATGCC TGGCAGAAGG TATGGGGCTG GCCTGGTCAA 1050
TTCCGGTTTT TGGCCGATCT GGGGGTATGG GCACTTGGGA AACTGGTACT CATCTCCGGC GTGGTGCTTC 1120
TGTTGTCGGC CGCTACGCCT GGTCTGTTGT ATCGGCTCCG TTTTGCTGAA CATTTGCTCA GCCTGCCCGT 1190
TATGCGCTTA TCGCACGAAA TCTCGGTCAT CATCGGAATT ATGCTTGTCG TTCTGTCCCA CGGAATCTCT 1260
CTGCGTATTC GCAGAGCATT GCGGCTGACC TTGATACTGC TGCTGACAGG AGCCATTTTC ACCTTCACTA 1330
AAGGTCTGGA TTTTGAAGAA GCCTTTTTCC TGCTGTTCGT GGCATTAATG CTGTGGATTT CGCGTTCACG 1400
GTTTTATCGG GTCAGTGCGC CGCTGAATCG GCACAACATT TTAATATGGG GCGGATTATC TCTACTCGTA 1470
ACTGGTGCTT ATTTTATAAT CGGGGCAGGC TCCAATACTC CATTTATGCG TCATTTGCAT GCCAAGGTCC 1540
ACCTGGACTT TTTTATGAAC CGCAGCGATT ACGGAGTTAC AGCCGTATTT AGTTTGATTT TGGCATGGGT 1610
ATTCTTGACG GTGTATTTCT TTCTTCGTCC TCAACGTAGC ATCAGCAATC TACCCGACGC ACAGGAACTG 1680
GTTAAGCTAA AAGAATTTTT GGAACGACAG GGTGGTAATC TCGTTTCTCA TATGCTTTTT CTCGGCGATA 1750
AATATCTGTA TTGGACCAAG GACGAACAGG TAGTTCTCCC CTATGCTCGC AGTCGGGACA AACTGATTGT 1820
ATTAGGTGAC CCCCTCGGTC CAAAGGAACG TGTGAGTGAA GCCATTCAGG AATTCCAACG GTTCGCGGAT 1890
CGCTATGCTT TGACGGCTGT ATTTTATCAA GCATCACCGG AATATTTGTC CATCTATCAC GAGAACGGCT 1960
ATCGCTTTTT TAAGTTGGGC GAGGAAGCGC TCGTGCCGCT GGAGTCCTTT ACACTAACGG GCAAAAGCAA 2030
TCAGGCGCTG CGAAGCGCCA AAAATCGCTT TGGCCGCGAA GGCTATTCAT TCGAAATGAT CCAGCCTCCT 2100
CTAGAGGCGT CATTGATTGA GGAGATGCGT CATATTTCGG ATATTTGGCT GGACGGGCGC AAGGAGAAGG 2170
GATATTCACT CGGCTGGTTC AAGGAATCTT ACCTTCAGTT GGCTCCAATT GCATTGCTGA AAGACTCTGA 2240
AGGTAAGGTT ATTGCTTTCG CCACGATGGC CCCTGCCTAT GATCATGGGC AGACGGTCTC TATCGATCTG 2310
ATGCGTCACC TGCCTGACAC ACCCAATGGA ACGATGGATT ACTTATTCAC ACGGGTCATC GAGTGGGCCA 2380
AGGAGAGTGG ATATACGACA TTTAATCTGG GCATGGCACC GCTGTCCCAG GTAGGACAAA GCGAAAAGGC 2450
ACTGCGCGAG GAAAAGCTGG CTCGACTCGT TTTTCAATAC GGGGGACATT TTTACGGCTT CCAGGGGCTC 2520
CGACGCTTCA AGGATAAGTT CAAGCCGCAG TGGGAGCCGC GCTATCTAGC CTATCCAGCT TCTGTTTTTC 2590
TACCGATCCT GACGCTGGAA CTGGTGTATC TCGTGTCCAA ACGCTCGGAC TAA                    2643
```

Figure 32: Nucleotide sequence of the *P. polymyxa* ATCC 842 aaPGS encoding gene
The aaPGS encoding nucleotide sequence from *P. polymyxa* ATCC 842 was amplified using random primers and the sequence was elucidated after cloning into vector pBAD-His-A (compare section 2.4.15).

8.2 Sequence identity determination of aaPGS enzymes

The C-terminal domains of aaPGS enzymes were defined based on a sequence alignment with the C-terminal domain of the A-PGS of *P. aeruginosa* (Hebecker *et al.*, 2011). Sequence identity values were calculated using the Lasergene® software package (DNASTAR, Madison, WI, USA) and are summarized in Figure 33.

	L_Mtb	L_Msm	L_Sth	L_Sa	L_Rtr	L_Lmo	L_Cpe	L_Ccre	L_Bthu	L_Bli	L_Ban	L_Atu	ALR_Efs	ALR_Efm	AL_Bsu	A_Pput	A_Ppoly	A_PA14	A_Mba	A_Kra	A_Cpe	A_Bph	A_PAO1
L_Mtb	-																						
L_Msm	79.6	-																					
L_Sth	16.9	17.2	-																				
L_Sa	19.9	19.3	31.9	-																			
L_Rtr	20.7	19.8	27.8	31.3	-																		
L_Lmo	17.7	16.9	39.8	37.2	32.0	-																	
L_Cpe	16.3	16.9	38.5	36.9	34.4	43.8	-																
L_Ccre	18.5	18.2	31.2	27.6	41.9	28.0	29.6	-															
L_Bthu	18.4	18.4	37.3	41.4	35.5	44.5	40.4	28.6	-														
L_Bli	18.9	19.8	44.2	45.2	37.6	44.6	47.0	31.4	63.6	-													
L_Ban	18.5	18.5	37.3	41.1	34.9	44.6	40.1	28.8	97.3	63.7	-												
L_Atu	21.3	19.2	27.8	30.1	66.4	28.2	32.3	41.3	34.3	36.7	33.7	-											
ALR_Efs	19.5	20.1	49.3	36.8	30.7	45.2	43.4	31.5	41.7	45.5	42.4	29.2	-										
ALR_Efm	18.6	19.1	47.7	38.3	31.3	44.7	41.5	28.1	41.2	48.8	41.3	31.6	67.8	-									
AL_Bsu	19.0	18.7	41.5	42.9	36.5	43.0	41.8	31.0	64.8	76.2	64.7	35.0	43.4	44.8	-								
A_Pput	23.8	23.2	27.9	30.9	43.0	30.1	30.4	43.0	32.1	33.8	31.8	41.8	30.0	30.0	32.8	-							
A_Ppoly	20.7	21.3	36.4	36.6	34.9	41.9	40.4	31.8	43.2	43.7	43.7	32.8	39.8	40.8	42.2	37.6	-						
A_PA14	22.6	21.7	29.7	30.9	44.8	30.4	30.7	44.5	30.9	32.0	30.3	42.7	29.7	30.3	32.5	85.3	37.0	-					
A_Mba	17.2	17.8	31.8	31.5	38.3	27.6	33.6	41.8	32.4	32.6	32.7	40.7	31.8	29.7	33.0	45.1	35.5	45.1	-				
A_Kra	22.5	21.9	26.3	32.2	41.4	30.3	30.3	39.3	35.5	35.2	36.4	41.1	31.5	30.1	35.5	40.5	36.7	39.6	41.8	-			
A_Cpe	19.1	18.2	37.7	36.6	35.4	38.3	40.4	28.4	42.4	43.7	41.9	32.1	38.3	43.2	40.4	33.5	43.9	33.2	34.3	31.2	-		
A_Bph	23.7	23.7	26.7	30.1	45.5	26.8	28.6	37.4	28.7	31.2	29.1	42.8	26.4	29.1	30.4	44.6	34.3	44.9	38.6	39.2	31.0	-	
A_PAO1	22.9	21.7	29.7	30.6	45.1	30.1	30.7	44.5	31.2	32.0	30.6	43.3	29.7	30.3	32.8	84.7	37.0	99.1	45.4	40.2	33.5	45.2	-

Figure 33: Identity analysis of C-terminal aaPGS domains

Sequence identity values were obtained by comparing the C-terminal catalytic domains from all enzymes with characterized amino acid substrate specificity (see Table 10 and Table 11) using the Lasergene® software package (DNASTAR, Madison, WI, USA). Results were grouped according to their aminoacyl-tRNA substrate specificity.

Light gray: comparison of the L-PGS group, dark gray: comparison of the A-PGS group, black: cross-comparison of L-PGS and A-PGS sequences, white: enzymes showing broadened substrate specificity. The initial character(s) of each sequence name indicates the amino acid substrate specificity of each enzyme.

PAO1: *P. aeruginosa* PAO1, Bph: *B. phymatum*, Cpe: *C. perfringens*, Kra: *K. radiotolerans*, Mba: *M. barkeri*, PA14: *P. aeruginosa* PA14, Ppoly: *P. polymyxa*, Pput: *P. putida*, Bsu: *B. subtilis*, Efm: *E. faecium*, Efs: *E. faecalis*, Atu: *A. tumefaciens*, Ban: *B. anthracis*, Bli: *B. licheniformis*, Bthu: *B. thuringiensis*, Ccre: *C. crescentus*, Lmo: *L. monocytogenes*, Rtr: *R. tropici*, Sa: *S. aureus*, Sth: *S. thermophilus*, Msm: *M. smegmatis*, Mtb: *M. tuberculosis*.

8.3 Antimicrobial compounds employed for MIC determination

The chemical structures of antimicrobial compounds used in this study for MIC determination and the P_{PA0920} promoter activity analysis are given in Figure 34.

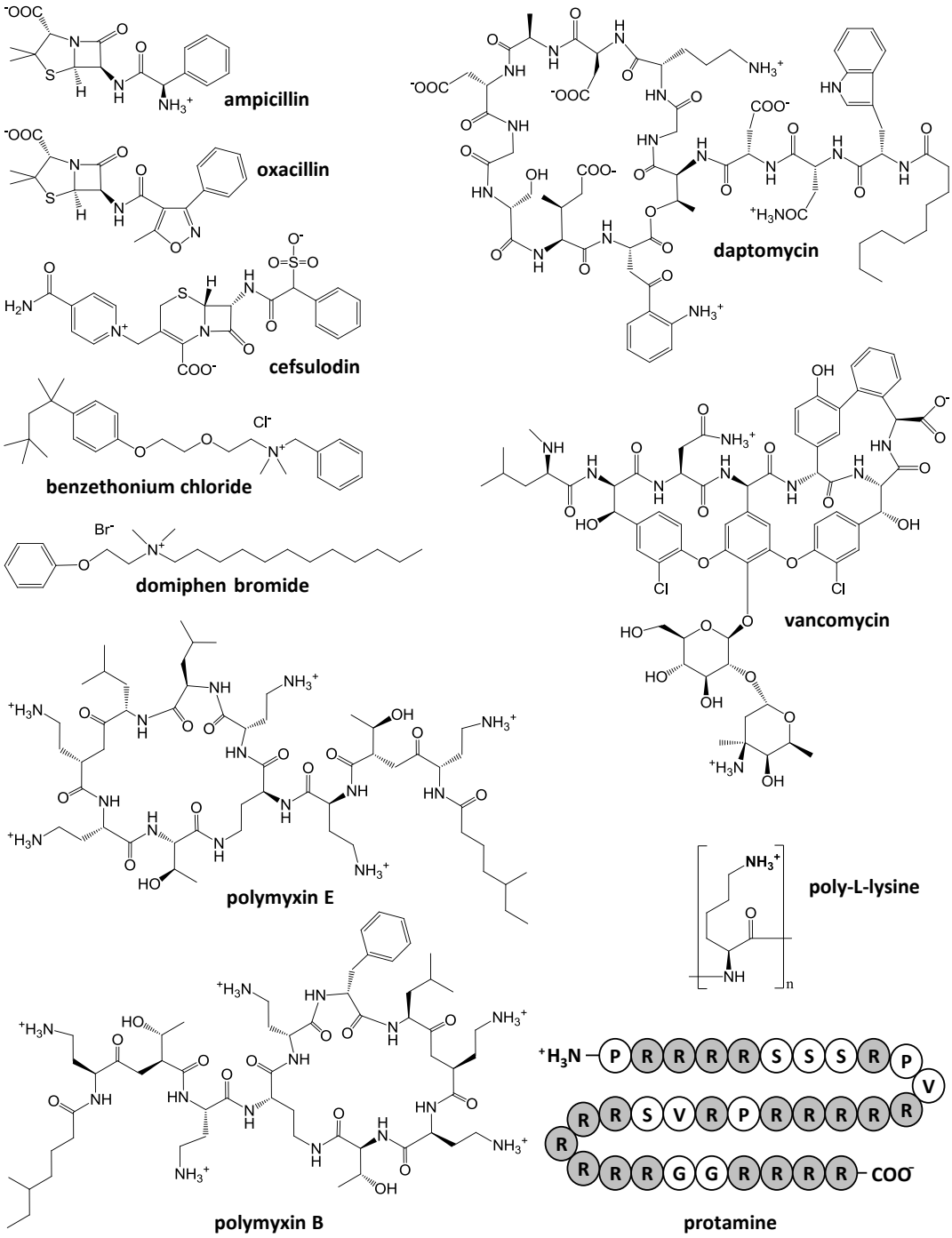

Figure 34: Chemical structures of antimicrobial compounds employed in this study
The antimicrobial peptides were used for MIC determination and P_{PA0920} promoter activity analysis. Positively charged amino acid residues of protamine are highlighted in gray.

8.4 Growth curves and lipid composition of ΔPA0919 complemented strains employed for the functional analysis of PA0919

Several strains were constructed for the analysis PA0919 *in vivo* (Δ19 P_{20}-19, Δ19 P_{19}-19, Δ19 P_{20} and Δ19 P_{19}) and cultivated under neutral conditions (pH 7.3). The corresponding growth curves and the lipid compositions of the strains are presented in Figure 35. For strain construction strategy, see section 3.5.2.

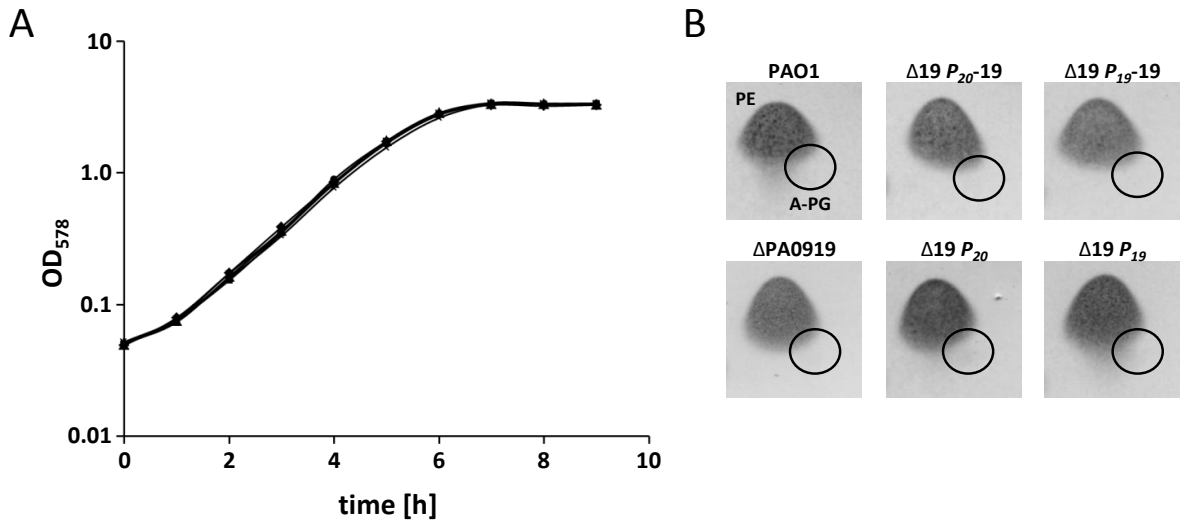

Figure 35: Growth curves (A) and lipid composition (B) of ΔPA0919 complemented strains for PA0919 function analysis

The various *P. aeruginosa* strains were cultured in AB medium pH 7.3 at 37 °C and 200 rpm (section 2.3.5). Culture turbidity was measured at 578 nm. After 24 h, polar lipids were extracted, separated by two-dimensional TLC and visualized by molybdato-phosphoric acid staining (sections 2.5.1 and 2.5.3). A-PG position is indicated by a circle.

Rhombus: PAO1 wild-type, square: PAO1 ΔPA0919, triangle: Δ19 P_{20}, cross: Δ19 P_{20}-19, star: Δ19 P_{19}, dot: Δ19 P_{19}-19.

A-PG: alanyl-phosphatidylglycerol, PE: phosphatidylethanolamine.

8.5 Sequence alignment of PA0919 homologous proteins

PA0919 homologous proteins were identified by BLAST analysis. Selected sequences were aligned using ClustalW2 (section 2.13.1). The obtained alignment is presented in Figure 36.

```
PA0919          ------------------------------------------------------------
PP_1201         ------------------------------------------------------------
Atu_AcvB        ------------------------------------------------------------
Atu_VirJ        ------------------------------------------------------------
Rtr_AtvA        ------------------------------------------------------------
Bphy_4018       ------------------------------------------------------------
Rpic_3994       MSWQAPRTQEARHRGVLRKGLRLAGHVGAVGMVLAASWAIAADAPAPTSKPTPVQGAVLV  60
XAC1368         ------------------------------------------------------------
XAC2411         ------------------------------------------------------------
Phep_2436       ------------------------------------------------------------
Phep_2437       ------------------------------------------------------------
Phep_2737       ------------------------------------------------------------
XF0754          ------------------------------------------------------------
XF2679          ------------------------------------------------------------
CJA_1309        ------------------------------------------------------------


PA0919          ------------------MSVVKRHWRR-----------FLVAALVLIVG--AALLLWSR  29
PP_1201         --------------------MTRRFLLY-----------LLVPLLLAALGGALAFWLWTR  29
Atu_AcvB        --------------------MMKRNLIG----------AFIAAST---LLSSSVAFSQDKP  28
Atu_VirJ        --------------------MAIKLVLIL----------VFTLFLA------ADAAYANDR-  25
Rtr_AtvA        --------------------MILKYAMSL----------AFACVLSTGLLMSGQARAEADDT  32
Bphy_4018       --------------------MIMQKFYR----------LAALASVSLCSLAGVAPTAHAYE  31
Rpic_3994       PPVGMTGASGVVAVPPRGDMPPRLQMSGPAVTANKAANGGVLSLPVVAPATPAAAPGAVE 120
XAC1368         --------------------MRRLEMWS-----------ALCGAAMLTLSGMAAAQA-PE  28
XAC2411         --------------------MGMGIKM----------FRWMIAILLIGGSSYAVARHLQD  30
Phep_2436       --------------------MANKNLYL-----------LIVTSLLSLSGCSLLKRERV  28
Phep_2437       ------------------------------------------------------------
Phep_2737       --MKGLMIRGLAQFMNKTLSMVKAGLTS-----------VFICLFLMLFYIKPALAIKEE  47
XF0754          ---------------------------------------MLLGG-SVAVCSHAYG  15
XF2679          --------------------MKQFKIRS-----------VLQSIALLVLAGTAAAEPKPE  29
CJA_1309        ------------------------------------------------------------


PA0919          PAAQAKLEALDLDDGGHATLAEPGEKP--------RSRVVVIAAPEQQLNDAQMLNLAHD  81
PP_1201         PAPEARLEQLSINDT-SITRVTPGVHP--------KARVAIGVPQDQALTGKQLLDLSQA  80
Atu_AcvB        AYETGMIPADHIMVPDGDIQASIFLISDANGWTEADETRAKALVEKGAAVVGIDFKEYLK  88
Atu_VirJ        --------ANGVMWSNG-----------------------------------------  34
Rtr_AtvA        KYDLGMIPAPHIMRPHGKVSNEVVLISDLAGWGDKEKAVADKLVANGSLVIGIDYPSFLA  92
Bphy_4018       TLPGGRYGNVTVTKPVADVRGFVVLFSRESGWNPADQQAADALAKNGAMVVGVDTAKYAA  91
Rpic_3994       FVTHGRFRDVPVYKPKGEIRSVVLMLSGDLGWTPAASRMAESLAQQGALVAGLSTPALFA 180
XAC1368         PVSHGRFEQVPVLMPKGEPQRVVIWLA-GAGNAATRQAQAESLRADGAMVAVVDTAHLYA  87
XAC2411         SNTAGHYGSVEVIRPEGTPKAMVILLP-DGDHPQDSQKLADMLSNDGALVAVVDTANYRE  89
Phep_2436       TRHNG------------------------------------------------------  33
Phep_2437       ------------------------------------------------------------
Phep_2737       VISHKTFGKTVIYIPQTIPTSVALFVSGDGGWQAGVINMAKNLALQGALVAGIDARQYMA 107
XF0754          DASDGRD----------------------------------------------------  22
XF2679          KITHGRFEQIPVLRPDGEPQRVVIWFS-DAGHVDQRTRQAEILRQDGAMVALVDTTHLYK  88
CJA_1309        -----------------------------------------MSQHGNLSAVLNIDNYLS  18
```

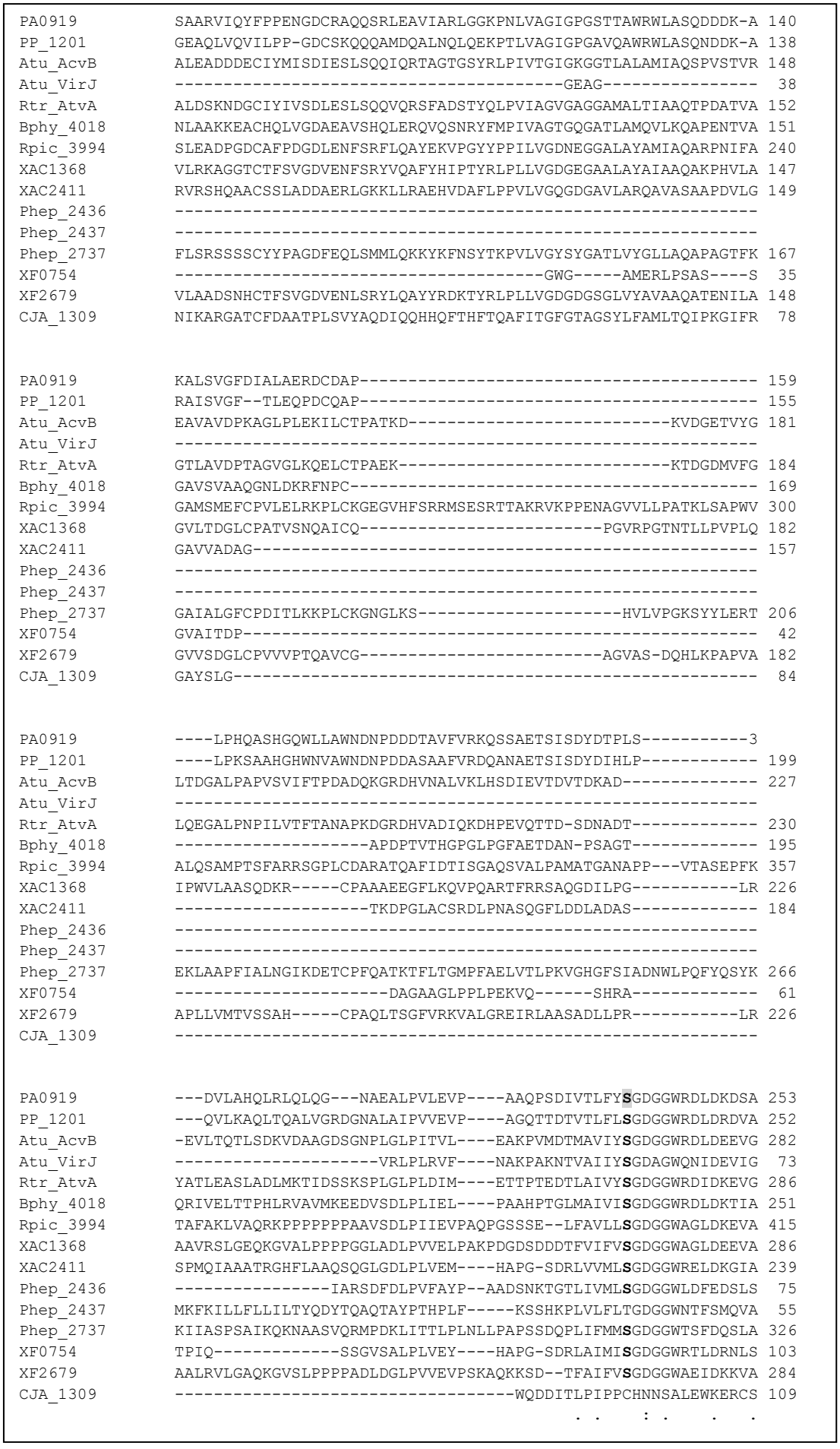
PA0919 SAARVIQYFPPENGDCRAQQSRLEAVIARLGGKPNLVAGIGPGSTTAWRWLASQDDDK-A 140
PP_1201 GEAQLVQVILPP-GDCSKQQQAMDQALNQLQEKPTLVAGIGPGAVQAWRWLASQNDDK-A 138
Atu_AcvB ALEADDDECIYMISDIESLSQQIQRTAGTGSYRLPIVTGIGKGGTLALAMIAQSPVSTVR 148
Atu_VirJ ----------GEAG---------- 38
Rtr_AtvA ALDSKNDGCIYIVSDLESLSQQVQRSFADSTYQLPVIAGVGAGGAMALTIAAQTPDATVA 152
Bphy_4018 NLAAKKEACHQLVGDAEAVSHQLERQVQSNRYFMPIVAGTGQGATLAMQVLKQAPENTVA 151
Rpic_3994 SLEADPGDCAFPDGDLENFSRFLQAYEKVPGYYPPILVGDNEGGALAYAMIAQARPNIFA 240
XAC1368 VLRKAGGTCTFSVGDVENFSRYVQAFYHIPTYRLPLLVGDGEGAALAYAIAAQAKPHVLA 147
XAC2411 RVRSHQAACSSLADDAERLGKKLLRAEHVDAFLPPVLVGQGDGAVLARQAVASAAPDVLG 149
Phep_2436 ----------
Phep_2437 ----------
Phep_2737 FLSRSSSSCYYPAGDFEQLSMMLQKKYKFNSYTKPVLVGYSYGATLVYGLLAQAPAGTFK 167
XF0754 ----------GWG-----AMERLPSAS----S 35
XF2679 VLAADSNHCTFSVGDVENLSRYLQAYYRDKTYRLPLLVGDGDGSGLVYAVAAQATENILA 148
CJA_1309 NIKARGATCFDAATPLSVYAQDIQQHHQFTHFTQAFITGFGTAGSYLFAMLTQIPKGIFR 78
PA0919 KALSVGFDIALAERDCDAP---------- 159
PP_1201 RAISVGF--TLEQPDCQAP---------- 155
Atu_AcvB EAVAVDPKAGLPLEKILCTPATKD----------KVDGETVYG 181
Atu_VirJ ----------
Rtr_AtvA GTLAVDPTAGVGLKQELCTPAEK----------KTDGDMVFG 184
Bphy_4018 GAVSVAAQGNLDKRFNPC---------- 169
Rpic_3994 GAMSMEFCPVLELRKPLCKGEGVHFSRRMSESRTTAKRVKPPENAGVVLLPATKLSAPWV 300
XAC1368 GVLTDGLCPATVSNQAICQ----------PGVRPGTNTLLPVPLQ 182
XAC2411 GAVVADAG---------- 157
Phep_2436 ----------
Phep_2437 ----------
Phep_2737 GAIALGFCPDITLKKPLCKGNGLKS----------HVLVPGKSYYLERT 206
XF0754 GVAITDP---------- 42
XF2679 GVVSDGLCPVVVPTQAVCG----------AGVAS-DQHLKPAPVA 182
CJA_1309 GAYSLG---------- 84
PA0919 ----LPHQASHGQWLLAWNDNPDDDTAVFVRKQSSAETSISDYDTPLS----------3
PP_1201 ----LPKSAAHGHWNVAWNDNPDDASAAFVRDQANAETSISDYDIHLP---------- 199
Atu_AcvB LTDGALPAPVSVIFTPDADQKGRDHVNALVKLHSDIEVTDVTDKAD---------- 227
Atu_VirJ ----------
Rtr_AtvA LQEGALPNPILVTFTANAPKDGRDHVADIQKDHPEVQTTD-SDNADT---------- 230
Bphy_4018 ----------APDPTVTHGPGLPGFAETDAN-PSAGT---------- 195
Rpic_3994 ALQSAMPTSFARRSGPLCDARATQAFIDTISGAQSVALPAMATGANAPP---VTASEPFK 357
XAC1368 IPWVLAASQDKR-----CPAAAEEGFLKQVPQARTFRRSAQGDILPG----------LR 226
XAC2411 ----------TKDPGLACSRDLPNASQGFLDDLADAS---------- 184
Phep_2436 ----------
Phep_2437 ----------
Phep_2737 EKLAAPFIALNGIKDETCPFQATKTFLTGMPFAELVTLPKVGHGFSIADNWLPQFYQSYK 266
XF0754 ----------DAGAAGLPPLPEKVQ------SHRA---------- 61
XF2679 APLLVMTVSSAH-----CPAQLTSGFVRKVALGREIRLAASADLLPR----------LR 226
CJA_1309 ----------
PA0919 ---DVLAHQLRLQLQG---NAEALPVLEVP----AAQPSDIVTLFYSGDGGWRDLDKDSA 253
PP_1201 ---QVLKAQLTQALVGRDGNALAIPVVEVP----AGQTTDTVTLFLSGDGGWRDLDRDVA 252
Atu_AcvB -EVLTQTLSDKVDAAGDSGNPLGLPITVL----EAKPVMDTMAVIYSGDGGWRDLDEEVG 282
Atu_VirJ ----------VRLPLRVF----NAKPAKNTVAIIYSGDAGWQNIDEVIG 73
Rtr_AtvA YATLEASLADLMKTIDSSKSPLGLPLDIM----ETTPTEDTLAIVYSGDGGWRDIDKEVG 286
Bphy_4018 QRIVELTTPHLRVAVMKEEDVSDLPLIEL----PAAHPTGLMAIVISGDGGWRDLDKTIA 251
Rpic_3994 TAFAKLVAQRKPPPPPPPAAVSDLPIIEVPAQPGSSSE--LFAVLLSGDGGWAGLDKEVA 415
XAC1368 AAVRSLGEQKGVALPPPPGGLADLPVVELPAKPDGDSDDDTFVIFVSGDGGWAGLDEEVA 286
XAC2411 SPMQIAAATRGHFLAAQSQGLGDLPLVEM----HAPG-SDRLVVMLSGDGGWRELDKGIA 239
Phep_2436 ----------IARSDFDLPVFAYP--AADSNKTGTLIVMLSGDGGWLDFEDSLS 75
Phep_2437 MKFKILLFLLILTYQDYTQAQTAYPTHPLF-----KSSHKPLVLFLTGDGGWNTFSMQVA 55
Phep_2737 KIIASPSAIKQKNAASVQRMPDKLITTLPLNLLPAPSSDQPLIFMMSGDGGWTSFDQSLA 326
XF0754 TPIQ----------SSGVSALPLVEY----HAPG-SDRLAIMISGDGGWRTLDRNLS 103
XF2679 AALRVLGAQKGVSLPPPPADLDGLPVVEVPSKAQKKSD--TFAIFVSGDGGWAEIDKKVA 284
CJA_1309 ----------WQDDITLPIPPCHNNSALEWKERCS 109

```
PA0919          EHMASMGYPVVGIDTLRYYWQHKSPEQSAADLSKLMQHYREKWGAKRFVLAGYSFGADIL 313
PP_1201         GEMAKLGYPVVGIDTLRYYWQHKTPEQSAADLSELMHHYRQKWGTKRFVLTGYSFGADVL 312
Atu_AcvB        SALQKQGVPVIGVDALRYFWKEKDPKEVAGDLARIIDTYRKEWKVKNVVLIGYSFGADII 342
Atu_VirJ        TYLQTEGIPVIGVSSLRYFWSERSPSETAKDLGHIIDVYTKHFGVQNVLLIGYSFGADVM 133
Rtr_AtvA        SYLQDQGIPVVGVDTLHYFWTEKDPQQTANDLGRIIDFYTKRFKVKHVVLVGYSFGADVL 346
Bphy_4018       EELQKDGVSVIGWDSLRYFWSEHSPQQTSHDLARVLQTYATRWHADHVALIGYSFGADVM 311
Rpic_3994       AALSKSGVPVVGIDSLRYFWTPRTPASAAADMDRLVRFYASRWKKQKALLIGYSQGADVL 475
XAC1368         DALAAQGIPVVGLDSLRYFWTERTPQGFADDLDRIARIYAQRWDRQRVVLIGFSQGADVL 346
XAC2411         AQLQQQGVSVVGWNSLRYFWGSRTPQQVGADLDRVIASYRQRWHIQHVALVGYSFGADVL 299
Phep_2436       VQFSKAGFNTVGFNCRDYFWERKTPRQTAEDLSMLLHVYIQQYNSTKIVLCGYSFGADVV 135
Phep_2437       DELGKNGYPVISLDTRKYFWEQKTPAGFAADVNTIVSKYLNQWNKDEFCVVGYSFGAEVG 115
Phep_2737       ESFAEKGMAVVGLDAQKYFWNAKTPQQTAAAIADAISYYMQNWKKKKFILAGYSFGACIA 386
XF0754          KELQRRGISVVGWNSLRYFWKLRTPEQLGDDLSRVIADYQRRWGAHQVILIGYSFGADVM 163
XF2679          GHLADADIPVVGLDSLRYFWSERTPEGFAKDLDRIARFYAHHWKRNRLLLVGFSQGADVL 344
CJA_1309        ELILHT----YPLPSTPWRLFNTHP---LKDLQAAIDYYTQAWAKSELLLIGFSMGADVM 162
                  :             :     *     :     *   :   .  : *:* ** :

PA0919          PAIYNRLPGKDQQQVKAMLLLALARTGSFEIEVEGWLGK--AGEEAATGPEMARLPAAKV 371
PP_1201         PAIYNRLPVEDQQRIDAVMLLAFARSGSFEIEVEGWLGK--EGQEAPTGPEMAKLPASKV 370
Atu_AcvB        PATYNLLPDRVKSSVAQLSLLGLSNEVDFEISVQGWLGVAGEGKGGKTVDDIAKIDPKLV 402
Atu_VirJ        PASFNRLTLEQKNRVKQISLLALSHQVDYVVSFRGWLQLETEGKGGNPLDDLRFIDPAIV 193
Rtr_AtvA        PASYNRLPQAEKDKIVQMSLLSLSQKVDYVISVMGWLGASSQGKGGDPVNDLKSINPKMV 406
Bphy_4018       PFAYNRLPDGLRAKVSLISLLGFAPSADFQIRVTGWLGMPASDKALPVKPEFERLPPRIV 371
Rpic_3994       PFIVNRLPAASREHVALAVMMGLGKRADFEFHMTNWVSS--SASGLLILPEVQKLPAGLG 533
XAC1368         PAAINKLPAATKQNLRMTALLSVGKLADYEFHVSNWLGS--DDEGLPIAPEVQRLPAGTT 404
XAC2411         PFAYPGLSPQQRASVQFVSLLGLGHEADFKVRVGGWLGW-HNDAERDVEPAIQALDAHRL 358
Phep_2436       PFIYNRLRPHLKSRITALGMLSPFATTDFKVHTSDLLNIAKDNRKYKVKAEIDRIRIP-V 194
Phep_2437       AFLPTHLPAATLEKFKSLVLLSPGYSNSFEVRFINMIATKNTNKDKYKVYPELLKSKIPV 175
Phep_2737       PFIANRLPENLQHNLSAVCMLSPDERADFEIHVADMLSIDGQDEPYNVLAEMKKARTFKL 446
XF0754          PFAYAHLMPTQRNGVDFISLLALGRKADFKARIFGWLGW-GEHGTRDVLTALGALDLHRV 222
XF2679          PAAINKLSPNTRQIIRMTALLSLGKYAHYEFHVSNWIST--DDEGIPIAPDMVKLRSTRT 402
CJA_1309        PFMVNRLDANTKHKIRSVNLLNPANTVDFVFHVSGWFST-AGELPYKLYPEMKDWTQWPV 221
                .     *       .    ::       :     . .

PA0919          FCIYGAEEKDESGCTQSQAVG-------EKLELPGGHHFDE-DYLSLAKKMLQAIRDREN 423
PP_1201         VCVYGVEETDESGCTEKTAVG-------ERLKLPGGHHFDE-NYPALAKRLIGEIETRQG 422
Atu_AcvB        QCVYGTEEEDEDPCPGLKAKGV------ETIGIEGGHHFDE-DYEALAKRIVTSLKTRLA 455
Atu_VirJ        QCMYGREDRNN-ACPSLRQTGA------EVIGFSGGHHFGN-DFKKLSTRVVSGLVARLS 245
Rtr_AtvA        QCVYGKDDDEDVACPLLKGTGA------EVIAMDGGHHFDD-DYEALANHIINGLKSRLG 459
Bphy_4018       QCFYG-EHEDETLCPTLTKTGI------EVIRTTGDHHFGH-DYVALEKRILNALKKQAN 423
Rpic_3994       MCIYG-KEEKDTNCPGLDPKQV------QLVKLPGGHHFDG-DYAKLARISLEGARAPGN 585
XAC1368         VCIYG-QDDDDALCPSLPANVA------RRVALPGDHHFKG-DYATLAKTIMDQLHALSK 456
XAC2411         QCIYG-DEEKDTLCPELRARGV------QVLARPGGHHFDH-DPVVLANLLMQGWQHAAQ 410
Phep_2436       FCFYG-KDEEPKAQENILKPGF------YLKLLAGDHRYEESTYQEIVNTLTNTINQK-- 245
Phep_2437       WCIFGEEEKTDISQELKETNKI------RKITIPGSHHYND-DVQLVVSGAIKGLVN--- 225
Phep_2737       IVLFG-DDEDPATTKQFRQETS------RVITLPGGHHYNN-DYTGIVNYVIKSL----- 493
XF0754          QCIYG-QNDKDAVCPELRERIF------DVVMRPGGHHFDG-DTVKLADAILQGWQRRIE 274
XF2679          VCIYG-VDDQETLCPSLPQ-QN------RRVALPGTHHFNG-DYETVAKTILAQMEAAP- 452
CJA_1309        NCFYS--ETQDSLCETIKANLPQKPDNQQLFYLSGDHHFNG-NYQQLIKWILANSKVPVR 278
                  .:.  .                          * *::       :

PA0919          APDA------- 427
PP_1201         KSSVAEQN--- 430
Atu_AcvB        K---------- 456
Atu_VirJ        HQYSSGPAPL- 255
Rtr_AtvA        E---------- 460
Bphy_4018       GV--------- 425
Rpic_3994       ASR-------- 588
XAC1368         P---------- 457
XAC2411         TPIAETASRS- 420
Phep_2436       ----------
Phep_2437       ----------
Phep_2737       ----------
XF0754          LREPRNADSPR 285
XF2679          ----------
CJA_1309        ----------
```

Figure 36: Sequence alignment of PA0919 homologous proteins (see previous pages)
PA0919 homologous proteins were identified by BLAST analysis and selected sequences were aligned by ClustalW2 (section 2.13.1). Conserved serines and histidines are indicated in bold letters and amino acid positions mutated by site-directed mutagenesis in PA0919 are highlighted gray. Conservation degrees are indicated: period (.): semiconserved, colon (:): conserved, asterisk (*): identical.
Gene names/locus tags: PA0919: *P. aeruginosa* PAO1, PP_1202: *P. putida* KT2440, Atu_AcvB: *A. tumefaciens* C58, Atu_VirJ: *A. tumefaciens* octopine-type Ti-plasmid pTiA6, Rtr_AtvA: *R. tropici* CIAT 899, Bphy_4018: *B. phymatum* STM815, Rpic_3994: *R. pickettii* 12J, XAC1368 and XAC2411: *X. axonopodis* 306, Phep_2436, Phep_2437 and Phep_2737: *P. heparinus* DSM2366, XF0754 and XF2679: *X. fastidiosa* 9a5c, CJA_1309: *C. japonicus* Ueda107.

8.6 Native molecular mass determination of the PA0919 protein

The native molecular mass of recombinant PA0919-Strep protein was determined by analytical gel permeation chromatography (section 2.10.6). The obtained chromatogram is given in Figure 37. The calculated native molecular mass of 57 kDa indicated a monomeric architecture of the recombinant PA0919-Strep protein.

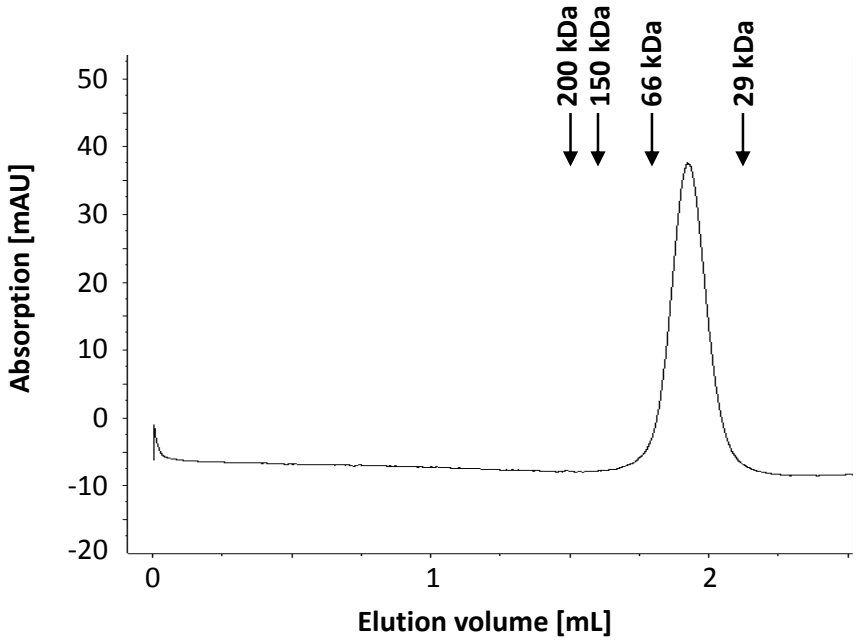

Figure 37: Analytical gel permeation chromatography of the recombinant PA0919-Strep protein
50 µg of purified recombinant PA0919-Strep protein were loaded onto a Superdex 200 5/150 GL column and eluted using a flow rate of 0.45 mL/min. Protein elution was monitored by measuring the absorption at 280 nm.
Protein standards: carbonic anhydrase (M_r = 29'000), bovine serum albumin (M_r = 66'000), yeast alcohol dehydrogenase (M_r = 150'000) and β-amylase (M_r = 200'000).

8.7 Topology analysis of the PA0919 protein

The PA0919 amino acid sequence was analyzed by the programs SignalP 4.1 and TMHMM for the identification of secretion signal sequences and transmembrane helices (section 2.13.5). The obtained output data are presented in Figure 38 (SignalP 4.1) and in Figure 39 (TMHMM). The analyses revealed the presence of one N-terminal transmembrane helix formed by amino acids 12 – 31 of the entire PA0919 protein. A secretion signal sequence was not predicted.

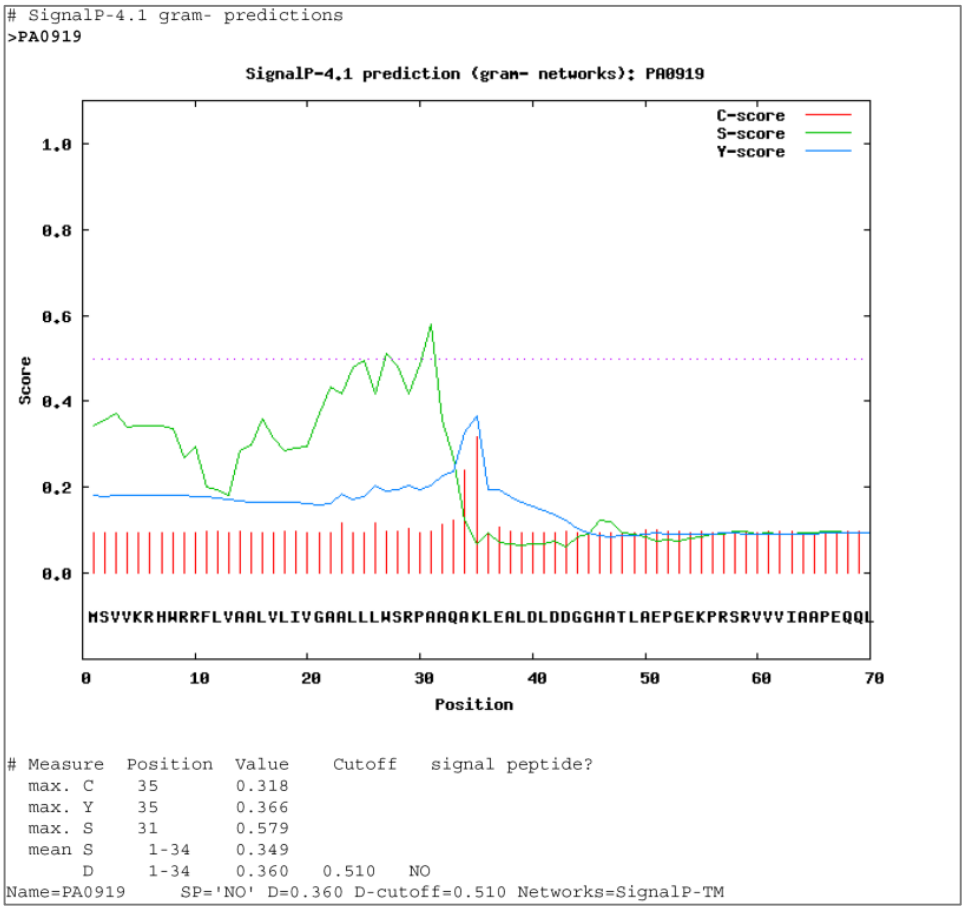

Figure 38: SignalP 4.1 output data for PA0919
The PA0919 amino acid sequence was analyzed by SignalP 4.1 to predict a potential secretion signal (Petersen *et al.*, 2011). Calculated scores were plotted against the specific amino acid position.
The obtained output data are presented: C-score (red): raw cleavage site score, S-score (green): signal peptide score, Y (blue): combined cleavage site score, D-score: discrimination score (distinguishes signal peptide sequences from non-signal sequences).

```
# PA0919 Length: 427
# PA0919 Number of predicted TMHs:  1
# PA0919 Exp number of AAs in TMHs: 20.0533
# PA0919 Exp number, first 60 AAs:  19.95012
# PA0919 Total prob of N-in:        0.99223
# PA0919 POSSIBLE N-term signal sequence
PA0919  TMHMM2.0        inside       1    11
PA0919  TMHMM2.0        TMhelix     12    31
PA0919  TMHMM2.0        outside     32   427
```

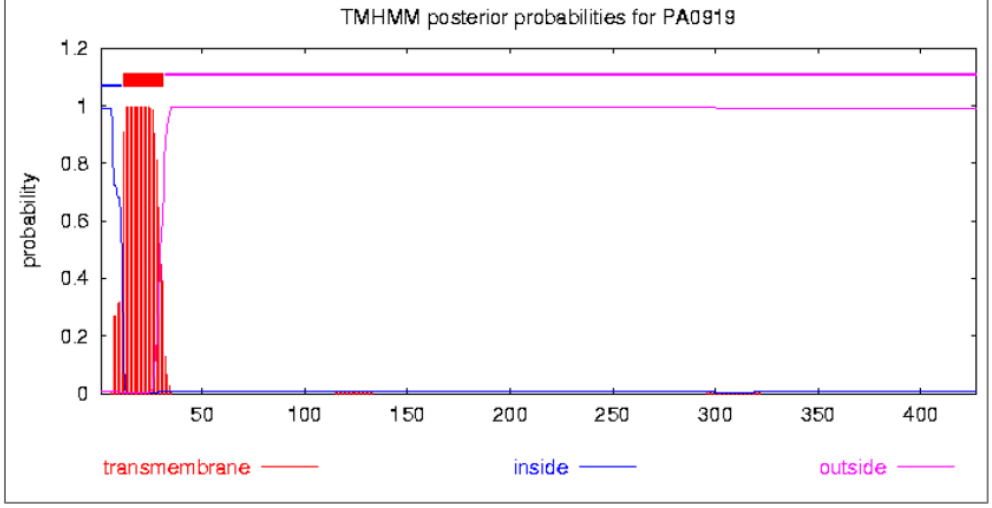

Figure 39: TMHMM output data for PA0919

The TMHMM online tool (Krogh *et al.*, 2001) was employed to detect transmembrane helices using the PA0919 amino acid sequence for query. Calculated probabilities for the location of specific amino acid residues were plotted against the specific amino acid moiety. The obtained output data are presented. One N-terminal located transmembrane helix was predicted by TMHMM consisting of PA0919 amino acids 12 to 31 and the program indicated the possibility of an N-terminal secretion signal sequence.

Protein sequences predicted to face the cytoplasm are indicated blue and fragments proposed to be located within the periplasm are given in magenta. Putative transmembrane helices are indicated in red.

AAs: amino acids, THMs: transmembrane helices.

8.8 Growth phenotype and lipid composition of ΔPA0919 complemented strains employed for PA0919 localization

Several *P. aeruginosa* strains (Δ19 19, Δ19 $19_{35\text{-}427}$, Δ19 pUC/19 and Δ19 pUC/$19_{35\text{-}427}$) were constructed based on the ΔPA0919 deletion mutant strain for the localization of PA0919 within its native host. The stains were analyzed together with their reference strains (PAO1, ΔPA0919 and Δ19 pUC) concerning their growth and lipid composition under neutral conditions. The obtained results are presented in Figure 40 and Figure 41. For strain designation and construction strategy, see section 3.8.1.

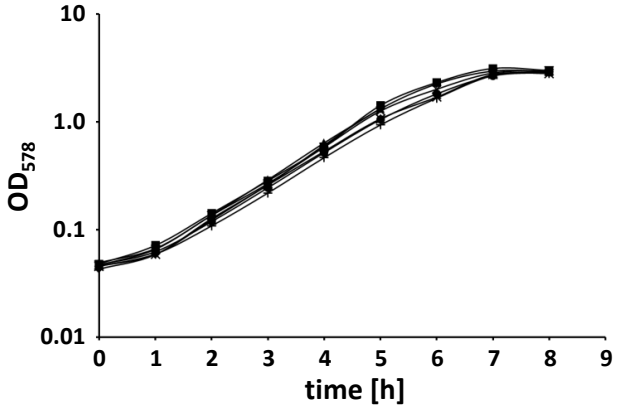

Figure 40: Growth curves of complemented ΔPA0919 for PA0919 localization
P. aeruginosa strains were cultured in AB medium pH 7.3 at 37 °C and 200 rpm (section 2.3.5). Culture turbidity was determined at 578 nm. For strain designation and construction details, see Figure 26 and section 2.4.19.
Rhombus: PAO1 wild-type, square: PAO1 ΔPA0919 deletion mutant, triangle: Δ19 19, cross: Δ19 $19_{35\text{-}427}$, star: Δ19 pUC/19, dot: Δ19 pUC/$19_{35\text{-}427}$, plus: Δ19 pUC.

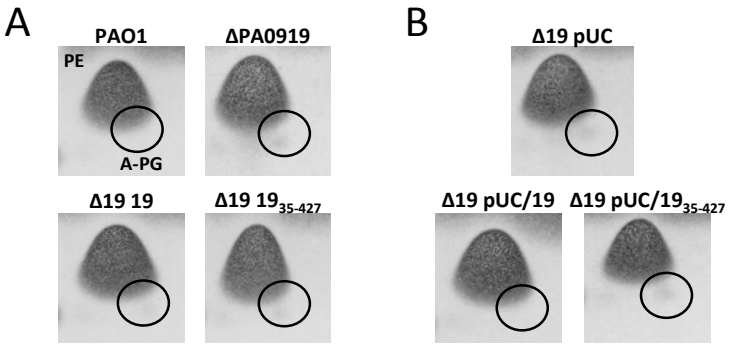

Figure 41: Lipid composition of complemented ΔPA0919 strains for PA0919 localization
Various *P. aeruginosa* strains were grown in AB medium pH 7.3 at 37 °C and 200 rpm for 24 h (section 2.3.5). Polar lipids were extracted, separated by two-dimensional TLC and detected by molybdatophosphoric acid staining (sections 2.5.1 and 2.5.3). A-PG position is indicated by a circle. For strain designation and construction details, see Figure 26 and section 2.4.19.
A-PG: alanyl-phosphatidylglycerol, PE: phosphatidylethanolamine.

Danksagung

Mein Dank gilt zuerst Herrn Prof. Dr. Dieter Jahn für die Möglichkeit, diese Arbeit in den letzten Jahren in seiner Arbeitsgruppe anfertigen zu können.

Herrn Prof. Dr. Ralf R. Mendel danke ich für die Übernahme des Prüfungsvorsitzes.

Bei Frau PD Dr. Gunhild Layer möchte ich mich für die Übernahme des Zweitgutachtens und für die vielen hilfreichen Diskussionen bedanken.

Mein ganz besonderer Dank gilt Dr. Jürgen Moser für die ausgezeichnete Betreuung, die gute Zusammenarbeit und seine unerschütterliche Zuversicht während der letzten Jahre.

Des Weiteren möchte ich mich bei Dr. Jeroen S. Dickschat und Henning Kuhz für die Synthese des Lys-ONp, bei Prof. Dr. Susanne Häußler für die Überlassung der Transposon-Mutanten und bei Beate Jaschok-Kentner für die N-terminale Sequenzierung bedanken.

Bei den derzeitigen und ehemaligen Mitgliedern der Arbeitsgruppe Moser, namentlich Dr. Stefanie Hebecker, Dr. Markus Bröcker, Christiane Lange, Svenja Kiesel, Simone Virus und Janis Rabe, möchte ich mich sehr herzlich für die gute Labor- und Diskussionsatmosphäre bedanken. Dr. Stefanie Hebecker sei insbesondere für die Bereitstellung der Ergebnisse zur Charakterisierung der AaPGS-Enzyme aus *B. phymatum*, *K. radiotolerans* und *M. barkeri*, die Durchführung der Promotoraktivitätsbestimmung in Gegenwart von Ampicillin, Oxacillin, Protaminsulfat, Polymyxin E und Domiphenbromid sowie die Bereitstellung der gereinigten A-$PGS_{543-881}$ gedankt. Bei Christiane Lange möchte ich mich insbesondere für ihr offenes Ohr und die Korrektur von weiten Teilen dieser Arbeit bedanken.

Des Weiteren möchte ich mich bei Maike Groenewold, Christin Uhlig, Timm Reichelt, Sonja Jäger und Franka Eichler bedanken, die mit ihren Bachelor- und Masterarbeiten meine Arbeit maßgeblich unterstützt haben. Mein besonderer Dank gilt Maike Groenewold, die mit der Erstellung des Stamms ΔPA0919 die Grundlage für viele weitere Experimente schuf und deren Arbeiten zur Lokalisierung und Inhibierung maßgeblich zur Charakterisierung der A-PGH beigetragen haben. Sonja Jäger sei für die Analyse der Substratspezifität der Aa-PGS-Enzyme aus *S. thermophilus* und *B. licheniformis* gedankt.

Außerdem möchte ich mich bei PD Dr. Max Schobert, Dr. Elisabeth Härtig, Dr. Maike Narten, Andrea Wesche-Franke, Ann-Kathrin Meyer, Anja Hartmann und Gabriele Günther für die Beantwortung all meiner Fragen zu Pseudomonas-Techniken und RNA-Methoden bedanken. Herzlichen Dank auch an die Arbeitsgruppen Layer und Härtig für die gute Nachbarschaft im S2-Labor und an die Arbeitsgruppe Schomburg, bei denen ich die Biolog-Experimente durchführen konnte.

Mein besonderer Dank gilt Tristan Nicke, der mir in den letzten Jahren mit seiner immerwährenden Diskussionsbereitschaft, seinem unendlichen Wissen zu Membranproteinen und deren Reinigung zur Seite gestanden hat und der immer ein offenes Ohr für mich hatte. Außerdem möchte ich mich bei Ann-Kathrin Meyer, Kristin Haufschildt, Judith Streif, Constanze Finger, Andrea Wesche-Franke, Jens Jäger, Claudia Frädrich und Dr. Johannes Walther für die gute Atmosphäre und den Wissenstransfer herzlich bedanken.

Christina Nitzsche und Daniela Schnobel gilt mein herzlichster Dank für ihre Offenheit und Herzlichkeit, aber insbesondere danke ich ihnen für den Satz „Das kriegen wir hin, gar kein Problem!“ und für all das, was darauf folgte. Bernd Hoppe, Dagmar Rose, Barbara Cwiklinski möchte ich für ihre Unterstützung danken, die mir so manche schlaflose Nacht ersparte.

Bei allen Mitarbeitern des Instituts für Mikrobiologie möchte ich mich für die freundliche Arbeitsatmosphäre, die hohe Diskussionsbereitschaft und die große Hilfsbereitschaft bedanken.

Meiner Familie und meine Freunden gilt mein Dank für ihre Unterstützung und ihre unendliche Geduld.

Abschließend gilt mein herzlichster Dank meinem Freund Tobias Keisenberg, der es in den letzten Wochen und Jahren nicht immer leicht mit mir hatte. Danke für deine Unterstützung!